Universidade do Porto
Faculdade de Engenharia
FEUP

Chemical Engineering Department

Multi-element Determination of Metal(loid)s in Surface Waters, at Trace Levels, Using Greener Voltammetric Approaches

Georgina Maria da Silva Alves

A thesis submitted in partial fulfilment of the requirement for the degree of

Doctor in Environmental Engineering

by

University of Porto

Supervisors

Doctor Helena Maria Vieira Monteiro Soares

Chemical Engineering Department

Faculty of Engineering of University of Porto

Doctor Júlia Maria Coelho Santos Magalhães

University of Porto

Acknowledgments

At the end of this thesis I would like to acknowledge all those who, of several ways, have made it possible.

First of all, I would like to express my gratitude to my supervisors, Professor Helena Soares and Doctor Júlia Magalhães, for giving me the opportunity to work on such an interesting project and for their great and continuous scientific guidance, advice, support and encouragment. It has been a pleasant and proficuous learning process throughout these last years.

For the facilities that allowed me to conduct the scientific experiments from which this thesis results, I would like to express my appreciation to the Department of Chemical Engineering of Faculty of Engineering of Porto and REQUIMTE.

I am also grateful to "Fundação para a Ciência e a Tecnologia" for the financial support under the Project PTDC/QUI-QUI/112439/2009 and for a PhD scholarship with reference SFRH/BD/46521/2008.

I wish to thank to Professor Constant van den Berg, who received me in his lab in the University of Liverpool. I also want to thank the opportunity of working with him. To Doctor Pascal Salaün from University of Liverpool, I have to thank for the valuable teachings about gold microwire electrodes and continuous support. To all friends that I made there, especially Rita, Bruno, Joana, Alessio, Shun and Kristopher, I wish to thank their support and friendship. It was a pleasure to meet you all.

Moreover, I am grateful to Professor Romà Tauler, who received me in the Institute (CSIC) in Barcelona. I would like to thank his patience and his intensive lessons about MCR-ALS. To all friends that I made there, especially Amrita, Marta, Mireia, Stefan and Xin, I wish to thank their support and friendship. It was a pleasure to meet you all.

I would also like to thank my colleagues from LAB 302B, namely Cristina, Manuela, João, Isabel Neto and Isabel Pinto. Thank you for the lovely working environment, support and friendship.

Finally, thank you to all my friends and to my closest family. Special thanks to my mother and my brother for their support, dedication, care and patience. Thank you for being always there for me.

"Challenges are what make life interesting; overcoming them is what makes life meaningful."

Charles Chaplin

Resumo

Os metais pesados e os metalóides são poluentes comuns; assim, a sua ocorrência em águas naturais constitui, por vezes, um dos principais problemas relacionados com a qualidade da água. A existência destes poluentes persistentes e não-biodegradáveis em ambientes aquáticos, provenientes de fontes naturais ou antropogénicas, mesmo em baixas concentrações, pode afetar a qualidade de vida dos animais e das plantas

As técnicas analíticas convencionais apresentam-se como inadequadas e/ou dispendiosas para a determinação simultânea de quantidades vestigiais de metais pesados e metalóides. Pelo contrário, a voltametria de redissolução, é uma técnica analítica simples, precisa, sensível e adequada para a determinação de traços ou ultra-traços de iões metálicos e metalóides.

Em conformidade com a tendência geral da electroanálise moderna, o objetivo desta tese consistiu no desenvolvimento de procedimentos voltamétricos simples e sensíveis para a deteção multi-elemento, baseados em metodologias ambientalmente mais amigáveis e usando macro ou microelétrodos não-tóxicos.

Em primeiro lugar, avaliou-se a utilização de um elétrodo de carbono vítreo com filme de bismuto depositado *in-situ*, juntamente com a aplicação da voltametria de redissolução anódica e da calibração multivariada por regressão por mínimos quadrados parciais, na determinação simultânea de cobre (Cu), chumbo (Pb) e zinco (Zn). A associação destas metodologias permitiu resolver os problemas relacionados com a sobreposição dos picos do bismuto (Bi) e do Cu e a formação de compostos intermetálicos de Cu-Zn. Os modelos de calibração multivariada desenvolvidos foram usados na determinação simultânea de Cu, Pb e Zn, a baixos níveis de concentração (μgL^{-1}), em amostras de água de rio, com resultados satisfatórios.

Posteriormente, explorou-se as potencialidades de um microelétrodo de fio de ouro (d = 25 μm), construído no laboratório, para a determinação multi-elemento de arsénio (As), cádmio (Cd), Cu, mercúrio (Hg), Pb e Zn, em condições ácidas e em meio salino (NaCl 0,5 $molL^{-1}$), usando um procedimento rápido e

simples (30 s de tempo e deposição sem desoxigenação) por voltametria de redissolução anódica diferencial com impulsos. Este microelétrodo foi usado como elétrodo de trabalho em duas configurações diferentes, isto é, como um elétrodo vibratório ou estacionário, respetivamente. Numa primeira fase, o microelétrodo vibratório de fio de ouro mostrou excelentes características para a determinação simultânea da concentração total de As, Cu, Hg e Pb, a pH 1, em águas doces não poluídas [os limites de deteção (LDs) para um tempo de deposição de 30 s foram 0,07; 0,4; 0,07 e 0,2 μgL^{-1}, respetivamente]. Por outro lado, a aplicação de duas medições sequenciais, a pH 3, usando o mesmo microelétrodo de ouro, em modo vibratório ou estacionário, numa mesma amostra e durante um curto período de tempo, permitiu quantificar as concentrações totais de Cu, Hg, Pb e Zn numa vasta gama de valores, típicos de águas não poluídas (para um tempo de deposição de 30 s, os limites de deteção foram 0,2 μgL^{-1} para Hg, 0,3 μgL^{-1} para o Pb e 0,4 μgL^{-1} para o Zn e Cu) ou poluídas (até concentrações cerca de cem vezes superiores aos valores dos LDs anteriormente mencionados), em águas superficiais (doces ou salinas) e em águas para consumo, na ausência da formação de compostos intermetálicos de Cu-Zn.

Além disso, a análise de uma mistura binária de Pb (até 15,0 μgL^{-1}) e Cd (até 10,0 μgL^{-1}) com o microelétrodo de ouro em modo vibratório, a pH 3, resultou numa forte sobreposição dos picos. A aplicação de modelos de calibração multivariada, quer o modelo que resultou da aplicação da restrição da correlação à resolução multivariada de curvas por mínimos quadrados alternados quer o modelo de calibração por mínimos quadrados parciais permitiram quantificar os dois metais; o modelo de resolução multivariada de curvas por mínimos quadrados alternados permitiu ainda resolver os metais. Ambos os modelos permitiram quantificar totalmente Pb e Cd em amostras de água fluviais superficiais, com resultados satisfatórios.

Finalmente, a utilização da voltametria adsorptiva de redissolução catódica de onda quadrada juntamente com um elétrodo vibratório sólido de bismuto, construído no laboratório, permitiu a deteção simultânea rápida e simples (30 s de tempo de acumulação sem desoxigenação) de níquel (Ni) e cobalto (Co). A

metodologia desenvolvida permitiu determinar Ni e Co (até 10 e 35 μgL^{-1}, respetivamente), em tampão amónia utilizando dimetilglioxima com LDs de 0,6 e 1,0 μgL^{-1}, respetivamente. O método proposto foi validado para a determinação simultânea de Ni e Co em águas doces.

Em conclusão, graças ao excelente desempenho analítico de dois elétrodos ambientalmente mais amigáveis [macroelétrodo de bismuto (filme ou sólido) e microelétrodo de ouro] e através da aplicação de técnicas voltamétricas de redissolução, por vezes coadjuvadas por ferramentas quimiométricas, foram desenvolvidas abordagens simples e rápidas para a determinação de concentrações totais de vários metais pesados (Cd, Co, Cu, Hg, Ni, Pb e Zn) e um metalóide (As), ao nível de traços, em águas superficiais.

Abstract

Heavy metals and metalloids are common pollutants; thus, their occurrence in natural waters is one of the major problems related with water quality. The existence of these persistent and non-biodegradable pollutants in aquatic environments, arising from natural or anthropogenic sources, even at trace levels, could affect the life of animals and plants.

Conventional analytical techniques appear to be inadequate and/or expensive for simultaneous determination of trace levels of heavy metals and metalloids. Unlike, stripping voltammetry is a simple, accurate and sensitive analytical technique, suitable for determination of trace and ultra-trace metal(loid) ions.

In line with the general trend of the modern electroanalysis, the aim of this thesis was the development of simple and sensitive voltammetric procedures for detection of multi-metal(loid) ions, based on "greener" approaches using non-toxic macro or microelectrodes.

Firstly, the use of a bismuth film plated *in-situ* at a glassy carbon electrode, coupled with the application of anodic stripping voltammetry and partial least squares regression chemometric tool, was evaluated for the simultaneous determination of copper (Cu), lead (Pb) and zinc (Zn). The association of these methodologies allowed solving problems related with the overlapping peaks of bismuth (Bi) and Cu and the formation of Cu-Zn intermetallic compounds. The built up partial least squares multivariate calibration models were used for simultaneous determination of Cu, Pb and Zn, at low concentration levels (μgL^{-1}), in river water samples with satisfactory results.

Later on, the potentialities of a "home-made" gold microwire electrode (25 μm diameter) for the multi-element determination of arsenic (As), cadmium (Cd), Cu, mercury (Hg), Pb and Zn, in acidic and saline (NaCl 0.5 $molL^{-1}$ medium) conditions, using simple and faster (30 s of deposition time without deoxygenation) subtractive diferential pulse anodic stripping procedures were explored. This microelectrode was used as a working electrode in two different

configurations, i.e., as a vibrating or as a stationary electrode, respectively. In a first attempt, the vibrating gold microwire electrode showed excellent characteristics for the simultaneous determination of total concentrations of As, Cu, Hg and Pb, at pH 1, in unpolluted fresh waters [the detection limits (DLs) for a deposition time of 30 s were 0.07, 0.4, 0.07 and 0.2 μgL^{-1}, respectively]. On the other hand, the application of two sequential measurements, at pH 3, using the same gold microelectrode under the vibrating or stationary mode in the same sample and during a short period of time, allowed quantification of total concentrations of Cu, Hg, Pb and Zn in a wider range of concentrations, typical of unpolluted (the DLs for a deposition time of 30 s were 0.2 μgL^{-1} for Hg, 0.3 μgL^{-1} for Pb and 0.4 μgL^{-1} for Zn and Cu) or polluted (up to about two orders of magnitude higher than the DLs mentioned previously) surface (fresh and saline) waters and in drinking waters without the formation of Cu-Zn intermetallic compounds.

Furthermore, the analysis of a binary mixture system of Pb (up to 15.0 μgL^{-1}) and Cd (up to 10.0 μgL^{-1}) using a vibrating gold microelectrode, at pH 3, resulted on strongly overlapping of the peaks. Application of multivariate curve resolution alternating least squares together with the correlation constraint or partial least squares regression allowed the resolution (only for multivariate curve resolution alternating least squares) and quantification of both metals. The built up multivariate calibration models, based either in multivariate curve resolution alternating least squares or partial least squares regression, allowed total quantification of Pb and Cd in surface river water samples, with satisfactory results.

Finally, square wave adsorptive cathodic stripping voltammetry, together with a "home-made" solid bismuth vibrating electrode, was used for the simultaneous, simple and fast (30 s of accumulation time without deoxygenation) detection of nickel (Ni) and cobalt (Co). The developed methodology enabled to determine Ni and Co (up to 10 and 35 μgL^{-1}, respectively), in ammonia buffer using dimethylglyoxime with detection limits of 0.6 and 1.0 μgL^{-1}, respectively.

The proposed method was validated for simultaneous determination of Ni and Co in fresh waters.

In conclusion, thanks to the excellent analytical performance of two "green" electrodes [a bismuth (film or solid) macroelectrode and a gold microelectrode] and through the application of voltammetric stripping techniques, in some instances assisted by chemommetrics tools, simple and rapid analytical approaches were developed for determination of total concentrations of several heavy metals (Cd, Co, Cu, Hg, Ni, Pb and Zn) and one metalloid (As), at trace levels, in surface waters.

Preface

Water pollution is an important global problem, which requires attention and continuous prevention. Among the different toxic compounds present in water bodies (e.g. lakes, rivers, oceans, aquifers and groundwater) heavy metals or metalloids, such as is the case of As, are considered among the most hazardous. The environmental impact of them is of particular concern because, unlike organic compounds, they are persistent and non-biodegradable pollutants. Thus, the European Union (EU) commission and the Environmental Protection Agency (EPA) from USA, provide guidelines and threshold limits for concentrations of these pollutants in waters.

The major existing techniques for trace metal analysis are expensive and time consuming; thus, the development of safe, low cost, quick and sensitive analytical methodologies are required. In this context, this work is an important contribution for the development of efficient, simple, relatively inexpensive, very sensitive and more "environmentally-friendly" approaches, to the simultaneous determination of total concentrations of multi-combinations of the following metal(loid)s: As, Cd, Co, Cu, Hg, Ni, Pb and Zn.

This thesis is organized in seven chapters. The first chapter comprises a general introduction to the problematic of the multi-element determination of heavy metals or metalloids, at trace levels, using "greener" voltammetric approaches with a review of the literature, which include the main works developed between 2003 and April of 2013. This review gives a survey of the application of non-toxic mercury-free electrodes associated with voltammetric stripping techniques for monitoring trace metals in environmental and/or biological samples. This chapter also provides a brief description of voltammetric techniques and chemometrics tools used in this work. The next five chapters contain a series of papers, elaborated during the PhD, which were published or accepted for publication.

Chapters 2 and 6 describe the work developed with two different bismuth macroelectrodes [bismuth film deposited *in-situ* on a glassy carbon electrode

(Chapter 2) and a solid bismuth vibrating electrode (Chapter 6)] for the simultaneous determination of (Cu, Pb and Zn) and (Co and Ni), respectively.

Chapters 3 to 5 are devoted to the multi-element determination of As, Cd, Cu, Hg, Pb and Zn using a gold microelectrode.

Finally, the main conclusions of this thesis are presented in chapter 7 together with some suggestions of future work.

List of original publications

This thesis is based on the following publications:

I. Georgina M. S. Alves, Júlia M. C. S. Magalhães, Helena M. V. M. Soares
Simultaneous Determination of Copper (II), Lead (II) and Zinc (II) at Bismuth Film Electrode by Multivariate Calibration.
Electroanalysis 2011, 23, 1410 – 1417
Impact Factor (5 years): 2.856; Number of Citations (Scopus): 7

II. Georgina M.S. Alves, Júlia M.C.S. Magalhães, Pascal Salaün, Constant M.G. van den Berg, Helena M.V.M. Soares
Simultaneous Electrochemical Determination of Arsenic, Copper, Lead and Mercury in Unpolluted Fresh Waters Using a Vibrating Gold Microwire Electrode
Analytica Chimica Acta 2011, 703, 1 – 7
Impact Factor (5 years): 4.144; Number of Citations (Scopus): 12
This paper was classified as feature article and was front page of the issue of the journal

III. Georgina M. S. Alves, Júlia M. C. S. Magalhães, Helena M. V. M. Soares
Voltammetric Quantification of Zn and Cu, Together with Hg and Pb, Based on a Gold Microwire Electrode, in a Wider Spectrum of Surface Waters
Electroanalysis 2013, 25, 493 – 502
Impact Factor (5 years): 2.856

IV. Georgina M.S. Alves, Júlia M.C.S. Magalhães, Roma Tauler and Helena M.V.M. Soares
Simultaneous Anodic Stripping Voltammetric Determination of Pb and Cd, Using a Vibrating Gold Microwire Electrode, Assisted by Chemometric Techniques
Electroanalysis 2013 (accepted for publication; reference: elan.201300198).
Impact Factor (5 years): 2.856

V. Georgina M. S. Alves, Júlia M. C. S. Magalhães and Helena M. V. M. Soares
Simultaneous Determination of Nickel and Cobalt Using a Solid Bismuth Vibrating Electrode by Adsorptive Cathodic Stripping Voltammetry
Electroanalysis 2013, 25, 1247-1255
Impact Factor (5 years): 2.856

Contents

Figure Captions

Table Captions

Symbols and Abbreviations

A	Area
AA	Annual average
AAS	Atomic absorption spectroscopy
AAS-CV	Atomic absorption spectroscopy with cold vapour
AAS-EA	Atomic absorption spectroscopy with electrotermal atomization
AAS-FA	Atomic absorption spectroscopy with flame atomization
AdCSV	Adsorptive cathodic striping voltammetry
AdSCCC	Adsorptive stripping constant current chronopotentiometry
AdSV	Adsorptive stripping voltammetry
A_G	Geometric area
ALS	Alternating least squares
A_R	Real surface area
ASV	Anodic stripping voltammetry
BIA	Batch injection analysis
BiFE(s)	Bismuth film electrode(s)
BiFμE(s)	Bismuth film microelectrode(s)
CCC	Criteria continuous concentration
CE	Counter electrode
CLS	Classical least squares
CMC	Criteria maximum concentration
CMEs	Chemically modified electrodes
CSV	Cathodic stripping voltammetry

CV	Cyclic voltammetry
d	Diameter
D	Diffusion coefficient
DCLS	Directly classical least squares
DL(s)	Detection limit(s)
DME	Dropping mercury electrode
DMG	Dimethylglyoxime
DP	Differential pulse
DPAdCSV	Differential pulse adsorptive cathodic stripping voltammetry
DPASV	Differential pulse anodic stripping voltammetry
E	Potential
E_{acc}	Accumulation potential
E_{cond}	Conditioning potential
E_{dep}	Deposition potential
EFA	Evolving factor analysis
EPA	Environmental protection agency
EQS	Environmental quality standards
EU	European Union
F	Faraday constant
FIA	Flow injection analysis
GC	Glassy carbon
HMDE	Hanging mercury drop electrode
I	Current

ICLS	Indirectly classical least squares
ICP-AES	Inductively coupled plasma mass atomic emission spectrometry
ICP-MS	Inductively coupled plasma mass spectrometry
ILS	Inverse least squares
l	Length
LCR	Linear concentration range
LD(s)	Limite(s) de deteção
Lof	Lack-of-fit
LS	Linear sweep
LSAdCSV	Linear sweep adsorptive cathodic stripping voltammetry
LSV	Linear sweep voltammetry
LVs	Latent variables
MAC	Maximum allowable concentration
MCR-ALS	Multivariate curve resolution alternating least squares
MFE	Mercury film electrode
PCA	Principal component analysis
PLS	Partial least squares
Pure	Purest variables
r	Radius
R	Roughness
RDE	Rotation rate of a rotating disc electrode
RE	Reference electrode
RE (%)	Relative percentage error in concentration predictions

RMSE	Root mean square error
RMSEP	Root mean square error of prediction
rpm	Rotation rate per minute
RWQCs	Recommended water quality criteria
SBiVE	Solid bismuth vibrating electrode
SEP	Standard error of prediction
SIA	Sequential injection analysis
SMDE	Static mercury drop electrode
SVD	Singular value decomposition
SW	Square wave
SWAdCSV	Square wave adsorptive cathodic stripping voltammetry
SWASV	Square wave anodic stripping voltametry
t	Time
t_{acc}	Accumulation time
t_{dep}	Deposition time
t_{eq}	Equilibration time
THGA	Transversely-heated graphite atomizer
UPD	Underpotential deposition
USA	United States of America
UV	Ultraviolet
VIP	Variable importance in the projection
$W_{1/2}$	Half width
δ	Diffusion layer thickness

υ	Kinematic viscosity

Chapter 1

INTRODUCTION

1.1. Trace metal analysis in surface waters: An overview

Heavy metals are considered harmful and dangerous pollutants because they are highly toxic, persistent and non-biodegradable [1]. As a result of their non-biodegradable nature, heavy metals tend to accumulate in ecological systems, particularly in an aquatic environment, and move up through the food chain [2]. The existence of these pollutants in water bodies, even at trace levels, could affect the life of animals and plants, thus this problem has focused the attention of both scientific community and the public in general.

Heavy metals are continuously released into aquatic systems from natural (weathering of rocks, erosion, volcanic activity and forest fires) but also from several anthropogenic sources, such as municipal sewage effluents, garbage incineration, combustion of fossil fuels, metallurgical, paper and textile industries, mining and agricultural activities [3,4].

The chemical state of trace metals in natural waters is important for understanding their reactivity, transport and toxicity [1]. Their physicochemical forms in natural waters may include particulate (> 1 μm) and dissolved (≤ 1 nm) form, such as inorganic species and organic complexes and metal ions adsorbed onto a variety of colloidal particles (1 nm – 1 μm) [4,5]. Measurements of total metal concentrations alone do not yield sufficient information on the ecotoxicological impact and fate of trace metals [5]. However, the characterization of chemical speciation of metals is laborious and time consuming. In addition, its knowledge is only relevant when the aquatic systems under study are polluted. Therefore, first *in-situ* or at least *on-site*, screening of the total concentrations of several metals is needed in order to evaluate if waters are

polluted or not; after this first evaluation, a subsequent exhaustive metal chemical speciation study can be required (or not) depending of the extent of the metal pollution found. This preliminary study enables a fast detection of metal pollutants present in the aquatic systems.

Due to their toxicity, even at low concentrations, the most hazardous and important elements are Pb, Cd, As, Hg, aluminum (Al) and chromium (Cr). On the other hand, Cu, Zn, Ni, Co, selenium (Se) and Bi are important because they may be essential or toxic depending on the amount of their concentrations and the nature of organisms considered [5]. In fact, when present above threshold concentrations, all elements can be toxic.

Environmental regulations from European Union (EU) commission [6] and Environmental Protection Agency (EPA) from United States of America (USA) [7] about heavy metals/metalloid pollution provide guidelines and threshold limits for these elements in surface waters. Directive 2008/105/EC of 16 December 2008 [6] about environmental quality standards in the field of water policy of the European Parliament and Council identified Cd, Pb, Hg and Ni as priority hazardous substances (Table 1.1). The contamination of surface waters (fresh and saline) by As, Cd, Cr^{6+},Cu, Pb, Hg, Ni, Se, silver (Ag) and Zn is classified as priority toxic metal pollutants by EPA [7] (Table 1.2).

Table 1.1 – EU Environmental Quality Standards (EQS) recommended, in μgL^{-1}, for priority toxic metal pollutants [6].

Element	Inland surface waters[a]	Other surfase waters
	MAC[b]/(AA[c]) – EQS	**MAC[b]/(AA[c]) – EQS**
Cd and its compounds	0.9[d]/(0.15)	0.9[d]/(0.2)
Hg and its compounds	0.07/(0.05)	0.07/(0.05)
Pb and its compounds	Not applicable/(7.2)	Not applicable/(7.2)
Ni and its compounds	Not applicable/(20)	Not applicable/(20)

[a] Inland surface waters encompass rivers and lakes and related artificial or heavily modified water bodies; [b]MAC: Maximum Allowable Concentration (MAC-EQS).; [c]AA: Annual Average value for total concentration. When the MAC-EQS are marked as "not applicable", the AA-EQS values are considered protective against short-term pollution peaks in continuous discharges since they are significantly lower than the values derived on the basis of acute toxicity and [e] For cadmium and its compounds the EQS values vary depending on the hardness of the water and in this case it assumes 100 to < 200 mg $CaCO_3$ /L hardness.

Table 1.2 – EPA-USA Recommended Water Quality Criteria (RWQCs), in μgL^{-1}, for priority toxic metal(loid)s pollutants [7].

Element	Fresh water		Saltwater	
	CMC[a]	**CCC[b]**	**CMC[a]**	**CCC[b]**
As	340	150	69.0	36.0
Cd	2.00	0.247	40.0	8.80
Cr^{6+}	16.0	11.0	1100	50.0
Cu	13.0	9.00	4.80	3.10
Pb	65.0	2.51	210	8.10
Hg	1.40	0.762	1.80	0.943
Ni	470	52.0	74.0	8.20
Se	---	5.00	290	71.0
Ag	3.20	---	1.90	---
Zn	120	120	90.0	81.0

Values represent total dissolved concentrations below which no significant detriment to aquatic life is predicted; Assumes 100 mg $CaCO_3$ /L hardness for freshwater.; [a]CMC: Criteria Maximum Concentration, acute exposure acceptable limit and [b]CCC: Criteria Continuous Concentration- maximum acceptable chronic exposure concentrations.

Current analytical techniques used for heavy metals detection include spectroscopic methods such as Atomic Absorption Spectroscopy (AAS), Inductively Coupled Plasma Mass Atomic Emission Spectrometry (ICP-AES), Inductively Coupled Plasma Mass Spectrometry (ICP-MS), fluorescence spectrometry, UV-vis spectroscopy and neutron activation analysis [3-5,8,9] Although these methods allow determining heavy metals in effective way they are time consuming, require sophisticated instrumentation and highly qualified technicians [3,8]. Further, these methods are expensive to run and maintain and are not suitable for *on-field* monitoring [3,8]. Therefore, from the environmental and economic point of view, it is important to develop simple, fast, accurate, sensitive, low cost and portable sensing devices for monitoring trace or ultra-trace metals/metalloids in surface water samples. Indeed single element detection is a particular case that we may not encounter in real water sample analysis. Hence, the multi-element capability, which enables to detect several metals/metalloids at the same time, is particularly important.

In this context, an electroanalytical methods supported by voltammetric stripping techniques [Anodic Stripping Voltammetry (ASV) and Adsorptive Cathodic Striping Voltammetry (AdCSV)] has been widely recognized as powerful methods [1,3-5]. These techniques are very sensitive, suitable for automatic *on-line* monitoring and for *on-field* and/or *in-situ* analysis and offers multi-element and speciation capabilities [1].

Mercury based electrodes have long been widely used for trace analysis of heavy metals [1]. However, the difficulties associated with handling, storage and disposal and essentially because the toxicity of Hg, becomes the application of these electrodes (especially *in-situ* or *on-field*) undesirable. In fact, environmental regulations and health considerations restrict its continuous application due to the high toxicity of mercury [10].

One of the most important advances in stripping analysis, towards the development of "greener" procedures for heavy metals/metalloids monitoring, has been the advent of mercury-free non-toxic electrodes. Simultaneous elements detection is another important step towards the implementation of a "greener"

analytical strategy because it is possible to perform the detection of several ion metals/metalloids using a single solution and a single instrument at the same time, saving energy and reagents and producing fewer amounts of residues.

Stripping voltammetry is a valuable technique for multi-element monitoring, at trace levels, in surface waters, once a single potential scan can display simultaneously several metals/metalloids and provide qualitative and quantitative relevant information. The major types of interferences, which can affect the accuracy and precision of stripping analysis in general and multi-element stripping measurements in particular are: (i) the formation of intermetallic compounds between the metals deposited or between the electrode material and a deposited metal; (ii) overlapping of the peaks caused by the similarity in the oxidation potentials of the metals and (iii) the presence of organic compounds that adsorb on the electrode surface. Further, contamination of samples and losses of analyte are other problems inherent to any kind of trace analysis [1]. To avoid contamination problems, if the analysis cannot be performed *in-situ*, all precautions related with sample handling and storage and proper attention to material and reagents purity must be taken. The interferences of intermetallic compounds can be minimized by the addition of a "third" element, that forms a more stable intermetallic compound with one of the components of the binary system or by the reducing the amounts of metals deposited by the adjustment of the time or deposition potential [1]. Problems related with the overlapping of the peaks can be reduced by the introduction of a separation step prior to the stripping measurement or by the judicious choice of the experimental conditions such as the suitable choice of the supporting electrolyte, exchange solution, electrode and deposition and stripping conditions, respectively [1]. Beyond all these chemical or instrumental solutions there are mathematical and computational approaches, based on chemometrics tools, especially suitable for multi-element determination. In order to overcome the organic interferences, destruction of organic matter by Ultraviolet (UV) irradiation may be considered prior to the stripping analysis. For samples with low organic content, a standard addition method can be one option. Finally, electrode coverage by different protective films may be considered [1].

Chemometric is a chemical discipline that uses mathematics, statistics and formal logic to (i) design or select optimal experimental conditions, (ii) provide maximum relevant chemical information by analyzing chemical data and (iii) obtain knowledge about chemical systems [11,12]. Chemometrics tools are important to explore the extraordinary potential of voltammetric techniques for the simultaneous trace elements determination once these tools are useful for resolution of overlapping signals, calibration, prediction and model identification.

Contamination of natural waters (rivers, lakes and oceans) by heavy metals/metalloids is a serious problem. The benefits of rapid real-time data are invaluable and thus the development of "green" stripping analytical methods for rapid *in-situ* or at least *on-field* measurements of mixtures of heavy metals/metalloids is of increasing importance.

1.2. Electroanalytical Methods: Voltammetry *vs.* Polarography

Electroanalytical methods are among the most powerful and popular tools used in analytical chemistry [13]. They are a class of techniques, which study an analyte by measuring the potential (E), time (t) and/or current (I) in an electrochemical cell containing the analyte.

The most widespread electroanalytical methods are voltammetry and polarography [13]. In voltammetry static or solid electrodes (e.g. solid electrodes made of carbon or noble metals) are used as working electrodes (WEs). Polarography is a subclass of voltammetry that uses a liquid WE whose surface can be renewed periodically (e.g. by drops). Polarography is applied mainly to the analysis of reducible species [1].

Voltammetric techniques are based on the recording of the current, I, which flows between the working (polarized) electrode and the counter electrode (CE), due to the reduction or oxidation of the analyte(s), as function of the potential, E, imposed on the WE and expressed with respect to that of a reference

electrode (RE). The current is proportional to the analyte(s) concentration in the sample [5].

1.2.1. Voltammetric stripping techniques

One of the most important electroanalytical voltammetric techniques used for monitoring and detection of trace or ultra-trace metals/metalloids in natural and waste waters is stripping voltammetry. This technique is based in two different steps, namely initial deposition/accumulation of the analyte(s), under a controlled potential on the surface of a suitable WE (pre-concentration step) followed by the voltammetric detection (measurement step). The pre-concentration step is based either on the electrolysis [ASV and Cathodic Stripping Voltammetry (CSV)] or on the physical adsorption [Adsorptive Stripping Voltammetry (AdSV)] of the analyte(s) at the electrode surface. The measurement step involves the oxidation or reduction of the deposited analyte(s) which return to the solution (stripping). The voltammetric response [current-potential (I = f (E)) plot], recorded during this step, is proportional to the analyte(s) concentration in or on the electrode and thus in the sample solution [13,14].

Usually the stripping step consists of scanning the potential linearly [Linear Sweep Voltammetry (LSV)] or in another potential wave form as a function of time, and the current response is recorded. The most popular modulation forms used for trace analysis are differential pulse (DP) and square wave (SW) pulse voltammetry, respectively. In LSV the applied potential takes the form of a linear ramp and the current is measured at regular intervals of time. In pulse voltammetry the applied potential consists of a linear ramp with superimposed voltage pulses (DP) or a staircase signal with superimposed square wave pulses (SW). In DP mode the difference in the current measured just before and at the end of each pulse is recorded and in SW mode the current is measured during the forward pulse and the reverse pulse and the difference is recorded [15].

The voltammetric stripping methodologies presents the following features [1,5,9,14,16]:

(i) High sensitivity;
(ii) Low detection limit;
(iii) Multi-element and speciation capabilities;
(iv) Wide spectrum of analytes with both organic and inorganic origin (electroactive chemical species) can be measured;
(v) Insignificant effect of the matrix (in certain instances);
(vi) Compatibility with other methods (hybridization of methods);
(vii) Relative simplicity, automated, miniaturized, portable and low cost of equipment;
(viii) Low energy requirements;
(ix) Automatic *on-line* and portable options

All of these features explain the suitability of stripping voltammetry for the environmental monitoring of trace metals.

The following sections briefly describe ASV and AdCSV which were the stripping voltammetric techniques used in this thesis.

1.2.1.1. Anodic stripping voltammetry

ASV is the one of the most sensitive electroanalytical techniques available [1,13] and has been the most widely used for stripping metal ions determination [5,13].

This technique is based on the pre-concentration through the application of a cathodic deposition at a controlled potential and time (electrolytic reduction of organic compound or metal ion on the electrode surface) followed by the subsequent anodic scanning (re-oxidation). Usually, the deposition potential is 0.3 – 0.5 V more negative than the reversible potential calculated from the Nernst equation for the least easily reduced metal ion to be determined [1,13]. The target analyte(s) reach the electrode surface by diffusion or convection where it/they is/are reduced and concentrated. The convection transport is achieved by solution

stirring or electrode rotation. The convection force is usually used to facilitate the deposition step. After the pre-concentration step, the convection is stopped and a rest period is employed before the measurement step. Linear Sweep (LS), DP and SW voltammetry or alternating current techniques can be used for the measurement step [1,13]. The resultant voltammogram provides two different types of analytical information: (i) quantitative information: the height/area or derivative of peak(s) are proportional to the metal(s) concentration in the sample solution and (ii) qualitative information: the potential (position) of the peak(s) serves to identify the analyte(s) in the sample [1,13].

1.2.1.2. Adsorptive cathodic stripping voltammetry

CSV is another stripping voltammetric technique similar to ASV. As a short description, it is the mirror image of ASV [13]. This technique is used to determine a wide range of organic and inorganic compounds that form insoluble salts with the electrode material [1]. In CSV, the pre-concentration step consists of the application of an oxidizing deposition at a controlled potential and time (electrolytic oxidation of organic compound or metal ion on the electrode surface) followed by the subsequent cathodic scanning (reduction). The stripping scan can be obtained using LS, DP and SW voltammetry or alternating current techniques [13].

AdSV is based on the adsorptive accumulation (physical adsorption) of the analytes (organic and inorganic compounds) on the electrode surface followed by the voltammetric scan, i.e., chemical reduction (the usual method) or oxidation of the adsorbed species [13]. The adsorptive approach offers improvements in selectivity and sensitivity when compared to ASV and CSV [13].

The applications of AdSV for the determination of trace metals together with a subsequent cathodic scan results in an AdCSV. AdCSV makes use of a specific ligand which is added to the sample solution and forms a complex with the metal (metal-complex). This surface active metal-complex is adsorbed on the

WE by means of a non-electrolytic process prior to the voltammetric scan. After an equilibration time (t_{eq}), the potential is scanned in the cathodic direction. The voltammetric response of such analyte provides the relationship between the surface and the bulk concentration of the analyte.

1.3. Multivariate calibration and prediction

Calibration is the process of construction a mathematical model that relates the output of an instrument with the properties of samples. Prediction is the process of using the model to predict properties of samples according to the instrument output [17]. To construct the model, instrument responses from samples with known concentration levels are measured and a mathematical relationship is established between the instrument response and the concentration of chemical component(s). Latter on, this model can be used to predict the concentration of a chemical component in new samples using the measured instrument response(s).

Calibration can be univariate or multivariate, respectively. In univariate calibration only the analyte of interest must contribute to the measured signal (selective response), i.e., only one instrument response is used per sample. Unlike, multivariate calibration is the process of relating multiple responses from an instrument to a property or properties of a sample [17].

When compared with univariate approaches, multivariate calibration allow to use non-selective signals and offers the following advantages [17]: (i) it is possible to analyze multiple components simultaneously which reduce the analysis time and (ii) allow to make multiple redundant measurements which can improve precision in prediction, fault and/or interference(s) detection.

Multivariate calibration models can be linear or non-linear. However, it is important to note that these linear methods tolerate some degree of non-linear behavior in the data.

Finally, multivariate calibration methods can be divided in two main groups designated by Classical Least Squares (CLS) and Inverse Least Squares (ILS), respectively. The difference between CLS and ILS methods lies in how they are formulated, i.e., CLS model is constructed from the instrumental responses whereas ILS model is built up from the concentrations of the components in the samples. CLS is applicable to simple systems, when all the analytes are known and pure response of each analyte can be obtained. On the other hand, ILS is employed to complex systems where it is not necessary to obtain the response of pure analytes

In this thesis it was used linear multivariate calibration models for voltammetric data analysis based on CLS and Partial Least Squares (PLS) regression methods. Additionally, for quantitative purposes, it was also used the Multivariate Curve Resolution Alternating Least Squares (MCR-ALS) together with the application of a correlation constraint. The following sections briefly describe CLS, PLS and MCR-ALS methods.

1.3.1. Classical least squares regression method

As described in section above, CLS regression method is based on a linear relationship between experimental measurements (voltammograms) and a parameter to be predicted (concentrations) and is only applicable when the concentration of all analytes in calibration samples and pure signals are known. Pure signals can be obtained using either directly (DCLS) or indirectly (ICLS) methods [17]. The difference between DCLS and ICLS is based on the way how the pure signals are obtained. For DCLS, the pure signals are directly measured at unit concentration for each analyte in the mixture while for ICLS the pure signals are estimated from mixture signals of calibration samples where the concentration of all analytes are known. Once the pure signals of analytes are obtained, then they are used to form the pure signals matrix ($\mathbf{S^T}$) and the calibration model is obtained from the pseudo-inverse of this $\mathbf{S^T}$ matrix. This calibration model is subsequently used to predict the concentrations of analytes in unknown samples.

1.3.2. Partial least squares regression method

PLS is a well-known ILS multivariate linear regression method based on a factor analysis, which has been frequently applied to electroanalytical data [12]. The goal of PLS is to build up a prediction model for the analyte(s) concentration(s). This method involves the factor decomposition of the experimental data, such as voltammetric data (**D** matrix), into a reduced set of latent variables (LVs) (components or factors). These LVs are linear combinations of original variables (**D** matrix) that correlate optimally with the variables to be predicted (c vector) [18]. To establish a calibration model, the PLS regression algorithm selects a few number of orthogonal factors, which maximizes the covariance between measured voltammograms (**D** matrix) and the analyte concentrations (c vector) of a set of calibration samples.

Mathematically speaking, PLS regression decomposes **D** and c into factor scores (**T**) and factor loadings (**P** and q) according to:

$$\mathbf{D} = \mathbf{T}\mathbf{P}^{\mathbf{T}} + \mathbf{E} \qquad \text{(Eq. 1.1)}$$

$$c = \mathbf{T}q + f \qquad \text{(Eq. 1.2)}$$

where **T** is the scores matrix, $\mathbf{P}^{\mathbf{T}}$ and q are the matrix and vector loadings describing the variance in **D** and c, respectively, and **E** and f are the residuals in **D** and c, respectively. This decomposition is performed simultaneously and in such way the first few factors should explain most of the covariance between **D** and c., respectively The remaining noise factors can thus be ignored, hence the addition of residuals E and f [19].

Finally, the obtained multivariate regression model is subsequently used to predict analyte(s) concentration values on new samples.

1.3.3. Multivariate curve resolution alternating least squares method

MCR-ALS, a technique developed by Tauler *et al*. [20,21], has become a popular chemometric method used for the resolution of multiple component responses in unknown unresolved mixtures [22]. Initially, this technique was used for the spectroscopic studies and latter was adapted for voltammetric studies.

In mathematical terms, MCR-ALS methods are based on a bilinear model analogous to the generalized Lambert-Beer's law [19,22-26], where the individual responses of each analyte are additive. In a matrix form, this bilinear model is expressed in the following way:

$$\mathbf{D} = \mathbf{C}\mathbf{V}^{\mathbf{T}} + \mathbf{E} \qquad \text{(Eq. 1.3)}$$

In voltammetric measurements, **D** matrix is the current experimental data matrix; **C** is the matrix of concentration profiles; $\mathbf{V}^{\mathbf{T}}$ is the matrix of pure voltammograms and **E** is the matrix associated to the experimental error. The superscript T means the transpose of matrix S.

Figure 1.1 summarizes, in a schematic flow-chart, the steps for MCR-ALS voltammetric data resolution. MCR-ALS solves iteratively Eq. 1.3 by an Alternating Least Squares (ALS) algorithm which calculates concentration (**C**) and pure voltammograms ($\mathbf{V}^{\mathbf{T}}$) matrices that fits optimally the experimental data matrix **D**. This optimization is carried out for a proposed number of components and using initial estimates of either **C** or $\mathbf{V}^{\mathbf{T}}$. The number of components can be determined by Principal Component Analysis (PCA) or using a Singular Value Decomposition (SVD) method. These methods perform a unique orthogonal decomposition of matrix **D**. Initial estimations can be obtained using Evolving Factor Analysis (EFA) or the determination of purest variables (Pure) [22,23]. These initial estimations are subsequently optimized by an iterative ALS process. During this iterative optimization process, several constraints can be imposed to model the shapes of the **C** and $\mathbf{V}^{\mathbf{T}}$ profiles in order obtain a limited number of

solutions with physical meaning and to minimize as much as possible rotational and intensity ambiguities [25]. ALS iteration process, according to the constraints postulated and the established convergence criteria, continues until an optimal solution is obtained.

In this work, the constraints used were: (i) non-negativity for concentrations and signals (concentration and voltammetric profiles are always positive or zero); (ii) selectivity (in a particular voltammogram if one or more components are not present, their concentrations is zero or if do not contribute to the response, their current intensity at a specific potentials is zero) and (iii) correlation [23].

This latter constraint has been introduced in 2002, by Tauler *et. al* [23], for the simultaneous quantitative determination of mixtures of metal ions using stripping voltammetric analysis. This correlation constraint consists of a series of steps, performed during each iteration step of the ALS optimization: (i) the concentrations of a particular analyte in calibration samples at each ALS iteration are forced to be correlated to previously known reference concentration values of the analyte in these samples; (ii) a local linear model between the ALS estimated values and the nominal concentrations is built by least squares linear regression; and finally (iii) concentration values are then updated according to the predicted values using the estimated parameters of the local model. In conclusion, the application of a correlation constraint during the MCR-ALS analysis implies the establishment of calibration models subsequently used for quantitative determination of analytes, in the presence of interferences, on new samples.

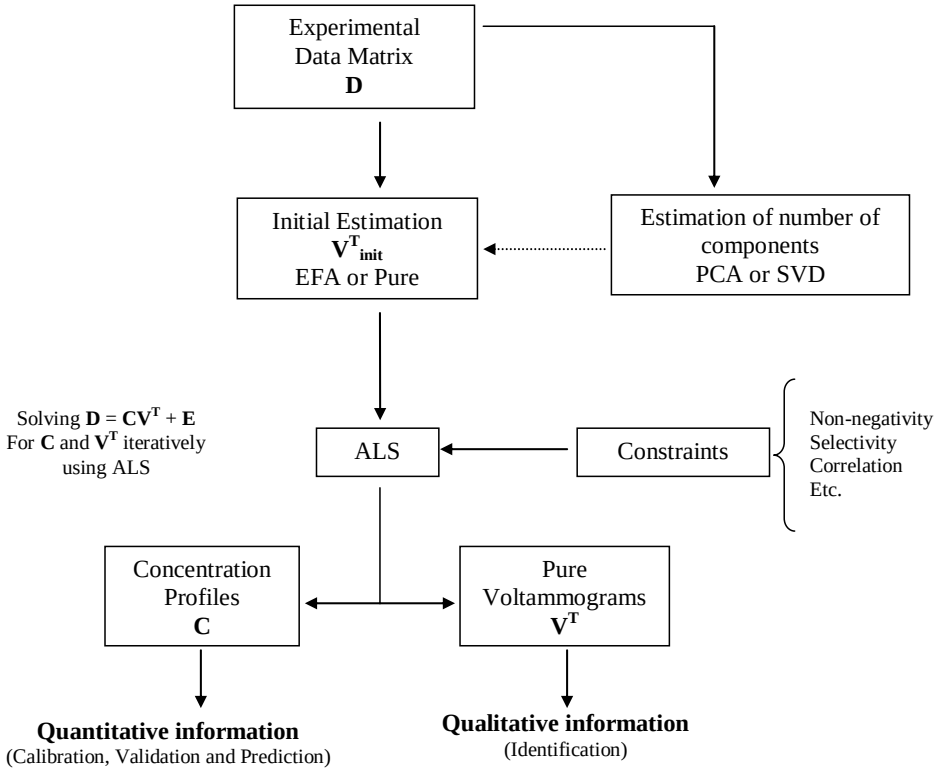

Figure 1.1 – Flowchart of the MCR-ALS procedure applied to voltammetric data (adapted from [19]).

1.4. Non-toxic mercury-free electrodes for multi-metal(loid)s voltammetric stripping analysis

Since the discovery of polarography by Heyrovsky in 1920 [1], mercury electrodes [DME (Dropping Mercury Electrode), HMDE (Hanging Mercury Drop Electrode), SMDE (Static Mercury Drop Electrode) and Mercury Film Electrode (MFE)] played a main role in the success of trace metals stripping analysis. This fact is due to the analytical advantageous of mercury in the negative potential range (high overvoltage towards the hydrogen evolution reaction) and because many metals of interest have fast electrode kinetics at mercury and form amalgams [27-29]. The additional advantage for dropping mercury electrodes is

the possibility to restore a new and clean electrode surface periodically [1]. However, due to the difficulties associated with handling, storage and disposal and essentially because the well known high toxicity of mercury salts these electrodes have been replaced by alternative more "environmentally friendly" electrode materials [28,30]. Therefore, at the same time has been developed and improved voltammetric stripping techniques, has continuously appeared new mercury-free electrodes used for simultaneous determination of trace metal(loid)s (please see Tables 1.3 up to 1.6): carbon (glassy carbon (GC); carbon fiber; carbon paste; graphite and thin-film boron doped diamond), bismuth, gold, iridium and other chemically modified electrodes (CMEs). The proper choice of the WE is very important for the sensitivity and reproducibility of stripping analysis [1,13,31,32]. In fact, the electrode material, as well as its geometry and surface properties, determines the course of the electrode reaction. For "green" and sustainable trace metals monitoring strategy, the ideal working electrode, should presents the following features [33]:

(i) Non-toxic;
(ii) Inexpensive;
(iii) Easy to handle;
(iv) Large useful potential window for cathodic and anodic reactions (high overvoltage towards hydrogen and oxygen evolution);
(v) Low residual (background) current;
(vi) Low ohmic resistence;
(vii) Reproducible surface;
(viii) Long-term stability;
(ix) Good analytical performance (high accuracy, sensitivity and stability during the time, low DLs and good reproducibility);

Two approaches have been generalized to replace mercury electrodes towards the simultaneous determination of heavy metals. The first one involves the use of other solid non-toxic unmodified electrodes (Table 1.4). The second

approach involves the use of CMEs (Table 1.3 and Table 1.5). The more frequently used CMEs are bismuth electrodes with their different configurations (Table 1.3). Unmodified solid electrodes based on carbon and metals such as gold and iridium (Table 1.4) were also used but more sporadically. According to their dimensions these electrodes are classified in macro (Tables 1.3 up to 1.5, respectively) or micro (Table 1.6) electrodes, respectively. The major works developed on field of voltammetric stripping analysis for simultaneous heavy metal(loid)s detection, performed between 2003 and April 2013 with macro (bismuth, solid, chemically modified) or microelectrodes are present and discussing in following sections.

1.4.1. Bismuth electrodes

Bismuth is an "environmentally-friendly" element, with very low toxicity, and a widespread pharmaceutical use [31,34,35]. Thirteen years ago, in 2000, a bismuth film electrode (BiFE) was introduced by Wang and co-workers as a favorable replacement for mercury electrodes [36] and by now, bismuth electrodes (bismuth thin films deposited simultaneously with the target metals (*in-situ* deposition) or pre-plated (*ex-situ* deposition) on a suitable substrate, bismuth bulk electrode, bismuth powder and bismuth oxide modified carbon paste electrodes) are widely accepted and has been used in numerous electrochemical laboratories worldwide (Table 1.3). The attractive stripping behavior of bismuth electrodes reflects the ability of bismuth to form "fused" multicomponent alloys with several heavy metals [31].

Regarding to different configurations, the most explored bismuth electrodes using for multi-metals analysis are bismuth thin films electroplated onto the carbon surface by reduction of Bi^{3+} ions (BiFEs) (Table 1.3). Different forms of carbon, with different sizes and geometries, such as a GC, carbon paste, wax-impregnated graphite, pencil-lead, boron-doped diamond and screen-printed carbon ink have been used as substrates for bismuth film deposition. However, the majority of studies employing a GC disk (Table 1.3). The use of metal supports

for bismuth films such as copper, gold and platinum is comparatively rather scarce because their lower chemical inertness and lower resistance to corrosion than carbon, as well as, their tendency to form intermetallic compounds with other metals [37]. On the other hand, iridium is a very convenient substrate material once its extreme chemical inertness, resistance to corrosion and to attack by common acids at room temperature and the fact that it does not form intermetallic compounds with bismuth or heavy metals [37]. Unlike to BiFEs, little work has been done using "non-film" configurations, such as bismuth bulk [38], bismuth powder and bismuth oxide modified carbon paste electrodes [39-41]. Bismuth oxide modified carbon paste electrode results from the incorporation of a bismuth precursor or powder into the bulk of the electrode, such as the incorporation of Bi_2O_3 and its subsequent reduction to metallic bismuth. Recently, bismuth precursors have been synthesized such as bismuth nanopowders and directly cast onto screen printed carbon substrates with Nafion [40]. Nafion is widely used as coating polymer and prevents the adsorption of organic surface active compounds on the electrode surface and improves sensitivity and mechanical stability [40]. Bismuth bulk electrode essentially consists of a polycrystalline pure metallic bismuth rod. This electrode is very attractive because is easily fabricated, cost-efficient, stable, reproducible and robust [38] and no bismuth plating step is necessary (its surface is easily regenerated by mechanical polishing) [42]. Finally, lithographic sputtering technique was also used to prepare bismuth electrodes [30].

As possible to see from Table 1.3, over the last ten years, combined with AdCSV but mainly with ASV, bismuth electrodes have been successfully used for simultaneous determinations of two (Ni and Co in AdCSV or Cd and Pb in ASV), three (Cd, Pb and Zn), more scarcely four (Cd, Cu, Pb and Zn) and five (Cd,Cu, Hg, Pb and Zn) metals (Table 1.3). These electrodes were also used for detection organic compounds [43]. Among the different multi-metals combinations, Table 1.3 shows that the development of highly sensitive method for determining trace amounts of Cd and Pb has received considerable attention. Another relevant aspect concerns the coupling of BiFEs with fully computer-controlled systems

such as flow injection analysis (FIA) [44], batch injection analysis (BIA) [45] and with sequential injection analysis (SIA) [28,44,46-48], respectivey.

In fact, BiFEs have several attractive properties that include their simple preparation, high sensitivity, well defined and undistorted stripping signal and in generally present good neighbouring peak resolution [31,35,39]. In addition, BiFEs are less susceptible to oxygen background interferences than mercury electrodes [31,39]. In most aspects, BiFEs exhibit comparable performance to MFEs with the notable exception of a narrower anodic potential range [37].

In conclusion, bismuth electrodes are one of the most viable alternative to mercury electrodes, for the simultaneously trace metals monitoring.

Table 1.3 – Simultaneous determination of heavy metals, at trace levels, on bismuth electrodes.

Electrode (diameter (d) or area (A))	**Modifier**	**Metals**	**Voltammetric stripping technique**	**Supporting electrolyte solution**	**E_{dep} (E_{acc}) / t_{dep} (t_{acc})**	**Analytical performance /µgL^{-1}**	**Samples analysed**	**Reference**
GC (d = 3 mm)	Nafion 2-mercaptoethanesulfonate –tethered polyaniline Bismuth film (*in-situ* deposition)	Cd and Pb	SWASV	0.1 molL^{-1} acetate buffer (pH 4.0)	-1.2 V (vs. SCE) for 300 s under stirring	*LCR:* Cd: 0.1 – 20 Pb: 0.1 – 30 *DL:* Cd: 0.04 Pb: 0.05	Tap water Spring water River water	[49]
Iridium microwire (d = 0.125 mm)	Bismuth film (*in-situ* deposition)	Cd, Pb (and potentially Zn)	SWASV	0.1 molL^{-1} acetate buffer (pH 4.5)	-1.2 V (vs. Ag/AgCl) for 300 s under stirring	*LCR:* --- DL: Cd: 1.5 Pb: 1	Waste water Tap water	[37]
GC (d = 3 mm)	Bismuth film (*in-situ* deposition)	Cd, Pb (and potentially Zn)	SWASV combined with SIA	0.5 molL^{-1} HCl	-1.4 V (vs. Ag/AgCl) for 100s	*LCR:* Cd: 3 – 140 Pb: 4 – 140 Zn: 10 – 40 *DL:* Cd: 1.0 Pb: 1.2 Zn: 3.0	Determination of Cd and Pb: Tap water	[46]

Table 1.3 – continuation…

Electrode (diameter (d) or area (A))	**Modifier**	**Metals**	**Voltammetric stripping technique**	**Supporting electrolyte solution**	**E_{dep} (E_{acc}) / t_{dep} (t_{acc})**	**Analytical performance /µgL^{-1}**	**Samples analysed**	**Reference**
Disposable electrode (wax impregnated graphite electrode)	Medical stone Nafion Bismuth film (*in-situ* deposition)	Cd and Pb	SWASV	0.1 molL^{-1} acetate buffer (pH 4.5)	-1.2 V (vs. SCE) for 300s under stirring	*LCR:* Cd: 2.0 – 12.0 Pb: 2.0 – 12.0 *DL:* Cd: 0.47 Pb: 0.07	Waste water	[50]
GC (d = 3 mm)	Nafion Poly (2,5 dimercapto-1,3,4-thiadiazole) Carbon nanotubes Bismuth film (*in-situ* deposition)	Cd and Pb	DPASV	0.1 molL^{-1} acetate buffer (pH 5.0)	-1.0 V (vs. SCE) for 360 s under stirring	*LCR:* Cd: 0.05 – 20 Pb: 0. 1 – 22 *DL:* Cd: 0.03 Pb: 0.05	Tap water Spring water River water	[51]

Table 1.3 – continuation…

Electrode (diameter (d) or area (A))	**Modifier**	**Metals**	**Voltammetric stripping technique**	**Supporting electrolyte solution**	**E_{dep} (E_{acc}) / t_{dep} (t_{acc})**	**Analytical performance /µgL^{-1}**	**Samples analysed**	**Reference**
GC (d = 3 mm)	Bismuth film (*in-situ* deposition)	Cd, Cu, Pb and Zn	SWASV	0.1 molL^{-1} acetate buffer (pH 4.5)	-1.4 V (vs. Ag/AgCl) for 180 s under stirring	*LCR:* Cd: 5 – 50 Cu: 10 – 80 Pb: 10 – 100 Zn: 20 – 280 *DL:* Cd: 0.10 Cu: 0.20 Pb: 0.40 Zn: 2.80	Tap water Certified reference water	[32]
Graphite-polyurethane composite (A = 0.126 cm^2)	Bismuth film (*in-situ* deposition)	Cd, Cu, Hg, Pb and Zn	SWASV	0.1 molL^{-1} acetate buffer (pH 4.5)	-1.4 V (vs. SCE) for 120 s under stirring	*LCR:* Cd: up to ~7 Cu: up to ~10 Hg: up to ~20 Pb: up to ~9 Zn: up to ~1 *DL:* Cd: 0.2 Cu: 0.2 Hg: 0.5 Pb: 0.2 Zn: 0.04	Tap Water	[52]

Table 1.3 – continuation…

Electrode (diameter (d) or area (A))	**Modifier**	**Metals**	**Voltammetric stripping technique**	**Supporting electrolyte solution**	**E_{dep} (E_{acc}) / t_{dep} (t_{acc})**	**Analytical performance /µgL^{-1}**	**Samples analysed**	**Reference**
Carbon screen-printed	Carbon nanotubes Bismuth film (*in-situ* (*on-line*) deposition)	Cd, Pb and Zn	SWASV Combined with SIA	1 molL^{-1} HCl	-1.4 V (vs. Ag/AgCl) for 180s	*LCR:* Cd: 2 – 100 Pb: 2 – 100 Zn: 12 – 100 *DL:* Cd: 0.8 Pb: 0.2 Zn: 11	Herb	[28]
Carbon screen-printed (A = 4 × 2 mm^2)	Bismuth film (*ex-situ* deposition)	Cd and Pb and Cd, Pb and Zn	DPASV	0.01 molL^{-1} KNO_3	Cd and Pb: -1.05V (vs. Ag/AgCl) for 60 s under stirring Cd, Pb and zn: -1.5 V (vs. Ag/AgCl) for 60 s under stirring $t_{deoxigenation}$: 15 min	*LCR* (Cd and Pb): Cd: 1.12 – 899 Pb: 2.07 – 932 *LCR* (Cd, Pb and Zn): Cd: 1.12 – 787 Pb: 2.07 – 622 Zn: 6.53 – 458	---	[53]

Table 1.3 – continuation…

Electrode (diameter (d) or area (A))	**Modifier**	**Metals**	**Voltammetric stripping technique**	**Supporting electrolyte solution**	**E_{dep} (E_{acc}) / t_{dep} (t_{acc})**	**Analytical performance /µgL^{-1}**	**Samples analysed**	**Reference**
GC (d = 3 mm) or Carbon fibres (d = 7 µm) (*)	Bismuth film (GC: *in-situ* or *ex-situ* deposition and Carbon fiber: *ex-situ* deposition, respectively)	Cd, Cu, Pb and Zn	SWASV	0.1 molL^{-1} acetate buffer (pH 4.5)	- 1.4 V (vs. Ag/AgCl) for 180 s under stirring	*LCR* *GC electrode:* Cd: 5 – 50 Cu: 10 – 80 Pb:10 – 100 Zn: 20 -280 *Carbon fiber electrode:* Cd: 2 – 120 Cu: 10 – 100 Pb:10 – 100 Zn: 20 -160 *DL:* *GC electrode:* Cd: 0.10 Cu: 0.2 Pb: 0.4 Zn: 2.80 *Carbon fiber electrode:* Cd: 0.30 Cu: 0.6 Pb: 0.5 Zn: 4.10	Certified reference materials: Bovine liver and mussel tissue.	[55]

Table 1.3 – continuation…

Electrode (diameter (d) or area (A))	**Modifier**	**Metals**	**Voltammetric stripping technique**	**Supporting electrolyte solution**	**E_{dep} (E_{acc}) / t_{dep} (t_{acc})**	**Analytical performance /µgL^{-1}**	**Samples analysed**	**Reference**
GC (d = 3 mm)	Graphite nanofibers Nafion Bismuth film (*in-situ* deposition)	Cd and Pb	DPASV	0.1 molL^{-1} acetate buffer (pH 4.5)	-1.2 V (vs. Ag/AgCl) for 120 s under stirring	*LCR* Cd and Pb: 0.2 – 50 *DL:* Cd: 0.26 Pb: 0.19	River water Human blood	[54]
Bismuth bulk (d = 1.5 mm)	---	Cd, Pb and Zn	SWASV	0.1 molL^{-1} acetate buffer (pH 5.0)	- 1.4 V (vs. Ag/AgCl) for 180 s under stirring	*LCR:* Pb, Cd and Zn: 10 – 100 *DL:* Cd: 0.054 Pb: 0.093 Zn: 0.396	River water	[38]
Carbon paste (d = 3 mm)	Montmorillonite Bismuth film (*in-situ* deposition)	Cd and Pb	SWASV	0.1 molL^{-1} acetate buffer (pH 4.5)	- 1.2 V (vs. SCE) for 120 s under sitirring	*LCR:* Cd and Pb: 1 – 24 *DL:* Cd: 0.35 Pb: 0.2	River water	[56]

Table 1.3 – continuation…

Electrode (diameter (d) or area (A))	**Modifier**	**Metals**	**Voltammetric stripping technique**	**Supporting electrolyte solution**	**E_{dep} (E_{acc}) / t_{dep} (t_{acc})**	**Analytical performance /µgL^{-1}**	**Samples analysed**	**Reference**
Screen-printed carbon paste (A = 10 mm^2)	Nafion Bi nanopowders with different particle size distribution: Nano A (d = 45.5 nm) Nano B (d = 90. 2 nm) Nano C (d = 2.17 nm)	Cd, Pb and Zn	SWASV	0.1 molL^{-1} acetate buffer and 0.025 molL^{-1} HCl solution (pH 5.0)	- 1.35 V (vs. SCE) for 180 s under stirring	*LCR Nano A:* Cd, Pb and Zn: 1 – 50 *DL NanoA (for 600 s):* Cd: 0.09 Pb: 0.17 Zn: 0.60	---	[40]
CG	Polyaniline Bismuth film (*in-situ* deposition)	Cd and Pb	SWASV	0.02 molL^{-1} H_2SO_4 and 0.03 molL^{-1} KCl	- 1.3 V (vs.Ag/AgCl) for 160 s under stirring Under nitrogen atmosphere	*LCR:* Cd: 2.8 – 16.9 Pb: 5.2 – 31.1 *DL:* Cd: 0.1 Pb: 3.4	---	[57]
GC (d = 3 mm)	Graphene nanosheets Nafion Bismuth film (*in-situ* deposition)	Cd and Pb	DPASV	0.1 molL^{-1} acetate buffer (pH 4.5)	-1.2 V (vs. Ag/AgCl) for 120s under stirring	*LCR:* Cd: 1.5 – 30 Pb: 0.5 – 50 *LD (for 300s):* Cd: 0.02 Pb: 0.02	Lake water	[58]

Table 1.3 – continuation…

Electrode (diameter (d) or area (A))	**Modifier**	**Metals**	**Voltammetric stripping technique**	**Supporting electrolyte solution**	**E_{dep} (E_{acc}) / t_{dep} (t_{acc})**	**Analytical performance /µgL^{-1}**	**Samples analysed**	**Reference**
GC (d = 3 mm)	2,2'-Azinobis(3-ethylbenzothiazoline-6-sulfonate) diammonium salt Carbon nanotubes Bismuth film (*in-situ* deposition)	Cd and Pb	DPASV	0.1 molL^{-1} acetate buffer (pH 4.0)	- 1.0 V (vs. SCE) for 300 s under stirring	*LCR:* Cd: 0.5 – 35 Pb: 0. 2 – 50 *DL:* Cd: 0.2 Pb: 0.1	Tap water Spring water River water	[59]
Carbon paste (A = 0.0707 cm^2)	Bismuth film (*in-situ* deposition)	Cd and Pb	SWASV	0.1 molL^{-1} acetate buffer (pH 4.5)	-1 V (vs. SCE) for 120 s under stirring	*LCR:* Cd and Pb: 5 – 150 *DL:* Cd: 0.27 Pb: 0.35	Canned foods	[60]
GC (d = 3 mm)	Nafion Bismuth film electrode (*in-situ* deposition)	Cd, Pb and Zn	DPASV	0.1 molL^{-1} acetate buffer (pH 4.5)	-1.4 V (vs. Ag/AgCl) for 180s under stirring	*LCR:* Cd, Pb and Zn: 4 – 36 *DL:* Cd: 0.17 Pb: 0.17 Zn: 0.3	Determination of Cd and Pb: Vegetable samples	[34]

Table 1.3 – continuation…

Electrode (diameter (d) or area (A))	**Modifier**	**Metals**	**Voltammetric stripping technique**	**Supporting electrolyte solution**	**E_{dep} (E_{acc}) / t_{dep} (t_{acc})**	**Analytical performance /µgL^{-1}**	**Samples analysed**	**Reference**
GC (d = 3 mm)	Carbon nanotubes Nafion Bismuth film (*in-situ* deposition)	Cd and Pb	DPASV	0.1 molL^{-1} acetate buffer (pH 4.5)	-1.2 V (vs. Ag/AgCl) for 120 s under stirring	*Two LCRs:* Cd: 0.08 – 5 (for 300 s) and 5 – 100 (for 120 s), respectively Pb: 0.05 – 5(for 300s) 5 – 100 (for 120s): *DL:* Cd: 0.04 Pb: 0.025	Tap water	[61]
GC (d = 3 mm)	Nafion Bismuth film (*in-situ* deposition)	Cd, Pb and Zn	DPASV	0.1 molL^{-1} acetate buffer (pH 4.5)	-1.3 V (vs. SCE) for 90 s under stirring	*LCR:* Cd: 1.3 – 20.5 Pb: 1.7 – 27.9 Zn: 3.5 – 79.6 *DL:* Cd: 0.09 Pb: 0.13 Zn: 0.97	Blood	[62]

Table 1.3 – continuation…

Electrode (diameter (d) or area (A))	**Modifier**	**Metals**	**Voltammetric stripping technique**	**Supporting electrolyte solution**	**E_{dep} (E_{acc}) / t_{dep} (t_{acc})**	**Analytical performance /µgL^{-1}**	**Samples analysed**	**Reference**
GC (d = 3 mm)	Poly(*p*-aminobenzene sulfonic acid) Bismuth film (*in-situ* deposition)	Cd, Pb and Zn	DPASV	0.1 molL^{-1} acetate buffer (pH 5.3)	-1.4 V (vs. Ag/AgCl) for 240 s under stirring	*LCR:* Cd and Zn: 1.00 – 110.00 Pb: 1.00 – 130.00 *DL:* Cd: 0.63 Pb:0.80 Zn: 0.62	Tap water River water	[63]
Boron doped diamond (d = 3 mm)	Bismuth nanoparticle (*in-situ* deposition)	Cd and Pb	SWASV	0.1 molL^{-1} $HClO_4$ (pH 1.2)	-1.2 V (vs. SCE) for 120 s under stirring	*Two LCRs:* Pb and Cd: 0.05 – 20 and 20 – 200 *DL:* Cd:2.3 Pb:1.9	---	[64]
Carbon Screen-printed disk (d = 3 mm)	Carbon nanotubes Bismuth film (*in-situ* deposition)	Cd, Pb and Zn	SWASV	0.1 molL^{-1} acetate buffer (pH 4.5)	-1.4 V (vs. SCE) for 300 s under stirring	*LCR:* Cd, Pb and Zn: 20 – 100 *DL:* Cd: 0.7 Pb: 1.3 Zn: 12	River water	[65]

Table 1.3 – continuation…

Electrode (diameter (d) or area (A))	**Modifier**	**Metals**	**Voltammetric stripping technique**	**Supporting electrolyte solution**	**E_{dep} (E_{acc}) / t_{dep} (t_{acc})**	**Analytical performance /µgL^{-1}**	**Samples analysed**	**Reference**
Silicon substrate (photolithographic fabrication) (d = 5 mm)	Bismuth film (sputtering of metallic bismuth on a silicon substrate)	Cd and Pb	SWASV	0.1 molL^{-1} acetate buffer solution (pH 4.5)	-1.2 V (vs. Ag/AgCl) for 120 s under stirring	*LCR:* Cd: 10 – 90 Pb: 5 – 45 *DL(for 240 s):* Cd: 1 Pb: 0.5	Certified river water Phosphate fertilizer	[30]
Carbon screen-printed	Bismuth film (*in-situ* (*on-line*) deposition)	Cd, Pb and Zn	SWASV combined with SIA	1.0 molL^{-1} HCl	-1.4V (vs. Ag/AgCl) for 180 s	*LCR:* Pb and Cd: 0 – 70 Zn: 75 – 200 *DL:* Cd: 0.69 Pb: 0.89 Zn: 54	River water	[47]
GC (d = 3 mm)	Carbon nanotubes Nafion Bismuth film (*in-situ* deposition)	Cd and Pb	SWASV	0.1 molL^{-1} acetate buffer (pH 4.5)	-1.2 V (vs. Ag/AgCl) for 120 s under stirring	*LCR:* Cd: 1.0 – 300.0 Pb: 1.0 – 600.0 *DL (for 600 s):* Cd: 0.08 Pb: 0.05	Tap water	[66]

Table 1.3 – continuation…

Electrode (diameter (d) or area (A))	**Modifier**	**Metals**	**Voltammetric stripping technique**	**Supporting electrolyte solution**	**E_{dep} (E_{acc}) / t_{dep} (t_{acc})**	**Analytical performance /µgL^{-1}**	**Samples analysed**	**Reference**
GC (d = 3 mm)	Nafion 2,2'- bipyridyl Bismuth film (*in-situ* deposition)	Cd, Pb and Zn	SWASV	0.1 molL^{-1} acetate buffer (pH 4.5)	-1.4 V (vs. Ag/AgCl) for 120 s under stirring	*LCR:* Cd: 0.4 – 56 Pb: 0.25 – 104 Zn: 1. 9 – 131 *DL:* Cd: 0.12 Pb: 0.077 Zn: 0.56	Tap water, Commercial natural water Wine	[67]
GC (d = 2 mm)	Nafion Bismuth film: Cd and Pb (*ex-situ* and *in-situ* (*on-line*) deposition) Ni and Co (*ex-situ* deposition)	Cd and Pb and Ni and Co	Cd and Pb: SWASV Ni and Co: SWAdSV Hybrid flow: FIA/SIA	Cd and Pb: 0.1 molL^{-1} acetate buffer (pH 4.5) Ni and Co: 0.1 molL^{-1} ammonia buffer (pH 9.2) Complexing agent: DMG	Cd and Pb: - 1.2 V or -0.4 V (vs. Ag/AgCl) for *in-situ* or *ex-situ* deposition, respectively Ni and Co: - 0.7 V (vs. Ag/AgCl)	*LCR (for 60s):* Cd: 0 – 56 Pb: 0 – 70 Ni and Co: 0 – 35 *DL (for 180 s):* Cd: 2 Pb: 1 Ni and Co: 1	Determination of Cd and Pb: Phosphate fertiliser Determination of Ni and Co: Iron ore	[44]

Table 1.3 – continuation…

Electrode (diameter (d) or area (A))	**Modifier**	**Metals**	**Voltammetric stripping technique**	**Supporting electrolyte solution**	**E_{dep} (E_{acc}) / t_{dep} (t_{acc})**	**Analytical performance /µgL^{-1}**	**Samples analysed**	**Reference**
GC (d = 3 mm)	Poly(sodium 4 styrenesulfonate) Nafion Bismuth film (*in-situ* deposition)	Cd and Pb	SWASV	0.2 molL^{-1} acetate buffer (pH 4.2)	-1.2 V (vs. Ag/AgCl) for 120 sunder stirring	*LCR:* Cd and Pb: 1.0 – 50.0 *DL:* Cd: 0.38 Pb: 0.53	Tap water Snow samples	[68]
Edge plane pyrolytic grafite (d = 4.9 mm)	Bismuth film (*in-situ* deposition)	Cd and pb	SWASV	0.1 molL^{-1} acetate buffer (pH 4.5)	-1.2 V (vs. SCE) for 240 s	*Two LCRs:* Cd: 0.1 – 10 and 10 – 100 Pb: 0.1 – 20 and 20 – 300 *DL:* Cd: 0.062 Pb: 0.084	River water	[29]
Carbon paste (d = 0.5 mm)	Fibrinogen protein Bismuth film (*on-line* deposition before metals deposition)	Cd and Pb	SWASV combined with BIA	0.1 molL^{-1} acetate buffer (pH 4.6)	-1.2 V (vs. SCE) for 60 s	*LCR:* Cd: 0.06 – 56 Pb: 0.1 – 104 *DL:* Pb: 0.1 Cd: 0.1	Tap water Tea	[45]

Table 1.3 – continuation…

Electrode (diameter (d) or area (A))	**Modifier**	**Metals**	**Voltammetric stripping technique**	**Supporting electrolyte solution**	**E_{dep} (E_{acc}) / t_{dep} (t_{acc})**	**Analytical performance /µgL^{-1}**	**Samples analysed**	**Reference**
GC (d = 3 mm)	Nafion Bismuth film (*in-situ* deposition)	Cd, Pb and Zn	SWASV combined with SIA	0.1 molL^{-1} acetate buffer (pH 4.5)	-1.4 V (vs. Ag/AgCl) for 120 s	*LCR:* Cd and Pb: 2 – 60 Zn: 6 – 80 *DL:* Cd: 2 Pb: 2 Zn: 6	Phosphate rock Urine	[48]
GC (d = 3 mm)	Poly(aniline) Bismuth film (*in-situ* deposition)	Cd and Pb	SWASV	0.1 molL^{-1} acetate buffer (pH 5.3)	-1.2 V (vs. SCE) for 240 s under stirring	*LCR:* Cd and Pb: 20 – 180 *DL:* Cd: 1.48 Pb: 1.03	Determination of Pb: Tap water	[69]
Carbon paste (d = 2 mm)	Bismuth powder	Cd and Pb	SWASV and Stripping chronopotentiometry	0.2 molL^{-1} acetate buffer (pH 4.5)	-1 V (vs. Ag/AgCl) for 90 s under stirring	*LCR:* Cd and Pb: 10 – 100 *DL (for 300s):* Cd: 1.2 Pb: 0.9	Tap water	[39]

Table 1.3 – continuation…

Electrode (diameter (d) or area (A))	**Modifier**	**Metals**	**Voltammetric stripping technique**	**Supporting electrolyte solution**	**E_{dep} (E_{acc}) / t_{dep} (t_{acc})**	**Analytical performance /µgL^{-1}**	**Samples analysed**	**Reference**
Graphite–epoxy composite paste (d = 6 mm)	Internal bismuth salt precursor for bismuth *in-situ* film formation	Cd and Pb	SWASV	0.1 molL^{-1} acetate buffer (pH 4.5)	-1.3 V (vs. Ag/AgCl) for 120 s under stirring	*LCR:* Pb: 10 – 40 Cd: 20 – 80 *DL:* Cd: 35.8 Pb: 19.1	---	[41]
Graphite–epoxy composite paste (d = 6 mm)	Bismuth film (*in-situ* deposition)	Cd and Pb	SWASV	0.1 molL^{-1} acetate buffer (pH 4.5)	-1.3 V (vs. Ag/AgCl) for 120 s under stirring	*LCR:* Cd and Pb: 30 – 90 *DL*: Cd and Pb: around 30	Tap water Contaminated soil	[70]
GC (d = 3 mm)	Bismuth film (*in-situ* or *ex-situ* deposition)	Cd, Pb and Zn	SWASV	0.1 molL^{-1} acetate buffer (pH 4.5)	-1.4V (vs. Ag/AgCl) for 180 s under stirring With deoxygenation	*LCR:* Cd, Pb and Zn: 1 – 20 *LD (for 600s):* Pb: 0.1 Cd: 0.1 Zn: 0.4	Determination of Pb with preplated BiFE: Tap water and wine Determination of Cd and Pb with preplated BiFE: Urine	[71]

Table 1.3 – continuation…

Electrode (diameter (d) or area (A))	**Modifier**	**Metals**	**Voltammetric stripping technique**	**Supporting electrolyte solution**	**E_{dep} (E_{acc}) / t_{dep} (t_{acc})**	**Analytical performance /µgL^{-1}**	**Samples analysed**	**Reference**
Pencil-lead (d = 0.5 mm)	Bismuth film (*in-situ* deposition)	Cd, Pb and Zn	SWASV	0.1 molL^{-1} acetate buffer (pH 4.5)	-1.4V (vs. Ag/AgCl) for 180 s under stirring	*LCR:* Cd, Pb and Zn: 2 – 24 *DL (for 600s):* Cd: 0.3 Pb and Zn: 0.4	Determination of Pb and Zn: Tap water	[72]
GC (d = 3 mm)	Bismuth film (*ex-situ* deposition)	Ni and Co	SWAdCSV Complexing agent : DMG	0.2 molL^{-1} ammonia buffer (pH 9.2)	-0.7 V (vs. Ag/AgCl) for 120 s under stirring	*LCR:* Ni and Co: 1 – 14 *DL (for 300s):* Ni: 0.1 Co: 0.07	Certified river water Iron ore Duraluminium	[73]

Table 1.3 – continuation…

Electrode (diameter (d) or area (A))	**Modifier**	**Metals**	**Voltammetric stripping technique**	**Supporting electrolyte solution**	**E_{dep} (E_{acc}) / t_{dep} (t_{acc})**	**Analytical performance /µgL^{-1}**	**Samples analysed**	**Reference**
GC (d = 2 mm)	Bismuth film (*ex-situ* deposition)	Co and Ni	AdSCCC Complexing agent : DMG	0.01 molL^{-1} ammonia buffer (pH 9.2)	-0.7 V (vs. Ag/AgCl) for 60 s under stirring	LCR: ---- DL: Co: 0.08 Ni: 0.26	----	[74]

(*) Microelectrode; LCR: Linear concentration range; DL: detection limit; SIA: Sequential injection analysis; FIA: Flow injection analysis; BIA: Batch injection analysis ; SWAdCSV: square wave adsorptive cathodic stripping voltammetry; AdSCCC: adsorptive stripping constant current chronopotentiometry; SWASV: square wave anodic stripping voltammetry; DPASV: differential pulse anodic stripping voltammetry and DMG: dimethylglyoxime.

1.4.2. Bare solid electrodes

In stripping analysis, the most commonly used bare solid electrodes are carbon and noble metal electrodes (e.g. gold, silver and platinum), respectively. Carbon is a current conducting material with a relatively wide potential range and is more chemically inert than noble metals and low cost [1]. One general advantage of metallic electrodes is their high conductivity which results in low (usually negligible) background currents [75]. Carbon and metallic bare solid electrodes are particularly attractive due to its mechanical simplicity and robustness and the possibility to adapt to different flow cells designs. However, the main difficulties associated with these electrodes are related with irreproducibility problems which result from non-homogeneous electrode surfaces, adsorption and/or interaction between metals co-deposited on the electrode surface [1]. Unlike to mercury electrodes, these solid electrodes, can be used for the stripping measurements of metals/metalloids which do not form amalgams or which have redox potentials positive with respect to mercury, such as selenium (Se), As, Hg, Ag, gold (Au) or tellurium (Te) [1,76].

At these electrodes the process of deposition is based on the formation of metallic layers on bare solid electrode surfaces. The metal ion is reduced to the metal at potential less (underpotential deposition, UPD) or more negative (overpotential deposition) than predicted by the Nernst equation. The underpotential phenomenon occurs when the electrode surface is covered only partially with a monolayer of the deposited metal. The activity of the deposit depends not only on the amount plated, but also on its interaction with the electrode material and distribution on the surface. In generally this process is a more complicated than in case of amalgams and requires electrode pretreatment and polishing to obtain reproducible results [1].

Table 1.4 summarizes the work developed between 2003 and April 2013 for the simultaneous determination of several metals using solid electrodes. Unlike to bismuth electrodes these electrodes have been scarcely explored. Using ASV, binary mixtures of Cd and Pb were determined in carbon [77] and gold [78] electrodes and Cu and Hg in gold electrodes [79], respectively. The analytical

performance of these electrodes is in generally worse than to the most bismuth electrodes described in previous section. The most important work was developed in carbon paste electrode using AdCSV and allows the determination of ternary mixture of Cu, Fe and Mn with good DLs [80].

Although a scarcely work reported about the determination of mixtures of heavy metals with solid electrodes (probably due to the complexity of the deposition process), this is an area which deserves to be continuously explored once the robustness of these electrodes could be particularly important for measurements *on-field.*

Table 1.4 – Simultaneous determination of heavy metals, at trace levels, on solid electrodes.

Electrode (diameter (d) or area (A))	**Metals**	**Voltammetric stripping technique**	**Supporting electrolyte solution**	**E_{dep} (E_{acc}) / t_{dep} (t_{acc})**	**Analytical performance /μgL^{-1}**	**Samples analysed**	**Reference**
Edge plane pyrolytic graphite (d = 4.9 mm)	Cd and Pb	LSASV	0.1 $molL^{-1}$ acetate buffer (pH 4.6)	-1.2 V (vs. SCE) for 240 s under stirring With deoxygenation	*Two LCRs:* Cd and Pb: 2.0 – 20 and 20 – 200 *DL:* Cd: 0.3 Pb: 0.2	---	[77]
Gold (A = 0.785 mm^2)	Cu and Hg	SWASV	0.1 $molL^{-1}$ $HClO_4$ or 0.01 $molL^{-1}$ EDTA-Na_2, 0.06 mol L^{-1} NaCl and 2.0 mol L^{-1} $HClO_4$ (the best supporting electrolyte) or 0.1 mol L^{-1} KSCN and 0.001 mol L^{-1} $HClO_4$	- 0.8 V (vs. Ag/AgCl) for 240 s under stirring $t_{deoxigenation}$: 5 min	*LCR:* Depends of Hg – Cu concentration ratios *DL (the best supporting electrolyte):* Cu: 0.15 Hg: 0.11	Standard reference materials: Estuarine Sediment BCR-CRM 277 River Sediment BCR-CRM 320 Mercury in Water NIST-SRM 1641d Sediments and sea waters sampled in a lagoon ecosystem	[79]

Table 1.4 – continuation…

Electrode (diameter (d) or area (A))	**Metals**	**Voltammetric stripping technique**	**Supporting electrolyte solution**	**E_{dep} (E_{acc}) / t_{dep} (t_{acc})**	**Analytical performance /µgL^{-1}**	**Samples analysed**	**Reference**
Carbon paste (d = 3 mm)	Cu, Fe and Mn	SWAdCSV Complexing agent: 2-(5_-bromo-2_-pyridylazo)-5-diethylaminophenol	0.1 molL^{-1} acetate buffer (pH 5)	1.0 V (vs. Ag/AgCl) for 240 s under stirring	*LCR:* Cu: 0.36 – 45 Fe: 0.31 – 25 Mn: 0.22 – 40 *DL:* Cu: 0.108 Fe: 0.093 Mn: 0.066	Ground water Tap water Bottled water	[80]
Gold	Cu and Pb	SWASV	0.05 molL^{-1} HCl	-0.35 V (vs. Ag/AgCl) for 30 s	*LCR:* Cu: 20 – 430 Pb: 250 – 430 *DL (for 900 s):* Cu: 0.12 Pb: 0.235	Ethanol fuel	[78]
Silver-bismuth alloy electrode	Co and Ni	DPAdCSV Complexing agent : DMG	.01 molL^{-1} ammonia buffer (pH 11)	-0.750 V (vs. Ag/AgCl) for t_{acc} s	----	Water from wastewater treatment process	[81]

LCR: Linear concentration range; DL: detection limit; SWAdCSV: square wave adsorptive stripping cathodic voltammetry; DPAdCSV: differential pulse adsorptive cathodic stripping voltammetry; LSASV: linear sweep anodic stripping voltammetry; SWASV: square wave anodic stripping voltammetry and DMG: dimethylglyoxime.

1.4.3. Chemical modified electrodes

CMEs represent a modern approach to replace mercury electrodes. The development and application of these electrodes for simultaneous determination of multi-metal(loid)s have received considerable attention in recent years (Table 1.5). These electrodes are conveniently prepared by the placement of a modifier onto the electrode surface in order to improve their surface properties and consequently to enhance the analytical performance. The huge success of CMEs arises most often from the remarkable and sometimes unique selectivity and/or sensitivity properties of the modifiers [9,10]. These modifiers can have electrostatic interaction or complexation with metal ions and pre-concentrate the metal ions at the electrode modifying surface [3].

Table 1.5 summarizes the main work developed between 2003 and April 2013 for the simultaneous determination of several metal(loid)s using CMEs. At present (Table 1.5), a variety of modifiers such as conductive polymers, ligands, inorganic ion exchangers, nanoparticles, thin films and carbon nanotubes had been used in simultaneous heavy metal(loid)s determinations. The synergistic contribution from different modifiers was also explored (Table 1.5).

In relation to the electrode, GC, carbon-paste and gold electrodes are the most explored (Table 1.5). Carbon paste electrodes, due to their easy construction, easy renewability of the surface, relatively residual currents and compatibility with various types of modifiers, have been widely used as suitable matrices for the preparation of the modified electrodes [9,82].

Considering a carefully choice of the modifier, the main advantage of CMEs in relation to bismuth and solid electrodes is the possibility to make the simultaneous determination of more than three metal(loid)s, i.e., Cd, Cu, Pb and Hg [83], Cd, Hg, Ni and Pb [84], As, Cd, Cu, Pb and Zn [85]. However, these determinations offers lower sensitivities and DLs even applying higher deposition times. Compared with previously described bismuth and solid electrodes (please see sections 1.41 and 1.42, respectively) these CMEs are more complicated to

prepare and some multi-element voltammetric procedures described in Table 1.5 requires longer deoxygenating times.

In conclusion, although these electrodes present good multi-element capabilities, they need further improvements especially related with sensitivity. In addition, before to submit CMEs to *on-field* trace metals monitoring some questions related with storage and operational stability due the possibility to continuous leaching of modifier during the prolonged electrochemical measurements should be considered.

Table 1.5 – Simultaneous determination of metal(loid)s, at trace levels, on CMEs electrodes.

Electrode (diameter (d) or area (A))	**Modifier**	**Metals**	**Voltammetric stripping technique**	**Supporting electrolyte solution**	**E_{dep} (E_{acc}) / t_{dep} (t_{acc})**	**Analytical performance /μgL^{-1}**	**Samples analysed**	**Reference**
Carbon paste (d = 1.5 mm)	Silica nanoparticles, Synthesized Schiff base: N,N_-bis(3(2 thenylidenimino)propyl)piperazine	Cd, Cu, Hg	SWASV	Britton–Robinson buffer (pH 2.0)	−1.1 V (vs. Ag/AgCl) for 60 s under stirring $t_{deoxigenation}$: 10 min	*LCR:* Cd: 1.5 –1000 Cu: 0.6 – 1100 Hg: 0.5 – 1000 *DL:* Cd: 0.3 Cu: 0.1 Hg:0.05	Tap water Persian Gulf water Tobacco Fish Shrimp tissues Human hair Rice	[86]
Carbon Paste (d = 1.5 mm)	Carbon nanotubes Synthesized Schiff base: (Z)-2-((3-(4-(3-(5-bromo-2-hydroxybenzylideneamino)propyl)piperazin-1-yl)propylimino)methyl)-4-bromophenol	Cd and Pb	SWASV	Britton–Robinson buffer (pH 5.3)	−1.1 V (vs. Ag/AgCl) for 190 s under stirring $t_{deoxigenation}$: 5 min	*LCR:* Cd: 1.00 – 1200 Pb: 0.40 – 1100 *DL:* Cd: 0.74 Pb: 0.25	Tobacco Human hair Soya Sugar Rice Tap water Waste water Shrimp tissues Fish.	[87]

Table 1.5 – continuation…

Electrode (diameter (d) or area (A))	**Modifier**	**Metals**	**Voltammetric stripping technique**	**Supporting electrolyte solution**	**E_{dep} (E_{acc}) / t_{dep} (t_{acc})**	**Analytical performance /μgL^{-1}**	**Samples analysed**	**Reference**
GC (A = 7.07 mm^2)	Silver nanonuts	Cd and Pb	DPASV	0.1 molL^{-1} acetate buffer solution (pH 5.3)	-1.4V (vs. SCE) for 120 s under stirring	*LCR:* Cd and Pb: 0.5 – 90 *DL:* Cd:0.15 Pb: 0.10	Waste water	[88]
GC (A = 0.07065 cm^2)	Poly(diphenylamine-co-2-aminobenzonitrile), a cyano group containing conducting polyaniline derivative	Cd and Pb	DPASV	KCl and HCl buffer solution (pH 2.01)	−1.0 V (vs. Ag/AgCl) for 60 s under stirring	*LCR:* Cd: (1.260 – 907.8) × 10^3 Pb: (0.26 – 58.73) × 10^3 *DL:* Cd: 0.255 × 10^3 Pb: 0.165 × 10^3	Tap water	[3]
Carbon Paste	Carbon nanotubes Synthesized Schiff base: 3- (4 methoxybenzylideneamino)-2-thioxothiazolodin-4-one ligand	Hg and Pb	SWASV	0.15 molL^{-1} KNO_3 (pH 3.0)	−1.2 V (vs. Ag/AgCl) for 90 s under stirring $t_{deoxigenation}$: 5 min	*LCR*: Hg: 0.5 – 140 Pb: 0.52 – 140 *DL:* Hg: 0.18 Pb: 0.12	Sea water Waste water Tobacco Marine and human teeth samples	[9]

Table 1.5 – continuation…

Electrode (diameter (d) or area (A))	**Modifier**	**Metals**	**Voltammetric stripping technique**	**Supporting electrolyte solution**	**E_{dep} (E_{acc}) / t_{dep} (t_{acc})**	**Analytical performance /µg L^{-1}**	**Samples analysed**	**Reference**
Graphitic carbon bulk (d = 5 mm)	4-aminosalicylic acid	Cd and Pb	DPASV	Acetate buffer (pH 8)	-0.8 V (vs. Ag/AgCl) for 240 sunder stirring $t_{deoxigenation:}$ 15 min	*LCR:* Cd: 11 – 90 Pb: 21 – 166 *DL:* Cd: 0.08 Pb: 0.2	Waste water from lead acid batteries	[89]
Carbon paste (d = 1.5 mm)	Synthesized phosphorous ylide nitro benzoyl diphenylmethylenphosphorane	Cd and Hg	SWASV	Britton–robinson buffer (pH 3.0)	-0.9 V (vs. Ag/AgCl) for 210 s under stirring	*LCR*: Cd and Hg : up to 2000 *DL:* Cd: 6.6 Hg: 8.2	Fish tissue Human hair Several plant foodstuffs Water samples	[82]
GC	Stannum–bismuth composite film (*in-situ* deposition)	Cd and Zn	DPASV	0.1 $molL^{-1}$ acetate buffer solution (pH 4.7)	-1.4V (vs. SCE) for 270 s under stirring	*LCR:* Cd and Zn: 2 – 80 *DL:* Cd: 0.86 Zn: 0.31	Tap water	[35]

Table 1.5 – continuation…

Electrode (diameter (d) or area (A))	**Modifier**	**Metals**	**Voltammetric stripping technique**	**Supporting electrolyte solution**	**E_{dep} (E_{acc}) / t_{dep} (t_{acc})**	**Analytical performance /μgL^{-1}**	**Samples analysed**	**Reference**
GC (d = 3mm)	Nafion Magnesium oxide	Cd and Pb	SWASV	0.1 molL^{-1} acetate buffer (pH 5.0)	-0.8 V (vs. Ag/AgCl) for 120 s	*LCR:* Cd: 4.5 – 16 Pb: 0.7 – 4.6 *DL:* Cd: 0.009 Pb: 0.0004	Water sample collected from Dongpu Reservoir in Hefei City	[90]
GC	Nafion Copper - Methyl 3,5-bis{bis-[(pyridin-2 yl)methyl]amino}methyl) benzoate complex	Cd and Pb	DPASV	0.1 molL^{-1} acetate buffer (pH 4)	-1.4 V (vs. Ag/AgCl) for 120 s under stirring	*LCR:* Cd: 0.6 - 5620 Pb: 1.0 – 10360 *DL:* Cd: 0.1 Pb: 0.4	Certified referenc material: Groundwater CRM 610 (BCR) River water	[10]
GC (d = 3 mm)	Polyaniline	Cd and Pb	SWASV	0.1 molL^{-1} acetate buffer (pH 5.3)	-1 V (vs. Ag/AgCl) for 120s under stirring With deoxygenation	*LCR:* Cd: 0 – 225 Pb: 0 – 414 *DL:* Cd: 14.6 Pb: 20.7	---	[92]

Table 1.5 – continuation…

Electrode (diameter (d) or area (A))	**Modifier**	**Metals**	**Voltammetric stripping technique**	**Supporting electrolyte solution**	**E_{dep} (E_{acc}) / t_{dep} (t_{acc})**	**Analytical performance /µgL^{-1}**	**Samples analysed**	**Reference**
Carbon paste (d = 3 mm)	Barium hydrogen phosphate or Nafion and barium hydrogen phosphate	Cd and Pb	DPASV	0.1 molL^{-1} KCl (pH 7)	-1.2 V (vs. SCE) for 300 s under stirring	*LCR using Barium hydrogen phosphate modifier:* Cd: 1.1 – 9.0 Pb: 2.1 – 17 *DL (for 900 s) using Barium hydrogen phosphate modifier:* Cd: 0.2 Pb: 0.6 or *LCR using nafion and barium hydrogen phosphate modifier:* Cd: 1.1 – 5.6 Pb: 2.1 – 10 DL (for 900 s) *using nafion and barium hydrogen phosphate modifier:* Cd: 0.09 Pb: 0.9	---	[91]

Table 1.5 – continuation…

Electrode (diameter (d) or area (A))	**Modifier**	**Metals**	**Voltammetric stripping technique**	**Supporting electrolyte solution**	**E_{dep} (E_{acc}) / t_{dep} (t_{acc})**	**Analytical performance /µgL^{-1}**	**Samples analysed**	**Reference**
GC (d = 3 mm) GC electrode was selected as the most satisfactory support. or Carbon paste (d = 5 mm) or Impregnated graphite electrode (d = 6 mm)	Tin film (*in-situ* deposition)	Cd and Zn and Cd and Pb and Cd, Cu, and Pb	SWASV	0.1 molL^{-1} acetate buffer (pH 4.5) the most suitable supporting electrolyte	-1.5 V (vs. Ag/AgCl) for 120 s under stirring	*LCR:* Cd and Zn: 4 – 60 and 10 – 200) *DL:* Cd: 0.7 Zn: 0.9 *LCR:* Cd and Pb: 0 – 52 *LCR:* Cu, Pb and Cd: 0 – 60	Tap water	[93]
Gold (d = 3mm)	Polymer film of dipicolinic acid Gold nanoparticle Cysteine	Cd and Zn	DPASV	0.1 molL^{-1} acetate buffer (pH 3.8)	-1.7 V (vs. SCE) for 180 s under stirring $t_{deoxigenation}$: at least 5 min	*LCR:* Cd: 5.0 – 1911 Zn: 1.3 – 1635 *DL:* Cd: 1.7 Zn: 0.5	Tap water Lake water River water Spring water	[94]

Table 1.5 – continuation…

Electrode (diameter (d) or area (A))	**Modifier**	**Metals**	**Voltammetric stripping technique**	**Supporting electrolyte solution**	**E_{dep} (E_{acc}) / t_{dep} (t_{acc})**	**Analytical performance /µg L^{-1}**	**Samples analysed**	**Reference**
Carbon paste (d = 3 mm)	Montmorillonite-calcium clay	Cd, Cu, Pb, and Hg	SWASV	0.1 $molL^{-1}$ HCl (pH 1)	-0.90V (vs. Ag/AgCl) for 300 s under stirring	*LCR:* Cd: 1.8 – 120 Cu: 2.5 – 130 Pb: 1 – 100 Hg: 3.5 – 150 *DL:* Cd: 0.54 Cu: 0.75 Pb: 0.30 Hg: 1.05	Tap water Bottled natural water Sea water	[83]
Glassy carbon electrode	Aromatic diazonium derivatives	Cd and Pb	SWASV	0.2 $molL^{-1}$ acetic buffer (pH 6.1)	-1.2 V (vs. Ag/AgCl) 120 s under stirring	*LCR:* Cd and Pb: 0.5 – 50 *DL:* Cd: 0.13 Pb: 0.20	Sewerage	[95]

Table 1.5 – continuation…

Electrode (diameter (d) or area (A))	**Modifier**	**Metals**	**Voltammetric stripping technique**	**Supporting electrolyte solution**	**E_{dep} (E_{acc}) / t_{dep} (t_{acc})**	**Analytical performance /µg L^{-1}**	**Samples analysed**	**Reference**
Carbon paste (d = 3.5 mm)	Polyaniline (PANI) or Polyaniline-poly(2,2_-dithiodianiline) (PANI-PDTDA) or Mercaptobenzothiazole (MBT) or Faujasite zeolite (FAUY)	Cd, Hg, Ni and Pb	DPASV	0.5 $molL^{-1}$ HCl	-0.4 V (vs. Ag/AgCl) for 120 s	*LCR:* Cd: $0.1 – 1 \times 10^5$ Hg: $0.2 – 2 \times 10^5$ Ni: $0.06 – 6 \times 10^4$ Pb: $0.2 – 2 \times 10^5$ *DL:* *(PANI):* Cd: 97 Hg: 3×10^3 Ni: 56 Pb: 269 *(PANI-PDTDA):* Cd: 33 Hg: 26 Ni: 19 Pb: 35 *(MBT):* Cd: 157 Hg: 8×10^3 Ni: 59 Pb: 1×10^4	River water	[84]

Table 1.5 – continuation…

Electrode (diameter (d) or area (A))	**Modifier**	**Metals**	**Voltammetric stripping technique**	**Supporting electrolyte solution**	**E_{dep} (E_{acc}) / t_{dep} (t_{acc})**	**Analytical performance /µg L^{-1}**	**Samples analysed**	**Reference**
GC (d = 3 mm)	Langmuir – Blodgett film of a 25,27-Dimethoxy-26-(N-trichloroacetyl) carbamoyloxy-p-tert-butylcalix[4]arene	Pb and Tl	SWASV	0.2 $molL^{-1}$ acetate buffer (pH 4.4)	-1.4 V (vs. SCE) for 90 s under stirring $t_{deoxigenation}$: 10 min	*LCR:* Pb: 41 – 4.1 x 10^3 Tl: 6.13 – 817 *DL:* Pb: 17 Tl: 4	Tap water Lake water	[96]
GC	Seven modified polymers based on aniline (ANI), 4.4′-diaminodiphenyl sulphone (DDS), PEDOT, diclofenac (DCF), sodium dodecyl sulfate (SDS), cetyl trimethyl ammonium bromide (CTAB): (1) Poly(ANI-co-DDS) (2) PEDOT (3) PEDOT/SDS (4) PEDOT/CTAB (5) Poly(EDOT-co-DCF) (6) Poly(EDOT-co-DCF)/SDS (7) Poly(EDOT-co DCF)/CTAB	As, Cd, Cu, Pb and Zn	SWASV	Britton-robinson buffer (pH 4.0)	0.3 V (vs SCE) for 60s under stirring $t_{deoxigenation}$: 20 min	*LCR:* *Modified system PEDOT/GCE:* As, Cd, Cu, Pb and Zn: (0.003 – 0.2) × 10^3 *DL:* *Modified system PEDOT/GCE:* As: 0.2 Cd: 1 Cu: 1 Pb: 1 Zn: 2	Plating wastewater	[85]

Table 1.5 – continuation…

Electrode (diameter (d) or area (A))	**Modifier**	**Metals**	**Voltammetric stripping technique**	**Supporting electrolyte solution**	**E_{dep} (E_{acc}) / t_{dep} (t_{acc})**	**Analytical performance /μgL^{-1}**	**Samples analysed**	**Reference**
GC (d = 3 mm)	Carbon nanotubes Sodium dodecyl benzene sulfonate Stannum film (*in-situ* deposition)	Cd and Zn	DPASV	0.1 molL^{-1} acetate buffer (pH 5.25)	-1.4 V (vs. Ag/AgCl) for 240 s under stirring	*LCR:* Cd and Zn: 5 – 100 *DL:* Cd: 0.8 Zn: 0.9	Tap water	[97]
Carbon paste (d = 1.8 mm)	Ionic liquid N octylpyridium hexafluorophosphate Hydroxyapatite	Cd and Pb	SWASV	0.1 molL^{-1} $HClO_4$ (pH 8.0)	- 1.1 V (vs. Ag/AgCl) for 180 s under stirring	*Linear range:* Cd: 0.1 – 11 Pb: 0.2 – 21 *DL:* Cd: 0.06 Pb: 0.04	Wastewater	[98]
Gold polycrystalline (d = 1.6 mm)	3-(Mercaptopropyl) trimethoxy silane Gold nanoparticles	As^{3+}, Cu and Hg	SWASV	1 molL^{-1} HCl	-0.35 V (vs. Ag/AgCl) for 100 s	*LCR:* Sub-μgL^{-1} *DL:* As^{3+} and Hg: 0.02	Determination of arsenic: Contaminated water	[99]

Table 1.5 – continuation…

Electrode (diameter (d) or area (A))	**Modifier**	**Metals**	**Voltammetric stripping technique**	**Supporting electrolyte solution**	**E_{dep} (E_{acc}) / t_{dep} (t_{acc})**	**Analytical performance /μgL^{-1}**	**Samples analysed**	**Reference**
Carbon paste (A = 0.16 cm^2)	SBA-15 nanostructured silica organofunctionalised with 2-benzothiazolethiol	Cu, Hg and Pb	DPASV	0.1 molL^{-1} phosphate solution (pH 3.0)	-0.80 V (vs. SCE) for 180 s $t_{deoxigenation}$: 15 min	*LCR:* Cu: 51 – 635 Hg: 401 – 2 × 10^3 Pb: 62 – 1.5 × 10^3 *DL:* Cu: 13 Hg: 80 Pb: 8	Well water Sugar cane spirit (*cachaça*)	[100]
Diamond carbon film (d = 7.2 mm)	Boron	Cd and Pb (and Zn)	DPASV	0.05 molL^{-1} acetate buffer (pH 4.8)	-1.9 V (vs. SCE) for 60 s under stirring With deoxygenating	*LCR:* Cd: 5 – 20 Pb: 5 – 70 Zn: --- *DL:* Pb and Cd: 1.5 Zn: ---	---	[101]
Gold array constituted with four electrodes	(1) Gly-Gly-His and thioctic acid; (2) γ-Glu-Cys Gly and thioctic acid; (3) Human angiotensin I and thioctic acid; (4) Thioctic acid	Cd, Cu and Pb	OSWV (Osteryoung square wave voltammetry) Medium exchange N-PLS calibration	0.05 molL^{-1} ammonium acetate (pH 7.0) and 0.05 mol L^{-1} NaCl	At open circuit potential for 600 s (vs. Ag/AgCl) under stirring	*LCR:* Cd: 11 – 1.1 × 10^3 Cu: 6.4 – 6.4 × 10^2 Pb: 21 – 2.1 × 10^3	---	[102]

Table 1.5 – continuation…

Electrode (diameter (d) or area (A))	**Modifier**	**Metals**	**Voltammetric stripping technique**	**Supporting electrolyte solution**	**E_{dep} (E_{acc}) / t_{dep} (t_{acc})**	**Analytical performance /μgL^{-1}**	**Samples analysed**	**Reference**
Gold disk (d = 2 mm)	Au nanoparicles ($\bar{d}$ = 20 – 40 nm) Mercaptoethanesulfonate	Cu, Hg and Pb	SWASV	0.01 molL^{-1} HNO_3 and 0.1 mol L^{-1} NaCl	-0.2 V (vs. Ag/AgCl) for 180 s under stirring	*LCR:* Cu, Hg and Pb: 1 – 100 μgL^{-1} *DL:* Cu: 0.15 Hg: 0.13 Pb: 0.16	Metallurgy wastewater	[103]
Carbon paste (A = 0.08 cm^2)	Carbamoylphosphonic acid (acetamide phosphonic acid) self-assembled monolayer (SAM) on mesoporous silica	Cd, Cu and Pb	SWAdSV With medium exchange	0.2 molL^{-1} HNO_3	Open circuit for 120 s and -1.0 V (vs. Ag/AgCl) for 120 s under stirring	*LCR:* Cd, Cu and Pb: 10 – 200 *DL:* Cd, Cu and Pb: 10	---	[104]
GC (d = 3mm)	9, 10-anthraquinone Na-montmorillonite nanoparticles (nano-SWy-2)	Cd and Pb	DPASV	0.1 molL^{-1} acetate buffer (pH 5.6)	-1.2 V (vs. SCE) 300 s under stirring	*LCR:* Cd: 0.9 – 112 Pb: 0.4 – 207 *DL:* Cd: 0.34 Pb: 0.21	Milk powder Lake water	[105]

Table 1.5 – continuation…

Electrode (diameter (d) or area (A))	**Modifier**	**Metals**	**Voltammetric stripping technique**	**Supporting electrolyte solution**	**E_{dep} (E_{acc}) / t_{dep} (t_{acc})**	**Analytical performance /μgL^{-1}**	**Samples analysed**	**Reference**
Carbon paste (d = 3 mm)	Diacetyldioxime	Cd and Pb	DPASV	0.1 molL^{-1} phosphate buffer (pH 5)	-1.1 V (vs. SCE) 300 s under stirring	*LCR:* Cd: 28 – 2.8 × 10^3 Pb: 21 – 3.1 × 10^3 *DL:* Cd: 4.5 Pb: 2.1	Water collected near steel mill.	[106]
GC	Dihexadecyl hydrogen phosphate Carbon nanotubes	Cd and Pb	DPASV	0.1 molL^{-1} acetate buffer with 0.02 molL^{-1} KI (pH 4.5)	-1.2 V (vs. SCE) 300 s under stirring	*LCR:* Cd: 2.8 – 1.1×10^3 Pb: 4.1 – 2.1×10^3 *DL:* Cd: 0.7 Pb: 0.8	Lake water	[107]

LCR: Linear concentration range; DL: detection limit; SWAdCSV: square wave adsorptive stripping cathodic voltammetry; SWASV: square wave anodic stripping voltammetry; DPASV: differential pulse anodic stripping voltammetry.

1.4.4. Microelectrodes

The size of the electrode affects the mass transport of redox species to and from the electrode surface and the bulk solution, which influences the observed electrochemical response [108]. When compared to macroelectrodes (e.g. bismuth, solid and CMEs previously described) which dimensions are commonly on the order of millimeters (typically greater than 100 μm [5,108]), microelectrodes [108] having at least one dimension less than 100 μm (typically 10 – 50 μm).

The microelectrode operational definition recommended by IUPAC in Pure and Applied Chemistry [109] is the following:

"A microelectrode is an electrode whose characteristic dimension is, under the given experimental conditions, comparable to or smaller than the diffusion layer thickness, δ. Under these conditions a steady-state or a pseudo steady state (cylindrical electrodes) is attained."

The major difference between macro and microelectrodes is that planar diffusion occurs on the former compared to radial diffusion in the latter. Radial diffusion occurs when the electrode radius, r (for spherical, hemispherical and disc electrodes) is much smaller than the diffusion layer thickness, δ ($r << \delta$; typically $r \leq 10$ μm) [5]. Compared to conventionally sized electrodes (1 – 5 mm radius) microelectrodes have a few unique characteristics that make them preferable to macroelectrodes for voltammetric environmental monitoring [4,5,16,76,109-111]:

(i) High mass transport;
(ii) Relatively low immunity to ohmic drop;
(iii) Reduced capacitive current;

(iv) Good signal-to-noise ratio
(v) Higher current densities;
(vi) Time-independent currents
(vii) The possibility of using very high scan rates
(viii) The possibility of carrying out measurements in solutions with very low conductivity (without addition of electrolyte).

Non-toxic mercury-free microelectrodes of various materials (e.g. carbon, noble metals and BiFEs) and geometries (microdisk, microring, microband, microcylinder, microsphere and microhemisfere, respectively [109] have been prepared mechanically or lithographically [76]. In addition to single electrodes, microelectrode arrays (microdisk, microband, microcylinder and interdigitated arrays, respectively [109]), have been prepared and used [76]. Arrays (uniform surface) and ensembles (random surface) of microelectrodes offer further advantage over individual microelectrode in stripping analysis because the very low current associated with a single microelectrode (typically in the pA to nA range [4]) is amplified and thus it is possible to use less sensitive instrumentation. Although microelectrodes exists in various geometries, in stripping analysis the most frequently used are those with geometries of disk, hemisphere, cylinder and arrays (or ensembles) of microdisks, microhemispheres, microbands and interdigitated structures [76].

Taking into account the advantages of microelectrodes, an increasing number of papers have appeared in the literature reporting the use of various types (modified or unmodified) of non-toxic mercury-free microelectrodes or arrays of microelectrodes (carbon, gold, platinum, silver and silver-copper alloys), combined with voltammetric stripping analysis to detect trace levels of As, Cd, Co, Cu, Hg, Pb, Ni, Mn, Tl and Zn [76]. However, until now, the application of microelectrodes for multi-element detection is not very often (Table 1.6). In fact, the main microelectrodes applied for simultaneous heavy metal(loid)s determinations are gold (bare or modified electrode) and bismuth films deposited on micro-subtracts of carbon (Table 1.6).

Bismuth film microelectrodes (BiFμEs) prepared *in-situ* or *ex-situ* were used for simultaneous detection of binary and tertiary combinations of Cd, Pb and Zn (for ASV) [33,112-114] or Co and Ni (for AdCSV) [115], respectively. The analytical performance of these bismuth microelectrodes is similar to the corresponding macroelectrodes (Table 1.3) but without stirring the electrode or solution and in some instances using unbuffered solutions.

Modified gold electrodes [114,116,117] were successfully used for simultaneous determination of Cu and Pb and Cu, Pb and Zn, respectively. Further, a vibrating bare gold microwire electrode was used for simultaneous determination of Cu and Hg in sea water using a subtractive anodic stripping voltametric technique [118]. In this case, the deposition procedure is based on UPD [27], i.e., as described before for solid metallic electrodes, the formation of a monolayer of the target metal at potentials more positive than those required for bulk-metal deposition. At underpotential and in conditions of trace metal analysis (low concentrations of metal being deposited), the metallic deposit of Cu or Hg covers a very low portion of the working electrode surface, the electrode surface remains practically unchanged, which results in good analytical repeatability. In addition, because of the limited amount of metal deposited at UPD (one monolayer maximum) and the application of a vibrating device the necessary deposition time is often short. The possibility of working in the presence of the dissolved oxygen is another important advantage.

In conclusion, these small-sized electrodes and their arrays should continue to be explored for trace metal simultaneous analysis. Further, these electrodes are usually prepared in the laboratory. The preparation procedures are not complicated but require very careful work and experience Thus, side by side with the continuous evolution of microelectronics technology, the future prospects related with the application with microelectrodes should be its automated mass production and marketing.

Table 1.6 – Simultaneous determination of meta(loid)s, at trace levels, on microelectrodes.

Microelectrode (diameter (d) or area (A))	**Modifier**	**Metals**	**Voltammetric stripping technique**	**Supporting electrolyte solution**	**E_{dep} (E_{acc}) / t_{dep} (t_{acc})**	**Analytical performance /μgL^{-1}**	**Samples analysed**	**Reference**
Gold in a chip configuration (A = 1 mm^2)	L-aspartic acid / L-cysteine Gold nanoparticles	Cu and Pb	SWASV	0.1 $molL^{-1}$ acetate buffer solution (pH 4.5)	At open-circuit potential (vs. SCE) for 300 s	*LCR:* Cu and Pb: 5 – 2000 *DL:* Cu and Pb:1	---	[116]
Gold in a chip configuration (A = 1 mm^2)	Gold nanoparticles Tin film (*in-situ* deposition)	Cu, Pb and Zn	SWASV	0.1 $molL^{-1}$ acetate buffer solution (pH 4.5)	-1.4 V (vs. Ag/AgCl) for 300 s	*LCR:* Cu: 5 – 100 Pb: 5 – 100 Zn: 10 – 500 *DL:* Cu: 2 Pb: 3 Zn: 5	Surface water	[117]
Pyrolyzed photoresist film in alumina supports (A = 4 × 4 mm^2)	Nafion Bismuth film (*in-situ* deposition)	Cd, Pb and Zn	SWASV	0.1 $molL^{-1}$ acetate buffer solution (pH 4.5)	-1.3V (vs. Ag/AgCl) for 180 s under stirring	*LCR:* Cd: 1.12 – 11.2 Pb: 2.07 – 20.7 Zn: 0.65 – 6.5 *DL:* Cd: 0.7 Pb: 0.6 Zn: 1.6	---	[33]

Table 1.6 – continuation…

Microelectrode (diameter (d) or area (A))	**Modifier**	**Metals**	**Voltammetric stripping technique**	**Supporting electrolyte solution**	**E_{dep} (E_{acc}) / t_{dep} (t_{acc})**	**Analytical performance /µgL^{-1}**	**Samples analysed**	**Reference**
Carbon fibre microdisk (d = 6 µm)	Bismuth film (*in-situ* deposition)	Zn and Cd	SWASV	0.1 molL^{-1} acetate buffer (pH 5.5)	- 1.6 V (vs. Ag/AgCl) for 800s	*LCR:* Cd: 0.06 – 1.1 Zn: 0.03 – 0.7 *DL:* Cd: 0.003 Zn: 0.05	Estuarine water	[112]
Carbon paste (d = 50–300 µm)	Bismuth film (*in-situ* deposition)	Cd and Pb	SWASV	Unbuffered solutions (pH 2.8) or acetate buffer (pH 4.7)	−1.1V (vs. SCE) for 600 s	*LCR:* Cd: 1.12 – 112 Pb: 2.07 – 207 *DL:* Pb: 0.16 (in 0.01 molL^{-1} acetate buffer) Cd: 0.14 (in 0.1 molL^{-1} acetate buffer)	Tap water	[113]

Table 1.6 – continuation…

Microelectrode (diameter (d) or area (A))	**Modifier**	**Metals**	**Voltammetric stripping technique**	**Supporting electrolyte solution**	**E_{dep} (E_{acc}) / t_{dep} (t_{acc})**	**Analytical performance /μgL^{-1}**	**Samples analysed**	**Reference**
Carbon and gold microdiscs ($d_{carbon\ electrode}$ = 30 μm and $d_{gold\ electrode}$ = 10 μm)	Bismuth film (*in-situ* deposition)	Cd and Pb	SWASV	Variable (0 – 0.1 molL^{-1}) acetate buffer (pH values between 3.7 4.6)	Carbon microelectrode: −1.1 V (vs. Ag/AgCl) for 600 s Gold microelectrode: −1.2 V (vs. Ag/AgCl) for 600 s	*LCR for carbon microelectrode in buffered solutions:* Cd: 5.62 – 112 Pb: 10.4 – 207 *LCR carbon microelectrode in unbuffered solutions:* Cd: 11.2 – 112 Pb: 20.7 – 207 *DL in buffered solutions:* Cd: 2.2 and Pb: 2.3 *DL in unbuffered solutions* Cd:16.9 and Pb: 9.3 *LCR for gold microelectrode in buffered solutions:* Cd: 33.7 – 1124 Pb: 14.5 – 1036 *DL in buffered solutions:* Cd: 9.0 and Pb: 12.4 *DL in unbuffered solutions:* Cd:22.5 Pb: 16.6	Determination of Pb in tap water using a carbon microelectrode	[114]

Table 1.6 – continuation…

Microelectrode (diameter (d) or area (A))	**Modifier**	**Metals**	**Voltammetric stripping technique**	**Supporting electrolyte solution**	**E_{dep} (E_{acc}) / t_{dep} (t_{acc})**	**Analytical performance /µgL^{-1}**	**Samples analysed**	**Reference**
Gold microwire (d = [5, 25 and 100] µm)	---	Cu and Hg	Subtractive SWASV	Sea water or 0.01 molL^{-1} HCl	-0.2 V (vs. Ag/AgCl) for 120 s for sea water or 0 V (vs. Ag/AgCl) for 120 s for0.01 molL^{-1} HCl Under stirring in both cases	*LCR:* --- *DL (for 300 s) in 0.01 molL^{-1} HCl with an electrode of 5 µm:* Cu: 0.0016 Hg: 0.001	Sea water	[118]
Single carbon fibre (d = 7 µm)	Bismuh film (*ex-situ* deposition)	Co and Ni	SWAdCSV Complexing agent: DMG	0.01 molL^{-1} ammonia buffer (pH 9.2)	-0.7 V (vs. Ag/AgCl) for 60 s under stirring	*LCR:* Co: 0.2 – 1.8 for 120 s and 2.0- 20.0 for 30 s Ni: 0.2 – 1.8 for 120 s and 2.0 – 16.0 for 30 s *DL:* Co: 0.069 Ni: 0.056	Simulated saliva, sweat and real aqueous humor, cerebrospinal fluid	[115]

LCR: linear concentration range; DL: detection limit; SWAdCSV: square wave adsorptive cathodic stripping voltammetry; SWASV: square wave anodic stripping voltammetry.

References

[1] J. Wang, Stripping Analysis, VCH, New York **1985**.

[2] G. Aragay, J. Pons, A. Merkoci, Chem. Reviews **2011,** 111, 3433.

[3] M.F. Philips, A.I. Gopalan, K.-P. Lee, J. of Hazardous Materials **2012**, 237, 46.

[4] X.D. Xie, D. Stueben, Z. Berner, Anal. Lett. **2005**, 38, 2281.

[5] J. Buffle, M.L. Tercier-Waeber, Trac-Trends in Anal. Chem. **2005**, 24, 172.

[6] European Comission, in "Directive 2008/105/EC on environmental quality standards in the field of water policy, amending and subsequently repealing Council Directives 82/176/EEC, 83/513/EEC, 84/156/EEC, 84/491/EEC, 86/280/EEC and amending Directive 2000/60/EC" **2008**.

[7] EPA, in "National Recommended Water Quality Criteria. United States Environmental Protection Agency, Office of Water/ Office of Science and Technology" **2009**.

[8] J. Morton, N. Havens, A. Mugweru, A.K. Wanekaya, Electroanalysis **2009**, 21, 1597.

[9] A. Afkhami, H. Bagheri, H. Khoshsafar, M. Saber-Tehrani, M. Tabatabaee, A. Shirzadmehr, Anal. Chim. Acta **2012**, 746, 98.

[10] D. Stankovic, D. Manojlovic, G. Roglic, S. Kostic-Rajacic, I. Andjelkovic, B. Dojcinovic, J. Mutic, Electroanalysis **2011**, 23, 1928.

[11] M. Esteban, C. Arino, J.M. Diaz-Cruz, Trac-Trends in Anal. Chem. **2006**, 25, 86.

[12] M. Esteban, C. Arino, J.M. Diaz-Cruz, Critical Rev. in Anal. Chem. **2006**, 36, 295.

[13] S.A. Ozkan, Current Pharmaceutical Analysis **2009**, 5, 127.

[14] K.Z. Brainina, N.A. Malakhova, N.Y. Stojko, Fresenius J. of Anal. Chem. **2000**, 368, 307.

[15] G. Henze, Monograph Metrohm: Introduction to polarography and voltammetry **2003**, pp. 11-16.

[16] E.P. Achterberg, C. Braungardt, Anal. Chim. Acta **1999**, 400, 381.

[17] R.K Beebe., R.J. Pell, M.B Seasholtz, Chemometrics: A Pratical Guide, Wiley-Interscience Publication **1998**, chapter 5.

[18] L.A. Fonseca de Godoy, L.W. Hantao, M.P. Pedroso, R.J. Poppi, F. Augusto, Anal. Chim. Acta **2011**, 699, 120.

[19] T. Azzouz, R. Tauler, Talanta **2008**, 74, 1201.

[20] R. Tauler, A. Izquierdoridorsa, E. Casassas, Chemom. and Intell. Lab. Syst. **1993**, 18, 293.

[21] R. Tauler, A. Smilde, B. Kowalski, J. of Chemom. **1995**, 9, 31.

[22] J. Jaumot, R. Gargallo, A. de Juan, R. Tauler, Chemom. and Intell. Lab. Syst. **2005**, 76, 101.

[23] M.C. Antunes, J.E.J. Simao, A.C. Duarte, R. Tauler, Analyst **2002**, 127, 809.

[24] H.C. Goicoechea, A.C. Olivieri, R. Tauler, Analyst **2010**, 135, 636.

[25] A. Jayaraman, S. Mas, R. Tauler, A. de Juan, J. of chromatog. B **2012**, 910 138.

[26] M. De Luca, G. Ioele, S. Mas, R. Tauler, G. Ragno, Analyst **2012**, 137, 5428.

[27] G. Herzog, D.W.M. Arrigan, Trac-Trends in Anal. Chem. **2005**, 24, 208.

[28] U. Injang, P. Noyrod, W. Siangproh, W. Dungchai, S. Motomizu, O. Chailapakul, Anal. Chim. Acta **2010**, 668, 54.

[29] R.T. Kachoosangi, C.E. Banks, X. Ji, R.G. Compton, Anal. Scien. **2007**, 23, 283.

[30] C. Kokkinos, A. Economou, I. Raptis, C.E. Efstathiou, Electrochim. Acta, **2008**, 53, 5294.

[31] J. Wang, Electroanalysis **2005**, 17, 1341.

[32] Z.D. Anastasiadou, I. Sipaki, P.D. Jannakoudakis, S.T. Girousi, Anal. Lett. **2011**, 44, 761.

[33] V. Rehacek, I. Hotovy, M. Vojs, T. Kups, L. Spiess, Electrochim. Acta **2012**, 63, 192.

[34] H. Xu, L. Zeng, D. Huang, Y. Man, L. Jin, Food Chem. **2008**, 109, 834.

[35] N.B. Li, W.W. Zhu, J.H. Luo, H.Q. Luo, Analyst **2012**, 137, 614.

[36] J. Wang, J.M. Lu, S.B. Hocevar, P.A.M. Farias, B. Ogorevc, Anal. Chem. **2000**, 72, 3218.

[37] C. Kyrisoglou, A. Economou, C.E. Efstathiou, Electroanalysis **2012**, 24, 1825.

[38] K.C. Armstrong, C.E. Tatum, R.N. Dansby-Sparks, J.Q. Chambers, Z.-L. Xue, Talanta **2010**, 82, 675.

[39] S.B. Hocevar, I. Svancara, K. Vytras, B. Ogorevc, Electrochim. Acta **2005**, 51, 706.

[40] G.-J. Lee, C.K. Kim, M.K. Lee, C.K. Rhee, Electroanalysis **2010**, 22, 530.

[41] M.T. Castaneda, B. Perez, M. Pumera, M. del Valle, A. Merkoci, S. Alegret, Analyst **2005**, 130, 971.

[42] A. Economou, Trac-Trends in Anal. Chem. **2005**, 24, 334.

[43] I. Svancara, C. Prior, S.B. Hocevar, J. Wang, Electroanalysis **2010**, 22, 1405.

[44] A. Economou, A. Voulgaropoulos, Talanta **2007**, 71, 758.

[45] I. Adraoui, M.E. Rhazi, A. Amine, Anal. Lett. **2007**, 40, 349.

[46] V. Guzsvany, H. Nakajima, N. Soh, K. Nakano, I. Svancara, K. Vytras, L. Bjelica, T. Imato, Electroanalysis **2011**, 23, 1593.

[47] S. Chuanuwatanakul, W. Dungchai, O. Chailapakul, S. Motomizu, Anal. Scien. **2008**, 24, 589.

[48] G. Kefala, A. Economou, Anal. Chim. Acta **2006**, 576, 283.

[49] L. Chen, Z. Su, X. He, Y. Liu, C. Qin, Y. Zhou, Z. Li, L. Wang, Q. Xie, S. Yao, Electrochem. Commun. **2012**, 15, 34.

[50] H. Li, J. Li, Z. Yang, Q. Xu, C. Hou, J. Peng, X. Hu, J. of Hazardous Materials **2011**, 191, 26.

[51] X. He, Z. Su, Q. Xie, C. Chen, Y. Fu, L. Chen, Y. Liu, M. Ma, L. Deng, D. Qin, Y. Luo, S. Yao, Microchim. Acta **2011**, 173, 95.

[52] I. Cesarino, C. Gouveia-Caridade, R. Pauliukaite, E.T.G. Cavalheiro, C.M.A. Brett, Electroanalysis **2010**, 22, 1437.

[53] N. Serrano, J. Manuel Diaz-Cruz, C. Arino, M. Esteban, Electroanalysis **2010**, 22, 1460.

[54] D. Li, J. Jia, J. Wang, Talanta **2010**, 83, 332.

[55] Z.D. Anastasiadou, P.D. Jannakoudakis, S.T. Girousi, Central European J. of Chem. **2010**, 8, 999.

[56] L. Luo, X. Wang, Y. Ding, Q. Li, J. Jia, D. Deng, Applied Clay Scien. **2010**, 50, 154.

[57] Z.M. Wang, H.W. Guo, E. Liu, G.C. Yang, N.W. Khun, Electroanalysis **2010**, 22, 209.

[58] J. Li, S. Guo, Y. Zhai, E. Wang, Anal. Chim. Acta **2009**, 649, 196.

[59] W. Deng, Y. Tan, Z. Fang, Q. Xie, Y. Li, X. Liang, S. Yao, Electroanalysis **2009**, 21, 2477.

[60] M.E.A. Ghanjaoui, M. Srij, M. El Rhazi, Anal. Lett. **2009**, 42, 1294.

[61] H. Xu, L. Zeng, S. Xing, Y. Xian, G. Shi, Electroanalysis **2008**, 20, 2655.

[62] B. Liu, L. Lu, M. Wang, Y. Zi, Electroanalysis **2008**, 20, 2363.

[63] Y. Wu, N.B. Li, H.Q. Luo, Sen. and Actuat. B-Chemical **2008**, 133, 677.

[64] K.E. Toghill, G.G. Wildgoose, A. Moshar, C. Mulcahy, R.G. Compton, Electroanalysis **2008**, 20, 1731.

[65] G.H. Hwang, W.K. Han, J.S. Park, S.G. Kang, Talanta **2008**, 76, 301.

[66] N. Wang, X. Dong, Anal. Lett. **2008**, 41, 1267.

[67] F. Torma, M. Kadar, K. Toth, E. Tatar, Anal. Chim. Acta **2008**, 619, 173.

[68] J. Jia, L. Cao, Z. Wang, Electroanalysis **2007**, 19, 1845.

[69] W.W. Zhu, N.B. Li, H.Q. Luo, Anal. Lett. **2006**, 39, 2273.

[70] U. Anik, S. Marin, M. Pumera, A. Merkoci, S. Alegret, Electroanalysis **2005**, 17, 881.

[71] G. Kefala, A. Economou, A. Voulgaropoulos, Analyst **2004**, 129, 1082.

[72] D. Demetriades, A. Economou, A. Voulgaropoulos, Anal. Chim. Acta **2004**, 519, 167.

[73] M. Morfobos, A. Economou, A. Voulgaropoulos, Anal. Chim. Acta **2004**, 519, 57.

[74] E.A. Hutton, S.B. Hocevar, B. Ogorevc, M.R. Smyth, Electrochem. Commun. **2003**, 5, 765.

[75] A.M.O. Brett, C.M.A. Brett, Electroquimica: Principios, metodos, e aplicacoes, Almedina Ed. **1993**, pp. 143-147.

[76] S. Daniele, M.A. Baldo, C. Bragato, Current Anal. Chem. **2008**, 4, 215.

[77] M. Lu, K.E. Toghill, R.G. Compton, Electroanalysis **2011**, 23, 1089.

[78] R.A.A. Munoz, L. Angnes, Microchem. J. **2004**, 77, 157.

[79] C. Locatelli, Anal. Methods **2010**, 2, 1784.

[80] E.M. Ghoneim, Talanta **2010**, 82, 646.

[81] O. Mikkelsen, S.M. Skogvold, K.H. Schroder, M.I. Gjerde, T.A. Aarhaug, Anal. and Bioanal. Chem. 2003, 377, 322.

[82] A. Afkhami, T. Madrakian, S.J. Sabounchei, M. Rezaei, S. Samiee, M. Pourshahbaz, Sens. and Actuat. B-Chemical **2012**, 161, 542.

[83] A.M. Beltagi, E.M. Ghoneim, M.M. Ghoneim, Int. J. of Environm. Anal. Chem. **2011**, 91, 17.

[84] V.S. Somerset, L.H. Hernandez, E.I. Iwuoha, J. of Environm, Scien. and Health Part A **2011**, 46, 17.

[85] C. Vedhi, G. Selvanathan, P. Arumugam, P. Manisankar, Ionics **2009**. 15, 377.

[86] A. Afkhami, F. Soltani-Felehgari, T. Madrakian, H. Ghaedi, M. Rezaeivala, Anal. Chim. Acta **2013**, 771, 21.

[87] A. Afkhami, H. Ghaedi, T. Madrakian, M. Rezaeivala, Electrochim. Acta, **2013**, 89, 377.

[88] S. Prakash, V. K. Shahi, Anal. Methods **2011**, 3, 2134.

[89] R.G. Kempegowda, P. Malingappa, Anal. Chim. Acta **2012**, 728, 9.

[90] Y. Wei, R. Yang, X.-Y. Yu, L. Wang, J.-H. Liu, X.-J. Huang, Analyst **2012**, 137, 2183.

[91] T. Sheela, S. Basavanna, R. Viswanatha, H.C.B. Kalachar, Y.A. Naik, Electroanalysis **2011**, 23, 1150.

[92] Z. Wang, E. Liu, X. Zhao, Thin Solid Films **2011**, 519, 5285.

[93] E. Czop, A. Economou, A. Bobrowski, Electrochim. Acta **2011**, 56, 2206.

[94] M.B. Gholivand, A. Azadbakht, A. Pashabadi, Electroanalysis **2011**, 23, 364.

[95] L. Fan, J. Chen, S. Zhu, M. Wang, G. Xu, Electrochem. Commun. **2009**, 11, 1823.

[96] L. Zou, Y. Zhang, H. Qin, B. Ye, Electroanalysis **2009**, 21, 2563.

[97] Y.Q. Tian, N.B. Li, H.Q. Luo, Electroanalysis **2009**, 21, 2584.

[98] Y. Li, X. Liu, X. Zeng, Y. Liu, X. Liu, W. Wei, S. Luo, Sens, and Act. B-Chem. **2009**, 139, 604.

[99] B.K. Jena, C.R. Raj, Anal. Chem. **2008**, 80, 4836.

[100] I. Cesarino, G. Marino, J. do Rosario Matos, E.T. Gomes Cavalheiro, Talanta **2008**, 75, 15.

[101] O. El Tall, N. Jaffrezic-Renault, M. Sigaud, O. Vittori, Electroanalysis **2007**, 19, 1152.

[102] E. Chow, D. Ebrahimi, J.J. Gooding, D.B. Hibbert, Analyst **2006**, 131, 1051.

[103] X.H. Gao, W.Z. Wei, L. Yang, T.J. Yin, Y. Wang, Anal. Lett. **2005**, 38, 2327.

[104] W. Yantasee, Y.H. Lin, G.E. Fryxell, B.J. Busche, Anal. Chim. Acta **2004**, 502, 207.

[105] S. Yuan, W.H. Chen, S.H. Hu, Talanta **2004**, 64, 922.

[106] C.G. Hu, K.B. Wu, X. Dai, S.S. Hu, Talanta **2003**, 60, 17.

[107] K.B. Wu, S.S. Hu, J.J. Fei, W. Bai, Anal. Chim. Acta **2003**, 489, 215.

[108] X.-J. Huang, A.M. O'Mahony, R.G. Compton, Small **2009**, 5, 776.

[109] K. Stulik, C. Amatore, K. Holub, V. Marecek, W. Kutner, Pure and Appl. Chem. **2000**, 72, 1483.

[110] L. Nyholm, G. Wikmark, Anal. Chim. Acta **1992**, 257, 7.

[111] I. Pizeta, G. Billon, J.C. Fischer, M. Wartel, Electroanalysis **2003**, 15, 1389.

[112] A.P.R. de Souza, M.O. Salles, E.S. Braga, M. Bertotti, Electroanalysis **2011**, 23, 2511.

[113] L. Baldrianova, I. Svancara, S. Sotiropoulos, Anal. Chim. Acta **2007**, 599, 249.

[114] L. Baldrianova, I. Svancara, A. Economou, S. Sotiropoulos, Anal. Chim. Acta **2006**, 580, 24.

[115] E.A. Hutton, B. Ogorevc, S.B. Hocevar, M.R. Smyth, Anal. Chim. Acta **2006**, 557, 57.

[116] J. Wang, C. Bian, J. Tong, J. Sun, S. Xia, Thin Solid Films **2012**, 520, 6658.

[117] J. Wang, C. Bian, J. Tong, J. Sun, S. Xia, Electroanalysis **2012**, 24, 1783.

[118] P. Salaun, C.M.G. van den Berg, Anal. Chem. **2006**, 78, 5052.

Chapter 2

SIMULTANEOUS DETERMINATION OF COPPER, LEAD AND ZINC AT A BISMUTH FILM ELECTRODE BY MULTIVARIATE CALIBRATION [1]

Graphical abstract

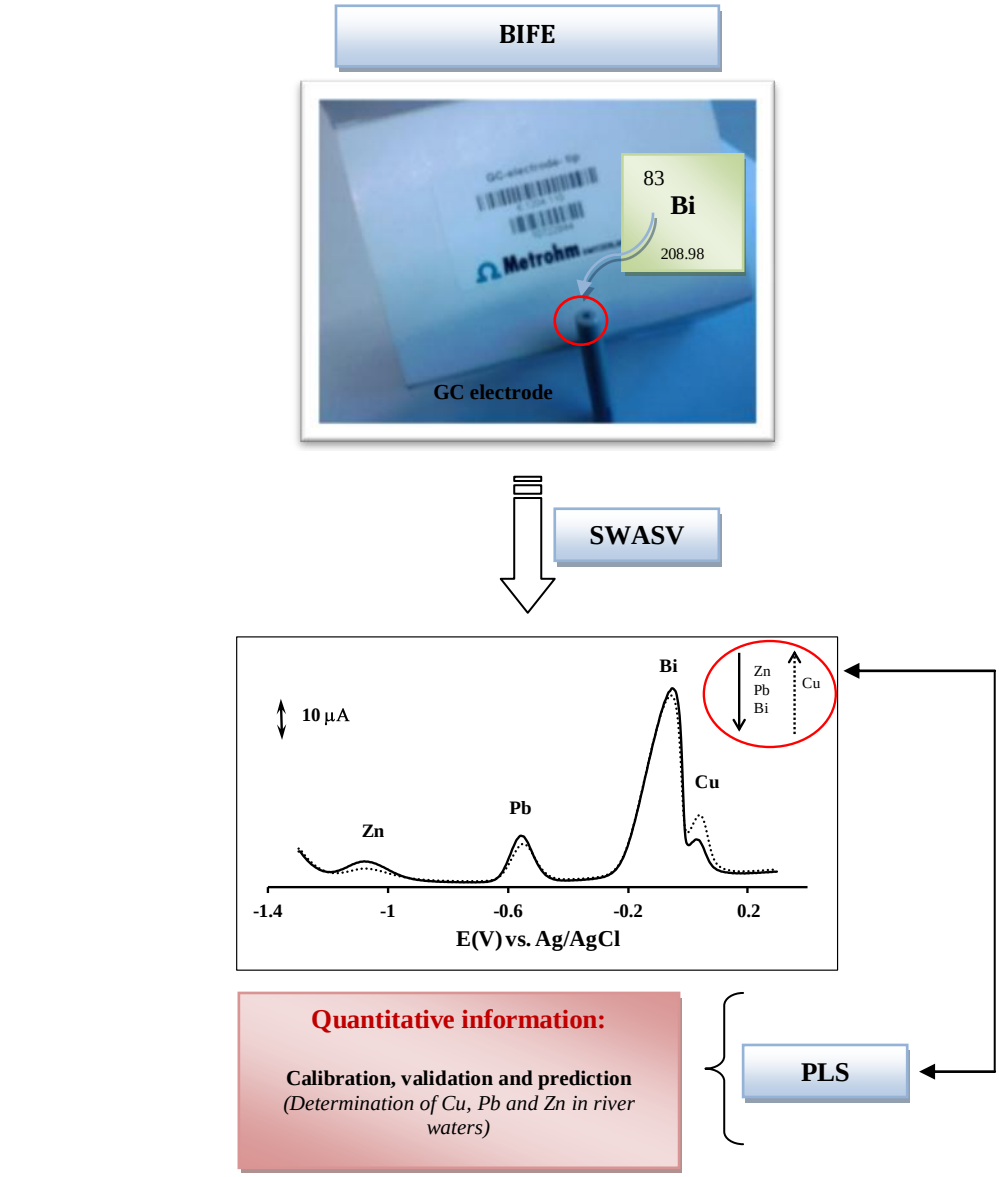

[1]Electroanalysis 2011, 23, 1410 – 1417

Abstract

In this work, simultaneous determination of Cu, Pb and Zn metal ions at low concentration levels (μgL^{-1}) by SWASV on a bismuth film electrode plated *in-situ* at a GC electrode is described. A chemometric approach was used to overcome the overlapping peaks of Cu and Bi metal ions, the competition of the electrodeposited Cu and Bi for the surface of the GC electrode and the formation of Cu-Zn intermetallic compounds. The construction of the multivariate calibration models, based on PLS regression, allowed the simultaneous determination of Cu (in the concentration range 8.0 to 20.1 μgL^{-1}), Pb (2.0 to 30.0 μgL^{-1}) and Zn (29.7 to 90.4 μgL^{-1}) with most of the prediction errors obtained in the external validation set for the three models lower than 11, 16 and 26%, respectively.

Finally, this method was used for the determination of these trace metal ions in surface river water samples with satisfactory results (errors below 10, 5 and 32% for Cu, Pb and Zn, respectively).

2.1. Introduction

Stripping techniques [1] are particularly suitable for the determination of trace metals in environmental water samples [2,3] due to their excellent DLs, sensitivity to the presence of different metal species, capacity to multi-element determinations and relatively low cost.

Mercury electrodes have been the most used WEs for electroanalytical purposes due to their wide cathodic range. However, due to environmental concerns, the development of alternative electrode materials is a subject of research nowadays [4–11]. Many studies have demonstrated the applicability of the BiFEs [9–11] as a possible alternative for electrochemical stripping analysis of trace heavy metals avoiding the use of mercury. Several attractive properties of the bismuth coated electrode include the simple *in-situ* preparation, high sensitivity, well defined and undistorted stripping signal and excellent resolution (of neighbouring peaks). Bismuth is also a more "environmentally-friendly" metal with a very low toxicity and less sensitive to oxygen (depending on the pH) than mercury electrodes.

Usually, metal ions with a stripping potential more negative than Bi are determined using BiFEs; it is also possible to determine Cu [12–19] and Hg [19] metal ions. However, determination of Cu on a BiFE [12–19] is usually prone to errors due to the partial overlapping of the Cu and Bi stripping peaks. Three different strategies have been proposed in the literature to overcome this limitation; specifically, (i) sequential determination of Cu at a GC electrode followed by the determination of other metals after addition of Bi [17,18], (ii) the addition of Ga^{3+} [12–14] or (iii) hydrogen peroxide [15,16]. Besides the difficulties related to the analytical determination of Cu, the interference of this metal ion on the determination of other trace metals using BiFEs has seldom been addressed [12,20]. Stripping voltammetry at mercury electrodes is prone to errors due to the formation of intermetallic Cu-Zn compounds [1, 21–23] in the mercury phase. The formation of these compounds in mercury electrodes is an equilibrium reaction and its importance increases with increasing metal concentration both in mercury and in solution phases [22]. A similar error has been observed on a BiFE

[12,20]; to overcome the problems related to the determination of Zn, addition of a masking reagent for Cu [20] gallium (Ga^{3+}) ions to form a preferential Cu-Ga intermetallic compound [12] have been suggested. However, the analysis of the literature shows that none of these approaches allows the simultaneous determination of Cu and Zn, as it was previously observed for mercury electrodes [21]. Furthermore, besides the formation of intermetallic compounds, the deposition potential for Cu is more anodic than for Bi; therefore, competition between the two metal ions for the surface of the GC electrode may occur, which can influence the deposition of other trace metal ions at the bismuth film [20].

Simultaneous determination of several metal ions is often complex because different metal ions undergo oxidation or reduction at close potential values leading to peak overlapping. In addition, interference due to the formation of intermetallic compounds, may also occur. Chemometric analysis offers several tools, for example, experimental design and PLS regression [24–35] to overcome these limitations in electroanalysis [35–41]. In this work, a chemometric approach, based on PLS multivariate calibration models was used to overcome the limitations of the BiFE electrode for simultaneous determination of Cu, Pb and Zn metal ions.

2.2. Experimental

2.2.1. Reagents and solutions

All reagents used were of analytical grade and purchased from Merck unless stated otherwise. Ultrapure water (18.2 $M\Omega cm^{-1}$), obtained from Millipore Direct-Q system, was used throughout. Working metal ion solutions were prepared from atomic absorption standard solutions [copper nitrate ($Cu(NO_3)_2$), zinc nitrate ($Zn(NO_3)_2$), cadmium nitrate ($Cd(NO_3)_2$) and bismuth nitrate ($Bi(NO_3)_3$) 1000 mgL^{-1} and lead nitrate ($Pb(NO_3)_2$) 2000 mgL^{-1}] after appropriate dilution with ultrapure water. A 0.1 $molL^{-1}$ acetate buffer stock solution (pH 4.5), prepared by mixing appropriate amounts of glacial acetic acid (100%) and sodium acetate (cryst. extra pure), was used as the supporting electrolyte. A 1.0 $molL^{-1}$

acetate buffer solution with pH 4.5 was also prepared and used for dilution of the surface water samples for electrochemical determination of the trace metals.

All material used for solutions preparations, as well as, electrochemical cells, were previously decontaminated. For this purpose, the material remained at least 2 h in a solution of 20 % nitric acid.

2.2.2. Instrumentation

Stripping voltammetric measurements were performed using a modular electrochemical workstation [microAutolab (Eco Chemie, Utrecht, The Netherlands) driven by the GPES 4.5 software (Eco Chemie) with IME 663 interface and a 663 VA stand from Metrohm]. A bismuth coated rotating GC disk (2 mm in diameter) electrode (6.1204.110 Metrohm) served as the WE, with an Ag/AgCl (sat. 3 M KCl) and a carbon road (6.1247.000 Metrohm) acting as the RE (all potential values are given *versus* Ag/AgCl RE) and CE, respectively. All measurements were carried out at room temperature in a 10 mL voltammetric cell.

All pH measurements were performed with a pH Meter GPL 22 with a 52 02 pH electrode from Crison.

For atomic absorption spectroscopy with electrotermal atomization (AAS-EA) measurements of Pb and Cu, a Perkin Elmer 600 AAnalyst atomic absorption spectrometer was used in combination with the transversely-heated graphite atomizer (THGA) furnace and the AS-800 autosampler module. Zn was determined by atomic absorption spectroscopy with flame atomization (AAS-FA) with an AAnalyst 400 from Perkin Elmer.

2.2.3. Preparation of the bismuth film electrode and measurement procedure

Square wave anodic stripping voltammetric measurements were performed by *in-situ* deposition of the Bi and the target metals in the presence of dissolved oxygen. Prior to use, the GC electrode, which served as the substrate electrode for

all experiments, was polished with polishing set 6.2802.000 from Metrohm and then rinsed thoroughly with ultrapure water. The three electrodes were immersed into the voltammetric cell, containing 0.1 $molL^{-1}$ acetate buffer (pH 4.5) and 500 μgL^{-1} of Bi and the target metals. The deposition potential (E_{dep}) of -1.3 V was applied for 120 s and the WE rotation speed was kept at 1500 rpm. Following the deposition step, rotation of the WE was stopped and after 10 s of t_{eq}, the voltammograms were recorded by applying a positive going square wave voltammetric potential scan from -1.3 to +0.3 V. Prior to each measurement, a 30 s conditioning step at +0.3 V was used in order to clean the substrate electrode surface.

2.2.4. Software, experimental design and multivariate calibration models

For the calculation of PLS multivariate calibration models, the PLS-Toolbox 5.5. chemometrics software from Eigenvector Research Inc with Matlab from MathWorks, was used.

The composition of the samples used for the construction of PLS multivariate calibration models, in the concentration ranges, 8.0 to 20.1, 2.0 to 30.0 and 29,7 to 90.4 μgL^{-1}, for Cu, Pb and Zn respectively, is summarized in table 2.1. The concentration of the three metal ions in the calibration set samples was designed according to a circumscribed central composite design (samples 1 to 15 in Table 2.1); to this design, six samples with composition designed according to a star design (samples 16 to 21 in Table 2.1) were added. Three independent determinations of the centre point of this design (sample 1 in Table 2.1) were assayed. For model building, the voltammogram obtained in the absence of the trace metal ions was also included in the calibration set. The external validation set was constituted by 12 samples (samples 22 to 33 in Table 2.1). The experiments corresponding to the calibration and the external validation sets were assayed separately; within each set, the samples were assayed randomly. For each sample, two voltammograms were obtained.

For the construction of the PLS calibration models, full cross-validation (leave one out) was used. Further validation of the models was carried out using external validation test set samples (see composition in Table 2.1).

2.2.5. Analysis of surface water samples

Three river water samples, designated as A, B and C, were collected, filtered, acidified to pH 2 with ultrapure HNO_3 and stored in the refrigerator. For the electrochemical determination of the metals, samples were buffered with acetate to pH 4.5. The voltammetric analysis was carried out as described above (see Section 2.2.3). The same water samples were also analyzed by AAS (Cu and Pb by AAS-EA and Zn by AAS-FA), which was used as a reference method.

Table 2.1 – Composition of the samples used for PLS calibration model building.

Sample	[Cu] /μgL^{-1}	[Pb] /μgL^{-1}	[Zn] /μgL^{-1}
Calibration set			
1	14.0	16.0	60.1
2	14.0	30.0	60.0
3	14.0	2.0	60.0
4	10.4	7.7	41.6
5	17.6	7.7	77.5
6	14.0	16.0	90.4
7	10.4	24.3	42.8
8	20.1	16.0	59.7
9	17.6	24.2	41.5
10	17.6	24.1	78.0
11	10.4	7.7	78.1
12	14.0	16.0	29.7
13	17.6	7.7	42.3
14	8.0	16.0	60.5
15	10.4	24.2	77.6
16	10.4	16.0	60.4
17	14.0	24.2	60.0
18	14.0	16.0	78.1
19	14.0	7.7	59.7
20	14.0	16.0	42.1
21	17.6	16.1	59.9
External validation Set			
22	12.5	11.0	63.4
23	14.4	19.2	69.3
24	12.6	16.8	51.6
25	14.4	11.9	50.8
26	12.2	16.0	70.7
27	14.7	20.2	49.4
28	15.4	12.7	64.0
29	15.8	17.6	53.3
30	11.8	20.2	61.9
31	14.0	11.0	67.1
32	16.2	20.8	59.7
33	15.4	17.7	69.4

2.3. Results and Discussion

2.3.1. Response of the bismuth film electrode to the metals

The SWASV parameters, which affect the response (frequency, step potential and pulse amplitude), were optimized univariantly using a solution containing 20 μgL^{-1} of Zn and 10 $\mu gL^{-1}$of Cd and Pb in 0.1 $molL^{-1}$ acetate buffer (pH 4.5). Based on the results obtained in these experiments, the square wave frequency was fixed to 80 Hz and the step potential and the pulse amplitude were fixed to 5 and 60 mV, respectively.

Independent calibrations for Cu, Pb, Cd and Zn were performed on a BiFE and the results obtained are summarized in table 2.2. Among the four metals studied, the electrode showed the lowest sensitivity of response towards Zn. The slope of the calibration curve, in the concentration range 20 to 200 μgL^{-1} of Zn was 195 $nA\mu g^{-1}L$ and the DL, calculated with the aid of a section of the calibration curves close to the origin and using both the slope and the standard deviation of y-residuals (Sy/x) [42], was 11 μgL^{-1}.

The electrode showed linear response to Cd in the range 2 to 80 μgL^{-1}, with a slope of 351 $nA\mu g^{-1}L$ ($r^2 = 0.9996$). The DL [42] for Cd was 2 μgL^{-1}; this value is above the values recommended by EU [43] commission and EPA [44] from USA for freshwaters.

For Pb, two linear ranges of response were identified, between 1 and 10 μgL^{-1} with a slope of response of 218 $nA\mu g^{-1}L$ ($r^2 = 0.997$), and between 10 and 100 μgL^{-1} with a slope of 626 $nA\mu g^{-1}L$ ($r^2 = 0.991$); the DL [42] was 0.7 μgL^{-1}.

The relative standard deviations (RSDs) (n = 7) in percentage of the response for a mixture of 20, 10 and 10 μgL^{-1} of Zn, Cd and Pb were 9.9, 5.5 and 7.2%, respectively. The peak for Cu is partially overlapped with the Bi peak; due to this reason, the DL [42] towards Cu was 2 μgL^{-1} despite of the value of the response slope, 840 $nA\mu g^{-1}L$.

For the analytical characteristics of the electrode towards Cu, Pb, Cd and Zn metal ions, the results obtained in this work for ASV determination of these metal ions using *in-situ* platted BiFE on carbon electrodes are comparable to those described in the literature [12, 45–49]. The comparison between the DLs obtained in this work for Cu, Pb, Cd and Zn, using univariate calibration, and the values recommended by EU [43] commission and EPA [44] from USA suggest that BiFE has potentialities for being used in the environmental monitoring of Cu, Pb and Zn in fresh waters.

According to the literature [12], Cu is a severe interference in the determination of Zn due to the formation of intermetallic compounds. In a BiFE case, besides this source of interference, Cu ion also competes with bismuth in the deposition step [12]; this fact is evident from the voltammograms obtained [12], which show a decrease of the Bi peak height with the increasing concentration of Cu. For these reasons, the interference of Cu on the response towards the other metals was studied. The voltammograms presented in figure 2.1 (A) were obtained for 200 μgL^{-1} of Zn without (curve a) and with increasing concentration of Cu (curves b to d); these voltammograms show that this metal produces simultaneously an increase of the Cu peak and a successive decrease of the Bi and Zn peaks; after addition of 20 and 40 μgL^{-1} of Cu, the peak of Zn is limited to 10% of its initial value and almost suppressed, respectively.

Results obtained in an identical experiment using the optimized SWASV parameters with 60 μgL^{-1} of Zn [Figure 2.1 (B)] showed that the peak current for this metal is reduced to 23% of its initial value upon addition of 15 μgL^{-1} of Cu. Additionally, the Cu peak was well defined only for concentrations above 15 μgL^{-1} of Cu; for Cu concentrations bellow this value, the Bi and Cu peaks were overlapped. The influence of Cu on Pb peak is also observed [20]. The voltammograms in figure 2.1 (C) show the effect of this metal on the peak obtained for 24 and 78 μgL^{-1} of Pb and Zn respectively, in the presence of 10 and 18 μgL^{-1} of Cu. Also, in this case, a decrease of Pb and Zn peak currents with increasing concentration of Cu was observed.

These results evidence that the presence of Cu is a severe interference on the determination of both Zn and Pb on a BiFE. This fact limits simultaneous determination of the three metal ions using univariate calibration. Due to this reason, we decided to evaluate the potentialities of PLS calibration models to minimize the interference of Cu in Pb and Zn determinations.

Table 2.2 – Analytical figures of merit of BiFE electrode for the determination of the metals studied.

Metals	**r^2**	**Sensitivity[a] /nAμg^{-1}L**	**Linear range /μgL^{-1}**	**Intercept[a] /nA**	**DL[b] /μgL^{-1}**
Cu	0.994	840 ± 22	8 – 30	-2251 ± 438	2
Pb	0.997	218 ± 6	1 – 10	8 ± 34	0.7
	0.991	626 ± 25	10-100	-6862 ± 1328	
Cd	0.9996	351 ± 3	2 – 80	-408 ± 96	2
Zn	0.997	195 ± 4	20 – 200	34 ± 460	11

[a] Standard error; [b] Detection limits were calculated from calibration curves.

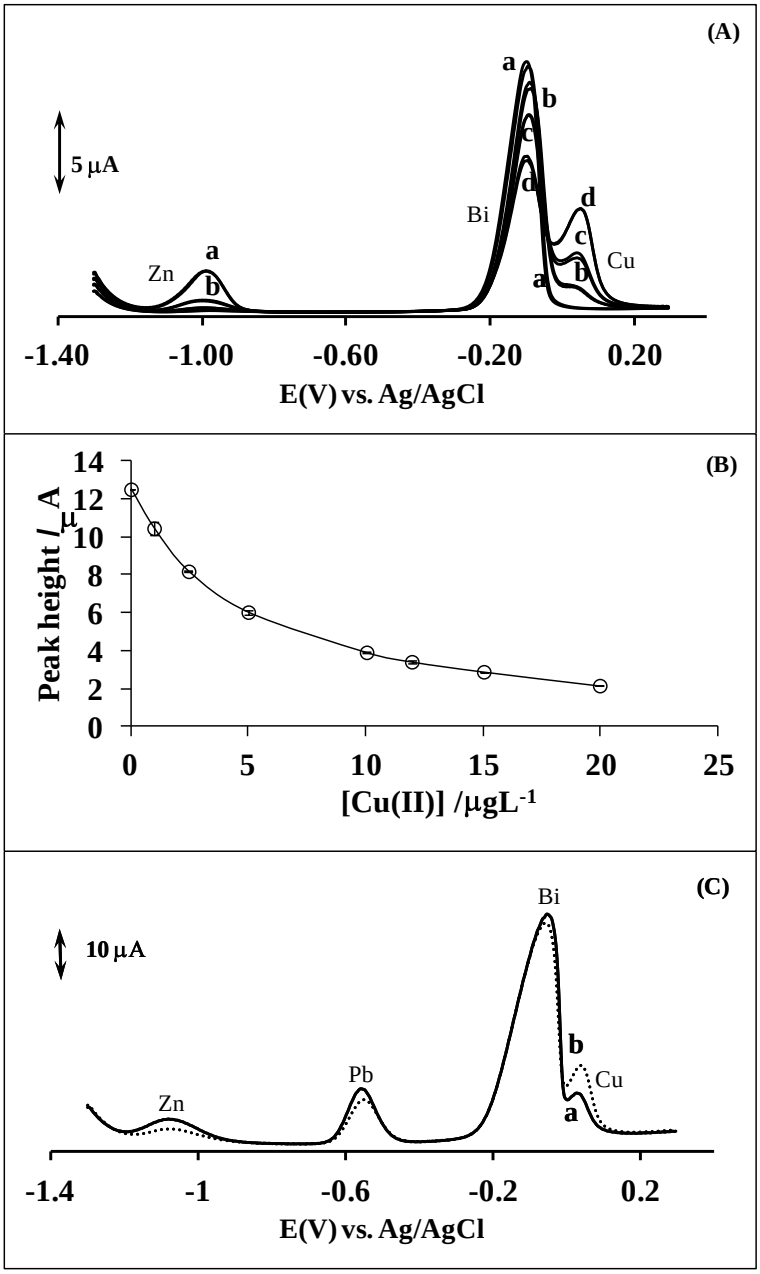

Figure 2.1 – **(A)** SWASV: voltammograms obtained for 200 μgL^{-1} of Zn (curve a) and 9.7 (curve b), 20.3 (curve c) and 39.6 μgL^{-1} (curve d) of Cu (frequency 20 Hz, step potential 5 mV and pulse amplitude 25 mV); **(B)** Peak height for 60 μgL^{-1} Zn upon successive additions of Cu (frequency 80 Hz, step potential 5 mV and pulse amplitude 60 mV). This is an example of an experiment, which was repeated two times; Average and standard deviations (vertical errors bars) of two replicates are present (n = 2); where no error bars are shown, they are within the points**; (C)** SWASV: voltammograms obtained for 78 μgL^{-1} of Zn, 24 μgL^{-1} of Pb and 10 (curve a) or 18 μgL^{-1} (curve b) of Cu [same conditions as in Figure 2.1 (B)].

2.3.2. PLS calibration models

PLS regression allows the use of whole voltammogram to extract the relevant information related to each metal. In this work, three independent PLS calibration models were built, using whole voltammograms, respectively for Cu, Pb and Zn. Data preprocessing is a key step for PLS model building and a lot of preprocessing techniques have been developed [50,51] and designed in order to remove spectral variation not due to the parameter of interest or to enhance spectral selectivity towards the parameter of interest. In this work, data preprocessing consisted on the normalization and the autoscaling of the variables; for Zn calibration models, an additional preprocessing step, consisting of first derivative (Satvisky – Golay second order polynomial and bandwidth of 15 data point), was also used. Autoscaling was used due to the large differences among current intensities corresponding to the peaks of the metals [50] [for example, see the voltammograms in Figure 2.1 (A)] and normalization was used to minimize multiplicative effects [50,51], mainly related to the *in-situ* deposition of the bismuth film. First derivative of data for Zn calibration model was applied to remove additive baseline effects [51], which are more relevant in the cathodic region of the voltammogram.

The number of the LVs for the PLS models was initially chosen based on the root mean square error (RMSE) values of the calibration and cross- validation (see Figure 2.2). The criteria used for the selection consisted on minimizing the value of the cross-validation RMSE. Figure 2.2 shows that, for Pb and Zn, the number of LVs in the model must be lower than 7 whereas for Cu up to 11 LVs could be considered. In order to avoid over-fitting, the model was further validated considering the RMSE for an external test set (samples 22 to 33 in Table 2.1) models with 5, 6 and 3 LVs selected for Cu, Pb and Zn, respectively.

The explained variance of the PLS models built with this number of LVs (the variance captured on the independent variables appears between brackets) was as follows: 99.7% (90.3%) for Cu with 5 latent variables, 96.5% (94.3%) for Pb with 6 latent variables, and 89.1% (74.8%) for Zn with 3 latent variables. All

the explained variance values are higher than 89%, which implies the adequacy of the fitting.

For the three models, the variable importance in the projection (VIP) is presented in figure 2.3. This figure shows that the potentials for Cu, Bi and Zn peaks are the most important variables for Cu PLS model [Figure 2.3 (A)], whereas the VIP for Pb model corresponds to the potentials for Pb and Bi peaks [Figure 2.3 (B)]. The contributes of the variables in the projection for the Zn model [Figure 2.3 (C)] show mainly the contribution from Bi and from variables in the cathodic region of the voltammograms including the usual location of Zn peak.

The results obtained in the external validation set for the three models are summarized in table 2.3. This table shows a good prediction ability of the models for Cu and Pb with most of the prediction errors lower than 10%. The performance of the Zn model is worst and prediction errors up to 26% were obtained.

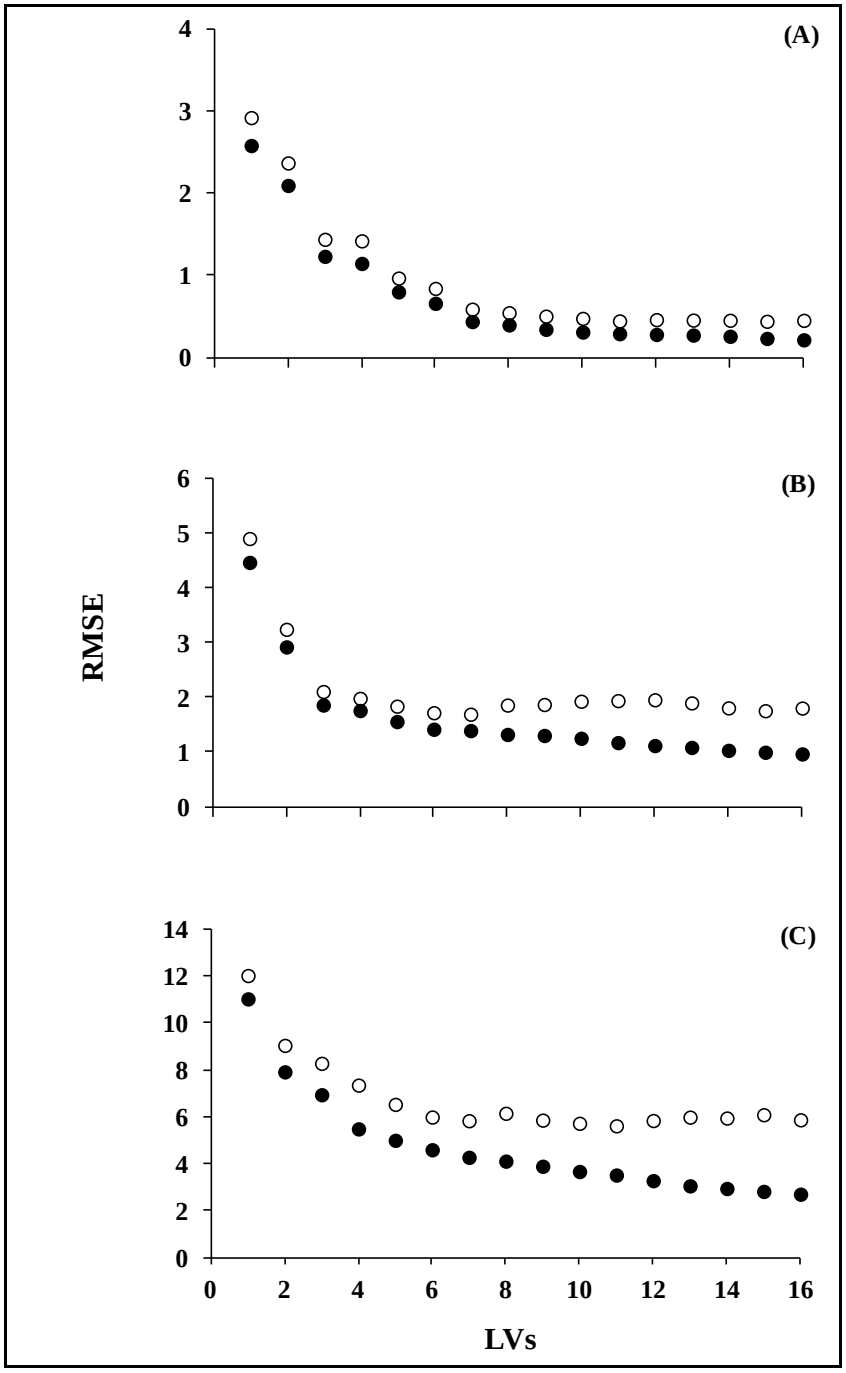

Figure 2.2 – Root mean squared error (RMSE) for calibration (●) and cross-validation (○) vs. the number of latent variables (LVs) in the PLS models for Cu (**A**), Pb (**B**) and Zn (**C**), obtained for model building with samples 1 to 21 in table 2.1.

Table 2.3 – Performance of the PLS calibration models in the external validation set samples: Cu, 5 LVs; Pb, 6 LVs; and Zn, 3 LVs.

Sample	Cu /μgL^{-1}			Pb /μgL^{-1}			Zn /μgL^{-1}		
	Expected	**Predicted**	**% Error**	**Expected**	**Predicted**	**% Error**	**Expected**	**Predicted**	**% Error**
22	12.5	12.4	-1.1	11.0	11.3	3.7	63.4	72.2	13.9
23	14.4	13.2	-8.6	19.2	18.9	-1.2	69.3	66.0	-4.8
24	12.6	13.8	9.2	16.8	18.2	8.1	51.6	56.0	8.5
25	14.4	15.6	8.5	11.9	11.2	-7.3	50.8	64.3	26.4
26	12.2	11.1	-9.3	16.0	16.8	5.3	70.7	73.9	4.5
27	14.7	14.9	1.3	20.2	21.3	5.5	49.4	61.1	23.5
28	15.4	15.5	0.7	12.7	12.7	0.1	64.0	65.0	1.5
29	15.8	15.8	0.0	17.6	19.3	9.9	53.3	58.8	10.3
30	11.8	12.1	2.8	20.2	22.2	10	61.9	65.1	5.2
31	14.0	12.5	-10.8	11.0	12.8	16.5	67.1	69.5	3.5
32	16.2	15.3	-5.8	20.8	19.3	7.2	59.7	68.0	13.9
33	15.4	13.8	-10.3	17.7	17.0	-3.7	69.4	68.2	-1.7

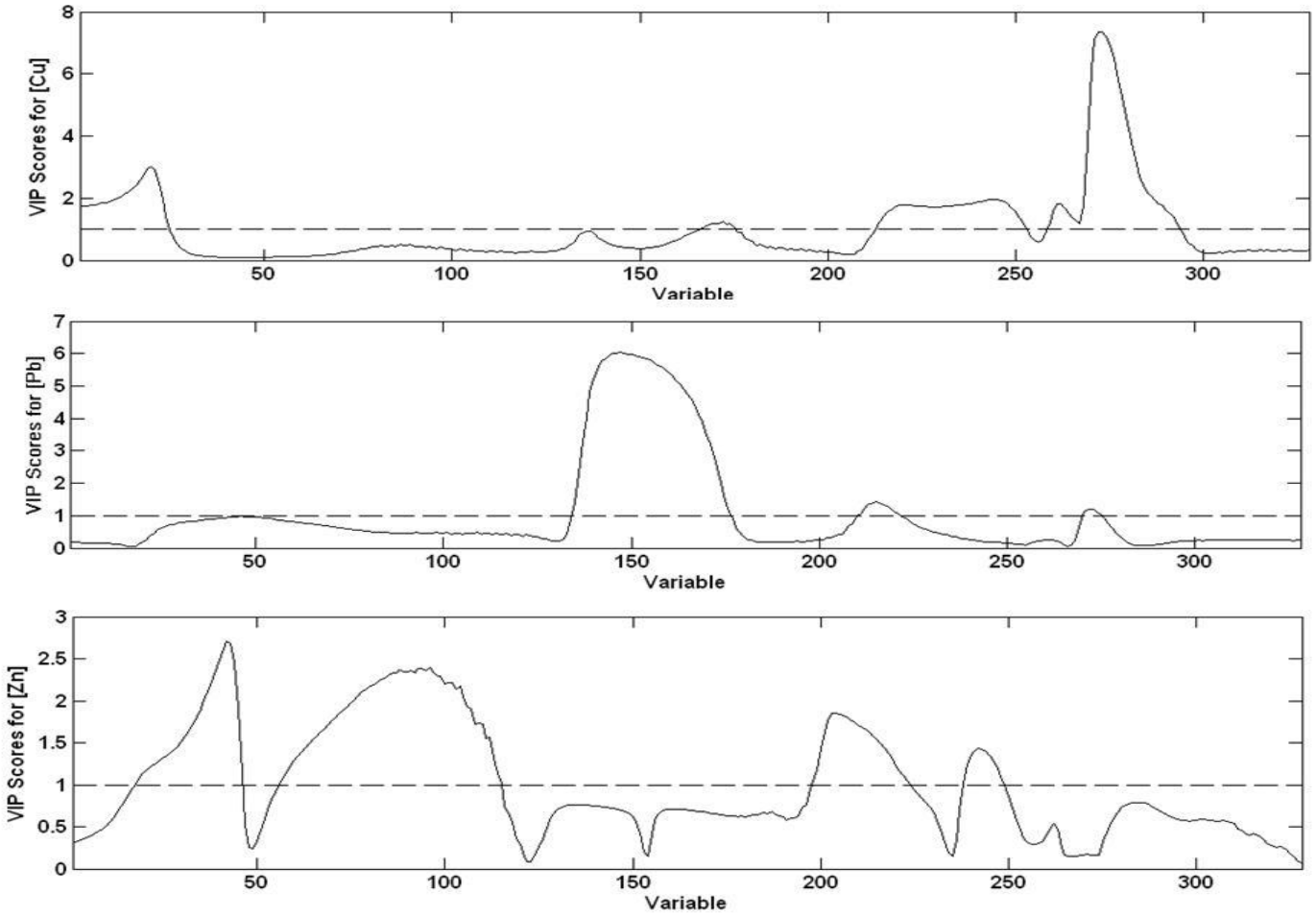

Figure 2.3 – Variable importance in the projection of the PLS calibration models for Cu (5 LVs), Pb (6 LVs) and Zn (3 LVs).

2.3.3. Analysis of Cu, Pb and Zn in the surface water samples

The concentrations of the three metal ions were determined in three surface river water samples (A, B and C) using a BiFE combined with the PLS calibration models. The results obtained were compared with those obtained by AAS (Table 2.4). A good agreement between the metal ion concentrations obtained by both methods was attained. In sample B, the concentration of Cu determined is much higher than the concentration measured by AAS-ET. This fact can be explained because the concentration of Cu is less than 8 μgL^{-1}, which was the minimum concentration of Cu used in the Cu PLS multivariate calibration model (Table 2.1).

The AAS results summarized in table 2.4 show that the concentration of Pb in the water samples were below or close to the lower limit of linear response range of the bismuth electrode. Therefore, in order to evaluate the prediction ability of the multivariate calibration models it was decided to fortify sample C with Pb. The results obtained (samples C1, C2 and C3 in Table 2.4) also show a good agreement between the metal concentrations obtained by both methods. To further test the calibration models, sample C was doped with Cu (samples C4 and C5 in Table 2.4). The analysis of the results show that increasing the concentration of Cu from 7.7 to 12.1 or 16.1 μgL^{-1} only influences the determination of Zn. Under these conditions, the concentration of this metal is underestimated by the PLS calibration model, a maximum relative error, ca. 32%, was obtained for 16 μgL^{-1} of Cu. Despite of this error in the determination of Zn, a significant improvement in the simultaneous determination of Zn and Cu, using the bismuth film electrode, is obtained when PLS multivariate calibration model is used. It is important to point out that the peak current of 60 μgL^{-1} of Zn is reduced to 23% of it's initial value upon the addition of 15 μgL^{-1} of Cu [Figure 2.2 (C)].

Table 2.4 - Results for the determination of Cu, Pb and Zn in river water samples.

Sample	Cu /μgL^{-1}			Pb /μgL^{-1}			Zn /μgL^{-1}		
	SWASV[a,b]	AAS[c]	% Error	SWASV[a,d]	AAS[c]	% Error	SWASV[a,e]	AAS[c]	% Error
A	14 ± 1	13.2 ± 0.2	6.1		2.4 ± 0.2		116 ± 8	120 ± 8	-3
B	9 ± 5	4.7 ± 0.1	91	n.d.	0.9 ± 0.3	___	72 ± 9	76.7 ± 0.9	-6
C	8.0 ± 0.3	7.6 ± 0.4	5.3		< DL		87 ± 9	89 ± 9	-9
Spiked river water samples									
C1[f]	7.7 ± 0.3	7.6	1.3	5.2 ± 0.7	5.0	4.0	76 ± 3	88.5	-14
C2[f]	7.9 ± 0.6	7.5	5.3	10.3 ± 0.2	10.0	3.0	76 ± 6	88.1	-14
C3[f]	8.2 ± 0.4	7.5	9.3	15.7 ± 0.5	15.0	4.7	81 ± 6	87.7	-8
C4[g]	11.9 ± 0.5	12.1	-1.7	14.7 ± 0.5	14.7	0	66 ± 5	87.3	-24
C5[g]	14.8 ± 0.7	16.1	-8.1	15 ± 1	14.7	2.0	59 ± 4	87.0	-32

n.d.: Not determined; DL: the AAS detection limit for Pb is 0.72 μgL^{-1} ; [a] Average of four determinations with confidence limits for 95% confidence level; [b] PLS calibration model for Cu with 5 LVs; [c] Average of three determinations with confidence limits for 95% confidence level; [d] PLS calibration model for Pb with 6 LVs; [e] PLS calibration model for Zn with 3 LVs; [f] sample C spiked with 5, 10 and 15 μgL^{-1} of Pb standard solution; [g] sample C spiked with 15 μgL^{-1} of Pb and 4.5 and 8.5 μgL^{-1} of Cu standard solutions.

2.4. Conclusions

The results obtained in this work demonstrated that the combined use of a non-toxic bismuth film, deposited *in-situ* on a GC electrode, in conjunction with PLS calibration models constitute an adequate and more robust analytical methodology for simultaneous determination of Cu, Pb and Zn metal ions. An advantage of using the *in-situ* deposited BiFE is that it is possible to determine metals reoxidized at potentials both more negative (e.g. Zn, Cd and Pb) and more positive (e.g. Cu) than Bi. This work shows that chemometrics tools were successful applied to design the experiments and to overcome problems related with the overlapped signals, competition for surface sites between Bi and Cu (minimization of interferences) and heavy metal interactions (e.g. interactions between Cu and Zn).

The developed methodology was successfully applied for determination of Cu, Pb and Zn in surface river water samples.

References

[1] J. Wang, Stripping Analysis, VCH, New York **1985**.

[2] M. Pesavento, G. Alberti, R. Biesuz, Anal. Chim. Acta **2009**, 631, 129.

[3] M. L. Tercier-Waeber, M. Taillefert, J. Environ. Monitoring **2008**, 10, 30.

[4] B. Yosypchuk, L. Novotny, Electroanalysis **2002**, 14, 1733.

[5] J. Barek, J. Fischer, T. Navratil, K. Peckova, B. Yosypchuk, J. Zima, Electroanalysis **2007**, 19, 2003.

[6] P. Cizkova, T. Navratil, I. Sestakova, B. Yosypchuk, Electroanalysis **2007**, 19, 161.

[7] S. Armenta, S. Garrigues, M. de la Guardia, Trac – Trends Anal. Chem. **2008**, 27, 497.

[8] B. Yosypchuk, J. Barek, Crit. Rev. Anal. Chem. **2009**, 39, 189.

[9] I. Svancara, C. Prior, S. B. Hocevar, J. Wang, Electroanalysis **2010**, 22, 1405.

[10] J. Wang, Electroanalysis **2005**, 17, 1341.

[11] I. Svancara, L. Baldrianova, E. Tesarova, S. B. Hocevar, S. A. A. Elsuccary, A. Economou, S. Sotiropoulos, B. Ogorevc, K. Vytras, Electroanalysis **2006**, 18, 177.

[12] J. Wang, J. M. Lu, U. A. Kirgoz, S. B. Hocevar, and B. Ogorevc, Anal. Chim. Acta **2001**, 434, 29.

[13] C. Prior, C. E. Lenehan, G. S. Walker, Electroanalysis **2006**, 18, 2486.

[14] C. Prior, C. E. Lenehan, G. S. Walker, Anal. Chim. Acta **2007**, 598, 65.

[15] W. R. Pacheco, E. M. Miguel, G. V. Ramos, C. E. Cardoso, P. A. M. Farias, R. Q. Aucelio, Anal. Chim. Acta **2008**, 625, 22.

[16] Z. D. Anastasiadou, P. D. Jannakoudakis, S. T. Girousi, Cent. Eur. J. Chem. **2010**, 8, 999.

[17] C. E. Cardoso, W. F. Pacheco, R. Sarubi, M. L. N. Ribeiro, P. A. M. Farias, R. Q. Aucelio, Anal. Sci. **2007**, 23, 1065.

[18] M. A. Baldo, S. Daniele, Anal. Lett. **2004**, 37, 995.

[19] I. Cesarino, C. Gouveia-Caridade, R. Pauliukaite, E. T. G. Cavalheiro, C. M. A. Brett, Electroanalysis **2010**, 22, 1437.

[20] R. O. Kadara, L. E. Tothill, Talanta **2005**, 66, 1089.

[21] C. M. A. Brett, M. B. Q. Garcia, J. Lima, Anal. Chim. Acta **1997**, 339, 167.

[22] J. H. Pei, M. L. Tercier-Waeber, J. Buffle, Anal. Chem. **2000**, 72, 161.

[23] C. Colombo, C. M. G. Van den Berg, Int. J. Environ. Anal. Chem. **1998**, 71, 1.

[24] D. Jagner, L. Renman, S. H. Stefansdottir, Anal. Chim. Acta **1993**, 281, 315.

[25] D. Jagner, L. Renman, S. H. Stefansdottir, Electroanalysis **1994**, 6, 201.

[26] Y. N. Ni and L. Wang, Anal. Lett. **1999**, 32, 2081.

[27] O. Dominguez, M. J. Arcos, Electroanalysis **2000**, 12, 449.

[28] O. Dominguez, M. J. Arcos, Anal. Chim. Acta **2002**, 470, 241.

[29] M. J. G. Gonzalez, O. D. Renedo, M. J. A. Martinez, Electroanalysis **2006**, 18, 1159.

[30] M. J. G. Gonzalez, O. D. Renedo, M. J. A. Martinez, Talanta **2007**, 71, 691.

[31] J. M. Palacios-Santander, L. M. Cubillana-Aguilera, I. Naranjo-Rodriguez, J. L. Hidalgo-Hidalgo-De-Cisneros, Chemom. Intell. Lab. Syst. **2007**, 85, 131.

[32] M. Cauchi, C. Bessant, S. Setford, Electroanalysis **2008**, 20, 2571.

[33] A. Niazi, E. Amjadi, D. Nori-Shargh, S. J. Bozorghi, J. Chin.

Chem. Soc. 2008, 55, 276.

[34] A. Niazi, S. Sharifi, E. Amjadi, J. Electroanal. Chem. **2008**, 623, 86.

[35] A. Herrero, M. C. Ortiz, Talanta **1999**, 49, 801.

[36] Y. N. Ni, S. Kokot, Anal. Chim. Acta **2008**, 626, 130.

[37] M. Esteban, C. Arino, J. M. Diaz-Cruz, Crit. Rev. Anal. Chem. **2006**, 36, 295.

[38] M. Esteban, C. Arino, J. M. Diaz-Cruz, Trac – Trends Anal. Chem. **2006**, 25, 86.

[39] M. B. Sanz, L. A. Sarabia, A. Herrero, M. C. Ortiz, Electroanalysis **2004**, 16, 748.

[40] M. B. Sanz, L. A. Sarabia, A. Herrero, M. C. Ortiz, Anal. Chim. Acta **2003**, 489, 85.

[41] A. Herrero, M. C. Ortiz, Anal. Chim. Acta **1999**, 378, 245.

[42] J.N. Miller, J.C. Miller, Statistics and Chemometrics for Analytical Chemistry, Pearson Education Limited, Fifth Edition, **2005**.

[43] European Comission, in "Directive 2008/105/EC on environmental quality standards in the field of water policy, amending and subsequently repealing Council Directives 82/176/EEC, 83/513/EEC, 84/156/EEC, 84/491/EEC, 86/280/EEC and amending Directive 2000/60/EC" **2008**.

[44] EPA, in "National Recommended Water Quality Criteria. United States Environmental Protection Agency, Office of Water/ Office of Science and Technology" **2009**.

[45] G. Kefala, A. Economou, A. Voulgaropoulos, M. Sofoniou, Talanta **2003**, 61, 603.

[46] S. B. Hocevar, B. Ogorevc, J. Wang, B. Pihlar, Electroanalysis **2002**, 14, 1707.

[47] D. Demetriades, A. Economou, A. Voulgaropoulos, Anal. Chim. Acta **2004**, 519, 167.

[48] R. Pauliukaite, C. M. A. Brett, Electroanalysis **2005**, 17, 1354.

[49] S. Legeai, K. Soropogui, M. Cretinon, O. Vittori, A. H. De Oliveira, F. Barbier, M. F. Grenier-Loustalot, Anal. Bioanal. Chem. **2005**, 383, 839.

[50] A. Craig, O. Cloareo, E. Holmes, J. K. Nicholson, J. C. Lindon, Anal. Chem. **2006**, 78, 2262.

[51] H. Swierenga, A. P. de Weijer, R. J. vanWijk, L. M. C. Buydens, Chemom. Intell. Lab. Sys. **1999**, 49, 1.

Chapter 3

SIMULTANEOUS ELECTROCHEMICAL DETERMINATION OF ARSENIC, COPPER, LEAD AND MERCURY, AT TRACE LEVELS, USING A VIBRATING GOLD MICROWIRE ELECTRODE[2]

Graphical abstract

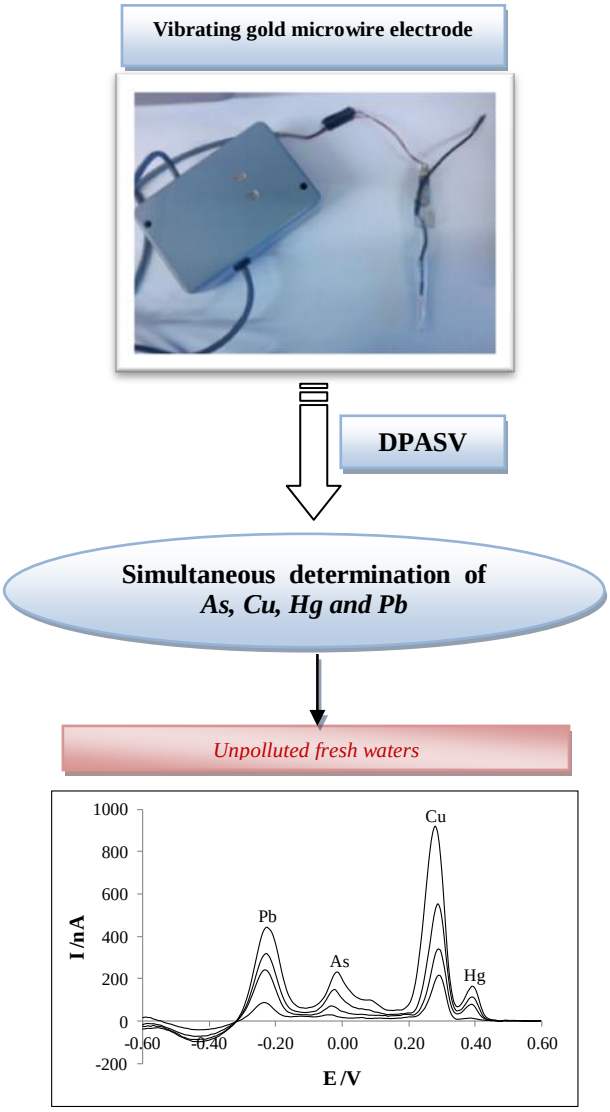

[2]*Analytica Chimica Acta* 2011, 703, 1 – 7

Abstract

In this work, a simple, rapid, reliable and low cost method for simultaneous electrochemical determination of As, Cu, Hg and Pb ions, on a vibrating gold microwire electrode combined with stripping voltammetry, is described for the first time.

The multi-element detection was performed in the presence of oxygen by DPASV, in hydrochloric acid 0.1 $molL^{-1}$ with sodium chloride 0.5 $molL^{-1}$. This medium was found optimum in terms of peak resolution, peak shape and sensitivities, and has a composition similar to sea water to which the method could potentially be applied. The gold microwire electrode presented well defined, undistorted, sharp and reproducible peaks for trace concentrations of Cu, Hg and Pb and As presented a reproducible peak with a small shoulder. Using a vibrating gold microwire electrode of 25 μm diameter and 30 s t_{dep}, the DLs of As, Cu, Hg and Pb were 0.07, 0.40, 0.07 and 0.2 μgL^{-1}, respectively. Possible effects of $Al^{3+,}$ $Cd^{2+,}$ Cr^{3+}, Cr^{6+}, Fe^{3+}, Mn^{2+}, Ni^{2+}, Sb^{3+} and Zn^{2+} were investigated but did not cause any significant interferences.

Finally, the method was applied for the simultaneous determination of these four metal(loid)s in unpolluted river water samples and the results were validated by AAS-EA or by ICP-MS.

3.1. Introduction

In-situ and *on-field* measurements of trace metals in natural environment represent a scientific challenge for analytical and environmental sciences. The electrochemical voltammetric stripping analysis is a unique tool, largely used for the detection of trace metals in environmental samples, including fresh and salt waters, due to the remarkably low DLs, high sensitivity and the ability to detect trace metal elements in different oxidation states [1-3]. Additionally, the basic instrumentation and operating costs required for voltammetric stripping analysis are relatively inexpensive. Another important advantage is the portability of the instrumentation and the ability to perform real-time analysis. However, the combination of these techniques with mercury electrodes, mainly MFE, should be limited or completely avoided because soluble salts of mercury are highly toxic.

According to this environmental conscience, several studies for detecting heavy metals, which use "greener" electrodes as potential substitutes of the mercury electrode, such as bismuth [Chapter 2 of this thesis, 4-6], antimony [7,8] silver [9-13], alloy [14,15] and gold [10-13,16-37] electrodes have been carried out. Gold electrodes with different sizes and forms have been used to detect heavy metals by stripping analysis: solid disk electrodes [16-18], films on GC [20,21], graphite [37] or on platinum [22], microelectrodes [13,19,23-30], modified gold electrodes [30-34], gold nanoparticles [32,33] and screen-printed [35,36] electrodes. Gold microelectrodes have special properties, which make them more suitable than macroelectrodes for *in-situ* detection due to the increase of mass transport, decrease of the influence of the solution resistance, better signal-to-noise ratio and low DLs [38-40].

Reliable simultaneous determination of more than one metal using stripping analysis is difficult due to the possibility of overlapping peaks, which can occur in the relatively narrow potential range where metals are reduced or oxidized. We are aware that few electrochemical studies have reported potentialities for simultaneous determination of more than one trace metal(loid)s in water samples at gold electrodes. As far as we know, the works available in the literature report the simultaneous determination of two metal/metaloid ions (Cu

and Hg [18,26,29], As and Hg [37], Cu and Pb [35], Cd and Pb [10] and Cd and Zn [41]) and only few studies were devoted to the simultaneous determination of three metal(loid)s ions [As^{3+}, Cu and Hg [32], Cu, Hg and Pb [33] and Cu, Pb and Zn [42] at gold modified electrodes, Cu, Pb and Zn [23] at gold microelectrodes, Cu, Hg and Pb [19] at a gold fiber electrode]. In recent times, Salaün *et .al*. [25] described a new approach, which opens the possibility of determining simultaneously Sb, Cu and Hg with a gold microwire electrode.

Recently, van den Berg and co-workers developed a gold microwire electrode, which allowed the detection of Cu and Hg [26], and the inorganic speciation of As in sea water [27] and in freshwater [24] with high sensitivity. Further works, where a vibrator was combined with the gold microwire electrode [28], produced a probe that was both highly sensitive and suitable for immersion to depths > 40 m. These results prompted us to investigate the potential of using this vibrating gold microwire electrode to perform the simultaneous determination of As, Cu, Hg and Pb by ASV.

3.2. Experimental

3.2.1. Reagents and solutions

Suprapur hydrochloric acid (HCl) 30 % and suprapur nitric acid (HNO_3) 65 % were purchased from Merck and used as received. Sulphuric acid (H_2SO_4) PA-ISO (96%) was obtained from Panreac, potassium peroxydisulfate ($K_2S_2O_8$) p.a. (≥ 99%) was obtained from sigma-aldrich and sodium chloride (NaCl) p.a. (99.5%), potassium hexacyanoferrate (III) ($K3[Fe(CN)_6]$) p.a. (99%), potassium chloride (KCl) p.a. (99.5%) and sodium nitrate ($NaNO_3$) p.a. (99.5%) were purchased from Merck.

In a similar way as it was described in sections 2.2.1 and 2.2.2, all solutions were prepared with Milli-Q water with resistivity of 18.2 $M\Omega cm^{-1}$ using decontaminated material. Metal(loid)s stock solutions were prepared by dilution with ultrapure water of 1000 mgL^{-1} atomic absorption standard solutions [mercury

nitrate ($Hg(NO_3)_2$), $Pb(NO_3)_2$, $Cu(NO_3)_2$, arsenic (V) acid H_3AsO_4]. The As^{3+} stock solution was prepared from sodium arsenite solution ($NaAsO_2$) obtained from Merck and wrapped in an aluminum foil to prevent oxidation by light. These stock solutions were acidified with HNO_3 to pH 2. Standard solutions of $Al^{3+,}$ Cd^{2+}, Cr^{3+}, Cr^{6+}, Fe^{3+}, $Mn^{2+,}$, Ni^{2+}, Sb^{3+} and Zn^{2+}, used for interference experiments, were diluted from AAS standard solutions from Merck.

An aqueous solution of 10 mM of $K_3[Fe(CN)_6]$ in 0.5 M of potassium chloride was prepared and used to determine the diffusion layer thickness (δ) of the gold microwire electrode.

3.2.2. Instrumentation and electrode preparation

Stripping voltammetric measurements were performed using a modular electrochemical workstation already describe in section 2.2.2. All measurements were carried out at room temperature in a 10 mL voltammetric cell with a vibrating gold microwire WE (10 or 25 μm diameter, purity: 99.99%, hard), an iridium CE [1 cm length (l), 150 μm diameter] and Ag/AgCl (3M) double junction RE with $NaNO_3$ 0.1 $molL^{-1}$ in the salt bridge. The gold and iridium wires were obtained from Goodfellow Company (UK). All potential values are given *versus* Ag/AgCl reference electrode. All electrical connections and cables were wrapped in aluminum foil and connected to ground to minimize electrical noise. Figure 3.1 presents the three electrodes used.

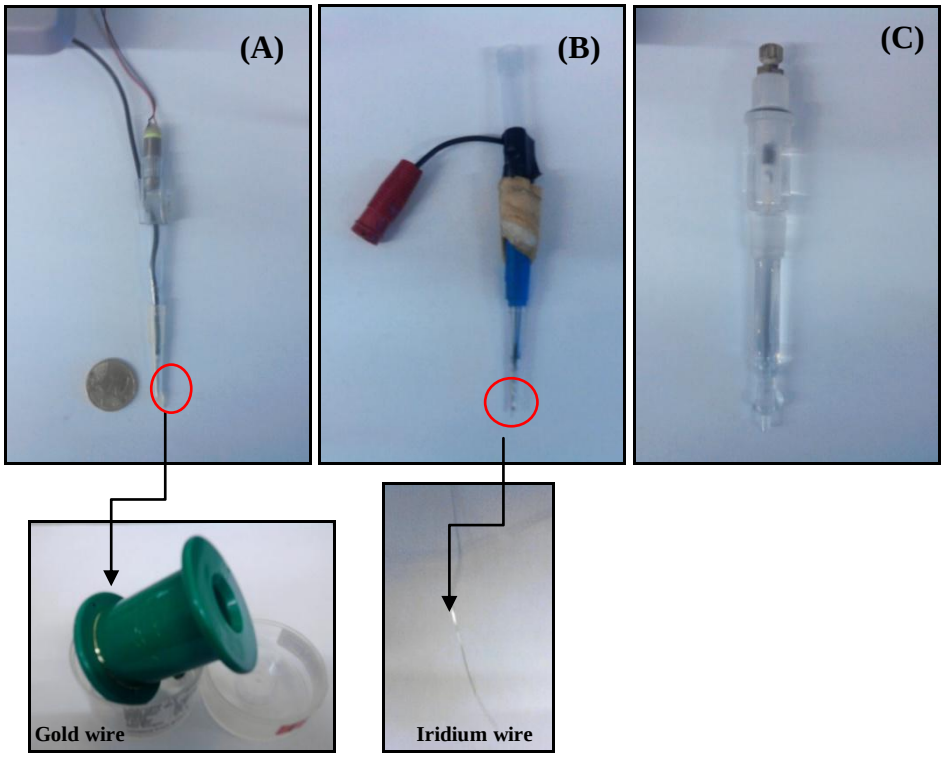

Figure 3.1 – **(A)** vibrating gold microwire WE; **(B)** iridium CE and **(C)** Ag/AgCl 3M double junction RE.

The gold microwire working and the iridium counter electrodes [Figures 3.1 (A) and (B)] were "home-made". The procedure used to prepare a vibrating gold microwire electrode was previously described [24-27]. Briefly, a copper wire ($l \approx 10$ cm and $d \approx 100$ μm) was passed through a 200 μm polyethylene tip. Its end was dipped in a conductive silver solution (Leitsiber L100), which had been freshly agitated and acted as a conductive adhesive. The copper wire was then attached to a 5 – 10 mm length of gold wire ($d = 10$ or 25 μm) by gently touching it; subsequently, the contact zone between gold and copper was exposed to the direct light of the lamp (approximately 10 s) in order to improve the electrical connection. The copper wire was then carefully pulled through the pipet tip until the gold microwire passed halfway through. The microwire was sealed in the tip by holding it in the top of the "home-made" oven [Figure 3.2 (A)], which had been set to 400 ºC, during 8 s to melt it uniformly or using a soldering iron [Figure 3.2 (B)]. The pipet tip was then held vertically in the air to cool. A robust electrical contact was made by back-filling the tip with a minimum of silver

conductive epoxy resin (SL65, Rite Lok) and inserting an electrical wire (d = 2 mm). Finally, the microwire was cut to the desired length with scissors. Before using, the electrode was UV digested for 30 minutes, in a mixture of H_2SO_4 0.5 $molL^{-1}$ and $K_2S_2O_8$ 10 $mmolL^{-1}$, using a "home-made" digester [Figure 3.2 (C)] [26] in order to clean the gold surface. A vibrator (1.5 V) [Figure 3.2 (D)] was fitted within the same tip allowing the electrode to vibrate, instead of the usual solution stirring, and connected via a cable to the IME interface which is attached to potentiostat. When not in use, the electrodes were dried and stored in the vertical position. The counter iridium electrode was fabricated in the same manner as the WEs.

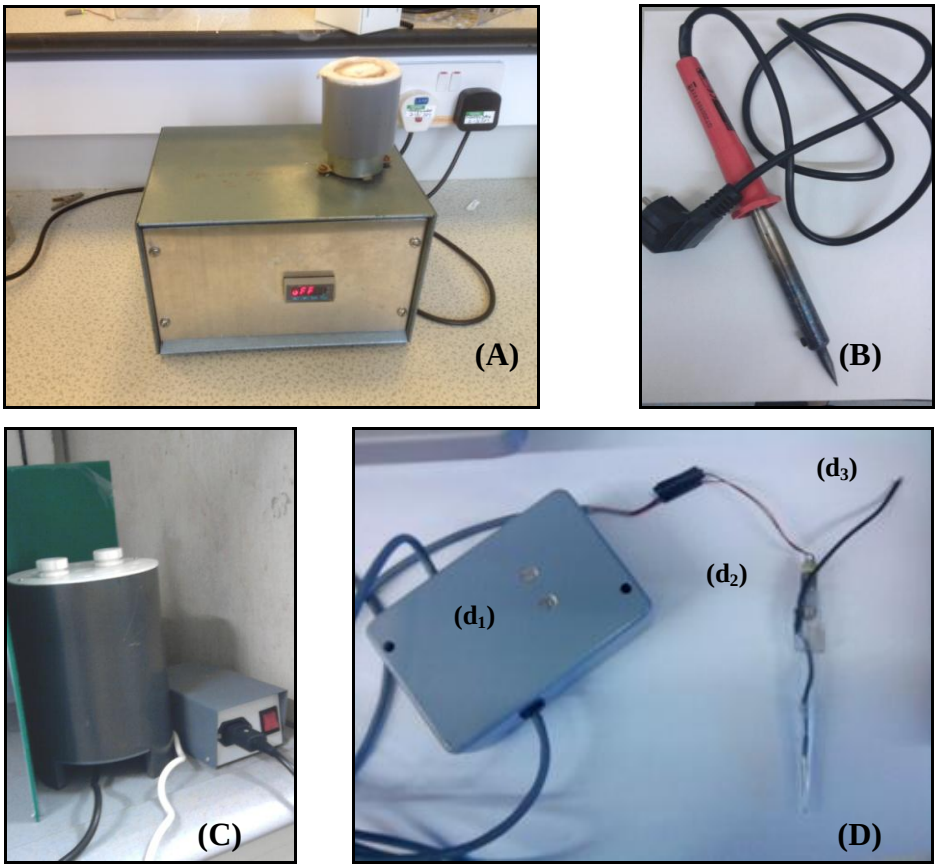

Figure 3.2 – **(A)** "Home-made" oven; (**B**) Soldering iron; (**C**) "Home-made" digester and **(D)** "Home-made" vibrating system (d_1 – vibrating interface; d_2 – vibrator and d_3 – potentiostat connection).

3.2.3. Characterization of the gold vibrating microwire electrodes: measurement of the surface area, length and the diffusion layer thickness of the electrode

Real surface area (A_R) was determined by cyclic voltammetry (CV) in 0.5 $molL^{-1}$ of H_2SO_4 [26]. Firstly, 5 cyclic voltammograms were made between 0 and 1.5 V at 100 mVs^{-1} (similar to scan 1 in Figure 3.3). Usually, the voltammograms are stable from the second scan. After find the E_{min} (point A in Figure 3.3), which indicates the completation of a monolayer coverage of the gold surface with oxide [26], 5 cyclic voltammograms were performed between 0 and E_{min} (similar to scan 2 in Figure 3.3), at the same scan rate. The cathodic peak (point B in Figure 3.3) corresponds to the reduction of the previously formed oxide. Thus, assuming a charge transfer of 450 μCcm^{-2} (monolayer cover of gold oxide) the charge of the gold oxide reduction peak (point B in Figure 3.3) was integrated (the average of the last three scans was used) and thus used to calculate A_R of the [26].

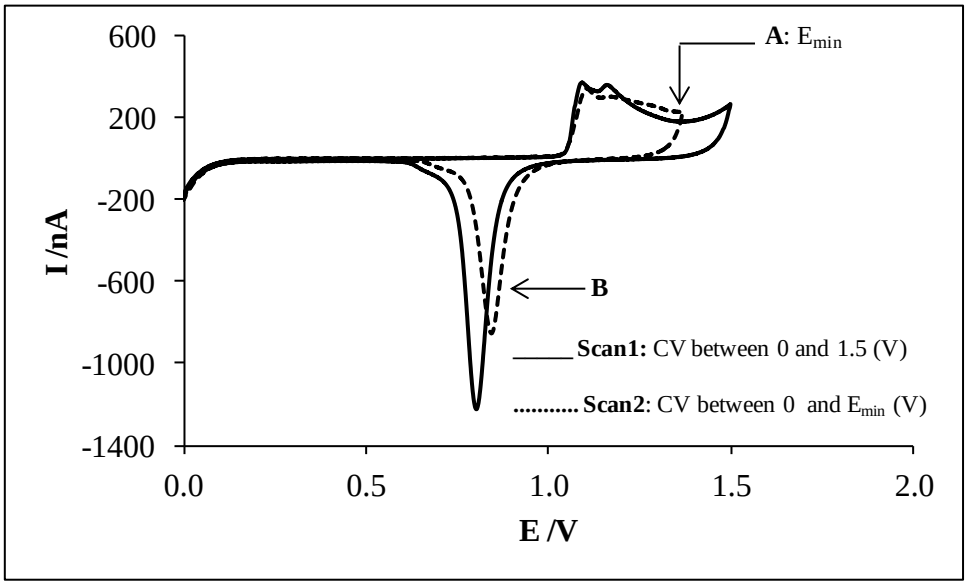

Figure 3.3 – Ciclic voltammogram for a gold microwire electrode (d = 25 μm) in 0.5 $molL^{-1}$ H_2SO_4 between 0 V and 1. 5 V (Scan 1) or E_{min} (Scan 2).

The length of the gold microwire electrode was determined by chronoamperometry at -0.3 V during 15 s (at a sampling frequency of 0.01 s^{-1}) in a stagnant solution of 10 $mmolL^{-1}$ $K_3[Fe(CN)_6]$ prepared in 0.5 $molL^{-1}$ KCl. The length of the electrode was calculated by fitting the experimental points obtained in the first seconds (5 – 7 s), i.e., when the evolving diffusion layer is not strongly influenced by the natural convection, to theoretical behavior [12,26]. The theoretical diffusion-limited current density, *I* (t), at a microwire electrode of length (l) and radius (r) (l >> r so that end effects are negligible) [26] is given by the equation 3.1:

$$I(t) = 2\pi nlFDC_b \left\{ \frac{e^{-0.1\sqrt{\frac{\pi Dt}{r^2}}}}{\sqrt{\frac{\pi Dt}{r^2}}} + \left[\ln\left(5.2945 + 1.4986\sqrt{\frac{Dt}{r^2}}\right) \right]^{-1} \right\} \quad \text{(Eq. 3.1)}$$

where n is the number of electrons involved, l (cm) is the electrode length, F (96485 $Cmol^{-1}$) is the faraday constant, D (cm^2s^{-1}) is the diffusion coefficient, t (s) is the electrolysis time and C_b ($molcm^{-3}$) is the bulk concentration. In $K_3[Fe(CN)_6]$ solution prepared in 0.5 $molL^{-1}$ KCl, n, D and C_b are 1, 7.17×10^{-6} cm^2s^{-1} and 1×10^{-5} $molcm^{-3}$, respectively.

The geometric area (A_G) was calculated taken into account the length and the diameter of the electrode; the roughness (R) was calculated as the A_R/A_G ratio.

The δ at the gold microwire was determined by chronoamperometric measurements in a solution of 10 $mmolL^{-1}$ $K_3[Fe(CN)_6]$ prepared in 0.5 $molL^{-1}$ KCl. The current was followed as a function of time for 120 s at a potential of -0.3 V (at a sampling frequency of 0.1 s^{-1}) with (or without) electrode agitation using the vibrator. The current average (in a steady state condition, $\bar{I}(t)$, was used to calculate the δ (μm), using the equation 3.2 [26, 28]:

$$\delta = 2\,\pi\, r / n\,F\,D\,C_b/\bar{I}(t) \qquad \text{(Eq. 3.2)}$$

All the parameters in this equation were previously identified in equation 3.1.

3.2.4. Trace metals determination

Trace metals analysis was carried out using either SWASV or DPASV with automatic peak search, depending on the stability of the signal. All measurements were carried out, at room temperature and without sample deoxygenation, in 0.1 $molL^{-1}$ HCl with 0.5 $molL^{-1}$ NaCl or in river water samples spiked with 0.5 $molL^{-1}$ NaCl and acidified with HCl to pH 1.

Each measurement consisted of three steps (see Table 3.1): conditioning of the electrode, analytical and background scan. The electrode was vibrating during the conditioning and deposition steps. For each addition, the measurements were repeated three times. The different steps were automated using the "project" option in the GPES software [24-27]. The background was automatically subtracted from the analytical scan. Both, peak height or peak derivative, can be used for quantification although the peak derivative was found more suitable (better reproducibility) at low concentrations levels because its value is unaffected by the choice of the baseline. The optimized voltammetric conditions to determine As, Cu, Hg and Pb are summarized in Table 3.1.

All experiments were performed in duplicate with a minimum of three repetitive scans per measurement.

Table 3.1 – Voltammetric parameters for As, Cu, Hg and Pb analysis by SWASV or DPASV

	SWASV	**DPASV**
Conditioning step		
Conditioning potential /V	0.55	0.55
Conditioning time /s	5	5
Analytical scan		
Deposition potential /V	-1.2	-1.2
Deposition time /s	32	32
Equilibration time /s	10	10
Potential window /V	-0.6 to 0.6	-0.6 to 0.6
Frequency /Hz	50	___
Step potential /mV	8	8
Amplitude /mV	50	50
Modulation time /s	___	0.002
Interval time /s	___	0.1
Standby potential /V	0.55	0.55
Background scan	The same conditions as the analytical scan with the deposition time reduced to 2 s	

3.2.5. Analysis of the surface river water samples

Two river water samples, designated as A and B, were collected from different sites, filtered with 0.45 μm membrane, acidified at pH 2 with suprapur HCl (for the electrochemical determination) or HNO_3 (for AAS-EA and ICP-MS determinations) and then stored in polyethylene bottles in the freezer. Prior to the analysis, the samples were digested with UV radiation for one hour using a "home-made" digester [Figure 3.2 (C)] [26].

For all electrochemical determinations, the pH of the samples was adjusted to pH 1 with suprapur HCl; NaCl solid powder was also added until the final concentration of 0.5 $molL^{-1}$. For all analyses, two independent assays were carried

out; a minimum of three repetitive scans were made per sample, as described above (see section 3.2.4). In the case of the standard addition method, all determinations consisted of three additions and three measurements per addition.

Comparative measurement of Cu was performed by AAS-EA using the same equipment described in section 2.2.2. Comparative measurement of As, Hg and Pb was made by ICP-MS with a Thermo X-Series quadrupole ICP-MS (Thermo Scientific), equipped with Ni cones and a glass concentric nebulizer (Meinhard, 1.0 mL min^{-1}) and refrigerated with a Peltier system. These techniques were used as reference methods.

3.3. Results and Discussion

3.3.1. Characterization of the gold vibrating microwire electrodes

The electrode A_R and A_G determined as described in section 3.2.3 was used to calculate R. The value of the R, obtained with four gold microwire electrodes with 10 μm of diameter, whose lengths ranged from 1.4 up to 1.8 mm, was 1.1 ± 0.1 [mean and standard deviation of three replicates of four independent experiments (n = 12)]; for a new gold electrode with d = 25 μm and l = 2.1 mm, the roughness was 1.13 ± 0.03 [mean and standard deviation of three replicates of two independent experiments (n = 6)]. The low roughness factor indicates that the gold microwires have a smooth surface. This property improves the ratio of faradaic/capacitive current resulting in a low DL. The R values obtained here are similar to those reported previously for similar electrodes [26].

In previous works, where gold microwire electrodes were used, it was found that the sensitivity was significantly improved when a vibrating electrode was used instead of stirring the solution [24,28]. This local motion, besides increasing the sensitivity, can also minimize the H_2 bubble formation at the WE, resulting in a reduced noise and increasing the stripping signal. The value of the δ, with the vibrator on the top of the pipette tip, were 0.92 ± 0.09 [mean and standard deviation of three replicates of four independent experiments (n = 12)] and 1.52 ±

0.01 μm [mean and standard deviation of three replicates (n = 3)] for 10 and 25 μm diameter electrodes, respectively. These diffusion layer sizes are amongst the lowest ever reported for such simple electrodes, thanks to the 200 Hz vibration frequency. Equation 3.3 is a modified version of the Levich equation and correlates the δ with the rotation rate of a rotating disc electrode (RDE) under laminar flow conditions for a reversible system:

$$\delta = 1.61\ D^{1/3}.(\pi.f/30)^{-1/2}.\ \upsilon^{1/6} \qquad \text{(Eq. 3.3)}$$

with D the diffusion coefficient (cm^2s^{-1}), f the rotation rate per minute (rpm) and υ the kinematic viscosity (cm^2s^{-1}). It can be calculated that the diffusion layer obtained at the 10 μm electrodes (0.92 μm) would only be achieved with a rotation rate of ~ 230,000 rpm, which is unattainable experimentally. A standard rotation rate of 10,000 rpm gives a δ of ~ 4.4 μm, i.e. 5 times higher than those obtained at the 10 μm wire electrodes. Such low diffusion layer sizes result in low DLs: (i) by providing high fluxes of metal towards the electrode during the deposition step and (ii) by providing well defined hydrodynamic conditions at the vicinity of the electrode, which improves the analytical reproducibility [5,28] when compared to standard stirring. It also means that shorter $t_{dep(s)}$ (e.g. 30 s) can be used thus decreasing considerably the experimental time. Finally, another important feature is the functional stability of the electrodes. The electrodes, used in this work, were stable during at least one month of intensive use. Generally speaking, the thicker electrodes were more robust and easier to handle.

3.3.2. Preliminary results

Literature reports that the magnitude of the stripping current for As depends on the choice of the supporting electrolyte [32]; higher stripping currents were obtained when HCl was used as the supporting electrolyte because Cl^- ions

complex with As^{3+} [32]. It was also described that bounded chloride ions, present in the double layer around the electrode, act as a bridge between the As ion and the electrode This makes the redox reaction more reversible and increases the peak current [20]. Based on these facts, we tested two different supporting electrolyte solutions: (i) HCl 0.1 $molL^{-1}$ and (ii) HCl 0.1 $molL^{-1}$ with NaCl 0.5 $molL^{-1}$ (a value quite close to the concentration level of chloride in sea water). For As the sensitivity and the separation of the peaks between As and Cu was improved when 0.5 $molL^{-1}$ NaCl was added, although it sometimes caused the formation of a small shoulder on the anodic side of the arsenic peak as previously observed on e.g. a gold foil electrode [43]. This shoulder might indicate slight differences in stripping processes of As adatoms from the polycrystalline gold surface. The stripping peak of Hg in 0.1 $molL^{-1}$ HCl was ~ 60 mV more positive than in 0.1 $molL^{-1}$ HCl / 0.5 $molL^{-1}$ NaCl, but the sensitivity was similar in both supporting electrolyte solutions. This behavior is in agreement with the fact that the formation of chlorocomplexes of Hg favours the oxidation of Hg, which occurs at a less positive potential [16]. For Cu and Pb, no substantial differences, in terms of sensitivity, were observed after the addition of NaCl. However, the peaks were slightly more positive when NaCl was added. According to these results, we chose HCl 0.1 $molL^{-1}$ with NaCl 0.5 $molL^{-1}$, as background electrolyte.

3.3.3. Effect of the deposition potential and of the deposition time

The effect of the t_{dep} and of the E_{dep} on the responses of As, Cu, Hg and Pb, recorded in SWASV mode, were determined using a 10 μm vibrating gold microwire electrode (Figure 3.4).

The t_{dep} was varied in the range 10 to 60 s at a fixed E_{dep} of -1.2 V. As expected, the stripping current peak intensities were found to increase in proportion to the t_{dep}. A t_{dep} of 30 s was chosen as a good compromise between the DL, linear concentration range (LCR) and the duration of the experiment.

The effect of the E_{dep} on the stripping current was evaluated in the potential range between -1.2 to -0.2 V for a fixed t_{dep} of 30 s. The $E_{dep(s)}$ studied had no significant effect on Cu and Hg signals. For Pb, the peak height increased when more negative $E_{dep(s)}$ were applied. For As, peaks were only observed when $E_{dep(s)} \leq$ -1 V were applied as previously reported [27]. According to these results, a E_{dep} of -1.2 V was chosen for further experiments. Please note that in these measuring conditions (acidic pH and low deposition potential), all As^{3+} originally present in the solution would be oxidized within seconds to As^{5+} by the chlorine generated at the auxiliary electrode during the deposition step [27]. Thus, the As peak response represents the total inorganic As [As^{3+} + As^{5+}]. As^{3+} can be determined selectively at a higher E_{dep} (and higher pH), i.e. in conditions where chlorine formation is prevented [27].

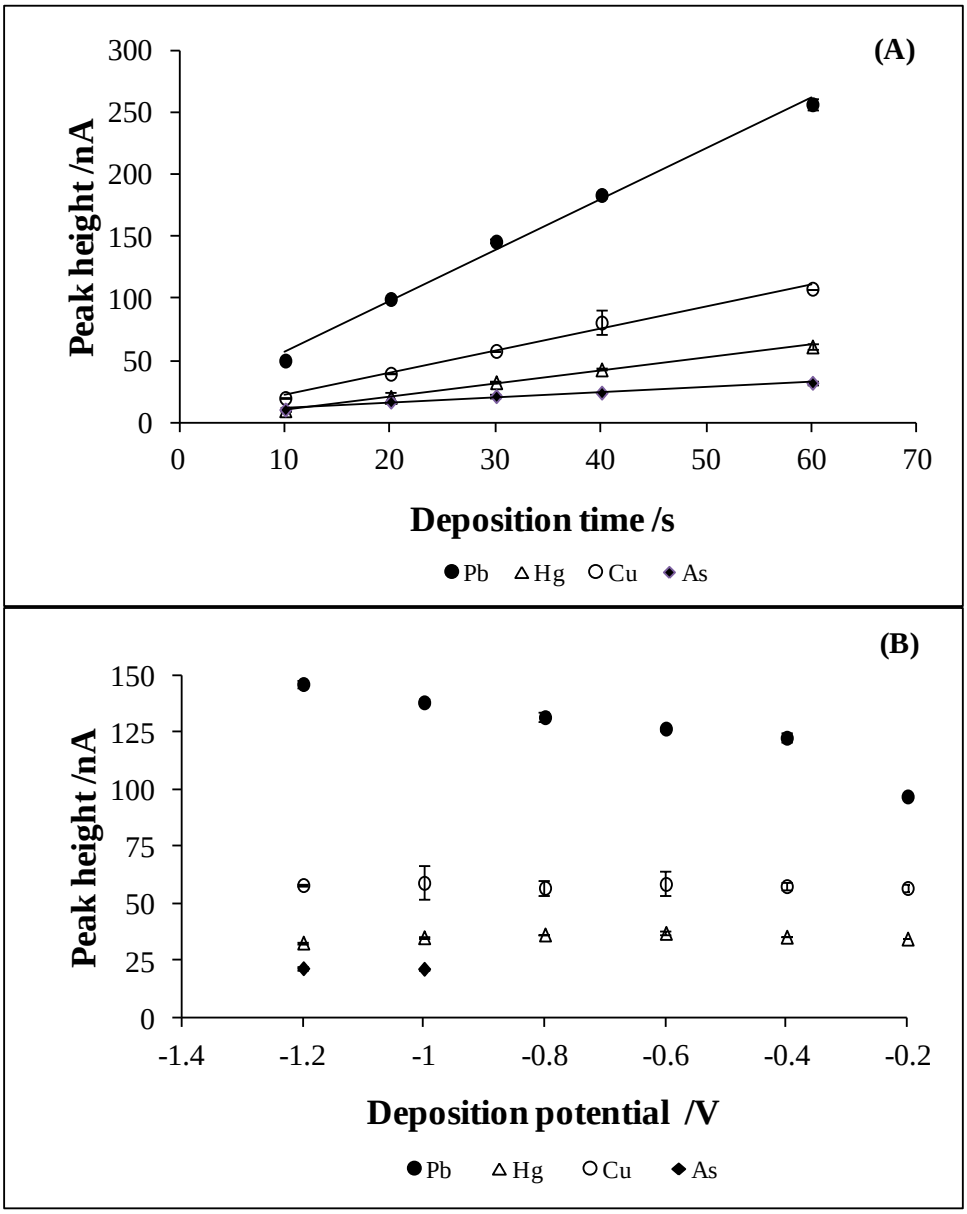

Figure 3.4 – Effect of the (**A**) deposition time at fixed -1.2 V deposition potential and of the (**B**) deposition potential using 30 s of deposition time on the peak heights response of 1.0, 1.0, 1.8 and 3.0 μgL^{-1} of As^{3+}, Cu, Hg and Pb, respectively, using a vibrating gold microwire electrode (d = 10 μm and l = 1.8 mm) in SWASV mode. Values are the average of two replicates with standard deviation (vertical error bars) are present (n = 2); where no error bars are shown, they are within the points**.** This is an example of an experiment repeated two times.

3.3.4 Optimization of ASV parameters

Firstly, independent calibrations of each metal(loid)s (As, Cu, Hg and Pb) were made by SWASV or DPASV. Both, SWASV (50 Hz frequency, 50 mV amplitude and 8 mV step) and DPASV (2 ms modulation time, 100 ms interval time, 50 mV amplitude and 8 mV step) parameters were chosen as they gave the best signal to noise ratio. The peak potential, half width ($W_{1/2}$), the sensitivity of the calibration curves, LCR, and the DLs, obtained by both techniques, are summarized in table 3.2. In order to eliminate any memory effects related with the adsorbed chloride ions [26], each calibration was preceded by three cyclic voltammetry scans made in H_2SO_4 0.5 $molL^{-1}$.

For individual calibration curves, the sensitivity, expressed as the ratio between the slope ($nAV^{-1}\mu g^{-1}L$) of each calibration curve and the length of the electrode (mm) (Table 3.2), decreased in the following orders: Cu > Hg > Pb > As (DPASV) and Cu > Pb > Hg > As (SWASV). For Cu, Hg and Pb, the sensitivities were much better when DPASV was used (Table 3.2) as expected from their respective pulse time (or frequency) which is 2 ms in DPASV (corresponding to 250 Hz in SW) over 10 ms in SWASV (50 Hz). However, the residual current also increased explaining why the DLs are rather similar between DPASV and SWASV. The fact that the sensitivity for As is similar using both techniques is characteristic of a lack of reversibility of the couple As^{3+}/As^0.

The DLs [44] were calculated as previously described in section 2.3.1. Relatively low DLs were achieved using a short t_{dep} and without deoxygenation. Oxygen can potentially be an interference for Pb determination as its peak is situated within the oxygen reduction wave (~ -0.2 V) whilst it does not affect the determination of As, Cu and Hg as their peaks are situated at potentials more positive than the oxygen reduction. It was found that the oxygen interference for Pb could be eliminated by background subtraction, and reproducible results were obtained for all four metals without the need for deoxygenation, which much simplifies the analytical procedure. The obtained DLs are low enough to determine trace metal concentrations according to the values of the EPA-USA

[45] and of the EU commission [46] guidelines but if lower levels need to be detected, increase of the t_{dep} is easily achieved.

The LCR was assessed by determining the DL, which gives an instrumental signal significantly different from the background signal, until the upper concentration limit, which corresponded to the saturation of the electrode surface; for As and Pb, table 3.2 evidences the LCRs attained whereas for Cu and Hg, 20.0 and 3.0 μgL^{-1} respectively, were the maximum concentrations tested. The LCRs can be extended by decreasing the t_{dep} [Figure 3.4 (A)] or increasing the length or diameter (Table 3.2) of the gold microwire electrode. Because elemental As is a very poor electrical conductor, the peak intensity of As is known to reach a limiting value when the active surface of the electrode is fully covered with As^0 [27]; this fact can explain the narrow LCR. The DLs and the LCR were not significantly affected by the length of the electrode, as expected.

In a second step, simultaneous determinations of As, Cu, Hg and Pb were made by SWASV and DPASV. Figure 3.5 (A) shows an example of the voltamogramms recorded when all four metal ions were determined simultaneously by DPASV or by SWASV. Additionally, for DPASV, figure 3.5 (B) evidences well defined peaks for all four metal ions in a wide concentration range tested. The comparison of the calibration curves of As, Cu, Hg and Pb, obtained individually or simultaneously by DPASV, also showed similar linear concentration dependence and equivalent sensitivities for all four metal ions (Table 3.2) indicating that the formation of intermetallic complexes is unlikely. It is interesting to note that in the case of SWASV, the large Cu peak at ~ +0.25 V interfered with the detection of Hg [Figure 3.5 (A)] while the two peaks were well separated in DPASV. Despite the higher stripping time when DPASV was used, its performance in terms of peak resolution was superior than the one obtained by SWASV. Based on these results, we decided to continue exploring the simultaneous determination of As, Cu, Hg and Pb by DPASV, using a gold vibrating microwire electrode with 25 μm of diameter, which presented a more extended LCR for Pb and As.

Garnier *et.al*. [23] reported that the response of Hg at a 25 μm gold microdisk electrode was poorly reproducible; this phenomenon was attributed to the formation of a strong amalgam with Au. However, deposition of Hg^0 and formation of an amalgam would only occur if mercury coverage exceeds a monolayer [47]. At sub-monolayer coverage, a symmetrical peak corresponding to the UPD of Hg^{2+}/Hg^{+} on gold is observed [48]. In the present work, the Hg calibration was kept low up to 3.0 μgL^{-1} (still much higher than the concentrations usually found in unpolluted salt and river waters) in order to remain within the sub-monolayer regime. As expected, a sharp and symmetrical peak was obtained and a good reproducibility of the results was also obtained either by DPASV or SWASV techniques, even over several days, highlighting the good stability of these electrodes.

Table 3.2 – Calibration parameters of the individual and simultaneous determinations of As, Cu, Hg and Pb at vibrating gold microwire electrodes.

Metal(loid)s	Pb	As	Cu	Hg
Vibrating gold microwire electrode (d = 10 μm)				
SWASV				
Linearity /μgL^{-1}	0.08– 4.0	0.08 – 2.0	0.3 – 20	0.06 – 2.0
DL /μgL^{-1}	0.08	0.08	0.3	0.06
Peak potential /V	-0.204	0.015	0.289 – 0.225	0.384
$W_{1/2}$ /V	0.130	0.126	0.063 – 0.111	0.045
Sensitivity /nAV^{-1} μg^{-1}L mm^{-1}	431 ± 13	239 ± 10	552 ± 16	319 ± 17
r^2	0.997 (n = 21)	0.994 (n = 18)	0.994 (n = 30)	0.988 (n = 21)
DPASV				
Linearity /μgL^{-1}	0.06– 4.0	0.1 – 2.0	0.2 – 20.0	0.07 – 2.0
LD /μgL^{-1}	0.06	0.1	0.2	0.07
Peak potential /V	-0.217	0.013	0.289 – 0.217	0.391
$W_{1/2}$ /V	0.090	0.146	0.056 – 0.087	0.045
Sensitivity /nAV^{-1} μg^{-1}L mm^{-1}	756 ± 10	238 ± 18	1646 ± 33	1164 ± 53
r^2	0.9995 (n = 21)	0.980 (n = 18)	0.997 (n = 30)	0.990 (n = 24)

Table 3.2 - continuation

Metals	Pb	As	Cu	Hg
Vibrating gold microwire electrode (d = 25 μm)				
DPASV				
Linearity /μgL^{-1}	0.2 – 8.0	0.07 – 3.0	0.4 – 20	0.07 – 3.0
LD /μgL^{-1}	0.2	0.07	0.4	0.07
Peak potential /V	-0.217	-0.019	0.313 – 0.225	0.397
$W_{1/2}$ /V	0.084	0.062	0.048 – 0.087	0.032 – 0.071
Sensitivity /nAV^{-1} μg^{-1}L mm^{-1}	1194 ± 35	1063 ± 25	2825 ± 65	1290 ± 26
r^2	0.995 (n = 27)	0.998 (n = 21)	0.997(n = 24)	0.998 (n = 27)
Simultaneous Determination				
Linearity /μgL^{-1}	Up to 8.0	Up to 3.0	Up to 10	Up to 3.0
Peak potential /V	-0.229	-0.015	0.305 – 0.249	0.389
$W_{1/2}$ /V	0.093	0.075	0.056 – 0.071	0.042
Sensitivity /nAV^{-1} μg^{-1}L mm^{-1}	1149 ± 46	1056 ± 34	2953 ± 104	1326 ± 44
r^2 (n = 26)	0.991	0.994	0.993	0.994

n –number of points in the calibration curve; The values of the sensitivities were calculated with a confidence interval of 95%.

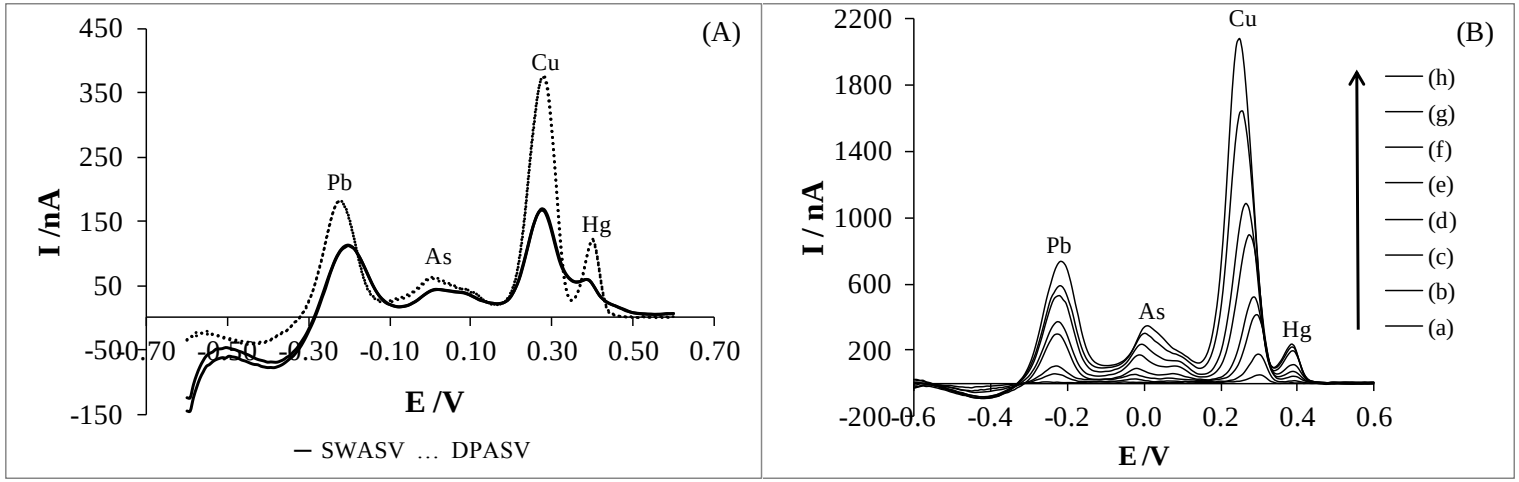

Figure 3.5 – Simultaneous determination of Pb, As, Cu and Hg response with background correction in HCl 0.1 M and NaCl 0.5 M: **(A)** DPASV and SWASV scans for ([Pb], [As], [Cu] and [Hg]) = (4.0, 3.0, 4.0, and 2.0) μgL^{-1} using a 10 µm electrode; **(B)** Simultaneous DPASV calibration response using a 25 µm electrode: **(a)** baseline; **(b** to **h)** increasing metal ion concentrations: Pb from 0.50 to 8.0 μgL^{-1}; As from 0.25 to 3.0 μgL^{-1}; Cu from 0.50 to10 μgL^{-1} and Hg from 0.10 to 3.0 μgL^{-1}. This is an example of an experiment repeated two times.

3.3.5. Repeatability and reproducibility

The stability of the electrodes was studied for microelectrodes with a diameter of either 10 or 25 μm. Firstly, a microelectrode with a diameter of 10 μm was tested for fifteen repetitive measurements by DPASV and SWASV, in a supporting electrolyte solution containing a mixture of 1.0 μgL^{-1} of each one of the following metals/metalloid As^{5+}, Cu, Hg and Pb. After several hours, the same electrode was cleaned with Milli-Q water, conditioned in H_2SO_4 0.5 $molL^{-1}$ by cyclic voltammetry and subjected to more fifteen repetitive measurements in a new mixture solution with the same concentrations of metal/metalloid ions. The RSDs in percentage obtained for As^{5+}, Cu and Pb, by SWASV, were 9, 7 and 4%, respectively, and for As^{5+}, Cu, Hg and Pb, by DPASV, were 12, 5, 5 and 2%, respectively. Similar stability was obtained at 25 μm diameter electrodes, under continuous use, for seven separate DPASV analyses at different days. The RSDs in percentage of the peak derivatives obtained by DPASV for As^{5+}, Cu, Hg and Pb were 9, 4, 11 and 9%, respectively. The stability of these microelectrodes can be considered satisfactory taking into account the relatively low concentration level of metal(loid)s ions involved.

3.3.6. Metal interferences

Metal interference studies were performed to examine the effect of other metals on the stripping signal of a mixture containing 1.0 μgL^{-1} of each one of the following metal/metalloid ions: As, Cu, Hg and Pb. DPASV experiments were carried out to establish interference from Al^{3+}, Cd^{2+}, Cr^{3+}, Cr^{6+}, Fe^{3+}, Mn^{2+}, Ni^{2+}, Sb^{3+} and Zn^{2+}. No significant effect was observed after the addition of up to 1000 μgL^{-1} of Al^{3+}, up to 300 μgL^{-1} of Mn^{2+} and up to 10 μgL^{-1} of Fe^{3+}. The addition of 100 μgL^{-1} of Fe^{3+} decreased by 25, 6, 14 and 10% the signals of As, Cu, Hg and Pb, respectively; in addition, the peaks heights decreased continuously after successive scans indicating the possible build up of interfering compounds at the surface of the gold electrode. The addition of 1μgL^{-1} of Ni^{2+} did not modify the stripping response of As, Cu, Hg and Pb; however, 10 μgL^{-1} of Ni^{2+} decreased by

24 % the response of As and 50 μgL^{-1} of Ni^{2+} reduced by 65 and 20% the As and Pb responses, respectively. Addition of 1 μgL^{-1} of Cr (Cr^{3+} or Cr^{6+}) did not have any interference but 10 μgL^{-1} of Cr (Cr^{3+} or Cr^{6+}) decreased by 30 % the response of Hg and 50 μgL^{-1} of Cr (Cr^{3+} or Cr^{6+}) decreased by 40 and 16 % the Hg and As responses, respectively. Addition of 10 μgL^{-1} of Zn^{2+} did not have any interference on the signals of Cu, Hg and Pb but 100 and 500 μgL^{-1} of Zn^{2+} decreased slightly (less than 10%) the response of these metals. The interference of Zn^{2+} was more severe in the case of As; 10, 100 and 500 $\mu gL^{-1}$of Zn^{2+} decreased 14, 58 and 100%, respectively, the signal of As.

Oxidation peak potentials of Pb and Cd^{2+} were located at -0.22 V and -0.12 V, respectively. The peak potentials were swapped regarding their position on the mercury electrode, in agreement with previous work [10]. For concentrations of Cd^{2+} higher than 1.0 μgL^{-1}, peak overlap prevented accurate Pb determination. In natural waters, the concentration of Pb is normally higher than that of Cd^{2+} [10] and under these conditions Pb could be detected without Cd^{2+} interferences. The same overlapped behaviour occurred for As (peak potential: -0.02 V) in regards to Sb (peak potential: 0.05 V). In these conditions of $E_{dep(s)}$ and acidity, all Sb^{3+} was found to get oxidized within seconds to Sb^{5+}. To remove this Sb interference, a higher E_{dep} (e.g. -0.9 V) can be chosen to selectively deposit As over Sb, as recently shown [25]. Such interference is however unlikely in natural systems where Sb levels are generally an order of magnitude lower than those of As [49].

Taken into account the results previously described, As was the element, which suffered most from these interferences. However, it is noteworthy that the concentration levels of the interfering metals were very high when compared with the concentration levels expected in unpolluted waters [45,46].

3.3.7. Measurements in river water samples

The proposed DPASV method was applied to determine simultaneously the concentration of As, Cu, Hg and Pb in two unpolluted surface river water samples (A and B). Since the presence of organic surface active substances, which tend to adsorb on the electrode surface, can interfere in the direct determination of total heavy metals in natural waters, all water samples were previously UV digested for one hour in order to remove organic compounds. Additionally**,** As, Cu, Hg and Pb concentrations were also determined by AAS-EA or ICP-MS, which were used as reference methods. Comparisons between all four metal/metalloid ions levels, determined by DPASV (either by interpolation using the calibration curve or by extrapolation using standard addition method), and values obtained by the reference methods (AAS-EA and ICP-MS) are presented in table 3.3. Additionally, figure 3.6 displays typical voltammograms recorded for sample B (UV digested and appropriately acidified) without and after standard additions of As, Cu, Hg and Pb; well defined peaks in a wide concentration range were obtained for the four metal/metalloid ions, in a similar way as it was obtained with the synthetic solutions (Figure 3.5). In fact, for both river water samples, table 3.3 evidences a good agreement between the values of As, Cu and Pb determined by the reference methods and DPASV (either by interpolation using calibration curves or by extrapolation using standard addition method). Hg levels were below the DLs of DPASV and ICP-MS methods. Note that no certified material for determining simultaneously all these four elements, in the concentration range of the DPASV method developed in this work, is commercially available. Thus, we decided to fortify sample A with 1.2 and 2.0 μgL^{-1} of As and Hg, respectively (Sample A1 – Table 3.3). A good agreement between the concentration of Hg determined by DPASV and the expected value was attained; in addition, the levels of As, determined by DPASV and ICP-MS were also in good agreement.

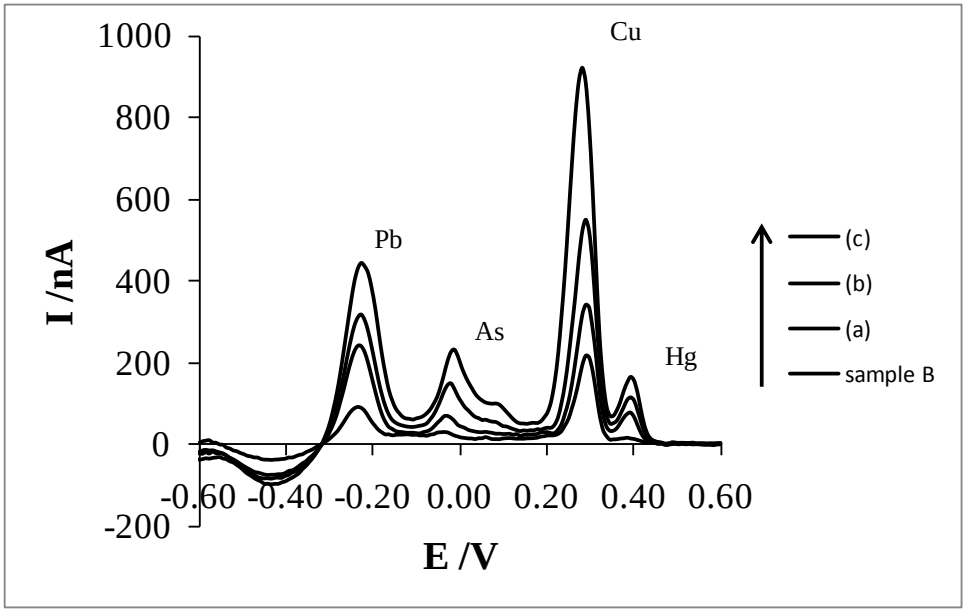

Figure 3.6 – Typical voltammograms (background corrected scans), recorded by DPASV with a 25 μm gold microwire electrode, for a UV digested and acidified river water (sample B) and after simultaneous standard additions of Pb, As, Cu and Hg, respectively: (**a**) 1.5, 0.5, 0.5, and 0.9 μgL^{-1}; (**b**) 2.5, 1.5, 2.0, and 1.5 μgL^{-1}; (**c**) 4.0, 2.5, 3.5, and 2.1 μgL^{-1}.

Table 3.3 – Comparison of As, Cu, Hg and Pb (μgL^{-1}) values determined in surface river water samples by DPASV and reference methods.

Metals	**Pb**		**As**		**Cu**		**Hg**	
				Calibration Curves [a]				
Sample	**DPASV**	**ICP-MS**	**DPASV**	**ICP-MS**	**DPASV**	**AAS-EA**	**DPASV**	**ICP-MS**
A	1.2 ± 0.2	1.03 ± 0.06	0.27 ± 0.02	0.35 ± 0.02	2.0 ± 0.4	1.7 ± 0.3	< DL	< DL
A1	1.46 ± 0.08	1.03 ± 0.06	1.49 ± 0.04	1.55	1.53 ± 0.08	1.7 ± 0.3	2.06 ± 0.05	≤ 2.05
B	1.18 ± 0.07	1.10 ± 0.06	0.39 ± 0.09	0.39 ± 0.02	0.7 ± 0.3	< DL	< DL	< DL
				Standard addition method [b]				
A	1.5 ± 0.3	1.03 ± 0.06	0.30 ± 0.03	0.35 ± 0.02	2.2 ± 0.1	1.7 ± 0.3	< DL	< DL
B	1.1 ± 0.2	1.10 ± 0.06	0.31 ± 0.04	0.39 ± 0.02	1.2 ± 0.3	< DL	0.09 ± 0.05	< DL

[a] Results obtained by interpolation using the calibration curves; [b] Results obtained by extrapolation using the standard addition method; DLs of As, Cu, Hg and Pb, determined by ICP-MS or AAS-EA, are 0.10, 1.3, 0.050 and 0.10 μgL^{-1}; the DLs of As, Cu, Hg and Pb, determined by DPASV, are 0.068, 0.40, 0.066 and 0.15 μgL^{-1}; A1 – sample A spiked with 1.2 and 2.0μgL^{-1} of As and Hg, respectively.

3.4. Conclusions

The use of gold microwire electrodes proved to be an easy task: (i) no need for polishing between runs; (ii) good ability to access negative potentials in acidic conditions; (iii) high sensitivity and stability; (iv) no requirement for removing dissolved oxygen. The ability to perform stripping analysis without deoxygenation greatly simplifies the stripping protocol and decreases the measurement time, which is particularly important to *on-site* or *on-line* applications. The combination of a vibrator with a gold microwire electrode resulted in a very small, stable and reproducible diffusion layer thickness (δ < 1 or 2 μm for a vibrating gold microwire electrode with d = 10 μm or d = 25 μm, respectively), which improved the sensitivity and reproducibility of the results and allowed making determinations with a very short t_{dep}.

This work proved that the vibrating gold microwire electrode is suitable and reliable for monitoring simultaneously As, Cu, Hg and Pb because: (i) the peak potentials of each metal/metalloid are well defined and sufficiently separated and thus the simultaneous voltammetric determination of neighboring elements is possible; (ii) the multi-element determination, in the presence of oxygen and with very short t_{dep}, where no medium exchange or film deposition was required, was attained; this provides fast information and can be easily adapted for on-field measurements; (iii) the DPASV procedure developed is simple, quick and sensitive enough for allowing simultaneous determination of these four elements with DLs in the range of nmol L^{-1}.

The proposed method was successfully applied to the simultaneous determination of these four elements in unpolluted river water samples at concentrations levels below the guidelines values given by EPA [45] and EU [46].

References

[1] M. Pesavento, G. Alberti, R. Biesuz, Anal. Chim. Acta **2009**, 631, 129.

[2] M.L. Tercier-Waeber, M. Taillefert, J. Environ. Monit. **2008**, 10, 30.

[3] J. Wang, Stripping Analysis, VCH Publishers, Inc., Deerfield Beach, Florida, **1985**.

[4] I. Cesarino, C. Gouveia-Caridade, R. Pauliukaite, E.T.G. Cavalheiro, C.M.A. Brett, Electroanalysis **2010**, 22, 1437.

[5] Z. Bi, C.S. Chapman, P. Salaün, C.M.G. van den Berg, Electroanalysis **2010**, 22, 2897.

[6] I. Svancara, C. Prior, S.B. Hocevar, J. Wang, Electroanalysis **2010**, 22, 1405.

[7] E. Tesarova, L. Baldrianova, S.B. Hocevar, I. Svancara, K. Vytras, B. Ogorevc, Electrochimica Acta **2009**, 54, 1506.

[8] M. Slavec, S.B. Hocevar, L. Baldrianova, E. Tesarova, I. Svancara, B. Ogorevc, K. Vytras, Electroanalysis **2010**, 22, 1617.

[9] Y. Bonfil, E. Kirowa-Eisner, Anal. Chim. Acta **2002**, 457, 285.

[10] Y. Bonfil, M. Brand, E. Kirowa-Eisner, Anal. Chim. Acta **2002**, 464, 99.

[11] O. Mikkelsen, K.H. Schroder, Electroanalysis **2001**, 13, 687.

[12] G. Billon, C.M.G. van den Berg, Electroanalysis **2004**, 16, 1583.

[13] I. Pizeta, G. Billon, J.C. Fischer, M. Wartel, Electroanalysis **2003**, 15, 1389.

[14] O. Mikkelsen, K.H. Schroder, Analyst **2000**, 125, 2163.

[15] Y. Bonfil, M. Brand, E. Kirowa-Eisner, Electroanalysis **2003**, 15, 1369.

[16] A. Giacomino, O. Abollino, M. Malandrino, E. Mentasti, Talanta **2008**, 75, 266.

[17] M. Kopanica, L. Novotny, Anal. Chim. Acta **1998**, 368, 211.

[18] C. Locatelli, Analytical Methods **2010**, 2, 1784.

[19] J. Wang, D. Larson, N. Foster, S. Armalis, J.M. Lu, X. Rongrong, K. Olsen, A. Zirino, Anal. Chem. **1995**, 67, 1481.

[20] Y.C. Sun, J. Mierzwa, M.H. Yang, Talanta **1997**, 44, 1379.

[21] J. Vandenhecke, M. Waeles, R. D. Riso, P. Le Corre, Anal. Bioanal. Chem. **2007**, 388, 929.

[22] H.L. Huang, P.K. Dasgupta, Anal. Chim. Acta **1999**, 380, 27.

[23] C. Garnier, L. Lesven, G. Billon, A. Magnier, O. Mikkelsen, I. Pizeta, Anal. Bioanal. Chem. **2006**, 386, 313.

[24] K. Gibbon-Walsh, P. Salaün, C.M.G. van den Berg, Anal. Chim. Acta **2010**, 662, 1.

[25] P. Salaün, K. Gibbon-Walsh, C.M.G. van den Berg, Anal. Chem. **2011**, 83, 3848.

[26] P. Salaün, C.M.G. van den Berg, Anal. Chem. **2006**, 78, 5052.

[27] P. Salaün, B. Planer-Friedrich, C.M.G. van den Berg, Anal. Chim. Acta **2007**, 585 312.

[28] C.S. Chapman, C.M.G. van den Berg, Electroanalysis **2007**, 19, 1347.

[29] S. Daniele, C. Bragato, M.A. Baldo, J. Wang, J.M. Lu, Analyst **2000**, 125, 731.

[30] A. Widmann, C.M.G. van den Berg, Electroanalysis **2005**, 17, 825.

[31] A. Profumo, M. Fagnoni, D. Merli, E. Quartarone, S. Protti, D. Dondi, A. Albini, Anal. Chem. **2006**, 78, 4194.

[32] B.K. Jena, C.R. Raj, Anal. Chem. **2008**, 80, 4836.

[33] X.H. Gao, W.Z. Wei, L. Yang, T.J. Yin, Y. Wang, Anal. Lett. **2005**, 38, 2327.

[34] T. Noyhouzer, D. Mandler, Anal. Chim. Acta **2011**, 684, 1.

[35] S. Laschi, I. Palchetti, M. Mascini, Sens. Actuators B **2006**, 114, 460.

[36] J. Wang, B. Tian, Anal. Chem. **1993**, 65, 1529.

[37] E.A. Viltchinskaia, L.L. Zeigman, D.M. Garcia, P.F. Santos, Electroanalysis **1997**, 9, 633.

[38] K. Stulik, C. Amatore, K. Holub, V. Marecek, W. Kutner, Pure Appl. Chem. **2000**, 72, 1483.

[39] X.D. Xie, D. Stueben, Z. Berner, Anal. Lett. **2005**, 38, 2281.

[40] L. Nyholm, G. Wikmark, Anal. Chim. Acta **1992**, 257, 7.

[41] M.B. Gholivand, A. Azadbakht, A. Pashabadi, Electroanalysis **2011**, 23, 364.

[42] J. Wang, C. Bian, J. Tong, J. Sun, S. Xia, Electroanalysis **2012**, 24, 1783.

[43] Y. Song, G.M. Swain, Anal. Chem. **2007**, 79, 2412.

[44] J.N. Miller, J.C. Miller, Statistics and Chemometrics for Analytical Chemistry,Pearson Education Limited, Fifth Edition, **2005**.

[45] EPA, in "National Recommended Water Quality Criteria. United States Environmental Protection Agency, Office of Water/ Office of Science and Technology" **2009**.

[46] European Comission, in "Directive 2008/105/EC on environmental quality standards in the field of water policy, amending and subsequently repealing Council Directives 82/176/EEC, 83/513/EEC, 84/156/EEC, 84/491/EEC, 86/280/EEC and amending Directive 2000/60/EC" **2008**.

[47] T.R. Lindstrom, D.C. Johnson, Anal. Chem. **1981**, 53, 1855.

[48] R.W. Andrews, J.H. Larochelle, D.C. Johnson, Anal. Chem. **1976**, 48, 212.

[49] M. Filella, N. Belzile, Y.W. Chen, Earth-Science Reviews **2002**, 59, 265.

Chapter 4

VOLTAMMETRIC QUANTIFICATION OF Zn AND Cu, TOGETHER WITH Hg AND Pb, BASED ON A GOLD MICROWIRE ELECTRODE, IN A WIDER SPECTRUM OF SURFACE WATERS[3]

Graphical abstract

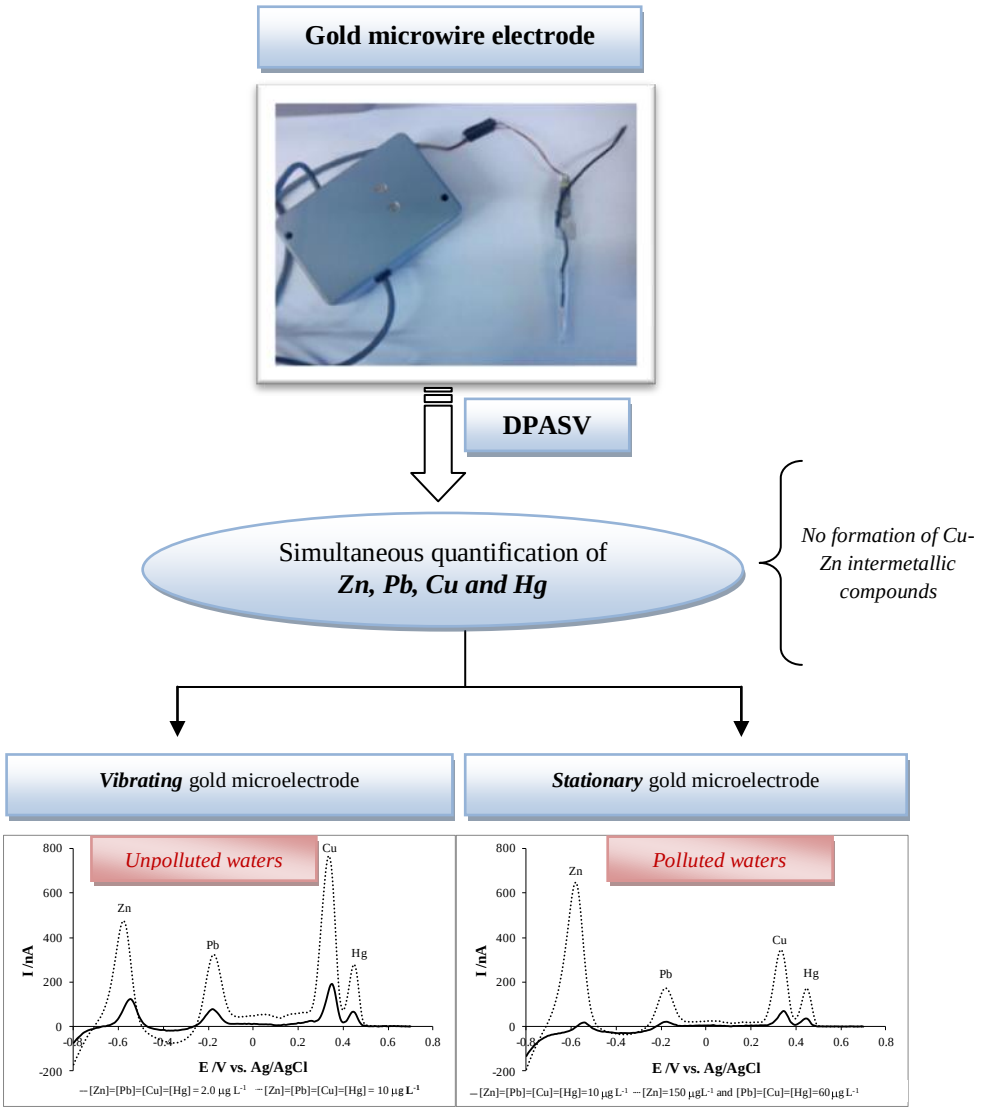

[3] *Electroanalysis* 2013, 25, 493 – 502

Abstract

The simultaneous determination of Zn and Cu by ASV is prone to errors due to the formation of Cu-Zn intermetallic compounds. The main aim of this work was to study the possibility of simultaneous determination of Zn and Cu, together with Hg and Pb, using a mercury-free solid gold microwire electrode. The multi-element detection was carried out by DPASV, in a chloride medium (0.5 $molL^{-1}$ NaCl) under moderate acid conditions (HCl 1.0 $mmolL^{-1}$) in the presence of oxygen, where the gold microwire electrode was used as stationary or vibrating WE during the deposition step. Under these conditions, no formation of Cu-Zn intermetallic compounds was found for concentrations usually determined in surface waters. In addition, quantification of Zn and Cu, together with Hg and Pb, can be performed in a wide range of concentrations (about two orders of magnitude) using the same sample, in a very short period of time. The DLs for Cu, Hg, Pb and Zn, using a vibrating electrode and 30 s of t_{dep}, were 0.2 μgL^{-1} for Hg, 0.3 μgL^{-1} for Pb and 0.4 μgL^{-1} for Zn and Cu, respectively.

The proposed DPASV methods were successfully applied to the determination of Cu, Hg, Pb, and Zn in a certified reference fresh water, river, tap and coastal sea waters. These results proved the applicability and versatility of the proposed methods for the analysis of different water matrices and showed that a gold microwire electrode is a suitable choice to determine simultaneously Zn and Cu.

4.1. Introduction

Heavy metals are recognized as highly toxic, dangerous, persistent and non-biodegradable pollutants [1] and are widely distributed around the Earth. These metals can accumulate in environmental samples and either high or trace levels can be found in river, lake and sea waters. Therefore, the trace metal monitoring in fresh and sea waters is essential for a better control of pollution.

ASV is an effective electroanalytical technique frequently used for determination of heavy metals, particularly in water samples [1-4]. The interest in voltammetry comes from its high sensitivity, low DLs and the possibility of multi-element measurements [1]; these features associated with the characteristics of the instrumentation, which is relatively inexpensive, easily miniaturized and portable, enables its use under field conditions.

Multi-element determination is an important characteristic because it implies a substantial reduction of time of analysis, sample volume and reagents used. However, when more than one metal ion are present in the same sample, the accurate multi-element quantification by ASV may be not possible due to the formation of intermetallic compounds, overlapping of neighboring peaks [Chapter 2 of this thesis,5,6] or simply because the determination of different metals requires different experimental conditions. When an intermetallic compound is formed, the stripping peaks for the metals of interest may be shifted, distorted and/or depressed [Chapter 2 of this thesis,1,7]. In the literature, formation of several intermetallic compounds have been addressed; among them, formation of intermetallic Cu-Zn compounds are commonly reported [Chapter 2 of this thesis, 5-14], especially at a mercury [6,8-11] and bismuth film electrodes [Chapter 2 in this thesis,5,12] but also for other electrodes such as a GC [13] and in a nanocrystalline diamond thin-film electrodes [7]. The formation of Cu-Zn intermetallic compound at a BiFE, previously reported in chapter 2 of this thesis, confirm the trend of BiFEs for the formation of these compounds.

Metals, such as Zn and Cu, are common in waters; so, chemical, mathematical and instrumental approaches have been suggested for minimizing or

eliminating this problem [6,8]. Frequently, to overcome this limitation, the addition of Ga^{3+} ions has been suggested [5,8,11] and Tyszczuk *et al*. [14] proposed the application of Ga film electrode for eliminating the Cu interference in the anodic voltammetric determination of Zn. In addition, to overcome this limitation, the application of chemometric tools proved to be an alternative to be considered, as it was demonstrated in chapter 2.

According to the assumptions above, a crucial point to the success of a voltammetric techhnique is the choice of a suitable WE [5,15]. Ideally, as it was described in chapter 1, a suitable WE must provide a good analytical performance (high sensitivity, robustness, stability, low DLs and application in a wider range of concentrations); additionally, the electrode should be non-toxic, operate using cost-efficient technology and be free of organic and or intermetallic interferences.

Both gold disk [16] and wire [17] microelectrodes have been recently proposed as good electrode materials to measure Zn in fresh and sea waters. These determinations were made at natural pH because the hydrogen wave on the gold electrode is more positive than on the mercury electrode; thus, the reduction potential for Zn is close to the hydrogen wave. However, as a result of UPD, peak potentials for metals deposited on gold microelectrodes are shifted to more positive potential compared to mercury electrodes; due to this reason, it is possible to quantify Zn at gold electrodes. Nevertheless, the determination of this metal at natural pH required sample deoxygenation to eliminate background current [16,17]. On the other hand, in chapter 3, we have shown that ASV using a vibrating gold microwire electrode allowed a simple, quick and reliable simultaneous determination of As, Cu, Hg and Pb in unpolluted river waters. But, the very acidic conditions of the electrolyte used unable the determination of Zn. Moreover, the method only allowed the determination of narrow concentration ranges typical of unpolluted surface natural waters according to the guidelines from EPA-USA [18] and EU [19]. Therefore, in this work, our aim was to explore and extend the potentialities of the gold microwire electrode for the simultaneous determination of Zn and Cu, together with Hg and Pb, in a suitable supporting

electrolyte and without removing oxygen, under a wide range of concentrations levels in different types (saline or fresh) of waters.

4.2. Experimental

4.2.1. Reagents and solutions

The Cu and Zn stock solutions were prepared by dilution of 2000 mgL^{-1} of $CuCl_2$ in Milli-Q water (18.2 $M\Omega cm^{-1}$) and $ZnCl_2$ in acidified Milli-Q water (0.06 % HCl). Solutions of $CuCl_2$ and $ZnCl_2$ were both purchased from Merck. More diluted unacidified stock solutions were prepared freshly for use. Sodium hydroxide (NaOH) p.a. (≥ 99%) from Merck where was used to adjust the pH of water samples

All remaining reagents and solutions, used in this chapter, were already described in sections 2.2.1 and 3.2.1 from chapter 2 and 3, respectively.

4.2.2. Equipment

All voltammetric measurements, performed with a gold microwire WE, were made with a potentiostat – galvanostat model PGSTAT12/30/302 coupled to an IME 663 interface both from Autolab driven by GPES 4.9 software (Eco Chemie) and using a "home-made" faraday cage. A 6.1415.210 voltammetric glass cell from Metrohm containing a gold microwire WE with 25 μm diameter was used. The remaining electrodes (CE and RE), as well as the procedure used to prepare the gold and iridium microwire electrodes [20-22] were already described in section 3.2.2

All pH measurements were performed with a pH Meter GPL 22 with a 52 02 pH electrode from Crison as described in section 2.2.2. Digestion of water samples was made in a similar way as it was described in section 3.2.5. In order to minimize contaminations all glass materials, including electrochemical cell, were decontaminated as reported in section 2.2.1.

4.2.3. Electrode conditioning and characterization

The gold microwire WE was cleaned in 0.5 $molL^{-1}$ H_2SO_4 solution by hydrogen generation at - 4 V (60 s), when the electrode was new, and at -2 V (30 s) when fouling was suspected [23]. In order to check how the electrode was working and to eliminate any memory effects related with the adsorbed chloride ions, the electrode was conditioned daily by cyclic voltammetry (5 scans) from 0 to 1.5 V (100 mVs^{-1}) [Chapter 3 in this thesis, 23].

The A_R, A_G, and the value of the δ were determined as described previously in section 3.2.3.

4.2.4. Voltammetric procedures for determination of metals

Trace metals were determined by DPASV using a gold microwire electrode as stationary or as vibrating WE during the deposition step. Measurements were carried out at room temperature, without sample deoxygenation, in HCl 1.0 $mmolL^{-1}$ with the addition of NaCl solid powder corresponding to 0.5 $molL^{-1}$.

Like in chapter 3, here it was used a subtractive DPASV procedure, i.e., each measurement consisted of two scans: an analytical scan and a background one. The background scan was made with 2s of t_{dep} and was automatically subtracted from the analytical scan; the peak derivative of the background corrected scan was used for quantification. Each measurement was repeated three times and the different steps were automated using the "project" option in the GPES software. Before the analytical and the background scans, a Conditioning potential (E_{cond}) of 0.55 V during 5 s was applied to the WE under vibration conditions. The E_{dep} was -1.0 V during 32 s, using a vibrating or a stationary WE, depending of the voltammetric procedure. After an t_{eq} of 1s, the voltammogram was recorded by applying a positive DPASV potential scan from -0.8 V to 0.7 V applying the same step potential, amplitude, modulation time, interval time and standby potential previously used for the DPASV simultaneous determination of

As, Cu, Pb and Hg, respectively (Table 3.1). When different conditions were used, they will be properly identified.

4.2.5. Analysis of water samples

The developed procedures were applied to multi-element (Cu, Zn, Hg and Pb) determination in river, sea and tap water samples, as well as in the certified reference surface fresh water sample (SPS-SW1 Batch 117 from LGC Standards).

River and coastal sea water samples were collected and filtered (with sterilized GN-6 Metricel membrane disc filters with 0.45 μm); tap water sample, collected from taps at home, was not filtered. River water sample was acidified to pH 2 with HCl and then stored in the refrigerator. Coastal sea water and tap water samples were frozen, at neutral pH, and then defrosted at the time of analysis.

As described in chapter 3, prior to electrochemical determinations all samples were UV digested for 1h to avoid possible organic interferences, caused by natural organic compounds, and to breakdown organic metal complexes. Then, a digested water sample was placed in the voltammetric cell and the pH of the samples was adjusted to pH 3 with a few micro liters of concentrated solutions of HCl or NaOH. After this correction of pH, the resulting variation of volume was less than 0.4 % and was not considered in the subsequent calculations. River, tap and certified reference water samples were spiked with NaCl corresponding to 0.5 $molL^{-1}$.

Finally, water samples were also analysed by AAS: Cu and Pb by AAS-EA, Zn by AAS-FA and Hg with atomic absorption spectroscopy with cold vapour (AAS-CV). The determination of Pb and Cu in coastal sea water sample was performed using a Metrohm 663 VA stand in combination with a microAutolab and an IME 663 interface from Eco Chemie using a MFE at -1.3 V (t_{dep} = 120s) [24]. The results obtained by these methods were used as reference values.

Measurements of Cu and Pb, made by AAS-EA, and of Zn, determined by AAS-FA, were made using the same spectrophotometers already described in section 2.2.2. Hg was quantified by AAS-CV with a FIAS 100 module from Perkin Elmer coupled to a Perkin-Elmer 3100 atomic absorption spectrophotometer; for this specific case, sample digestion, prior to Hg determination, was performed using a Milestone 1200 mega microwave-digester.

All experiments were performed in duplicate at room temperature.

4.3. Results and discussion

4.3.1. Optimization of the analytical parameters for the determinations

4.3.1.1. Effect of the pH on the Zn DPASV response

The determination of Zn in natural waters at bare gold electrodes has seldom been described and is usually performed at natural pH [16,17] because the peak potential of this metal in acid medium is located on the cathodic limit of the potential window for gold electrodes. This process was described as an example of UPD on gold microelectrodes, with a positive shift of the Zn oxidation peak potential compared to mercury electrodes. This shift to more positive potential values allowed easier analysis of Zn at natural pH [16, 17]. Moreover, literature reports that the addition of acid improves the determination of Pb [25,26], Cd [25,26], Cu [20] and Hg [27,28] at gold electrodes. Another key factor in UPD deposition is the anionic composition of the samples because anions are involved in the deposition step. For instance, the presence of chloride ions is necessary and has a significant contribution in the resolution of Hg peak due to the formation of chlorocomplexes of this metal [Chapter 3 in this thesis, 20,27].

So, based on all the statements mentioned above, and in order to optimize Zn determination and keeping open the possibility to make together the accurate analysis of Cu, Hg, Pb, and Zn, we decided to study the effect of the pH of the supporting electrolyte solution for acid and moderated acidic conditions (initially, the pH was 4.22 and then, it was lowered until 1.08 by adding HNO_3) without

previous deoxygenation. These measurements were carried out on the DPASV mode, for 5.0 μgL^{-1} of Zn, using a 25 µm gold microwire vibrating electrode and the supporting electrolyte solution was constituted by NaCl 0.5 $molL^{-1}$.

For the analysis of the pH effect, two points are important: (i) the peak position and (ii) the sensitivity of the response (peak height of Zn). For these experiments, the results are presented in figure 4.1.

Garnier *et al.* [16] reported that the response of Zn in sea and river waters at natural pH and at a 25 µm gold microdisk electrode was characterized by two successive peaks. This phenomenon was attributed to a mixed process including UPD deposition forming a metal monolayer on the gold electrode surface (Au-Zn monolayer) and a further deposition of a multiple layer of Zn (Zn-Zn deposits). In this work, a single well defined peak was observed for Zn [Figure 4.1 (A)]; this behavior suggests UPD deposition of the metal on the gold electrode and is consistent with recent results obtained in sea water, at natural pH, using a gold microwire electrode [17].

The results of this experiment clearly evidence that Zn can be detected under mild acid conditions (at pH 3) without previous deoxygenation. So, further work was performed under these experimental conditions.

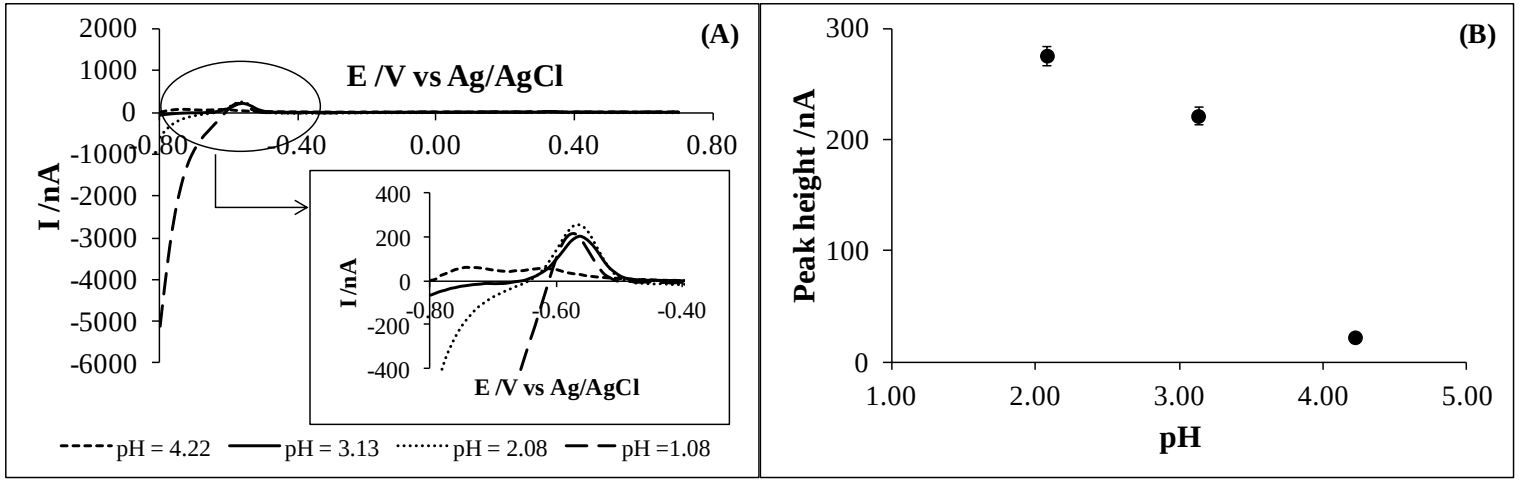

Figure 4.1 – Effect of the pH on the voltammetric response for 5.0 μgL^{-1} of Zn. **(A)** DPASV response using a vibrating 25 µm gold microwire electrode with 1.3 mm of length (E_{dep} = -1.2 V and t_{dep} = 32 s), with background (t_{dep} = 2s) subtraction and without deoxygenation, in 0.5 M NaCl at the pH values indicated. (**B**) Effect of the pH on the Zn peak height. Mean and standard deviation (vertical error bars) of three replicates of two independent experiments (n = 6); where no error bars are shown, they are within the points.

4.3.1.2. Effect of the deposition potential on the Cu, Hg, Pb and Zn DPASV responses

The effect of the E_{dep}, using a vibrating working electrode, on the stripping current for the multi-element determination of 1 μgL^{-1} of Cu, Hg, Pb and Zn in HCl 1.0 $mmolL^{-1}$ with NaCl 0.5 $molL^{-1}$ electrolyte solution was evaluated in the potential range between -1.4 V and -0.60 V. The $E_{dep(s)}$ had no significant effect on Pb, Cu and Hg peak derivative signals. On the other hand, for Zn, peaks were only observed for $E_{dep(s)}$ between -0.8 to -1.4 V; a maximum peak height was attained at E_{dep} of -1.0 V.

According to these results, for further work, the following conditions were used: a supporting electrolyte constituted by HCl 1.0 $mmolL^{-1}$ (pH 3) with NaCl 0.5 $molL^{-1}$ and a E_{dep} of -1.0 V.

4.3.2. Zn DPASV response and Cu interference

According to the literature [5-14] and as it was previously discussed in chapter 2, Cu is a severe interference in the Zn determination due to the formation of Cu-Zn intermetallic compounds in different electrode substrates. For this reason, the interference of Cu on the electrode response towards Zn was investigated.

Firstly, the response of the electrode towards Zn was studied. So, individual calibration for Zn with a vibrating gold microwire electrode, using the previous optimized conditions, was performed; the results obtained are summarized in table 4.1. These results evidence that the removal of oxygen was not necessary; consequently, this fact decreased the analysis time. This is an important improvement because dissolved oxygen was found to interfere with Zn determination at the gold microelectrodes [16,17].

Results presented in table 4.1 also show that, using an electrode with a length of 1.3 mm, Zn response was linear for concentration values up to 15 μgL^{-1} and the DL [29] obtained was 0.4 μgL^{-1}. These results are in good agreement with

results obtained for Zn, in sea water samples at natural pH, by Gibbon- Walsh *et al*. [17], despite mildly acidic conditions were used in the present work.

Under the present experimental conditions, the linear concentration range for Zn was quite narrow and concentrations of Zn corresponding to the criterion continuous concentration – maximum acceptable chronic exposure (81 and 120 μgL^{-1} in salt and fresh waters, respectively), established by EPA-USA [18] guidelines, could not be measured without previous sample dilution. In surface waters, the Zn background concentrations are usually <50 μgL^{-1}, but, in surface and ground waters, concentrations of Zn can range from 0.002 to 50 mgL^{-1} [30]. So, the possibility of extending the LCR was studied in order to encompass the guidelines values from EPA [18] in surface waters and allow quantifying this metal in more polluted waters. To accomplish this aim, three possibilities were considered: (i) to decrease the t_{dep}, (ii) to increase the area of the electrode, which corresponded to increase the length and/or the diameter of the electrode and (iii) to make measurements using the gold microwire electrode as a stationary WE during the deposition step. Under these last experimental conditions, the value of δ increases and thus, sensitivity and LCR are decreased and increased, respectively. The t_{dep} used was very short (30 s); so, we decided to keep this value. According to results obtained in chapter 3, the increasing of the area of the working electrode provoked a limited effect on the LCR of the metals studied. In addition, the analytical procedures become more complicated since it is necessary to use two different electrodes. Therefore, we decided to do the Zn calibration curve using the gold microwire electrode as a stationary WE during the deposition step. The results obtained are presented in table 4.1. Under these experimental conditions, the LCR was considerably wider (up to 200 μgL^{-1}) and the sensitivity was at least 10 times lower than the one obtained when the gold microwire electrode was used in the vibrating mode. The values of the diffusion layer size (μm), determined for vibrating and stationary gold microwire electrodes [Chapter 3 in this thesis, 20] were 1.92 ± 0.01 and 34 ± 2 [average with standard deviation for three replicates (n = 3)], respectively; these results confirm that the decrease in sensitivity of the stationary electrode was due to the increase of the diffusion layer size.

Table 4.1 – Calibration parameters of the individual determination of Zn using a vibrating and a stationary gold microwire electrode during the deposition step (30 s).

Gold microwire electrode	**Linearity /μgL^{-1}**	**DL /μgL^{-1}**	**Peak Potential /V**	**Width (1/2) /V**	**Sensitivity /nAV^{-1} μg^{-1}L mm^{-1}**	**r^2**
Vibrating	0.4 – 15	0.4	(-0.562)–(-0.594)	0.071 – 0.087	869 ± 32	0.993 (n=24)
Stationary	3 – 200	3	(-0.562)–(-0.594)	0.079 – 0.087	70 ± 3	0.995 (n=42)

n –number of points in the calibration curve; The values of the sensitivities were calculated with a confidence interval of 95%.

According to Gibbon- Walsh *et al*. [17], an addition of 50 $\mu molL^{-1}$ of Cu decreased the Zn peak by 75%. However, this metal addition was at least 1000 times greater than the Cu natural levels [17]. Levels of Cu in surface waters can range from 0.5 to 1000 μgL^{-1}, with a median of 10 μgL^{-1} [31]. In sea waters, Cu concentrations are usually lower than 1–5 μgL^{-1} [31]. So, special attention of Cu interference on the Zn response should be taken into account. Based on the typical median Cu concentration values, that can be found in waters [31], the possible interference of Cu on the response of 5 and 100 μgL^{-1} of Zn, using a vibrating [Figure 4.2 (A)] or a stationary [Figure 4.2 (B)] gold microwire electrode, respectively, was studied. The voltammograms, presented in figure 4.2 (A), were recorded for 5 μgL^{-1} of Zn without and with increasing concentrations of Cu, using the electrode in a higher sensitive mode (vibrating electrode). These voltammograms evidenced that no significant influence of Cu on the Zn peak height was observed under the experimental conditions used. Similar results were obtained when the gold microwire electrode was used in a stationary mode with 10 or 100 μgL^{-1} [Figure 4.2 (B)] of Zn. From the analysis of figure 4.2, we can conclude that there is no evidence of Cu-Zn intermetallic compounds for the conditions tested since both peaks were well defined and no depression or increase of the signals were observed [5]. These results suggest that the gold microwire electrode seems to be a good choice to determine Zn and Cu simultaneously.

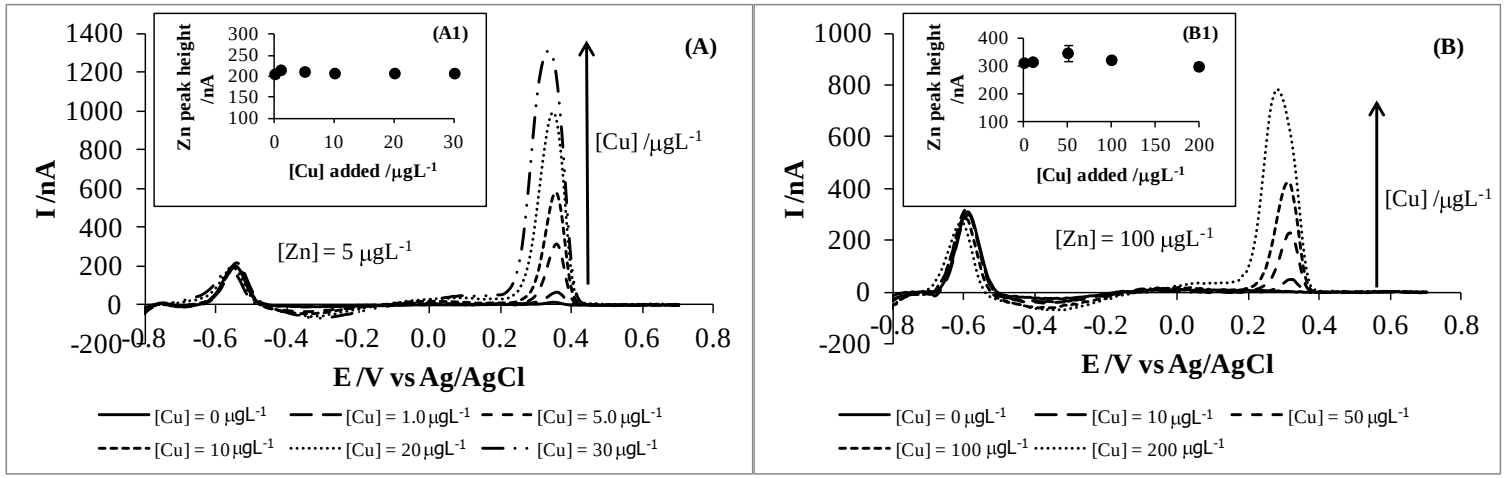

Figure 4.2 –Background subtracted voltammograms obtained, with a gold microwire electrode with 1.3 mm of length, for simultaneous determination of Zn and Cu by DPASV using **(A)** the vibration or **(B)** the stationary mode. **Inserts**: Zn response (peak height) in function of the addition of increasing concentrations of Cu. Values are the average of three replicates; standard deviation (vertical error bars) are present (n = 3); where no error bars are shown, they are within the points.

4.3.3. Simultaneous determination of Cu, Hg, Pb and Zn

From results presented in section 3.3.6, we have learned that concentrations of Zn up to 500 μgL^{-1} caused variations less than 10% on the determination of Cu, Hg, and Pb, respectively. Additionally, in this work, we demonstrated that it is possible to determine Cu and Zn in a single scan without intermetallic interferences (Section 4.3.2). Furthermore, the electrolyte solution was chosen to keep open the possibility of simultaneous determination of Pb and Hg (Section 4.3.1.1).

According to the literature, a vibrating gold microwire electrode has a high potential for determination of trace metals levels (μgL^{-1} or ngL^{-1}); this electrode has been often applied for this purpose in unpolluted waters [Chapter 3 of this thesis, 20,23]. In general, this electrode is very sensitive; thus, the linear response range is very tight due to the rapid saturation of its surface. In order to increase the potential of application of this electrode for simultaneous monitoring of total metals in a wider spectrum of surface waters, we decided to study the possibility of simultaneous determination of Cu, Hg, Pb and Zn, using the gold microwire electrode in stationary mode, and thus to increase the linear concentration range response for each metal.

Initially, the previous optimized conditions were used to make individual calibrations of these metals (Cu, Pb, Hg and Zn), using a vibrating or a stationary WE during the deposition step, in the presence of oxygen; the obtained results are summarized in table 4.2. For both modes (vibrating or stationary), the sensitivity towards the metals (Table 4.2) decreased in the following order: Cu > Zn > (or ~) Hg > Pb. Additionally, when the gold microwire electrode is used as a stationary electrode, the sensitivity is about 10 times lower than when it is used in the vibrating mode; as a consequence, a considerable increase of LCRs can be achieved (Table 4.2). These differences of sensitivities were reflected in the DLs. For a E_{dep} of -1.0 V during 30 s, the DLs [29] obtained, when the electrode was used in the vibrating mode, were: 0.2 μgL^{-1} for Hg, 0.3 μgL^{-1} for Pb and 0.4 μgL^{-1} for Cu and Zn; these DLs are low enough to determine the concentrations of these metals according to the guidelines values of the EPA-USA [18] and of the EU

[19]. On the other hand, when the electrode was used in the stationary mode, the DLs [29] obtained were: 5.0 μgL^{-1} for Hg, 4.0 μgL^{-1} for Pb and 3.0 μgL^{-1} for Cu and Zn.

In the next step, the simultaneous determination of the four metals (Cu, Hg, Pb and Zn), using a vibrating or a stationary WE, was tried in order to access the potentialities of quantifying these four metals in the same scan [Table 4.2 and Figure 4.3 (A)]. To avoid the progressive saturation of the gold electrode surface, the maximum concentration of each metal used was lower than the upper limit of the LCR (Table 4.2). Figure 4.3 shows an example of the voltammograms recorded for the simultaneous calibration of all four metal ions; figure evidences that all peaks, recorded for a wide range of concentrations, were well defined, sharp and symmetrical and no overlapping of the peaks occurred; additionally, no significant differences in the peak potential and $W_{1/2}$ were observed. For all four metals, the comparison between the calibration curves for each metal obtained individually or simultaneously (Table 4.2) showed similar linear concentration dependence, equivalent sensitivities and good correlation coefficients. These results demonstrate that, under the experimental conditions used, there is no formation of intermetallic compounds between the four metal ions tested. Thus, the application of the present experimental conditions (pH 3 and E_{dep} = -1.0 V) allows determining concentrations of Cu, Hg and Pb up 60 μgL^{-1} and for Zn up to 150 μgL^{-1} in the same scan without any mutual interferences.

In chapter 3, As was determined instead of Zn, together with Cu, Hg and Pb under different experimental conditions (pH 1 and E_{dep} = -1.2V). The procedure proposed in the present work does not allow determining total As since very acidic conditions (pH 1) are needed for this purpose. On the other hand, it has the advantage of determining Zn (together with Cu, Hg and Pb), which is usually more widely spread. Additionally, the new procedure also expands the LCRs for Cu, Hg and Pb (Table 4.2) without compromising significantly the DLs (see Table 3.2.). These results are particularly interesting because they point out that performing two sequential scans with the same electrode (using as vibrating or stationary working electrode) in the same sample during a short period of time

(2 × 30 s), it is possible to quantify the four metals in a wide range of concentrations (about two orders of magnitude; Table 4.2). Finally, the stability and reproducibility of the electrode monitored during several days were satisfactory: (i) for a mixture containing 1 μgL^{-1} of each metal and using the gold microwire as a vibrating electrode, the RSDs in percentage (n = 21) were 10, 7, 6 and 8% for Zn, Pb, Cu and Hg, respectively; (ii) for a mixture containing 20 μgL^{-1} of each metal and using the gold microwire as a stationary electrode, the RSDs in percentage (n = 9) were 9, 6, 8 and 6% for Zn, Pb, Cu and Hg, respectively.

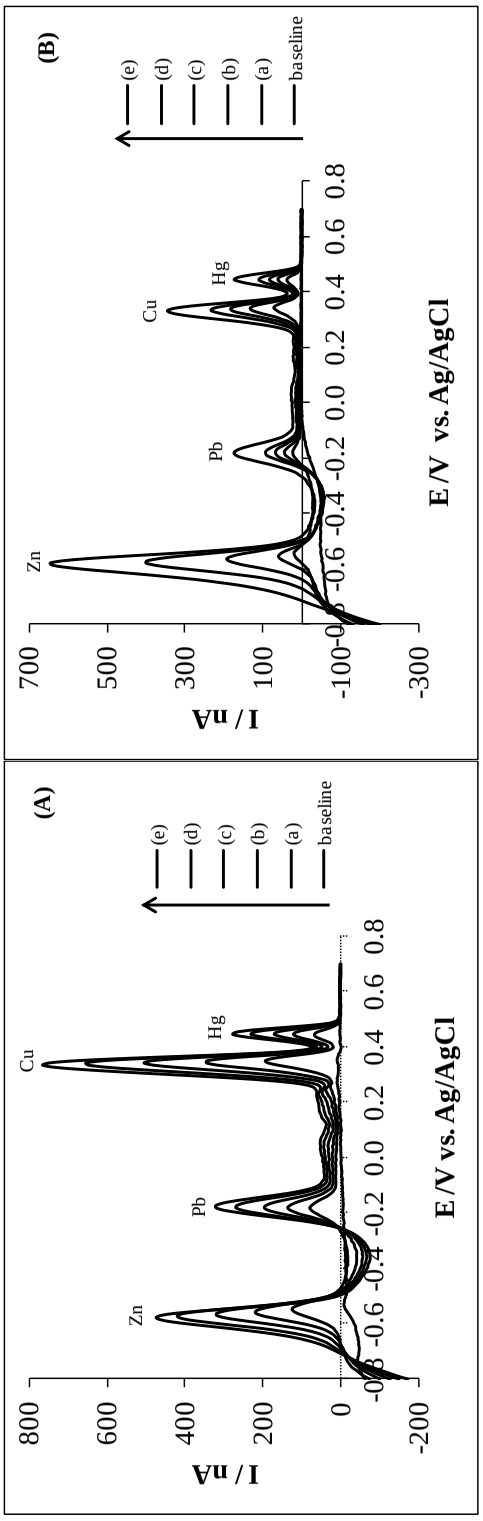

Figure 4.3 – Background subtracted voltammograms obtained for simultaneous DPASV calibration of Cu, Hg, Pb and Zn using a gold microwire electrode with 1.6 mm of length: **(A)** with vibration, **(a)-(e)** increasing metal concentrations, from 2.0 to 10.0 μgL^{-1}, for Zn, Pb, Cu and Hg; and **(B)** without vibration**, (a)-(e)** increasing metal concentration from 10 to 150 for Zn and from 10 to 60 μgL^{-1} for Pb, Cu and Hg. This is an example of an experiment repeated two times.

Table 4.2 – Calibration parameters of the individual and simultaneous determinations of Cu, Hg, Pb and Zn using a vibrating or a stationary gold microwire electrode during the deposition step (30 s).

Metals	Analytical parameters	Vibrating gold microelectrode		Stationary gold microelectrode	
		Individual calibration	Simultaneous calibration	Individual calibration	Simultaneous calibration
Cu	Sensitivity /nAV^{-1} μg^{-1}L mm^{-1}	1715 ± 48	1601 ± 76	115 ± 3	123 ± 7
	Linearity /μgL^{-1}	0.4 – 30	2 – 10	3 – 80	10 – 60
	r^2	0.994 (n=34)	0.992 (n=18)	0.996 (n=21)	0.987 (n=18)
Hg	Sensitivity /nAV^{-1} μg^{-1}L mm^{-1}	658 ± 23	662 ± 25	76 ± 3	68 ± 4
	Linearity/μgL^{-1}	0.2 – 20	2 – 10	5 – 100	10 – 60
	r^2	0.991 (n=33)	0.995 (n=18)	0.994 (n=23)	0.988 (n=18)
Pb	Sensitivity /nAV^{-1} μg^{-1}L mm^{-1}	625 ± 18	611 ± 19	58 ± 2	53 ± 2
	Linearity/μgL^{-1}	0.3 – 15	2 – 10	4 – 100	10 – 60
	r^2	0.995 (n=27)	0.997 (n=18)	0.994 (n=24)	0.993 (n=18)
Zn	Sensitivity /nAV^{-1} μg^{-1}L mm^{-1}	869 ± 32	826 ± 30	70 ± 3	76 ± 2
	Linearity/μgL^{-1}	0.4 – 15	2 – 10	3 – 200	10 – 150
	r^2	0.993 (n=24)	0.995 (n=18)	0.995 (n=42)	0.996 (n=18)

The values of the sensitivities were calculated with a confidence interval of 95%; n – number of points in the calibration curve.

At this point, it is important to compare the results obtained in this work with those reported in the literature. Literature described the application of a bismuth-film modified graphite-polyurethane composite electrode as an attractive option for simultaneous determination of Zn, Cd, Pb, Cu and Hg [32]. In this work [32], in a similar way to our results, no evidence of Cu-Zn intermetallic compounds formation was described. In relation to the DLs, after normalizing the DLs values by the different $t_{dep(s)}$ used, the DLs for Pb, Cu and especially for Hg, determined in our work, are lower than the ones described by Cezarino *et. al*. [32]; in the case of Zn, the DL is of the same order of magnitude. Although, it is not possible to determine Cd simultaneously with Cu, Hg, Pb and Zn using the gold microwire electrode in a conventional approach, the application of the gold microwire electrode demonstrated the ability of determining rapidly these four metals (Cu, Hg, Pb and Zn) in a wider range of concentrations. Cezarino *et. al*. [32] reported that surface active compounds influenced the square wave ASV response of heavy metals. This is a common problem of voltammetric metals determination in natural samples. The previous UV digestion of the samples, as it was done in this work, is an effective procedure to overcome this problem since it destroys the dissolved organic matter, which can complex trace metals or/and interact with the electrode materials, as surfactants. The comparative analysis of other works, where the simultaneous determination of metals, including Zn and Cu, were performed using bismuth electrodes [Chapter 2 of this thesis, 12 and references therein] evidences that in the present work low DLs and wider LCRs were achieved without being necessary additional reagents or the application of chemometrics treatments.

4.3.4. Metal interferences

Interferences of 10 μgL^{-1} of As [As^{3+} or As^{5+}], Cr [Cr^{3+} or Cr^{6+}], Fe^{3+}, Mn^{2+}, Ni^{2+} and Sb^{3+} and 0.5, 2.0 and 5.0 μgL^{-1} of Cd^{2+} in the simultaneous determination of a mixture containing 1.0 μgL^{-1} of Cu, Hg, Pb and Zn were evaluated using the gold vibrating electrode. No significant effect was observed after the addition of 10 μgL^{-1} of [As^{3+} or As^{5+}], Cr [Cr^{3+} or Cr^{6+}], Fe^{3+}, Mn^{2+} and

Sb^{3+}. In the case of As, it is important to note that despite the known Zn interference with the As determination, described in chapter 3, the reverse situation was not observed. However, 10 μgL^{-1} of As [As^{3+} or As^{5+}] resulted in a large peak, at ~ -0.05 V, with a small shoulder on the anodic side but did not interfere with the determination of Pb; this last response was more sensitive for As^{3+} than for As^{5+}. These results evidence that, under these experimental conditions, a correct quantification of As [As^{3+}, As^{5+} or total As] is not possible.

In the case of Cd^{2+}, it was possible to detect as low concentrations of Cd^{2+} as 0.5 μgL^{-1} in the presence of 1.0 μgL^{-1} of Pb but it was not possible to quantify correctly 2.0 or 5.0 μgL^{-1} of Cd^{2+} and 1.0 μgL^{-1} of Pb, simultaneously (data not shown). The use of a gold electrode for quantifying simultaneously Cd^{2+} and Pb using a conventional approach is restricted because Cd^{2+} and Pb peaks are overlapped. Our results are in agreement with the literature [26]. Considering that the sensitivity of the gold microwire electrode for Pb is higher than for Cd^{2+} and the concentration levels of Pb in natural waters are usually higher than for Cd^{2+} [26], under these conditions, Pb can be detected without Cd^{2+} interferences.

The addition of 1 μgL^{-1} of Ni^{2+} did not modify the stripping response of Cu, Hg, Pb and Zn when a vibrating gold microwire electrode was used. However, the addition of 10 μgL^{-1} of this metal caused a modification of the shape of the voltammogram in the cathodic side, which interfered with Pb and mainly with Zn peaks. As a consequence, there was an increase of about 27 and 22 % of the peak derivative of Pb and Zn, respectively, whereas the peaks of Cu and Hg did not suffer any interference. Additionally, the possible interferences due to the addition of 10 or 50 μgL^{-1} of Ni^{2+} with the simultaneous measurement of a mixture containing 20 μgL^{-1} of Cu, Hg, Pb and Zn, using a stationary gold electrode during the deposition step, were studied; no interference was observed. These results clearly indicate that the phenomenon of metal interferences depends not only of the concentration ratios of the metals involved but also of the amount of metal, which is deposited on the electrode surface.

4.3.5. Determination of metals in water samples

The developed DPASV methods were applied to quantify the concentrations of Cu, Hg, Pb and Zn in a certified reference (SPS-SW1 surface fresh water), river, coastal sea and tap water samples. Except for the certified reference sample, the concentrations of Cu, Hg, Pb and Zn were also determined by reference methods. The results obtained for the four metals, determined by DPASV (by interpolation using the calibration curve and by extrapolation using the standard addition method, if necessary) or by the reference methods, are presented in table 4.3.

The certified reference water sample is a surface fresh water, which contains 45 elements including 0.52 μgL^{-1} of Cd, 10.0 μgL^{-1} of As and 10 μgL^{-1} of Ni. Considering the amounts of metals present, a sequential multi-element determination, performed in the original sample, was adopted; in a first attempt, Cu and Zn were quantified using a stationary gold microelectrode [voltammogram a) in Figure 4.4] followed by the determination of Hg and Pb using a vibrating gold microelectrode [voltammogram b) in Figure 4.4]. No peaks were detected for As and Cd in this sample, which is in agreement with our previous results (see section 4.3.4.); thus, no interference with the determination of Pb was observed. As it was pointed out previously (see section 4.3.4.), 10 μgL^{-1} Ni can potentially interfere in the determination of Pb and Zn using a vibrating electrode. However, no distortion of the baseline seems to occur and the determination of Pb was not affected [see voltammogram b) in Figure 4.4]. The results obtained showed a satisfactory agreement between the concentration values determined by the DPASV methods proposed and the reference values (Table 4.3). This sample was also analyzed by DPASV using a vibrating electrode after 5 fold dilution and being spiked with 1.5 μgL^{-1} of Hg [voltammogram c) in Figure 4.4, and Table 4.3]. Please note that we decided to dope this sample with Hg because no certified material is commercially available for determining all four metals in the concentration ranges of the DPASV methods developed in this work. A good correlation between the concentration of the four metals determined by the DPASV method and the expected values were attained (Table 4.3). Besides this

certified reference material, metals contents present in another fresh water sample (river water in Table 4.3) were also analyzed using a sequential multi-element determination: (i) Zn was quantified using a stationary gold microelectrode and (ii) Cu, Hg and Pb were quantified using a vibrating gold microelectrode. A good agreement between the concentrations of Cu, Pb and Zn determined by the DPASV and the reference methods was attained. Concentration of Hg was below the DLs for both methods (DPASV with vibrating electrode and reference one).

In order to broad the field of application of the DPASV methods, developed in this work, the metals were also quantified in other types of water samples, specifically a tap water (as an example of a drinking water) (Table 4.3), which can contain up to a few mgL^{-1} of Zn [18], and a coastal sea water (Table 4.3). A first tentative to determine metals in the original tap water sample using a stationary electrode evidenced that the concentration of Zn was above the LCR whereas the concentrations of the other metals (Cu, Hg and Pb) were below the detection limits of this less sensitive method. In a subsequent run, Cu and Pb were determined directly in the same original sample using the vibrating electrode (Table 4.3); concentration of Hg was below the DL (Table 4.3). Then, Zn was quantified in a 5 fold diluted sample using a stationary electrode. A good agreement between the concentrations of Cu, Pb and Zn, determined by the DPASV and reference methods were attained (Table 4.3). It is important to point out that, despite the high concentration of Zn present in the undiluted sample, the concentrations of Cu and Pb were accurately determined by the DPASV method.

For coastal seawater, all metals were quantified in the same original sample using a sequential multi-element strategy; Cu, Hg and Pb were determined using a vibrating electrode and Zn was quantified using a stationary electrode (Table 4.3). Besides Hg, which concentration was below the DL (Table 4.3), good agreement between the values determined by the reference and the DPASV methods was obtained. In this case, the result obtained for Cu using the standard addition method (Table 4.3) was more in agreement with the one determined by the reference method than the value calculated by the direct calibration of the

DPASV method; this fact can probably be due to some modifications of the voltammogram, as a consequence of matrix effects.

The obtained results proved that using the same WE (as a vibrating or stationary gold microwire electrode), it is possible to quantify quickly four metals (Cu, Hg, Pb and Zn), present at different and wide ranges of concentrations in different type of samples (drinking, fresh and sea waters).

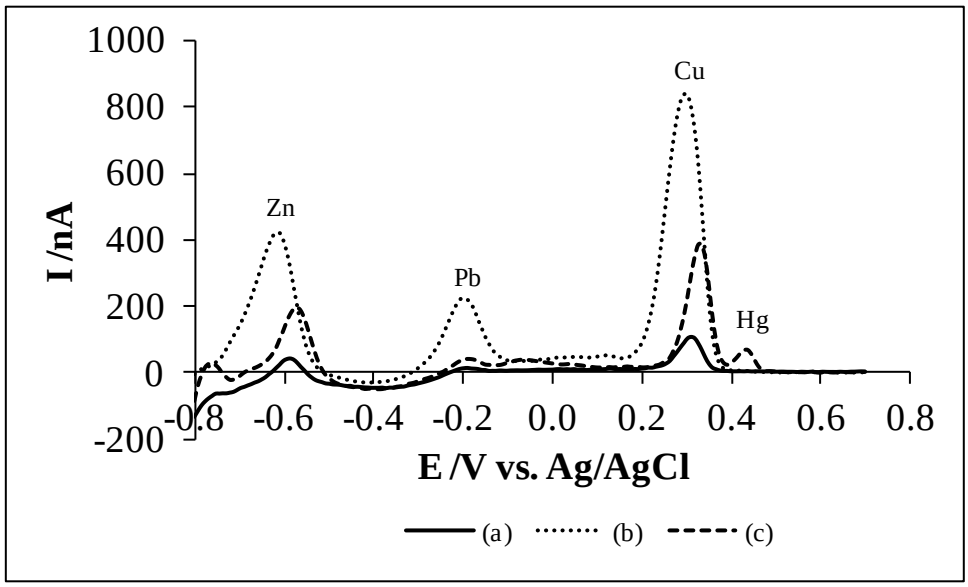

Figure 4.4 – Background corrected voltammograms obtained for UV digested certified fresh water sample (SPS-SW1) using the sationary (**a**) or vibrating (**b**) microwire electrode during the deposition and (**c**) as (**b**) but diluted 5 fold and doped with 1.5 μgL^{-1} of Hg.

Table 4.3 – Comparison of Zn, Pb, Cu and Hg (μgL^{-1}) values present in a certified water material or determined in water samples by the DPASV or reference methods [a].

Sample	Zn		Pb		Cu		Hg	
	DPASV	**Certified / Reference value**	**DPASV**	**Certified / Reference value**	**DPASV**	**Certified / Reference value**	**DPASV**	**Certified / Reference value**
Calibration curves [b]								
SPS-SW1[c]	20.4±0.5[d]	20 [e]	5 ± 1	5.0 ± 0.1[e]	19.3±0.4[d]	20 ± 1 [e]	< DL[f]	---
SPS-SW1 diluted 5 fold and spiked with 1.5 μgL^{-1} of Hg	4.7 ± 0.6	4	0.8 ± 0.1	1	5.0 ± 0.9	4	1.6 ± 0.2	1.5
River Water	32.3±0.4[d]	35 ± 2	6.0 ± 0.3	6 ± 1	1.1 ± 0.3	< DL[f]	< DL[f]	< DL[f]
Tap water	> 150 [d]	369 ± 2	2.1 ± 0.2	2.2 ± 0.2	4.3 ± 0.2	4.1 ± 0.1	< DL[f]	< DL[f]
Tap water diluted 5 fold	69 ± 2 [d]	74	---	---	---	---	---	---
Coastal seawater	17 ± 3[d]	16 ± 1	< DL[f]	0.15 ± 0.06	0.88 ± 0.06	0.69 ± 0.02	< DL[f]	< DL[f]
Standard addition method[g]								
Coastal seawater	19 ± 1 [d]	16 ± 1	< DL[f]	0.15 ± 0.06	0.69 ± 0.02	0.69 ± 0.02	< DL[f]	< DL[f]

[a] The values presented are the average with standard deviation of two independent determinations performed in triplicate (n = 6); for DPASV, all results present were determined using a gold vibrating microelectrode, unless otherwise stated; [b] Results obtained by interpolation of the calibration curves; [c] Certified reference fresh water; [d] Concentrations determined using a stationary gold microelectrode; [e] Information provided by the certificate of analysis; [f] The DL for Cu determined by AAS-EA was 1.1 μgL^{-1}. The DLs for Hg and Pb, determined by the DPASV using a vibrating gold microelectrode during the deposition step, were 0.2 and 0.3 μgL^{-1}, respectively. The DLs for Hg, determined by AAS-CV were 0.3 μgL^{-1} for river and sea waters and 0.07 μgL^{-1} for tap water, respectively and [g] Results obtained by extrapolation using the standard addition method.

4.4. Conclusions

The results obtained in this work demonstrated that, a gold microwire electrode can be applied for simultaneous determination of Zn and Cu, together with Hg and Pb, in mild acidic (pH 3) and saline (0.5 $molL^{-1}$ NaCl) conditions. These new electroanalytical procedures, besides allowing faster (30 s of t_{dep} without removing dissolved oxygen) and sensitive (using a vibrating electrode and 30 s of t_{dep}, the DLs were 0.2 μgL^{-1} for Hg, 0.3 μgL^{-1} for Pb and 0.4 μgL^{-1} for Zn and Cu, respectively) quantification of metals, also permit to quantify these metals (Cu, Hg, Pb and Zn) at much higher concentrations (about two orders of magnitude) using the same electrode in the same sample by performing two sequential scans (using as a stationary or vibrating WE), without formation of Cu-Zn intermetallic compounds.

The proposed methods were successfully applied to the determination of total concentrations of Cu, Hg, Pb and Zn in certified reference fresh (SPS-SW1 material), river, tap and coastal sea waters. The results proved the applicability and versatility of the proposed methods for the analysis of the total concentration of all four metals, present at different concentrations levels in various types (fresh, drinking and saline) of waters.

References

[1] J. Wang, Stripping Analysis, VCH Publishers, Inc., Deerfield Beach, Florida, **1985**.

[2] M. Pesavento, G. Alberti, R. Biesuz, Anal. Chim. Acta **2009**, 631,129.

[3] E.P. Achterberg, C. Braungardt, Anal. Chim. Acta **1999**, 400, 381.

[4] S.B. Saban, R.B. Darling, Sens. Actuat. B- Chem. **1999**, 61, 128.

[5] J. Wang, J.M. Lu, U.A. Kirgoz, S.B. Hocevar, B. Ogorevc, Anal. Chim. Acta **2001**, 434, 29.

[6] J.M. Zen, H.Y. Lin, H.H. Yang, Electroanalysis **2001**, 13, 505.

[7] P. Sonthalia, E. McGaw, Y. Show, G.M. Swain, Anal. Chim. Acta **2004**, 522, 35.

[8] C.M.A. Brett, M.B.Q. Garcia, J. Lima, Anal. Chim. Acta **1997**, 339, 167.

[9] M.S. Shuman, G.P. Woodward, Anal. Chem **1976**, 48, 1979.

[10] E. Lastres, G. deArmas, M. Catasus, J. Alpizar, L. Garcia, V. Cerda, Electroanalysis **1997**, 9, 251.

[11] E. Munoz, S. Palmero, M.A. Garcia-Garcia, Talanta **2002**, 57, 985.

[12] Z.D. Anastasiadou, I. Sipaki, P.D. Jannakoudakis, S.T. Girousi, Anal. Lett. **2011**, 44, 761.

[13] J.F. van Staden, M.C. Matoetoe, Anal. Chim. Acta **2000**, 411, 201.

[14] K. Tyszczuk, M. Korolczuk, M. Grabarczyk, Talanta **2007**, 71, 2098.

[15] R. Ouyang, Z. Zhu, C.E. Tatum, J.Q. Chambers, Z.-L. Xue, J. of Electroanal. Chem. **2011**, 656, 78.

[16] C. Garnier, L. Lesven, G. Billon, A. Magnier, O. Mikkelsen, I. Pizeta, Anal. and Bioanal. Chemis. **2006**, 386, 313.

[17] K. Gibbon-Walsh, P. Salauen, C.M.G. van den Berg, Environ. Chem. **2011**, 8, 475.

[18] EPA, in "National Recommended Water Quality Criteria. United States Environmental Protection Agency, Office of Water/ Office of Science and Technology" **2009**.

[19] European Comission, in "Directive 2008/105/EC on environmental quality standards in the field of water policy, amending and subsequently repealing Council Directives 82/176/EEC, 83/513/EEC, 84/156/EEC, 84/491/EEC, 86/280/EEC and amending Directive 2000/60/EC" **2008**.

[20] P. Salaun, C.M.G. van den Berg, Anal. Chem. **2006**, 78, 5052.

[21] C.S. Chapman, C.M.G. van den Berg, Electroanalysis **2007**, 19, 1347.

[22] G. Billon, C.M.G. van den Berg, Electroanalysis **2004**, 16, 1583.

[23] P. Salaün, K. Gibbon-Walsh, C.M.G. van den Berg, Anal. Chem. **2011**, 83, 3848.

[24] L.M. de Carvalho, P.C. do Nasciniento, A. Koschinsky, M. Bau, R.F. Stefanello, C. Spengler, D. Bohrer, C. Jost, Electroanalysis **2007**, 19, 1719.

[25] G. Herzog, D.W.M. Arrigan, Trac-Trends in Anal. Chem. **2005**, 24, 208.

[26] Y. Bonfil, M. Brand, E. Kirowa-Eisner, Anal. Chim. Acta **2002**, 464, 99.

[27] A. Giacomino, O. Abollino, M. Malandrino, E. Mentasti, Talanta **2008**, 75, 266.

[28] Y. Bonfil, M. Brand, E. Kirowa-Eisner, Anal. Chim. Acta **2000**, 424, 65.

[29] J.N. Miller, J.C. Miller, Statistics and Chemometrics for Analytical Chemistry,Pearson Education Limited, Fifth Edition, **2005**.

[30] ATSDR (2005). Toxicological profile for Zinc. Agency for Toxic Substances and Disease Registry (ATSDR). U.S. Department of Health and Human Services – Public Health Service.

[31] ATSDR (2004). Toxicological profile for copper. Agency for Toxic Substances and Disease Registry (ATSDR). U.S. Department of Health and Human Services - Public Health Service.

[32] I. Cesarino, C. Gouveia-Caridade, R. Pauliukaite, E.T.G. Cavalheiro, C.M.A. Brett, Electroanalysis **2010**, 22, 1437.

Chapter 5

SIMULTANEOUS ANODIC STRIPPING VOLTAMMETRIC DETERMINATION OF Pb AND Cd, USING A VIBRATING GOLD MICROWIRE ELECTRODE, ASSISTED BY CHEMOMETRIC TECHNIQUES[4]

Graphical Abstract

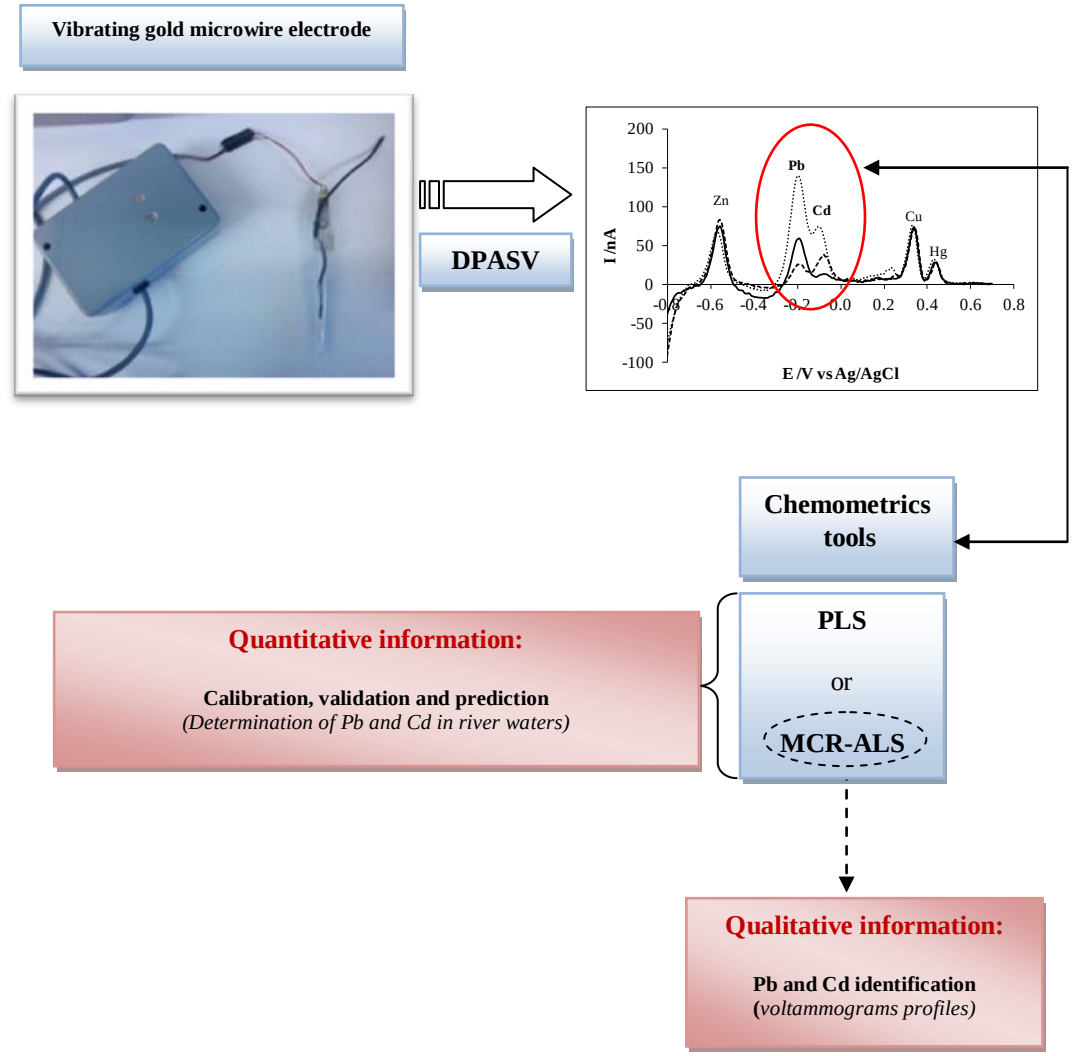

[4] Electroanalysis 2013 (accepted for publication; reference elan.201300198)

Abstract

Simultaneous anodic stripping voltammetric determination of Pb and Cd is restricted on gold electrodes as a result of the overlapping of these two peaks.

This work describes the quantitative determination of a binary mixture system of Pb and Cd, at low concentration levels (up to 15.0 and 10.0 μgL^{-1} for Pb and Cd, respectively) by DPASV (t_{dep} of 30s), using a "green" electrode (vibrating gold microwire electrode) without purging in a chloride medium (0.5$molL^{-1}$ NaCl) under moderate acidic conditions (HCl 1.0 $mmolL^{-1}$), assisted by chemometrics tools.

The application of MCR-ALS for the resolution and quantification of both metals is shown. The optimized MCR-ALS models showed good prediction ability with concentration prediction errors of 12.4 and 11.4% for Pb and Cd, respectively. The quantitative results obtained by MCR-ALS were compared to those obtained with PLS and CLS regression methods. For both metals, PLS and MCR-ALS results are comparable and superior to CLS. For Cd, as a result of the peak shift problem, the application of CLS was unsuitable. MCR-ALS provides additional advantage compared to PLS since it estimates the pure response of the analytes signal.

Finally, the built up multivariate calibration models, based either in MCR-ALS or PLS regression, allowed to quantify concentrations of Pb and Cd in surface river water samples, with satisfactory results.

5.1. Introduction

In chapters 3 and 4, the excellent characteristics of gold microwire electrodes for simultaneous anodic stripping voltammetric determination of Cu, Hg, Pb and As [Chapter 3 of this thesis] or Zn [Chapter 4 of this thesis] metal ions in surface waters was reported. Simultaneous metals determination was achieved, without removing oxygen, through the application of a subtractive anodic stripping procedure (background correction) using an automatic, simple and quick sequence [Chapters 3 and 4 of this thesis]. However, as a result of the strongly overlapped peaks, this electrode and unmodified gold electrodes [1] are, in general, unsuitable to determine simultaneously mixtures of Pb and Cd. In fact, at gold electrodes, Pb and Cd stripping peaks are very close to each other and a large excess of one of these metals creates the distortion of the other peak [1]. Therefore, it is not surprising that mixtures of these two metals have usually been addressed on mercury-free bismuth [2-6], silver [1,7,8] and antimony [9-11] electrodes instead of on gold electrodes. As far as we know, there is only one paper, described in the literature, which reports the simultaneous quantification of Pb and Cd at a bare solid gold electrode [1]. In this paper, Bonfil *et al.* [1] reported that the analysis of these two metals was possible on a silver electrode but was restricted on a gold electrode.

According to the described above, it is obvious that anodic stripping voltammetric analysis, based on bare gold electrodes, seems not to be the best option for the simultaneous determination of Pb and Cd. On the other hand, as it was demonstrated in chapter 4, a gold microwire electrode is a good choice to quantify simultaneously Zn, Cu, Hg and Pb. Thus, in this case, there is a great interest to explore the possibility to determine Cd together with Pb, using the analytical procedure described in chapter 4, as it will allow determining in a single scan, quickly and simultaneously, a total of five metal ions (Zn, Cu, Hg, Pb and Cd, respectively). The development of this multi-element analysis, through the use of a non-toxic gold microwire electrode and a simple stripping voltammetric procedure, enables a profitable work in an effective way and ensures to save material, reagents, time and energy.

The electroanalytical methods have been improved through the application of chemometrics methodologies [12-14]. Thus, chemometrics tools, such as MCR-ALS [15], can allow the extraction of analytical information from these unresolved peaks of Pb and Cd.

MCR-ALS [15-31] has become a popular chemometric method which is used for the resolution of multiple component responses in unknown and unresolved mixtures (recognition ability) [15,17,19]. Thus, the main aim of MCR-ALS is the recovery of pure response profiles (pure signals and concentrations) of unresolved species obtained in chemical processes where the information about the nature and composition of the analyzed mixture is only partial or non-existent [20], i.e., species identification, description and system interpretation of unresolved multivariate responses [15]. This chemometric method has been used to extract qualitative information in different analytical fields, such as in spectroscopic studies of bimolecules [20-24], in chromatographic and environmental applications [19,25-27], in electroanalytical studies [28-31] and, not so often, to extract quantitative analytical information [15,16,18,32,33]. When MCR-ALS is applied to second order calibration data (when measuring one sample a multivariate data matrix or data table is obtained), relative quantitative information is derived directly from the signal areas of the analyte in different samples. Absolute calibration is therefore possible if a set of calibration samples with known analyte concentrations are included in the analysis. In the case of first order calibration data (measuring one sample gives a multivariate data vector), quantitative information can be still achieved by the MCR-ALS method if it is applied together with the so-called correlation constraint [15,16,18]. This constraint has been firstly introduced for the simultaneous quantitative analysis of synthetic mixtures of metal ions using voltammetric data [15]. More recently, this correlation constraint was also applied for the quantification of a mixture of analytes in pharmaceutical and agricultural [16], and in juices and serum [18] samples, using first order spectrophotometric data.

Thus, in this work the possibility to extract qualitative and quantitative analytical information through the application of MCR-ALS to unresolved

voltammetric peaks of Pb and Cd recorded using a vibrating gold microwire electrode is explored. Since other multivariate calibration methods, particularly based on PLS regression, are also frequently used to extract analytical information from spectrometric and also voltammetric signals [Chapter 2 of this thesis,13,34], the results obtained by the MCR-ALS method were compared with those achieved by the PLS and CLS methods.

Finally, the developed multivariate calibration models (MCR-ALS and PLS, respectively) were used to quantify these two metal ions in river water samples.

5.2. Experimental

5.2.1. Reagents and solutions

All reagents and preparation of solutions reported in this work were performed as previously described in sections 3.2.1 and 4.2.1.

5.2.2. Equipment

All equipment/electrodes used in this work were previously described in section 4.2.2. WE used in this work was a vibrating gold microwire electrode with 1.5 mm length and 25 μm diameter.

Quantification of Pb and Cd in river water samples was performed by AAS-EA, using the equipment described in section 2.2.2 and by ICP-MS using the equipment described in section 3.2.5. These techniques were used as reference methods.

5.2.3. Electrode characterization and voltammetric procedures

The WE was constructed, characterized, cleaned and conditioned as reported [Sections 3.2.3 and 4.2.3 of this thesis].

In this work, subtractive DPASV procedure, previously applied to the simultaneous determination of Cu, Hg, Pb and Zn [chapter 4 of this thesis] was used.

5.2.4. Analysis of river water samples

River water samples were collected and processed as described in section 4.2.5. The voltammograms of the river water samples were obtained as described in section 4.2.4. For all river water samples, two independent assays were carried out; three replicates were obtained per measurement.

Concentrations of Pb and Cd were also analysed in these samples either by AAS-EA or ICP-MS. The results determined by these methods, which were used as reference values, were compared with the results obtained by the best MCR-ALS and PLS models.

5.3. Chemometrics Methodologies

5.3.1. Chemometric Software

All calculations related to MCR-ALS, initial estimates and constraints selected were performed in the MATLAB computation and visualization environment (The MathWorks, Natick, MA, USA), and using MCR-ALS toolbox with a graphical user-friendly interface [15-18].

For the calculation of the CLS and PLS multivariate calibration models, like in chapter 2, a PLS_Toolbox version 5.5 for MATLAB, from Eigenvector Research Inc., was used.

5.3.2. Experimental data sets

The composition of the samples used for the construction of the multivariate calibration models (concentrations up to 15.0 and 10.0 μgL^{-1} for Pb and Cd, respectively) is summarized in table 5.1. Twenty five synthetic binary mixtures of Pb and Cd, prepared with a composition designed according to a full factorial design with two factors ([Pb] and [Cd] in μgL^{-1}, respectively) and five concentration levels for each metal ion, were prepared. A central point (sample 6 in Table 5.1) was assayed two times and the baseline voltammogram ([Cd] = [Pb] = 0 μgL^{-1}) was also obtained. This sample set was divided in two independent data subsets: a calibration subset (samples 1 to 14 in Table 5.1) and an external validation subset constituted by 12 samples (samples 23 to 34 in Table 5.1). Calibration samples were selected trying to cover all the signal data variance.

Apart from the metal mixtures, the voltammograms of pure Pb and Cd samples were also obtained (pure samples set in Table 5.1) and were used together with the calibration subset for the construction of some multivariate calibration models.

The experiments corresponding to the calibration and the external validation subsets were assayed separately and within each subset the samples were assayed randomly. For each sample, three consecutive voltammetric measurements were made, as it was already mentioned above.

Table 5.1 – Concentration data for the calibration and external validation subsets used for building the multivariate calibration models.

Sample	[Pb] /μgL^{-1}	[Cd] /μgL^{-1}
Calibration subset		
1	0.00	0.00
2	1.02	1.02
3	8.01	1.02
4	15.0	1.01
5	1.02	5.54
6	8.00	5.50
7	14.9	5.50
8	1.02	10.0
9	8.01	9.98
10	15.0	9.88
11	4.50	3.27
12	11.5	3.26
13	4.50	7.76
14	11.4	7.76
Pure samples set		
15	0.00	1.50
16	0.00	3.00
17	0.00	4.50
18	0.00	6.00
19	3.00	0.00
20	6.00	0.00
21	9.00	0.00
22	12.0	0.00

Table 5.1 continuation…

Sample	[Pb] /μgL^{-1}	[Cd] /μgL^{-1}
External validation subset		
23	4.53	1.02
24	4.51	5.50
25	4.49	10.0
26	8.01	7.75
27	15.1	3.25
28	15.1	9.97
29	11.5	1.01
30	11.5	5.50
31	1.02	3.25
32	1.02	7.76
33	8.04	3.25
34	15.0	7.75

Sample 1 – baseline; Sample 6 – central point; Samples 15 up to 18 – selective information about Cd; Samples 19 up to 22 – selective information about Pb.

5.3.3. Data pre-processing

As described in the experimental section, each independent sample (Table 5.1) was analyzed by DPASV and consequently a data vector [voltammogram: I = f (E), where I is current intensity in nanoamperes (nA) and E is potential in volts (V), respectively] with 190 points was obtained.

Before submitting the voltammograms obtained to MCR-ALS, PLS or CLS analysis and in order to improve the quality of the original data and to reduce their size, these voltammograms were pre-processed. Thus, for each voltamogram, pre-processing steps consisted on: (i) normalization of the recorded current intensity values by dividing them by the length of the WE and (ii) elimination of negative data values, by taking the minimum current value of the normalized

voltammograms and subtracting it from every measured voltammetric value in order to ensure that all current values resulted positive ($I > 0$). Subsequently, all the voltammogramms were digitalized in the potential range from -0.411 to 0.144, resulting in 72 points per voltammogram.

Figure 5.1 shows the calibration data subset, including binary mixtures of Pb and Cd and pure samples (Table 5.1), before and after pre-processing. As it can be seen, peak shift and overlapping are simultaneously present and difficult to be discerned.

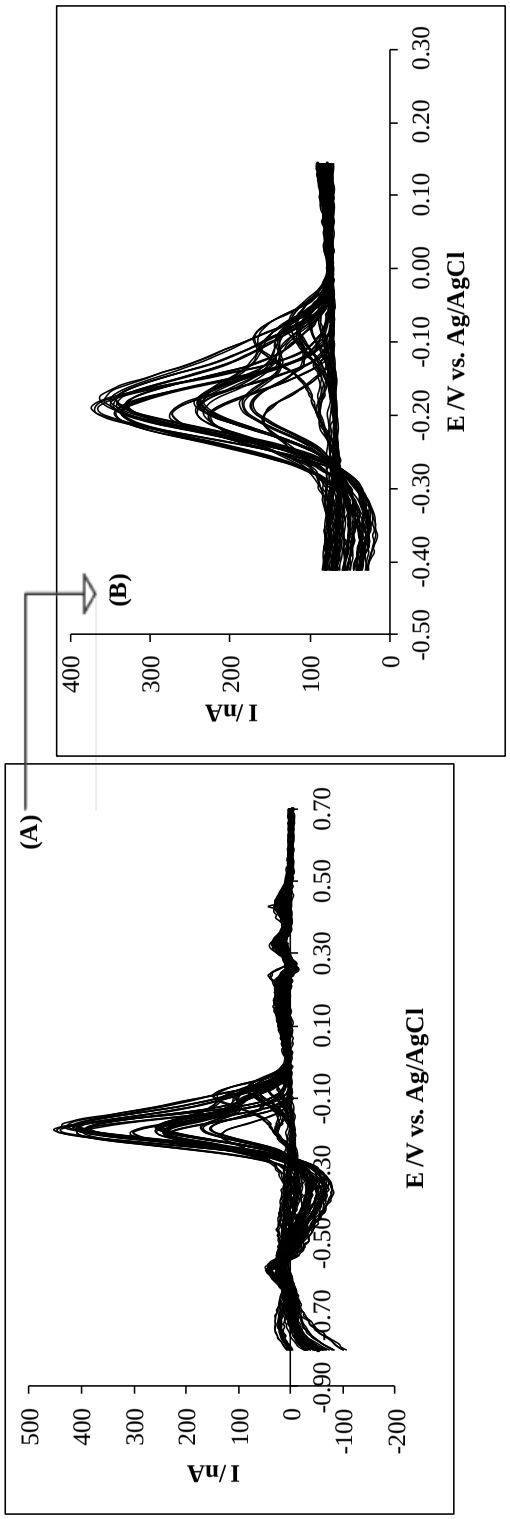

Figure 5.1 – Calibration data subset, including binary mixtures of Pb and Cd and pure samples, before (**A**) and after (**B**) pre-processing.

5.3.4. Application of MCR-ALS *for the resolution and quantification of unresolved mixtures of Pb and Cd*

Mathematically, MCR-ALS methods are based on a bilinear model analogous to the generalized Lambert-Beer's law [15-20], where the individual responses of each analyte are additive. The contribution of each analyte, Pb and Cd in this case, depends on its concentration and on its own response sensitivity.

The pre-processed voltammograms for the different samples analyzed (calibration and external validation data subsets), corresponding to different concentration values of Pb and Cd (Table 5.1), were arranged in a data matrix of current intensities (**D**). The data matrix, **D**, was built up under assumption of a bilinear model that can be expressed according to equation 1.3 presented in section 1.3.3. In this particular case, **D** *(i,j*) is the data matrix of current intensities with *i* rows of *i* sample voltammograms and *j* columns of *j* potential values; **C**(*i,k*) is the matrix of concentration profiles of *k* analytes present in these *i* samples; $\mathbf{V^T}$ (*k,j)* is the matrix of voltammograms of these *k* analytes recorded at *j* potential values and **E** (*i,j)* is the matrix associated to the experimental error.

Before a bilinear decomposition of **D** matrix into the "true" response profiles (**C** and $\mathbf{V^T}$ for Pb and Cd, respectively) by an iterative optimized ALS procedure, the number of components present was estimated by the inspection of singular values [15-18] plot and initial estimations of the voltammetric Pb and Cd profiles for these number of components were then obtained from the purest experimental ones estimated using a method similar to SIMPLISMA [15]. During the ALS iterative optimization, the following constraints were applied: (i) non-negativity; (ii) selectivity and (iii) correlation. Non-negativity constraints were applied to Pb and Cd concentration and voltammetric profiles. This non-negativity constraint was applied using a fast non-negative least squares method [35]. The selectivity constraint refers to the case where in a particular voltammogram one or more components (Pb and/or Cd) are known not to be present or that they do not contribute significantly to the measured response. This constrain was applied to pure samples of Pb or Cd included in the calibration data subset. Finally, the correlation constraint was implemented as proposed in [15,16,18]. Using this

correlation constraint, during the MCR-ALS iterative optimization, calibration models for quantitative determination of Pb and Cd can be established. Known concentrations of Pb and/or Cd corresponding to a set of calibration samples are provided as initial inputs during the ALS optimization, and they are correlated to the current ALS concentration estimations. A local linear model is built between known calibration values and those estimated by ALS, and the parameters of this local model are used then for the prediction of Pb and Cd concentration values for both calibration and unknown samples (which include the validation subset and new real samples, respectively).

5.3.5. Application of PLS for quantification of unresolved mixtures of Pb and Cd

In this work, quantitative results obtained for Pb and Cd by MCR-ALS methods are compared with those obtained with PLS and CLS methods, respectively.

The purpose of the application of PLS and CLS regression methods were to build up a prediction model for the concentration of Pb and Cd in unknown samples using efficiently the information contained in the voltammograms and the concentration of the analytes (Pb and Cd) in the calibration samples.

To establish a calibration model, the PLS regression algorithm selects a few number of orthogonal factors, which maximizes the covariance between measured voltammograms and the analyte (Pb and Cd) concentrations of a set of calibration samples. Then, the obtained multivariate regression model is subsequently used to predict their concentration values on new samples (validation subset and real samples, respectively) with unknown concentrations of them.

For multicomponent analysis, CLS is only applicable when the concentration of all analytes in calibration samples are known and pure signals can be obtained using either directly (DCLS) or indirectly (ICLS) methods [36]. In this work, the pure signals of Pb and Cd were estimated using the indirect

approach, ICLS. Once the pure signals of both metals were obtained, they were then used to form the pure signals matrix and the calibration model was obtained from the pseudo-inverse of this matrix. This calibration model was subsequently used to predict the concentrations of Pb and Cd in unknown samples.

5.3.6 Comparison between models and validation of results

To evaluate the performance of MCR-ALS method using different constraints, the percentage of lack-of-fit (lof) [15,17,19] was used. Lof was calculated according to the following expression*:*

$$\mathrm{lof}(\%) = 100 \sqrt{\frac{\sum_{ij}(d_{ij} - d'_{ij})^2}{\sum_{ij} d_{ij}^2}} \qquad \text{(Eq. 5.1)}$$

where d_{ij} is the element of the experimental data matrix (**D**), i.e., the current intensity measured for sample *i* at potential *j*, and d'_{ij} is the corresponding element calculated by ALS).

Validation of voltammetric and concentration profiles recovered by the ALS optimization can be obtained by calculating the similarity values (correlation coefficients) between the previously known pure voltammograms and true concentration values (when they are known in samples used for validation purposes) of Pb and Cd, comparing them with the MCR-ALS resolved ones.

For comparison of MCR-ALS and PLS models, the following figures of merit were used to express the quality of prediction in the quantitative determination of Pb and Cd concentrations in the external validation subset of samples:

Root mean square error of prediction (RMSEP):

$$\mathrm{RMSEP} = \sqrt{\frac{\sum_{i=1}^{n}(c_i - c'_i)^2}{n}} \qquad \text{(Eq. 5.2)}$$

Standard error of prediction (SEP):

$$\mathrm{SEP} = \sqrt{\frac{\sum_{i=1}^{n}(c_i - c'_i - \mathrm{Bias})^2}{n-1}} \qquad \text{(Eq. 5.3)}$$

Bias:

$$\mathrm{Bias} = \frac{\sum_{i=1}^{n}(c_i - c'_i)}{n} \qquad \text{(Eq. 5.4)}$$

Relative percentage error in concentration predictions (RE):

$$\mathrm{RE}(\%) = 100\sqrt{\frac{\sum_{i=1}^{n}(c_i - c'_i)^2}{\sum_{i=1}^{n} c_i^2}} \qquad \text{(Eq. 5.5)}$$

In all these expressions, c_i is the predicted analyte concentration and c'_i is the known concentration of the considered analyte in the mixture. All sums were taken for $i = 1$ to the number of samples used in the external validation data subset where these parameters were evaluated (n).

5.4. Results and Discussion

5.4.1. Individual versus simultaneous determination of Pb and Cd

Table 5.2 summarizes the results obtained for individual calibrations of Pb (already described in table 4.2 and emphasized here again) and Cd using a gold

microwire electrode under vibration conditions. The sensitivity [ratio between the slope ($nAV^{-1}\mu g^{-1}L$) of the calibration curve and the length of the electrode (mm)] and the linear response range were higher for Pb than for Cd (Table 5.2). The peak potential for Pb was independent of the metal ion concentration but the peak of Cd shifted to more negative potentials as the concentration values increased. These results evidenced that separate quantification of these metal ions is feasible but simultaneous determination of Pb and Cd is restricted because the peaks are strongly overlapped. Figure 5.2 shows the voltammograms obtained for mixtures of Zn, Pb, Cd Hg and Cu. The voltammograms in figure 5.2 evidence well defined peaks for Zn, Cu and Hg; this figure also shows that stripping peaks of Cd and Pb are not well separated and at higher concentrations their peaks are strongly overlapped. Difficulties for quantifying both metals arise when the concentration of Cd is of the same order of the concentration of Pb. Then, the possibility of simultaneous quantification of Pb and Cd, using a gold microwire electrode, by univariate analysis is not feasible or only in a very limited way.

Taken into account that, the concentration levels of Pb in natural waters are usually higher than those of Cd, in the previous chapter we have limited this study to the simultaneous determination of Cu and Zn together with Pb and Hg. Now, in order to open the possibility to determine all five metals (Zn, Pb, Cd, Cu and Hg) in a single voltammetric scan, the quantification of Pb together with Cd using a chemometric approach was firstly evaluated.

Table 5.2 – Individual calibration parameters for Cd and Pb using a vibrating gold microwire electrode.

Metals	**Linearity** /μgL^{-1}	**DL** /μgL^{-1}	**Peak Potential** /V	**$W_{1/2}$** /V	**Sensitivity** /nAV^{-1} μg^{-1}L mm^{-1}	**r^2**
Cd	Up to 10	0.3	(-0.054) – (-0.094)	0.071 – 0.095	355 ± 7	0.998 (n = 27)
Pb	Up to 15	0.3	-0.202	0.071 – 0.087	625 ± 18	0.995 (n = 27)

The values of the sensitivities were calculated with a confidence interval of 95%; WE: 25 μm/1.3 mm; n – number of points in the calibration curve

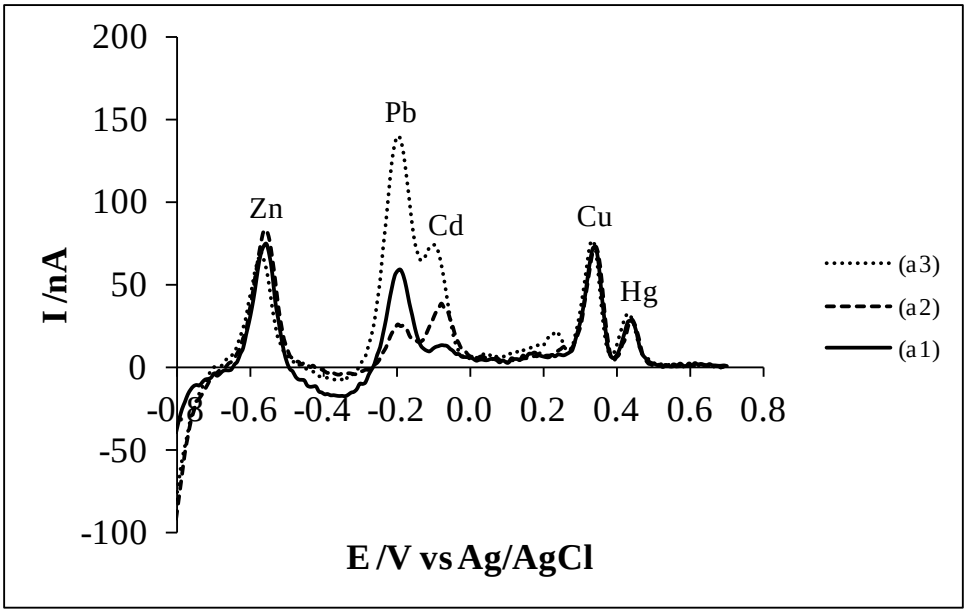

Figure 5.2 – Background subtracted voltammograms obtained, using a vibrating gold microwire electrode with 1.6 mm of length, for simultaneous determination of Zn, Pb, Cd, Cu and Hg by DPASV: [Zn], [Pb], [Cd], [Cu] and [Hg**]** **(**μgL^{-1}**)** **(a1)** 1.0, 2.0, 0.5, 1.0, 1.0 ; (**a2**) 1.0, 1.0, 2.0, 1.0, 1.0 and (**a3**) 1.0, 5.0, 5.0, 1.0, 1.0**.**

5.4.2. MCR-ALS results

In order to study the influence of several possible situations on the resolution of Pb and Cd in the binary mixtures, the effect of the number of components used and of the constraints applied were evaluated. The possible cases of application of constraints investigated were: (i) non-negativity for concentration and voltammetric profiles; (ii) non-negativity and correlation; (iii) non-negativity and selectivity and (iv) non-negativity, selectivity and correlation (Part A and Part B of Table 5.3 for Pb and Cd, respectively). To test the above conditions, two arrangements of the calibration data set, using the sample composition described in Table 5.1, were considered: (i) data set 1: samples 1 – 14 (without pure samples) and (ii) data set 2: samples 1 – 14 plus samples 15 - 22 (with Pb and Cd pure samples), whereas samples 23 – 34 (Table 5.1) were always used as validation data set. With the goal to study the effect of the selectivity constraint, data set 2 was subdivided in three sets: (i) data set 2a (with selective information about Pb); (ii) data set 2b (with selective information about Cd) and (iii) data set 2c (with selective information about both metals).

As described previously (section 5.3.4.), the number of components was initially estimated by SVD method. For samples containing metal ion binary mixtures, the number of significant singular values is comprised between 2 and 5. Initial estimations of the number of components were refined always considering a larger or/and a lower number of components (Table 5.3). In principle, if the experimental system behaves in a bilinear way as postulated by Equation 1.3, and if no important contributions of baseline drift, peak shifts or other additional interferences are present, the number of components estimated should be directly related to the number of chemical components contributing significantly to the measured signals [15]. However, for voltammetric signals, a larger number of singular components are frequently found because of the deviation of the experimental data from the theoretical bilinear model as a consequence of the peak shift of component signals when their concentration change. In fact, voltammetric signals of samples, which only contain a single metal ion, Pb or Cd, needed 2 and 5 singular values, respectively, to explain their experimental variation when their concentration change. Considering that usually one additional component is needed for the electrochemical background signal, these results seem to indicate that whereas Pb measurements can be well described by one component in the bilinear model, Cd signals need more bilinear components (up to 5) to explain their variation when its concentration changes. This significant deviating of behaviour for Cd measurements from one single component bilinear model is due to the strong peak shift effects observed for this metal ion.

Table 5.3 (Part A) gives an overview of the results obtained for Pb according to the number of factors and constraints tested in this work. As it can be seen from Table 5.3 (Part A), for the same number of components, final solutions obtained by MCR-ALS using the different constraints scenarios gave similar results. The ALS lack of fit values, which gives a measure of the fit quality in relative terms and in the same units as the measurements, decreased with the number of components used. In general, slightly better similarity between the concentrations and voltammetric profiles recovered by MCR-ALS and those obtained experimentally (please see the correlation coefficients values) were obtained with the implementation of the correlation and selectivity constraints.

The best correlation coefficients for concentration and voltammetric profiles were achieved with 2 and 3 components, respectively. The best recovery Pb voltammetric profile (0.998) was obtained with data set 2 (3 components) with the application of selective information about Pb and non-negativity constraint (Table 5.3 – Part A). This result is comparable to the correlation voltammetric profile value obtained (0.996) after the application of the correlation constrain to the same experimental data [Figure 5.3 (A1)]. Figure 5.3 (A1) represents the comparative analysis between normalized Pb voltammetric profiles recovered by MCR-ALS and experimental pre-processed voltammogram; this figure evidences a good agreement between them.

For Pb, all results evidenced that the application of the correlation constraint, used for quantification purposes, gave more reliable results. Thus, after inspection of all these parameters and taking into accounts a minimum relative percentage error in its concentration predictions [RE (%)], the optimal model for quantification of Pb was selected. A model built up with data set 2c, using the non-negativity, selectivity and correlation constraints, showed the lowest RE (%) concentration predictions values (7.8 and 12.4% for calibration and validation, respectively); this model was chosen for subsequent quantitative analysis. Figure 5.3 (B1) shows the regression line obtained from this optimized calibration model. Predicted concentration values for the external validation subset are also shown [Figure 5.3 (B1)].

Table 5.3 (Part B) summarizes the effect of the number of components and the constraints used on the resolution of Cd. As it was already mentioned above and according to the results obtained (Table 5.3 – Part B), Cd was more difficult to model than Pb (more components were needed). The analysis of Table 5.3 (Part B) shows that the correlation values for Cd concentration and voltammetric profiles improved with the application of the correlation and selectivity constraints. The MCR-ALS profiles obtained with the application of only non-negativity constraint (data set 1) were wrong (see corresponding correlation values in Table 5.3 – Part B), even though a good data fitting (see corresponding lof values in Table 5.3 – Part B) would imply that in this situation, rotational

ambiguities for Cd profiles were rather high. As it was already indicated (section 5.4.1), whereas peak potential of Pb signal was independent of the metal ion concentration, peak potential of Cd signal was shifted to more negative potentials (in the direction of the peak potential of Pb) with the increase of concentration of Cd. This fact, together with the lower concentrations of Cd in the analyzed samples (Cd was the minor analyte) and the lower sensitivity of this metal, when compared with Pb, explain why these worse correlation values were obtained (Table 5.3 – Part B).

For Cd, satisfactory results were only obtained using 4 or 5 components and using non-negativity, selectivity and correlation constraints. For the model built up with 5 components, RE (%) concentration prediction values for calibration and validation sets were 11.8 and 11.4 %, respectively. This model was better than the one obtained with 4 components, especially with respect to the resolution of the Cd voltammetric profile. Figures 5.3 (A2) and (B2) represent the best results obtained for Cd. In Figure 5.3 (A2), the MCR-ALS estimated Cd (normalized) voltammogram is compared with the pre-processed voltammogram of a pure Cd sample (also normalized). Unlike Pb, for Cd, there is a significative shift disagreement between the experimental and the MCR-ALS estimated voltammograms, which is also shown in the rather low correlation value (0.944) obtained (Table 5.3 – Part B). Figure 5.3 (B2) shows the quantitative estimation of Cd concentrations, i.e., the best regression line obtained from the calibration samples is plotted together with the predicted Cd concentration values for the validation data set samples.

The results above indicate that Pb results agree with the bilinear assumption of this metal signal; on the other hand, for Cd, a larger number of components was necessary, which evidences that the analyte signal has a non-bilinear behavior as a result of Cd signal shift. Therefore, extra components are needed to model Cd shift in MCR-ALS (as it also occurs in PLS results; please see below).

Table 5.3 – MCR-ALS results of Pb (**Part A**) and Cd (**Part B**): effect of the number of components and constraints.

Calibration data set	Nº components	Constraints	lof (%)[c]	Correlation of the concentration profiles	Correlation of the voltammetric profiles	N.it[d]
Part A: Pb						
Data set 1	2	non-negativity	9.67	0.991	0.965	500[e]
	3		4.30	0.942	0.911	158
	4		2.61	0.934	0.877	500[e]
Data set 1	2	non-negativity correlation[a]	9.67	0.991	0.965	4[e]
	3		4.36	0.963	0.924	14
	4		2.61	0.956	0.921	104
Data set 2a	2	non-negativity selectivity	13.9	0.991	0.969	48
	3		4.60	0.962	0.998	186
	4		3.16	0.891	0.961	426
Data set 2b	2		11.6	0.993	0.975	20
	3		4.67	0.960	0.990	22
	4		3.17	0.925	0.922	140
Data set 2c	2		15.3	0.991	0.970	14
	3		4.68	0.978	0.998	103
	4		3.17	0.925	0.953	265
Data set 2a	2	non-negativity selectivity correlation[a]	11.6	0.993	0.978	2[e]
	3		4.67	0.972	0.996	11
	4		3.25	0.972	0.957	96
Data set 2c	2	non-negativity selectivity correlation[b]	25.1	0.993	0.975	2[e]
	3		5.18	0.983	0.937	30
	4		3.12	0.982	0.945	56

Table 5.3 continuation…

Calibration data set	Nº components	Constraints	lof (%)[c]	Correlation of the concentration profiles	Correlation of the voltammetric profiles	N.it[d]
Part B: Cd						
Data set 1	3	non-negativity	4.30	0.379	0.964	158
	4		2.61	0.379	0.762	500[e]
	5		1.71	0.383	0.731	500[e]
Data set 1	3	non-negativity correlation[a]	14.0	0.757	0.940	12
	4		16.1	0.818	0.916	24[e]
	5		16.7	0.662	0.938	4[e]
Data set 2a	3	non-negativity	4.59	0.906	0.709	186
	4		3.16	0.984	0.890	426
	5		1.96	0.984	0.946	500[e]
	6		1.37	0.876	0.948	128
Data set 2b	3	Selectivity	4.67	0.306	0.770	22
	4		3.17	0.550	0.939	140
	5		1.96	0.563	0.905	251
	6		1.33	0.562	0.922	248
Data set 2c	3		4.68	0.909	0.771	103
	4		3.17	0.983	0.879	265
	5		1.97	0.983	0.945	400
	6		1.35	0.935	0.951	454
Data set 2c	3	non-negativity selectivity correlation[b]	5.18	0.864	0.790	30
	4		3.21	0.985	0.905	56
	5		1.99	0.985	0.944	196
	6		1.70	0.976	0.886	60

[a] Estimations of ALS concentrations were correlated with known Pb (Part A) and Cd (Part B) concentration values; [b] Estimations of ALS concentrations were correlated with known Pb and Cd concentration values, respectively; [c] lof (%) is the percentage of lack-of-fit calculated according to equation 5.1 (see text above); [d] N.it. is the number of ALS optimization iterations used and [e]Divergence occurred (results given are for the best iteration) or the maximum number of iterations (500) tested was applied.

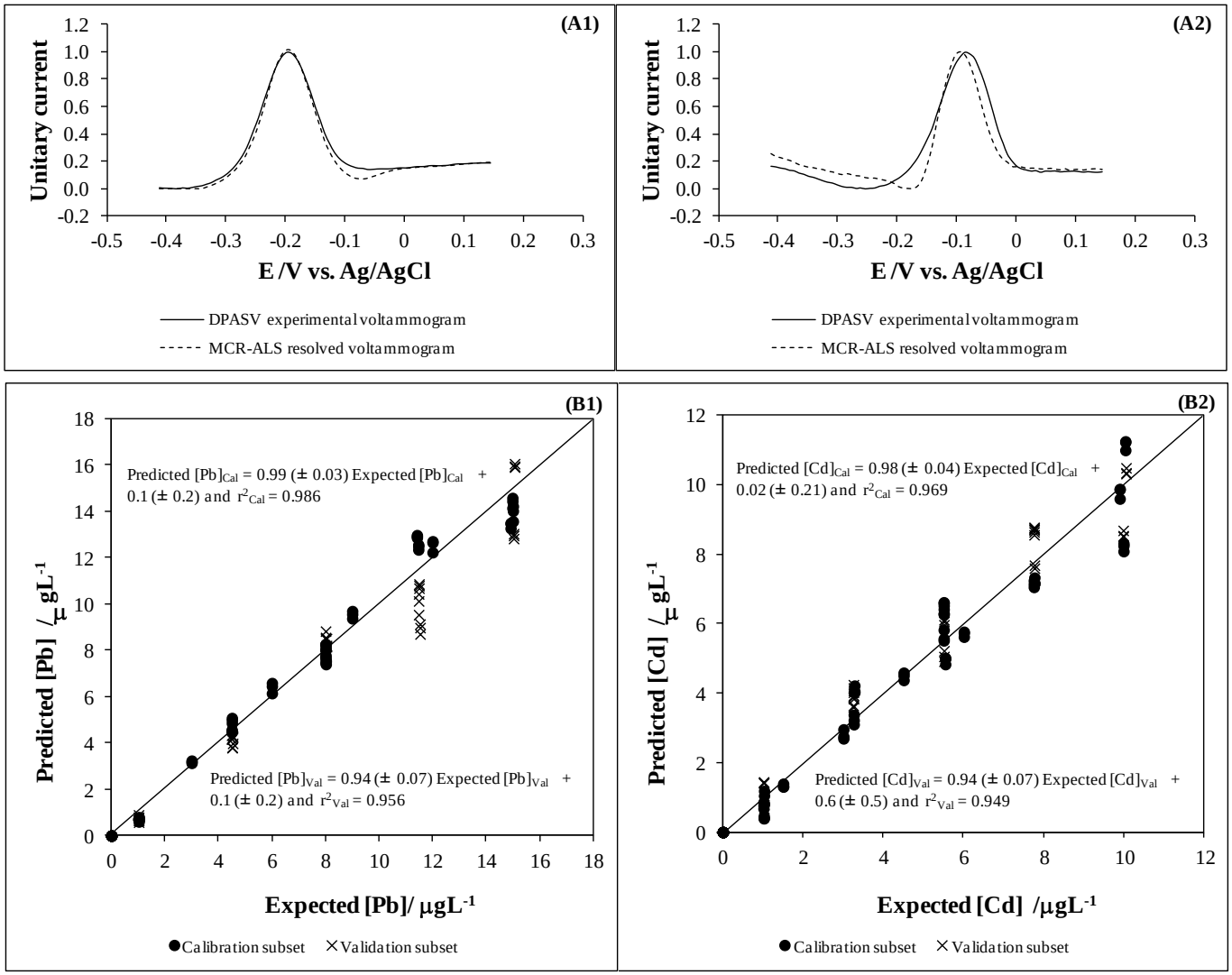

Figure 5.3 – MRC qualitative **(A)** and quantitative **(B)** results: Comparison of the pre-processed voltammograms (solid lines) with the optimized MCR-ALS resolved voltammograms (dashed lines) of (**A1**) Pb (data set 2a with 3 components) and (**A2**) Cd (data set 2c with 5 components) metal ions, respectively. Performance ability of the optimized MCR-ALS models: calibration and external validation subsets concentration values for (**B1**) Pb and (**B2**) Cd obtained by MCR-ALS versus true concentrations. The regression lines (95% confidence level) for the calibration and external validation subsets were also included in the line equations given in the figure.

5.4.3. Comparison of MCR-ALS, PLS and CLS results

Quantitative prediction results obtained by the MCR-ALS method were compared with those obtained by the application of the PLS and CLS regression methods, respectively.

For the construction of the PLS multivariate calibration models, the same input information (calibration data subset plus pure Pb and Cd samples, respectively; see Table 5.1) as for MCR-ALS models, was given. PLS was applied considering that the concentration of only one of the two metal ions in the calibration samples was known. Separate models were developed for Pb and Cd, respectively. The voltammograms data matrix was mean centered prior to PLS decomposition. The number of significant components (LVs) were chosen by a full cross-validation (leave one out) method. Further validation of the models was carried out using the external validation sample subset (Table 5.1). The number of selected LVs was 2 and 5 for Pb and Cd, respectively, in a similar way as it was for MCR-ALS. These LVs were chosen based on the minimum value of the RMSE in the calibration and cross-validation procedures (and avoid over-fitting). With these number of LVs, the explained variance of the PLS models was 98.6 and 97.3 %, for Pb and Cd, respectively.

Quantitative results obtained by the optimized MCR-ALS and PLS methods are compared in Table 5.4. These results indicate that quantitative performances of MCR-ALS and PLS methods were similar.

For comparison, after estimation of the pure voltammograms of Pb and Cd, results by ICLS are presented (Table 5.4). Regression results obtained for Pb were reasonable (Table 5.4). However, whereas for Cd its non bilinear behavior could be modeled by MCR-ALS and PLS by the inclusion of a larger number of components, this was not possible by ICLS. The ICLS performance for Cd was very poor (Table 5.4). The main disadvantage of ICLS is that all contributions should be explicitly included in the bilinear model.

MCR-ALS and PLS methods, unlike ICLS, could solve rather efficiently the same problems (Pb and Cd overlapping peaks and Cd peak shift);

consequently, these chemometric methods were able to resolve the binary mixtures and perform their quantitative analysis with good results. In conclusion, it can be derived that MCR-ALS and PLS methods could tolerate some deviation of the non bilinear behavior observed for Cd in the experimental electrode measurements. However MCR-ALS shows a better qualitative interpretation of the signals behavior of both metals; this fact is especially important in the case of Cd, where strong peak signal shifts were observed. This quantitative information can be used to investigate the electrode responses, including their reversibility and the bilinear or non bilinear behavior of the electrode.

Table 5.4 – Statistical comparison between MCR-ALS, PLS and CLS multivariate calibration models in the quantification of Pb and Cd in the external validation subset samples.

Metals	Multivariate calibration model	RMSEP[a]	SEP[b]	Bias[c]	RE(%)[d]	Slope[e]	Offset[f]	r^{2}[g]
Pb	MCR-ALS	1.16	1.02	0.58	12.4	0.940	0.1	0.956
	PLS	1.16	1.05	0.51	12.4	0.925	0.1	0.953
	CLS	1.20	1.19	0.23	12.8	0.818	1.24	0.960
Cd	MCR-ALS	0.72	0.69	-0.24	11.4	0.942	0.6	0.949
	PLS	0.68	0.69	-0.05	10.8	0.989	0.1	0.952
	CLS	2.60	2.68	0.37	41.3	0.416	3.59	0.317

[a],[b],[c] and [d] RMSEP, SEP, Bias and RE correspond to the root mean square error of prediction, standard error of prediction, Bias and relative percentage error in concentration prediction, respectively; these parameters were previously defined in equations 5.2, 5.3, 5.4 and 5.5, respectively (see text); [e], [f] and [g] Parameters of the regression line between the prediction and the expected concentration values in the external validation subset samples.

5.4.4. Determination of Pb and Cd in river water samples

Finally, the developed MCR-ALS and PLS models were tested in river water samples and the results are summarized in Table 5.5. In these samples, Pb and Cd concentration levels were previously determined by reference methods (AAS-EA or ICP-MS).

For all samples, original concentrations of Cd, determined by the AAS-EA reference method, were below the DL (DL = 0.15 μgL^{-1}). Therefore, in order to evaluate the prediction ability of the multivariate calibration models, samples A, B and C were spiked with 3.0, 7.0 and 2.0 μgL^{-1} of Cd (Table 5.5), respectively. For Pb, samples A and C were analyzed by ICP-MS and sample B was analyzed by AAS-EA. Results are presented in Table 5.5. Sample C, which nominal concentration of Pb was (0.47 ± 0.03) μgL^{-1} was spiked with 6.0 μgL^{-1} of Pb (Table 5.5). To test the reliability of the MCR-ALS and PLS estimations, the concentration values obtained by the reference method or after spiking with metals were used as reference values (Table 5.5).

No difficulties related to matrix effects were detected probably due to the previous UV digestion of the samples. However, if matrix effect problems are detected, the inclusion of natural water samples during the construction of the calibration model should be considered.

Results obtained by MCR-ALS and PLS models are presented in Table 5.5 and compared with the reference values. For both metals, a good agreement between the results obtained by the developed chemometric models and the reference values was attained (Table 5.5). In all cases, the differences observed in the results obtained by the application of MCR-ALS or PLS models were found to be negligible (Table 5.5), proving that both methods work properly in the determination of both metals in river water samples.

Table 5.5 – Determination of Pb and Cd in river water samples.

	[Pb] /μgL^{-1}			**[Cd] /μgL^{-1}**		
Sample	**DPASV + MCR-ALS**	**DPASV + PLS**	**Reference value**	**DPASV + MCR-ALS**	**DPASV + PLS**	**Reference value**
A	0.8 ± 0.1	1.1 ± 0.1	1.10 ± 0.05	0.5 ± 0.3	0.4 ± 0.1	< 0.15[a]
A_1	1.03±0.07	1.18±0.09	1.10 ± 0.05	3.0 ± 0.2	2.9 ± 0.2	3.0[b]
B	3.5 ± 0.2	3.6 ± 0.2	3.0 ± 0.2	7.6 ± 0.5	7.1 ± 0.3	7.0[a, b]
C	6.6 ± 0.2	6.7 ± 0.1	6.47[c]	2.2 ± 0.8	2.0 ± 0.5	2.0[a, b]

[a]Originally, concentrations of Cd present in samples A, B and C, determined by AAS-ET reference method, were below the DL (0.15 μgL^{-1}); [b]Samples A_1, B and C were spiked with 3.0, 7.0 and 2.0 μgL^{-1} of Cd, respectively; [c]The nominal concentration of Pb in sample C was 0.47 μgL^{-1}. This sample was spiked with 6.0 μgL^{-1} of Pb.

5.5. Conclusions

This work shows that it is possible to resolve strongly overlapped voltammetric signals of binary mixtures of Pb and Cd using a vibrating gold microwire electrode), through the application of the MCR-ALS method. The optimized multivariate calibration models, based on MCR-ALS, allowed the simultaneous determination of Pb and Cd (up to 15.0 and 10.0 μgL^{-1}, respectively) with prediction errors in external validation samples lower than 13% for both metals.

These quantitative results obtained by MCR-ALS, when the correlation constraint was applied, were comparable to those obtained by PLS regression calibration approaches. Both methods, MCR-ALS and PLS, gave similar results. On the other hand, the application of ICLS gave reasonable results only for the quantitative determination of Pb but not for Cd.

The application of the developed MCR-ALS and PLS models for the determination of Pb and Cd in river water samples proved that the proposed chemometric approaches coupled to a vibrating gold microwire electrode measurements allow the simultaneous quantification of these metals in river water samples.

The results presented in this chapter constitute a valuable improvement of the performance of the electrochemical method described in chapter 4 and opens the possibility of the simultaneous determination of Cd, Cu, Hg, Pb and Zn, using a vibrating gold microwire electrode in the presence of oxygen and without the need of further experimental manipulations.

References

[1] Y. Bonfil, M. Brand, E. Kirowa-Eisner, Anal. Chim. Acta **2002**, 464, 99.

[2] M. Lu, K.E. Toghill, R.G. Compton, Electroanalysis **2011**, 23, 1089.

[3] C. Kokkinos, A. Economou, I. Raptis, C.E. Efstathiou, Electrochim. Acta **2008**, 53, 5294.

[4] G.H. Hwang, W.K. Han, S.J. Hong, J.S. Park, S.G. Kang, Talanta **2009**, 77, 1432.

[5] D. Li, J. Jia, J. Wang, Talanta **2010**, 83, 332.

[6] Z.S. Bi, C.S. Chapman, P. Salaün, C.M.G. van den Berg, Electroanalysis **2010**, 22, 2897.

[7] Y. Bonfil, E. Kirowa-Eisner, Anal. Chim. Acta **2002**, 457, 285.

[8] O. Mikkelsen, K.H. Schroder, Electroanalysis **2001**, 13, 687.

[9] K.E. Toghill, L. Xiao, G.G. Wildgoose, R.G. Compton, Electroanalysis **2009**, 21, 1113.

[10] M. Slavec, S.B. Hocevar, L. Baldrianova, E. Tesarova, I. Svancara, B. Ogorevc, K. Vytras, Electroanalysis **2010**, 22, 1617.

[11] E. Svobodova-Tesarova, L. Baldrianova, M. Stoces, I. Svancara, K. Vytras, S.B. Hocevar, B. Ogorevc, Electrochim. Acta **2011**, 56, 6673.

[12] Y. Ni, S. Kokot, Anal. Chim. Acta **2008**, 626, 130.

[13] M. Esteban, C. Arino, J.M. Diaz-Cruz, Critical Rev. in Anal. Chem. **2006**, 36, 295.

[14] M. Esteban, C. Arino, J.M. Diaz-Cruz, Trac-Trends in Anal. Chem. **2006**, 25, 86.

[15] M.C. Antunes, J.E.J. Simao, A.C. Duarte, R. Tauler, Analyst **2002**, 127, 809.

[16] T. Azzouz, R. Tauler, Talanta **2008**, 74, 1201.

[17] J. Jaumot, R. Gargallo, A. de Juan, R. Tauler, Chemom. Intell. Lab. Syst. **2005**, 76, 101.

[18] H.C. Goicoechea, A.C. Olivieri, R. Tauler, Analyst **2010**, 135, 636.

[10] A. Jayaraman, S. Mas, R. Tauler, A. de Juan, J. Chromatog. B **2012**, 910, 138.

[20] M. De Luca, G. Ioele, S. Mas, R. Tauler, G. Ragno, Analyst **2012**, 137, 5428.

[21] J. Jaumot, V. Marchan, R. Gargallo, A. Grandas, R. Tauler, Anal. Chem. **2004**, 76, 7094.

[22] J. Blobel, P. Bernado, D.I. Svergun, R. Tauler, M. Pons, J. Am. Chem. Soc. **2009**, 131, 4378.

[23] J. Ghasemi, S. Ahmadi, A.I. Ahmad, S. Ghobadi, Appl. Biochem. Biotechnol. **2008**, 149, 9.

[24] M. Vives, R. Tauler, R. Eritja, R. Gargallo, Anal. Bioanal. Chem. **2007**, 387, 311.

[25] S. Mas, G. Fonrodona, R. Tauler, J. Barbosa, Talanta **2007**, 71, 1455.

[26] E. Pere-Trepat, R. Tauler, J. Chromatog. A. **2006**, 1131, 85.

[27] M. Terrado, D. Barcelo, R. Tauler, Anal. Chim. Acta **2010**, 657, 19.

[28] Y. Wang, Y. Ni, S. Kokot, Anal. Biochem. **2011**, 419, 76.

[29] R. Gusmao, C. Arino, J. Manuel Diaz-Cruz, M. Esteban, Anal. Biochem. **2010**, 406, 61.

[30] M.S. Diaz-Cruz, J. Mendieta, R. Tauler, M. Esteban, Anal. Chem. **1999**, 71, 4629.

[31] R. Gusmao, C. Arino, J. Manuel Diaz-Cruz, M. Esteban, Anal. Bioanal. Chem. **2009**, 394, 1137.

[32] A.R. Khataee, A. Naseri, M. Zarei, M. Safarpour, L. Moradkhannejhad, Environ. Techn. **2012**, 33, 2305.

[33] L.A. Fonseca de Godoy, L.W. Hantao, M.P. Pedroso, R.J. Poppi, F. Augusto, Anal. Chim. Acta **2011**, 699, 120.

[34] M.C. Antunes, J.E. Simao, R.C. Duarte, Electroanalysis **2001**, 13, 1041.

[35] R. Bro, S. De Jong, J. Chemom. **1997**, 11, 393.

[36] R.K Beebe., R.J. Pell, M.B Seasholtz, Chemometrics: A Pratical Guide, Wiley-Interscience Publication **1998**, pp. 188-210.

Chapter 6

SIMULTANEOUS DETERMINATION OF NICKEL AND COBALT, USING A SOLID BISMUTH VIBRATING ELECTRODE, BY ADSORPTIVE CATHODIC STRIPPING VOLTAMMETRY[5]

Graphical abstract

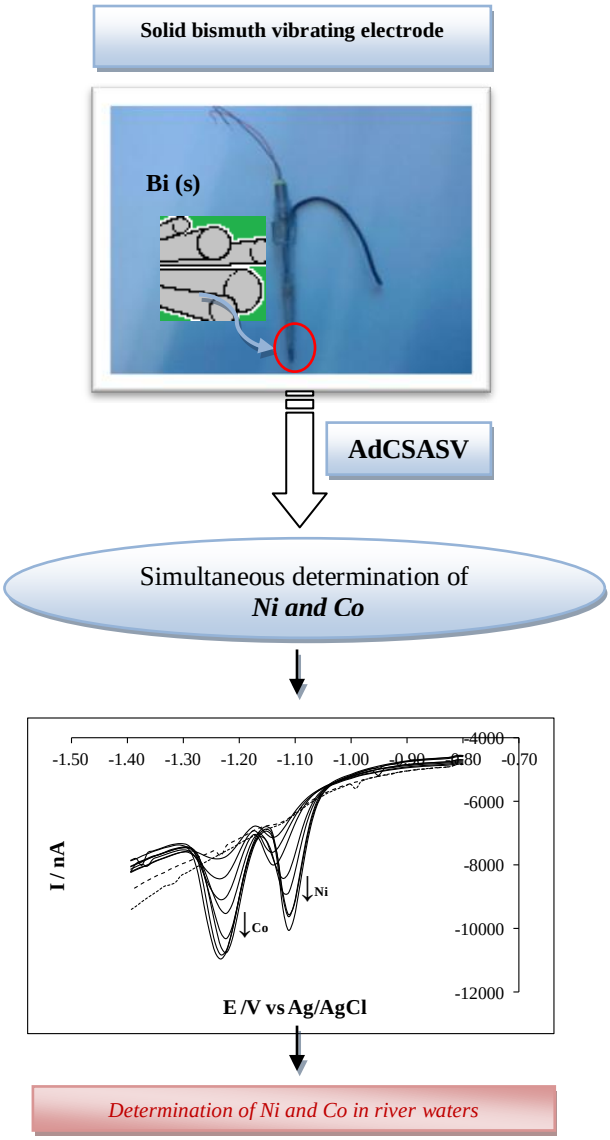

[5]*Electroanalysis* 2013, 25, 1247-1255

Abstract

A simple, fast, sensitive and "greener" voltammetric procedure for simultaneous analysis of Ni and Co by SWAdCSV using a solid bismuth vibrating electrode (SBiVE) is presented for the first time. The procedure enables to determine Ni together with Co, in ammonia buffer 0.1 $molL^{-1}$ (pH 9.2) and in the presence of oxygen, and involves an adsorptive accumulation of metal-dimethylglyoxime (Ni-DMG and Co-DMG) complexes on the electrode surface.

For Ni and Co, the DLs, obtained with 30 s of t_{acc}, were 0.6 and 1.0 μgL^{-1}, respectively.

The method was free of metals (Cd^{2+}, Cr^{3+}, Cr^{6+}, Cu^{2+}, Fe^{3+} and Pb^{2+} up to 50 μgL^{-1}, Al^{3+} and Mn^{2+} up to 500 μgL^{-1}; Zn^{2+} up to 300 μgL^{-1}) interferences up to the concentrations mentioned in brackets.

The proposed method was validated for simultaneous determination of Ni and Co in a certified reference surface and river waters with good results.

6.1. Introduction

Stripping voltammetry is a sensitive, simple and inexpensive electroanalytical technique for trace metal measurements [1-9], particularly in natural waters [2,3]. The previous chapters (Chapters 2 up to 5) support this idea, since they show that, using ASV is possible to make the multi-element detection of (Cu, Pb and Zn) and (As, Cd, Cu, Hg, Pb and Zn) in surface waters, using a BiFE and a gold microwire electrode, respectively.

Ni is usually present in natural water samples at low ($\leq$ μgL^{-1}) concentration levels [10,11]; therefore, monitoring of Ni in water samples requires sensitive voltammetric procedures. Conventionally, analysis of Ni by electroanalytical voltammetric procedures is performed by AdCSV in ammonia buffer [12]. The process usually involves the formation of complexes with dioximes [nioxime or dimethylglyoxime (DMG)] and an accumulation on mercury [10,13] or bismuth film [4-9,12,14-23] electrodes followed by the subsequent measurement of the reduction peak of the accumulated complex.

BiFEs, introduced by Wang and co-workers in 2000 [24], have been established as an appropriate alternative to mercury electrodes in the stripping analysis [25-28]. The most important advantages of BiFEs, compared to mercury electrodes, are its lower toxicity (Bi is an "environmental-friendly" metal) and lower sensitivity to the presence of the dissolved oxygen, (this is an essential property for *on-site* monitoring) without compromising the stripping performance [Chapter 2 of this thesis and 5,15,16,18,22,23,29].

AdCSV, using *ex-situ* [4-9,14-23] and more recently *in-situ* [12,30] prepared BiFEs, have been introduced as an effective alternative to the mercury electrodes for Ni and/or Co determination. The *ex-situ* plating (pre-plating) requires an adequate choice of the conductive electrode substrate and an additional formation of the bismuth film, prior to the analytical sequence, from a separate plating Bi^{3+} solution [31]. When the *in-situ* mode is used, the formation of the metallic film, in a conductive support, occurs simultaneously (co-deposition) with the deposition of the target metals during the deposition step

[31]. The analysis of Ni and/or Co using AdCSV usually involves neutral or alkaline electrolyte solutions and *ex-situ* deposition is frequently used due to the instability of the Bi^{3+} salts at these pH conditions. In addition, in AdCSV, the accumulation potential is usually not sufficiently negative for quantitative Bi^{3+} reduction and *in-situ* film formation [6,7]. However, recently Korolczuk M. *et al* [12,30] demonstrated that when bismuth is added to the sample solution in the form of its complex with tartrate, together with the introduction of an additional plating step in AdCSV analytical procedure, it is possible to form an *in- situ* bismuth film.

During the last decade, BiFEs have received strong attention and were successfully used in the stripping voltammetric trace metals analysis [25-28]. On the other hand, other studies, which used solid bismuth electrodes, have been reported for quantification of organic compounds [32-35] or heavy metals [2, 35-38]. The use of solid electrodes in voltammetric systems, in this particular case a "mercury-free" solid bismuth electrode, can offer many advantages. The main advantages of a solid bismuth electrode are: (i) it is easier to convert to flow analysis (simple handling and mechanical robustness); (ii) there is no time-consuming steps to deposit, clean or regenerate the film; (iii) it allows developing more "environmental-friendly" analytical protocols since there is minimization of the production of wastes (a solution of a salt of bismuth is not needed to prepare the film). All these reasons make a solid bismuth electrode more suitable for *on-field* measurements.

Up to now, the applicability of solid bismuth electrodes for trace metals analysis has been mainly focused on the anodic stripping voltammetric determination of Cd [2,35-37], Pb [2,36,37] and Zn [36,37] and more scarcely to other metals, such as is the case of Fe [38] by adsorptive constant-current stripping chronopotentiometric analysis. Even though, quantification of Ni has been widely described using BiFEs [4-9,12,14-23], as far as we know, no attempts have been made for its quantification using a solid bismuth electrode. Considering the advantages of the implementation of the solid bismuth electrodes, already mentioned above, the feasibility of using an easily fabricated, cost-efficient, stable

(under potential control) and robust solid bismuth disk electrode, together with a vibrating device [2], for the simultaneous determination of Ni and Co by AdCSV was evaluated in this work. The results obtained were critically compared with other works where other bismuth electrodes have been applied.

6.2. Experimental

6.2.1. Reagents and solutions

Heavy metal standard solutions used in this work were previously identified in section 3.2.1. These solutions were diluted with ultrapure water as required.

A stock aqueous solution of 0.1 $molL^{-1}$ of DMG was prepared in 0.35 $molL^{-1}$ NaOH [39]; more diluted solutions of DMG were prepared daily in pure water.

A 0.1 $molL^{-1}$ ammonia buffer solution (pH 9.2), which served as supporting electrolyte, was prepared with suprapur 25% ammonia solution and suprapur ammonium chloride, both from Merck.

6.2.2. Equipment

To perform measurements of SWAdCSV, all the equipment described in section 4.2.2 were used unless the WE, which was a solid bismuth disk vibrating electrode (~1mm diameter, supplied and "home-made" prepared by Professor van den Berg laboratory [2]). The movement of the WE was achieved using a vibrating device described in section 3.2.2.

The surface of the WE was polished using a polishing cloth with wet aluminum oxide powder with a grain size of 0.3 µm (polishing set for solid-state electrodes reference 6.2802.000 from Metrohm), followed by rinsing with water at the beginning of the day to avoid problems related with air exposition overnight.

Before stripping measurement, the certified water sample (SPS-SW1 Batch 117 from LGC Standards) and all other river water samples were UV digested [2] in a similar way as it was described in section 3.2.5.

All pH measurements were performed with a pH Meter described in section 2.2.2.

All measurements were carried out at room temperature

6.2.3. Voltammetric procedures for metals determination

A 15 mL supporting electrolyte solution [0.1 $molL^{-1}$ ammonia buffer (pH 9.2)] containing 0.04 $mmolL^{-1}$ DMG was used in the stripping analysis without removing the oxygen. The optimized SWAdCSV experimental conditions to determine Ni and Co were the following: a conditioning step [E_{cond} = -3 V for 2 s] was applied followed by the accumulation step [accumulation potential (E_{acc}) = -0.8 V for 30 s] while the electrode was vibrating. Then, the vibration of the electrode was stopped and after 10 s of t_{eq}, the voltammogram was recorded by applying a negative-going square wave scan (frequency: 50 Hz; amplitude: 25 mV and step potential: 10 mV) from -0.8 to -1.4 V. Between measurements, a standby controlled potential of -0.5 V was used.

For all experiments, at least two independent assays were carried out; a minimum of three repetitive scans were made per measurement.

6.2.4. Analysis of Ni and Co in real water samples

The developed square wave adsorptive cathodic voltammetric procedure was tested, using the standard additions method, in a certified water (sample SPS-SW1 from LGC Standards) and in two river water samples, designated as A and B, respectively. These river water samples were previously filtered, acidified to pH 2 with ultrapure HNO_3 and stored in the refrigerator. All samples were UV digested for one hour [2].

For the adsorptive stripping determination of Ni and Co, using a SBiVE, samples were diluted and buffered with 0.2 $molL^{-1}$ ammonia buffer solution pH 9.2. Certified water sample and sample A were diluted two times by adding 7.5 mL of the water sample plus 7.5 mL of ammonia buffer solution; sample B was diluted five times by adding 3.0 mL of the water sample plus 7.5 mL of ammonia buffer solution and 4.5 mL of ultrapure water. For all samples, final pH was adjusted to 9.2 with a few micro liters of NH_3 25% suprapure solution. The certified water sample was analyzed in triplicate and samples A and B in duplicate. The analysis was carried out as described above (see Section 6.2.3) and the results were validated by AAS-EA for Ni and by SWAdCSV using a HMDE for Co.

Measurements of Ni, made by AAS-EA, were performed with the spectrophotometer described in section 2.2.2. The determination of Co was performed using a Metrohm 663 VA stand together with a potentiostat – galvanostat model PGSTAT12/30/302 from Autolab and an IME 663 interface from Eco Chemie. For the determination of Co at a HMDE, samples were previously UV digested for one hour [2], buffered with ammonia 1.0 $molL^{-1}$ until pH 9.2 and spiked with 0.04 $mmolL^{-1}$ of DMG. The following SWAdCSV experimental conditions were used: E_{acc} = -0.7 V (60 s) under a rotation speed of 1500 rpm followed by 10 s of t_{eq}; subsequently, the voltammogram was recorded by applying a negative-going square wave scan (frequency: 50 Hz; amplitude: 20 mV and step potential: 5 mV) from -0.7 to -1.5 V.

6.3. Results and Discussion

In this work, the determination of Ni was performed in the presence of oxygen by SWAdCSV using a potential window from -0.8 to -1.4 V, ammonia buffer 0.1 mol L^{-1} (pH 9.2) as electrolyte solution and DMG as complexing agent. Additionally, a vibrating device [2] was used for improving the sensitivity. Under these experimental conditions, no evidence of hydrogen ions reduction at negative

potentials or oxidation of the metallic bismuth in the anodic limit seems to occur. These facts are in agreement with the literature [32,35,40].

The following sections describe the optimization and the evaluation of the analytical performance of a SBiVE for Ni and Co analysis.

6.3.1 Optimization of the experimental conditions for AdCSV of Ni

6.3.1.1. Effect of ligand concentration

The dependence of Ni-DMG peak current in function of the DMG concentration was studied. Figure 6.1 (A) shows the effect of increasing DMG concentration, over the range 0.005 – 0.32 $mmolL^{-1}$, on the peak height of 5.0 μgL^{-1} Ni using a constant accumulation potential (E_{acc} = -0.8 V) during 30 s. The Ni peak height increased with successive additions of DMG concentrations up to 0.08 mmol L^{-1}; at higher DMG concentrations, the signal stabilized. However for DMG concentrations higher than 0.04 $mmolL^{-1}$, a reduction peak for DMG occurred in the same position of Ni peak. Consequently, an optimum DMG concentration of 0.04 $mmolL^{-1}$ was selected for further experiments.

6.3.1.2. Effect of accumulation potential and accumulation time

The effect of E_{acc} was studied for a solution containing 5.0 μgL^{-1} of Ni and an optimized concentration of DMG (0.04 $mmolL^{-1}$) at a fixed t_{acc} (30 s). The E_{acc} was changed from -0.9 to -0.6 V. The obtained results are present in Figure 6.1 (B). Ni peak height was maximum when an E_{acc} from -0.8 to -0.7 V was applied and diminished when an E_{acc} more negative than -0.8 V or more positive than -0.7 V, respectively, were used. For an E_{acc} of -0.9 V there was a slight decrease (14%), which could be related with the reduction of the Ni-DMG complex [23]. Thus, for further studies, an E_{acc} of -0.8 V was chosen.

The influence of t_{acc} on the stripping signal was also investigated by varying its value in the range 0 to 60 s [Figure 6.1 (C)] using previously optimized

conditions ([DMG] = 0.04 mmolL^{-1} and E_{acc} = -0.8 V) for 2.0 μgL^{-1} and 5.0 μgL^{-1} of Ni, respectively. As expected, the influence of this experimental parameter depends on sample concentration. For 5.0 μgL^{-1} of Ni, the peak height increases linearly with t_{acc} up to 40 s; after, the peak height remained almost constant until 60 s. For a lower concentration of Ni (2 μgL^{-1}), the stripping signal increased linearly with the accumulation time up to 60 s. Considering these results, a 30 s t_{acc} was selected for subsequent measurements as this gave a good compromise between sensitivity and analysis time.

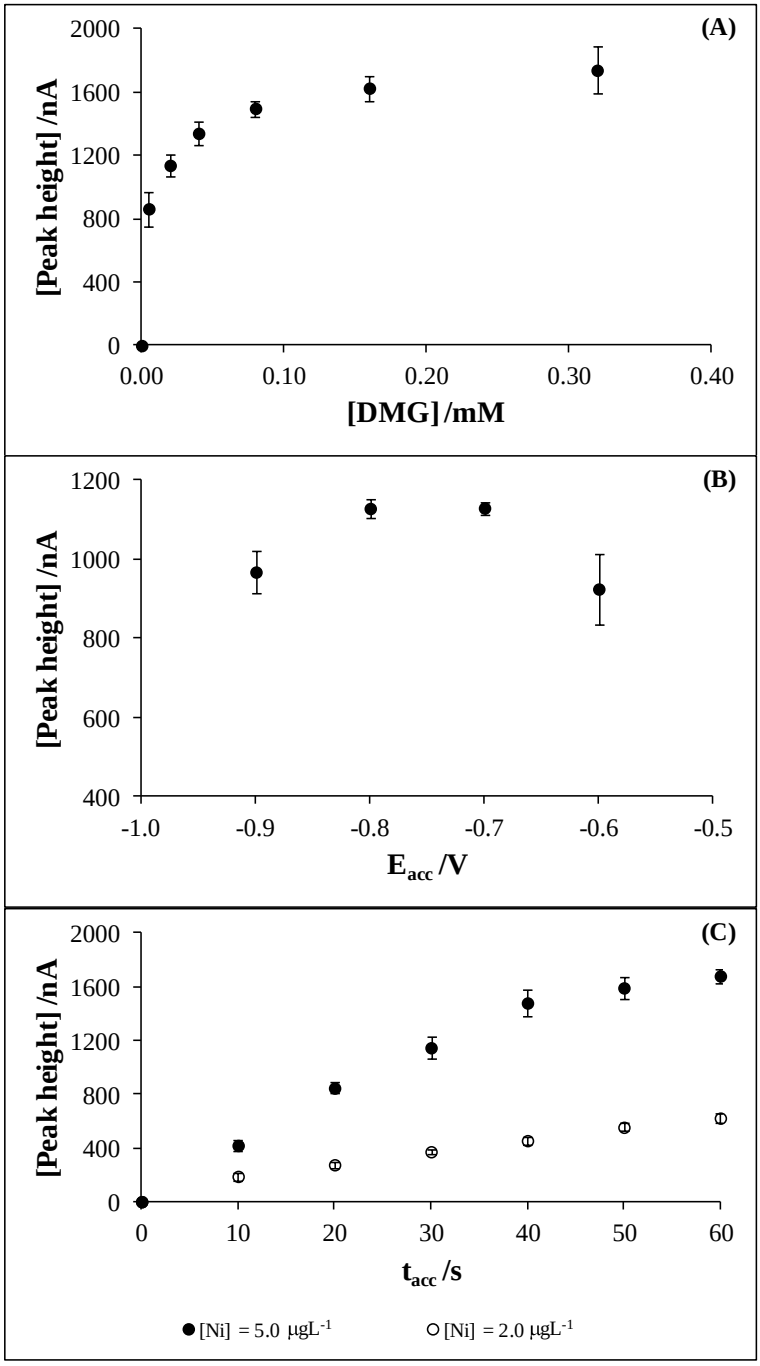

Figure 6.1 – Effect of several experimental parameters on the peak current intensity of Ni determined by SWAdCSV. **(A)**: Effect of the variation of [DMG] on the stripping signal obtained for 5.0 μgL^{-1} Ni (E_{acc} = -0.8 V and t_{acc} = 30 s); **(B)**: Effect of E_{acc} on the stripping signal for 5.0 μgL^{-1} Ni (t_{acc} = 30 s and [DMG] = 0.04 $mmolL^{-1}$) and **(C)**: Effect of t_{acc} on the stripping signals for the indicated Ni concentration levels (E_{acc} = -0.8 V and [DMG] = 0.04 $mmolL^{-1}$). Values are the average of three replicates of three (A and C) or two (B) independent experiments; Standard deviation (vertical error bars; where no error bars are shown, they are within the points) are presented (n = 9 for A and C; n = 6 for B).

6.3.2. Analytical performance

6.3.2.1. Trace nickel determination

In order to evaluate the analytical performance of a SBiVE for trace analysis of Ni under previous optimized conditions, the LCR and the DL were established.

Figure 6.2 shows the voltammograms [Figigure 6.2 (A)] recorded for increasing concentrations of Ni (increments of 2.0 μgL^{-1}) and the corresponding calibration curve [Figure 6.2 (B)]. Ni presented a cathodic well-defined sharp peak at -1.11 V. A linear response with a good correlation coefficient ($r^2_{(n=16)}$ = 0.991) was obtained for Ni up to 10 μgL^{-1} and obeyed the equation $I_{[peak\ height]}$ (nA) = (233 ± 13) × [Ni] μgL^{-1} + (7 ± 83) nA, calculated with a confidence interval of 95 %. The DL, calculated using the approximation of Miller and Miller [41] for the calibration curve, with a t_{acc} of 30 s, was 0.6 μgL^{-1}. The sensitivity and the LCR are convenient for monitoring Ni in natural surface waters [10]. Moreover, the DL achieved with the present analytical methodology comprises perfectly the values of Ni concentration according to the EPA of the USA [42] and of the EU [43] guidelines.

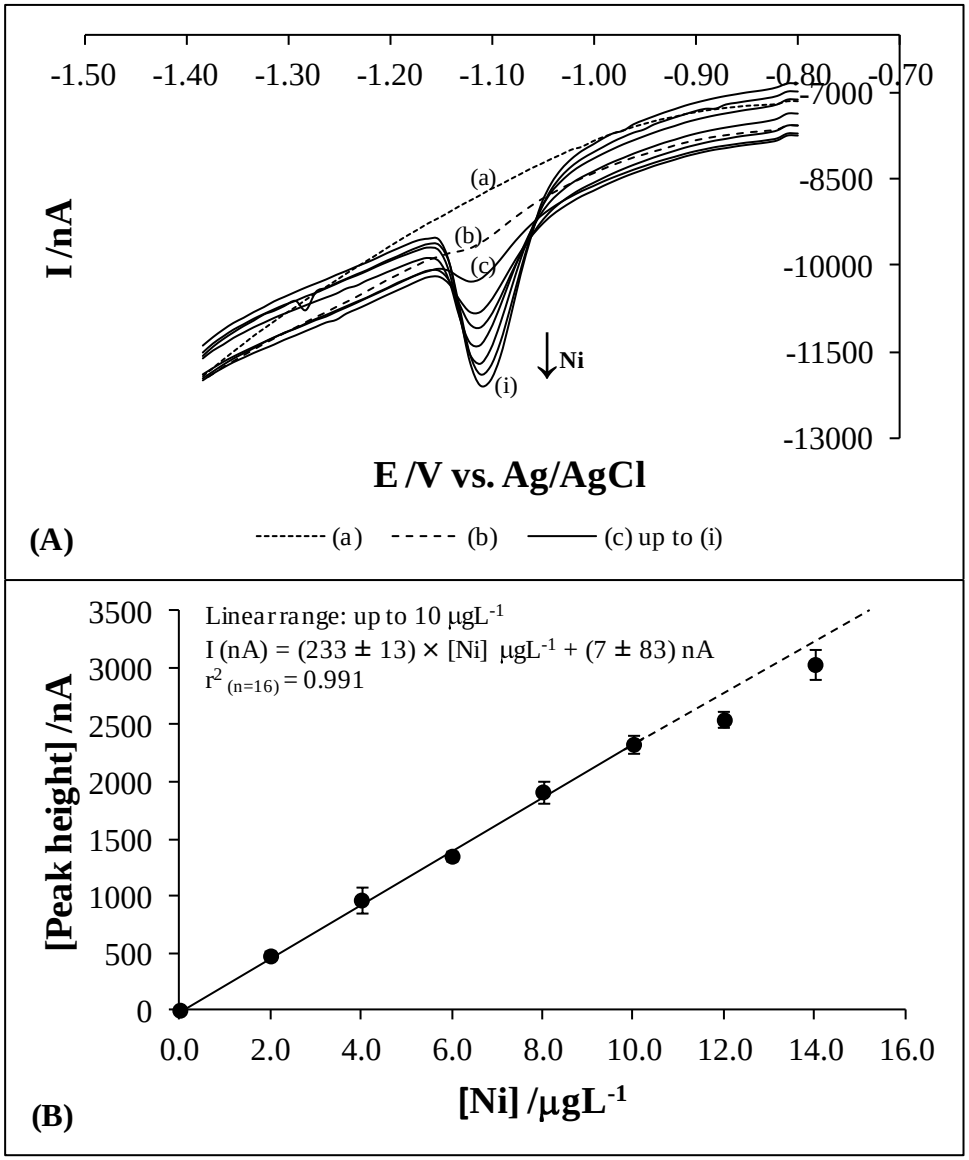

Figure 6.2 – (A) SWAdCSV voltammograms obtained in (a) 0.1 $molL^{-1}$ ammonia buffer solution (pH 9.2), (b) buffer solution with 0.04 $mmolL^{-1}$ of DMG and [(c) up to (i)] with increasing Ni concentration, at optimized conditions (E_{acc} = -0.8 V; t_{acc} = 30s); **(B)** Ni calibration curve. This is an example of an experiment repeated 3 times; in figure 6.2 (B), values are the average of three replicates; standard deviation (vertical error bars are shown; where no error bars are shown, they are within the points) are presented (n = 3).

Table 6.1 summarizes the literature results for Ni (DL and LCR) using different bismuth electrodes under different adsorptive stripping voltammetric

procedures. It should be noted that, the results were obtained with different t_{acc} and using electrodes with different areas, including micro and macro electrodes, respectively. After normalizing the DLs values by the different t_{acc} used, a comparative analysis between the results obtained in this work with others recorded under similar experimental conditions (SWAdCSV or AdSCCC with DMG) evidence that, unless the DL obtained with a BiFμE [20], our result is comparable [8,9,14,15,19] or better than the results obtained with a bismuth microelectrode arrays [16,17] and macro BiFEs [4,5,7,18,22] (Table 6.1). This result, together with the advantages presented by the solid bismuth electrode (briefly, it is mechanically more robust and it allows the development of faster and more environmental-friendly analytical protocols than the BiFEs), makes this SBiVE more suitable for the future development of greener automatized methods for *on-site* determination of Ni.

Table 6.1 – Adsorptive stripping voltammetric determination of Ni at various bismuth electrodes.

Working electrode	**Technique (t_{acc} (s))**	**Complexing agent**	**Linear range /μgL^{-1}**	**DL /μgL^{-1}**	**Reference**
Solid bismuth vibrating electrode (d = 1 mm)	SWAdCSV [a] (t_{acc} = 30 s)	DMG	Up to 10	0.6	Our work
Carbon screen-printed electrodes modified with bismuth nanoparticles (A = 0.10 cm^2)	LSAdCSV (t_{acc} = 120 s)	DMG	0.50 – 5.0	0.2	[14]
BiFE/GC (d = 1 mm) (*in-situ* deposition)	SWAdCSV (t_{acc} = 120 s)	Nioxime	0.30 – 3.0	0.06	[12]
Sputtered BiFE (A= 4 x 5 mm^2)	SWAdCSV (t_{acc} = 90s)	DMG	Up to 20 (90s) and Up to 40 (60s)	0.1	[15]
Sputtered BiFE (A = 5 x 5 mm^2)	SWAdCSV (t_{acc} = 60s)	DMG	0 – 14	0.4	[9]

Table 6.1 – Continuation…

Working electrode	**Technique (t_{acc} (s))**	**Complexing agent**	**Linear range /μgL^{-1}**	**DL /μgL^{-1}**	**Reference**
Sputtered Bi film microdisk array (A = 5 x 5 mm^2)	SWAdCSV (t_{acc} = 60s)	DMG	0 – 15	0.7	[16]
Sputtered Bi film microdisk array (A = 5 x 5 mm^2)	SWAdCSV[b] (t_{acc} = 60s)	DMG	0 – 60	2.7	[17]
BiFE/GC (d = 3 mm)	SWAdCSV [a] (t_{acc} = 300 s)	DMG	----	0.1	[18]
BiFME/Carbon fibre (d = 7μm) (*ex-situ* deposition)	SWAdCSV (t_{acc} = 120 s)	DMG	---	0.09	[19]
BiFμE/Carbon fibre (d = 7μm) (*ex-situ* deposition)	SWAdCSV[a] (t_{acc} = 60 s)	DMG	0.2 – 1.8 (120 s) and 2.0 – 16.0 (30s)	0.06	[20]
BiFE/GC (d = 3.0mm) (*ex-situ* deposition)	SWAdCSV (t_{acc} = 60 s)	1-nitroso-2-napthol	15 – 70 and 80 – 200	0.1	[21]

Table 6.1 – Continuation…

Working electrode	**Technique (t_{acc} (s))**	**Complexing agent**	**Linear range /μgL^{-1}**	**DL /μgL^{-1}**	**Reference**
BiFE/GC (*ex-situ* deposition)	LSAdCSV (t_{acc} = 180 s)	DMG	20 – 80 (30s)	0.8	[4]
BiFE/GC (d = 1.0 mm) (*ex-situ* deposition)	DPAdCSV [c] (t_{acc} = 300 s)	DMG	Up to 10	0.1	[22]
BiFE/GC (d = 3mm) (*ex-situ*: in line plated)	SWAdCSV[a][d] (t_{acc} = 120 s)	DMG	1 – 20	---	[23]
BiFE/Cu (d = 3.1 mm) (*ex-situ* deposition)	SWAdCSV (t_{acc} = 600 s)	DMG	5.9 – 59	6	[5]
BiFE/GC (d = 2 mm) (*ex-situ* deposition)	SWAdCSV (t_{acc} = 60 s)	DMG	Up to 70	----	[6]
BiFE/GC (d = 2 mm) (*ex-situ* deposition)	SWAdCSV[a] (t_{acc} = 180 s)	DMG	----	1	[7]

Table 6.1 – Continuation…

Working electrode	Technique (t_{acc} (s))	Complexing agent	Linear range /μgL^{-1}	DL /μgL^{-1}	Reference
BiFE/GC (d =2 mm) (*ex-situ* deposition)	AdSCCC[a] (t_{acc} = 60 s)	DMG	---	0.26	[8]
Silver-bismuth alloy electrode (BiAgE)	DP-AdCSV[a][c]	DMG	---	---	[44]

SWAdCSV: Square wave adsorptive cathodic stripping voltammetry; DPAdCSV: Differential pulse adsorptive cathodic stripping voltammetry; LSAdCSV – Linear sweep adsorptive cathodic stripping voltammetry; AdSCCC – Adsorptive stripping constant current chronopotentiometry.

[a] Simultaneous determination of Ni and Co; [b] Static mode; [c] Automatic system and [d] Flow system.

6.3.2.2. Simultaneous determination of Ni and Co

According to EPA RWQCs (Table 1.1), Co is not considered a toxic metal pollutant [42]. However, in this work, the possibility of determining Co simultaneously with Ni was also studied using the experimental conditions previously optimized for Ni. Firstly, the determination of Co solely was attempted; in Figure 6.3, the voltammograms [Figure 6.3 (A)] and the calibration curve (increments of 5.0 μgL^{-1}) [Figure 6.3 (B)] of Co are presented. In a similar way as it was observed for Ni, a well-defined Co peak, located at -1.22 V [Figure 6.3 (A)], was recorded. For an t_{acc} of 30 s, the calibration curve was linear up to 40 μgL^{-1} and obeyed to the equation $I_{[peak\ height]}$ (nA) = (128 ± 3) × [Co] μgL^{-1} – (39 ± 71) nA ($r^2_{(n=25)}$ = 0.997), calculated with a confidence interval of 95 %. The calculated DL [41] was 1.0 μgL^{-1}. The sensitivity obtained for Co was lower than the one recorded for Ni. The DL and the LCR were about two and four times higher, respectively, than the respective values calculated for Ni. In general, the DL reported for Co obtained with other bismuth electrodes was lower than the one obtained in this work [30,45-48]. However, it is important to point out that Co was determined under experimental conditions, which were not optimized for Co but for Ni; thus, the DL obtained for Co here seems to be satisfactory. If further enhancement of the Co-DMG response is desirable, a catalytic adsorptive stripping analysis using nitrite, usually described in the literature [23,30,47,48], can be used.

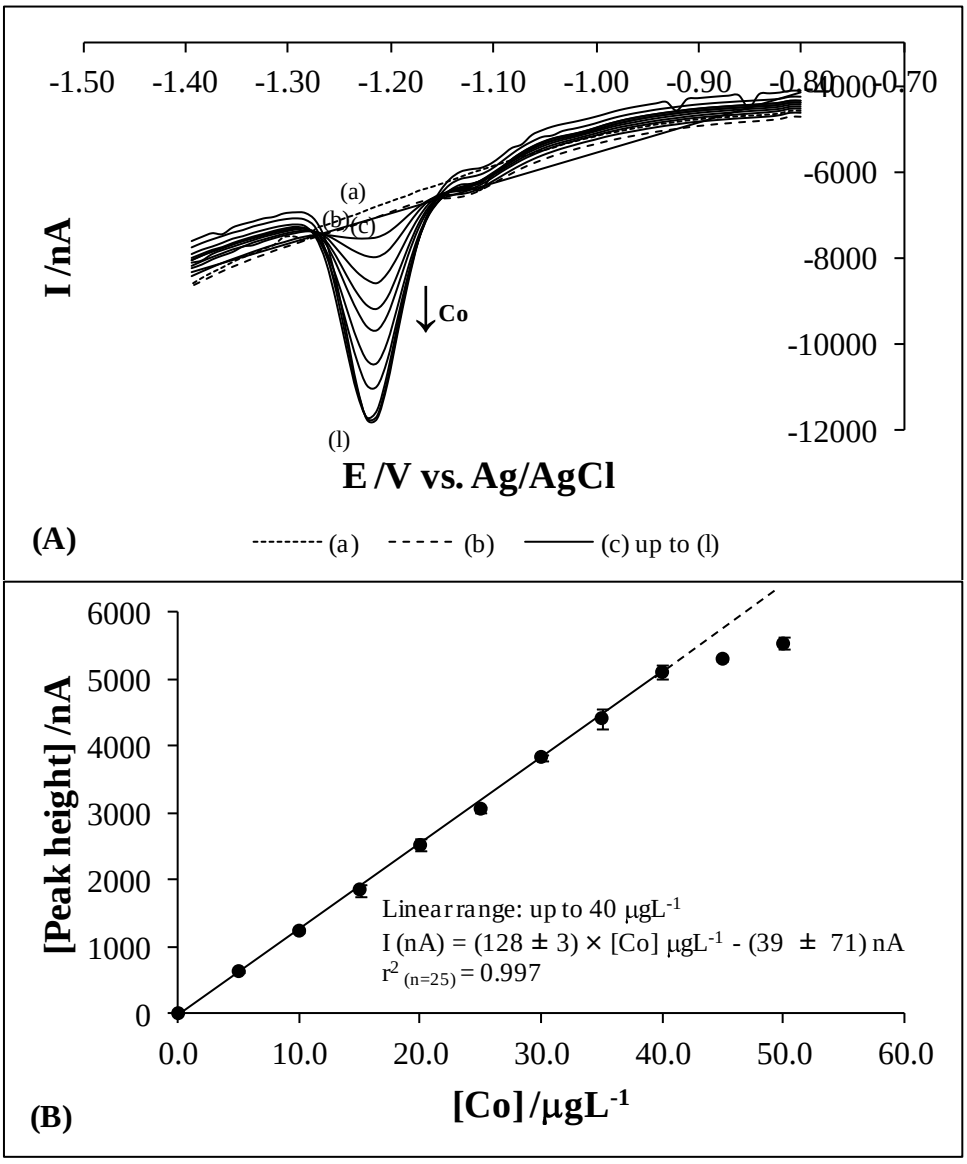

Figure 6.3 – (A) SWAdCSV voltammogramms obtained in (a) 0.1 $molL^{-1}$ ammonia buffer solution (pH 9.2), (b) buffer solution with 0.04 $mmolL^{-1}$ of DMG and [(c) up to (l)] with increasing Co concentration, at Ni optimized conditions (E_{acc} = -0.8 V; t_{acc} = 30s); **(B)** Calibration curve of Co. This is an example of an experiment repeated 3 times; in figure 6.3(B), values are the average of three replicates; standard deviation (vertical error bars are shown; where no error bars are shown, they are within the points) are presented (n = 3).

According to the results presented above, a SBiVE allows making individual determination of Ni and Co. So, the next step was to study the possibility of determining simultaneously these two metals. As it was mentioned above, in real samples, Ni is usually present at higher concentrations than Co [49]; so, the interference of Co on the Ni stripping signal seems not to be a usual problem. However, the interference of successive additions of Co on the determination of Ni ([Ni] = 5.0 μgL^{-1}) was studied; the results obtained are presented in figure 6.4. This figure shows that the stripping signal corresponding to 5.0 μgL^{-1} of Ni was not affected by the successive additions of Co, even in the presence of concentrations of Co ten times higher than the concentration of Ni.

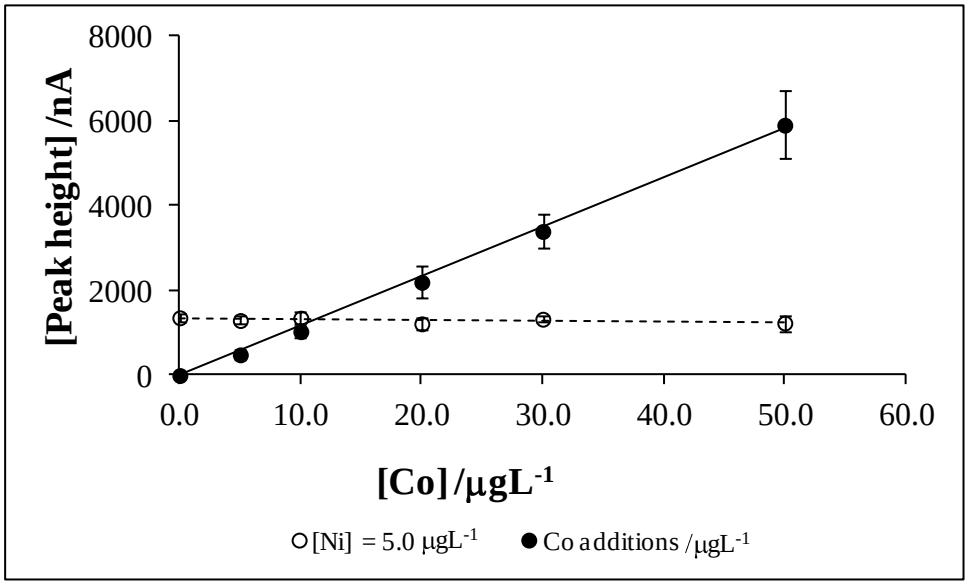

Figure 6.4 – Effect of successive additions of Co (up to 50 μgL^{-1}) on the Ni response (5 μgL^{-1}), using the optimized SWAdCSV Ni conditions (DMG = 0.04 $mmolL^{-1}$; E_{acc} = -0.8 V and t_{acc} = 30s). Values are the average of three replicates of three independent experiments; standard deviation (vertical error bars) are present (n = 9).

Finally, simultaneous determination of Ni and Co was performed using the same experimental conditions applied for the individual experiments. Figure 6.5 (A) represents an example of a series of voltammogramms recorded with solutions containing increasing concentrations of both metals. Well-defined and separated peaks for Ni and Co, located at ~ -1.12 and ~ -1.23 V, respectively,

were observed. Without prejudice the analysis, for concentrations of Ni higher than 10 μgL^{-1} (upper limit of linearity), the peak becomes narrow and shifts in the anodic direction [Figure 5 (A)]. The simultaneous calibration curve [Figure 6.5 (B)] obtained for Ni exhibits the same linearity range and equivalent sensitivity when compared with the individual analysis [Figure 6.2 (B)]. For Co, the peak shape is similar in individual [Figure 6.3 (A)] and simultaneous [Figure 6.5 (A)] determinations, respectively. In the simultaneous determination, the Co peak height current – concentration relationship is linear up to 35 μgL^{-1} and is represented by the equation $I_{[peak\ height]}$ (nA) = (111 ± 5) × [Co] μgL^{-1} + (57 ± 103) nA ($r^2_{(n=22)}$ = 0.990), calculated with a confidence interval of 95%. The sensitivity obtained remained relatively unchanged (~13%) when compared with the individual calibration of Co.

The results obtained above clearly showed the suitability of the solid bismuth vibrating electrode to determine Ni and Co simultaneously. In a similar way as described for the BiFEs, the solid bismuth electrode is insensitive to dissolved oxygen. Therefore, the procedure developed in this work is simpler, faster and the analytical performance of the electrode proved to be comparable to the BiFEs. These characteristics, together with the fact that this electrode does not require bismuth film formation, as well as the subsequent cleaning or activating procedures to regenerate the electrode surface, allowed us to develop a "greener" electrochemical analytical procedure for determination of Ni and Co.

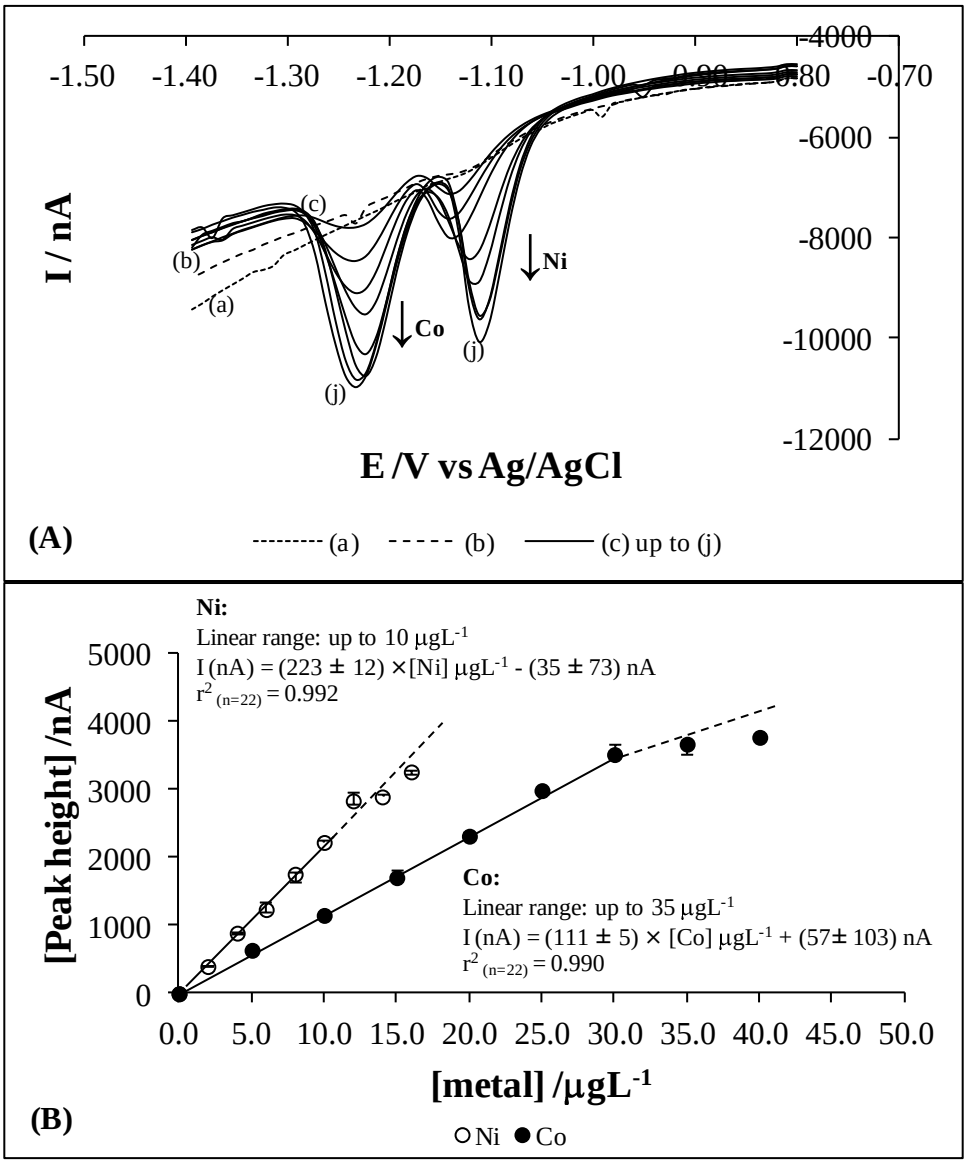

Figure 6.5 – (A) SWAdCSV voltammogramms obtained in (a) 0.1 $molL^{-1}$ ammonia buffer solution (pH 9.2), (b) buffer solution with 0.04 $mmolL^{-1}$ of DMG and [(c) up to (j)] with increasing Ni and Co concentrations, at Ni optimized conditions (E_{acc} = -0.8 V; t_{acc} = 30s); **(B)** Ni and Co calibration curves. This is an example of an experiment repeated 3 times; in figure 6.5B, values are the average of three replicates; standard deviation (vertical error bars are shown; where no error bars are shown, they are within the points) are presented (n = 3).

6.3.2.3. Repeatability and Reproducibility

The response of the solid bismuth electrode is stable when the electrode is used continuously under a controlled potential to prevent the oxidation of the electrode [2]. Mechanical polishing of the bismuth solid electrode is only

necessary after its exposition to air for more than one hour. According to this, in the beginning of the day, the electrode was polished to avoid oxidation problems related to air exposition overnight and used thereafter.

Using a freshly polished electrode, a series of 14 repetitive measurements of a mixture with 5.0 μgL^{-1} of Ni and 5.0 μgL^{-1} of Co, gave a stable response (relative standard deviations of 11 and 7% for Ni and Co, respectively), which reflected a rapid desorption of the complexes of Ni-DMG and Co-DMG from the electrode surface.

Additionally, the stability and reproducibility of a SBiVE were tested for the same metal concentrations performing 14 independent determinations. For Ni and Co, values of 13 and 18% (n = 14), respectively, were attained. These results showed that the solid bismuth electrode evidenced a satisfactory mechanical and electrochemical stability.

6.3.2.4. Metals interferences studies

Possible interferences of foreign metal ions (Al^{3+}, Cd^{2+}, Cr^{3+}, Cr^{6+}, Cu^{2+}, Fe^{3+}, Mn^{2+}, Pb^{2+} and Zn^{2+}) on the simultaneous AdCSV determination of Ni and Co were investigated using a mixture of 5.0 μgL^{-1} of Ni and 5.0 μgL^{-1} of Co, in the presence of different amounts of the interferent metal ion (0.5, 5.0 and 50 μgL^{-1}; in the case of Al^{3+}, Mn^{2+} and Zn^{2+}, concentrations of the foreign metal ions up to 500 μgL^{-1} were also tested.

Taking into account the results of the repeatability and reproducibility reported above, none of these metal ions (Cd^{2+}, Cr^{3+}, Cr^{6+}, Cu^{2+}, Fe^{3+} and Pb^{2+} up to 50 μgL^{-1}; Al^{3+} and Mn^{2+} up to 500 μgL^{-1}; Zn^{2+} up to 300 μgL^{-1}) seems to interfere on the determination of Ni and Co up to the concentrations mentioned.

6.3.2.5. Simultaneous determination of Ni and Co in real water samples

The utility of a SBiVE for the simultaneous analysis of Ni and Co using the adsorptive stripping method described above was tested in a certified water material (sample SPS-SW1 from LGC Standards) and in two river water samples (samples A and B, respectively).

The certified reference sample is a surface water, which contains 45 elements including (10.0 ± 0.1) μgL^{-1} of Ni and (2.00 ± 0.02) μgL^{-1} of Co. Except for the certified water material, the concentrations of Ni and Co were also determined by reference methods.

After being collected, all the samples were acidified (pH ≤ 2); before Ni and Co measurement by SWAdCSV, all samples were diluted and buffered with ammonia buffer at pH 9.2. The DL for Co determined by SWAdCSV using a SBiVE was 1.0 μgL^{-1}; the concentration of Co in samples A and B could not be measured by the developed method because the values were below the DL. These results were corroborated by the Co concentrations, determined by the reference method, which were less than 0.4 μgL^{-1} and (1.0 ± 0.2) μgL^{-1} for samples A and B, respectively. Therefore, to prove the applicability of the SWAdCSV method to simultaneous determination of Ni and Co in real surface water samples, sample A was diluted two times and doped with 5.0 μgL^{-1} of Co (Sample A1) and subsequently analyzed.

The comparative analysis between the results obtained with a SBiVE and the reference values evidence a good agreement for both metals (Table 6.2), even for Co determined in the certified water material, which concentration was near the DL. These results confirm the potentiality of a SBiVE as an alternative to mercury or BiFE electrodes for monitoring Ni and Co in fresh surface waters.

Table 6.2 – Comparison of Ni and Co (μgL^{-1}) concentration values present in a certified water material or determined in river water samples by SWAdCSV with a SBiVE or with reference methods [a].

Sample	Reference Values		SWAdCSV	
	Ni	Co	Ni	Co
SPS-SW1[b] diluted 2 times	5.00	1.00	4.9 ± 0.5	1.1 ± 0.2
A[c] diluted 2 times	1.49	< 0.4	1.28 ± 0.07	< DL [f]
A1[d]	1.49	≥ 5.0	1.46 ± 0.02	4.8 ± 0.1
B[e] diluted 5 times	3.16	0.20	3.13 ± 0.01	< DL[f]

[a] The values presented are the average of three replicates of three (n = 9) (Ni AAS determinations and Ni and Co SWAdCSV with a SBiVE analysis of a certified water material) or two (n = 6) (SWAdCSV, either with a HMDE or a SBiVE, analysis of samples A and B) independent experiments; [b] Certified water material: $[Ni]_{certified\ value}$ = (10.0 ± 0.1) μgL^{-1} and $[Co]_{certified\ value}$ = (2.00 ± 0.02) μgL^{-1} according to the information provided by the certificate of analysis; [c] River water sample A: $[Ni]_{reference\ value\ determined\ by\ AAS\text{-}EA}$ = (2.98 ± 0.09) μgL^{-1} and $[Co]_{reference\ value\ determined\ by\ SW\text{-}AdCSV\ with\ HMDE}$ < DL (0.4 μgL^{-1}); [d] Sample A1 corresponds to sample A diluted 2 times and doped with 5.0 μgL^{-1} of Co; [e] River water sample B: $[Ni]_{reference\ value\ determined\ by\ AAS\text{-}EA}$ = (15.8 ± 0.7) μgL^{-1} and $[Co]_{reference\ value\ determined\ by\ SW\text{-}AdCSV\ with\ HMDE}$ = (1.0 ± 0.2) μgL^{-1} and [f] DL for Co determined by SWAdCSV using a SBiVE was 1.0 μgL^{-1}.

6.4. Conclusions

For the first time, a SBiVE was successfully applied for the simultaneous determination of Ni and Co by SWAdCSV.

The analytical performance of the SBiVE proved to be comparable or better than the BiFEs with the advantage of allowing a faster and simpler adsorptive methodology [it does not require the bismuth film formation (either *ex-situ* or *in-situ* deposition), as well as the subsequent cleaning or activating procedures to regenerate the electrode surface] than the ones previously described with BiFEs. These properties, together with the fact that this solid electrode avoids the application of the traditional mercury toxic electrodes and has more mechanical robustness than the BiFEs, make this SBiVE easier to convert to flow analysis and thus, more suitable for field measurements of Ni and Co by SWAdCSV.

References

[1] J. Wang, Stripping Analysis, VCH Publishers, Inc., Deerfield Beach, Florida, **1985**.

[2] Z.S Bi, C.S. Chapman, P. Salaun, C.M.G. van den Berg, Electroanalysis **2010**, 22, 2897.

[3] M. Pesavento, G. Alberti, R. Biesuz, Anal. Chim. Acta **2009**, 631, 129.

[4] J. Wang, J.M. Lu, Electrochem. Comm. **2000**, 2, 390.

[5] S. Legeai, S. Bois, O. Vittori, J. of Electroanal. Chem. **2006**, 591, 93.

[6] A. Economou, A. Voulgaropoulos, Electroanalysis **2010**, 22, 1468.

[7] A. Economou, A. Voulgaropoulos, Talanta **2007**, 71, 758.

[8] E.A. Hutton, S.B. Hocevar, B. Ogorevc, M.R. Smyth, Electrochem. Comm. **2003**, 5, 765.

[9] C. Kokkinos, A. Economou, L. Raptis, C.E. Efstathiou, T. Speliotis, Electrochem. Comm. **2007**, 9, 2795.

[10] A. Aouarram, M.D. Galindo-Riano, M. Garcia-Vargas, M. Stitou, F. El Yousfi, E. Espada-Bellido, Talanta **2010**, 82, 1749.

[11] ATSDR (**2005**). Toxicological profile for nickel. Agency for Toxic Substances and Disease Registry (ATSDR). U.S. Department of Health and Human Services - Public Health Service.

[12] M. Korolczuk, I. Rutyna, K. Tyszczuk, Electroanalysis **2010**, 22, 1494.

[13] A. Bobrowski, J. Zarebski, Current Anal. Chem. **2008**, 4, 191.

[14] L.A. Piankova, N.A. Malakhova, N.Y. Stozhko, K.Z. Brainina, A.M. Murzakaev, O.R. Timoshenkova, Electrochem. Comm. **2011**, 13, 981.

[15] C. Kokkinos, A. Economou, I. Raptis, T. Speliotis, Anal. Chim. Acta **2008**, 622, 111.

[16] C. Kokkinos, A. Economou, I. Raptis, Anal. Chim. Acta **2012**, 710, 1.

[17] C. Kokkinos, A. Economou, I. Raptis, T. Speliotis, Electrochem. Comm. **2011**, 13, 391.

[18] M. Morfobos, A. Economou, A. Voulgaropoulos, Anal. Chim. Acta **2004**, 519, 57.

[19] E.A. Hutton, S.B. Hocevar, M. Ogorevc, Anal. Chim. Acta **2005**, 537, 285.

[20] E.A. Hutton, B. Ogorevc, S.B. Hocevar, M.R. Smyth, Anal. Chim. Acta **2006**, 557, 57.

[21] R. Segura, M. Pradena, D. Pinto, F. Godoy, E. Nagles, V. Arancibia, Talanta **2011**, 85, 2316.

[22] D. Ruhlig, A. Schulte, W. Schuhmann, Electroanalysis **2006**, 18, 53.

[23] N.G. Naseri, S.J. Baldock, A. Economou, N.J. Goddard, P.R. Fielden, Anal. and Bioanal. Chem. **2008**, 391, 1283.

[24] J. Wang, J.M. Lu, S.B. Hocevar, P.A.M. Farias, B. Ogorevc, Anal. Chem. **2000**, 72, 3218.

[25] S. Hocevar, I. Svancara, Electroanalysis **2010**, 22, 1405.

[26] J. Wang, Electroanalysis **2005**, 17, 1341.

[27] C. Kokkinos, A. Economou, Current Anal. Chem. **2008**, 4, 183.

[28] A. Economou, Trac-Trends in Anal. Chem. **2005**, 24, 334.

[29] M. Korolczuk, K. Tyszczuk, M. Grabarczyk, Electrochem. Comm. **2005**, 7, 1185.

[30] I. Rutyna, M. Korolczuk, Electroanalysis **2011**, 23, 637.

[31] A. Krolicka, A. Bobrowski, Electrochem. Comm. **2004**, 6, 99.

[32] M. Buckova, P. Grundler, G.U. Flechsig, Electroanalysis **2005**, 17, 440.

[33] M. Adamovski, A. Zajac, P. Grundler, G.U. Flechsig, Electrochem. Comm. **2006**, 8, 932.

[34] O. El Tall, D. Beh, N. Jaffrezic-Renault, O. Vittori, Inter. J. of Environm. Anal. Chem. **2010**, 90, 40.

[35] R. Pauliukaite, S.B. Hocevar, B. Ogorevc, J. Wang, Electroanalysis **2004**, 16, 719.

[36] K.C. Armstrong, C.E. Tatum, R.N. Dansby-Sparks, J.Q. Chambers, Z.-L. Xue, Talanta **2010**, 82, 675.

[37] M. de la Gala Morales, M.R. Palomo Marin, L. Calvo Blazquez, E. Pinilla Gil, Electroanalysis **2012**, 24, 1170.

[38] W. Pimrote, R. Ratana-Ohpas, L. Renman, Electroanalysis **2011**, 23, 1607.

[39] J. Santos-Echeandia, Talanta **2011**, 85, 506.

[40] E.A. Hutton, B. Ogorevc, S.B. Hocevar, F. Weldon, M.R. Smyth, J. Wang, Electrochem. Comm. 2001, 3, 707.

[41] J.N. Miller, J.C. Miller, Statistics and Chemometrics for Analytical Chemistry, Pearson Education Limited, Fifth Edition, **2005**.

[42] EPA, in "National Recommended Water Quality Criteria. United States Environmental Protection Agency, Office of Water/ Office of Science and Technology" **2009**.

[43] European Commission, in "Directive 2008/105/EC on environmental quality standards in the field of water policy, amending and subsequently repealing Council Directives 82/176/EEC, 83/513/EEC, 84/156/EEC, 84/491/EEC, 86/280/EEC and amending Directive 2000/60/EC" **2008**.

[44] O. Mikkelsen, S.M. Skogvold, K.H. Schroder, M.I. Gjerde, T.A. Aarhaug, Anal. and Bioanal. Chem. **2003**, 377, 322.

[45] C. Kokkinos, A. Economou, M. Koupparis, Talanta **2009**, 77, 1137.

[46] M. Korolczuk, A. Moroziewicz, M. Grabarczyk, Anal. and Bioanal. Chem. **2005**, 382, 1678.

[47] K. Nowak, A. Bobrowski, Anal. Lett. **2005**, 38, 1887.

[48] A. Krolicka, A. Bobrowski, K. Kalcher, J. Mocak, I. Svancara, K. Vytras, Electroanalysis **2003**, 15, 1859.

[49] K. Tysczuk, M. Korolczuk, Electroanalysis **2007**, 19, 1539.

Chapter 7

MAIN CONCLUSIONS AND FUTURE WORK

7.1. Conclusions

In this thesis, the potentialities of two different "green" electrodes namely (i) a bismuth macroelectrode [bismuth film deposited *in-situ* on a GC electrode (Chaper 2) and a SBiVE (Chapter 6)] and (ii) a gold microwire electrode (Chapters 3, 4 and 5, respectively) for voltammetric detection of total concentrations of multi-combinations of metal(loid)s (As, Cd, Co, Cu, Hg, Pb, Ni and Zn), at trace levels in surface waters, was evaluated.

Figure 7.1 summarizes the overall voltammetric "greener" approaches developed in this work. Through the application of ASV technique (either with a square wave or a differential pulse mode), it is possible to make the simultaneous determination of (i) Cu, Pb and Zn (Chapter 2) with a bismuth film macroelectrode and (ii) As, Cu, Hg and Pb, (Chapter 3), (iii), Zn, Cu, Hg and Pb (Chapter 4) and (iv) Cd and Pb (chapter 5) with a gold microelectrode, respectively. Furthermore, the application of SWAdCSV technique, using a solid bismuth vibrating macroelectrode, allowed simultaneous quantification of Co and Ni (Chapter 6).

The use of chemometrics in electroanalytical chemistry is not as popular as in spectroscopy. However, the work developed in this thesis clearly indicated that the application of these tools for (i) mathematical resolution of overlapping signals [(Bi and Cu) in Chapter 2 and (Cd and Pb) in chapter 5], (ii) establishment of calibration models from multivariate voltammetric measurements [(Cu, Pb and Zn PLS models) in Chapter 2 and (Cd and Pb MCR-ALS together with a correlation constraint and PLS models) in Chapter 5, respectively] and (iii) species identification [(Cd and Pb) in Chapter 5] was essential to extract

maximum relevant chemical information from the complexity of the voltammograms obtained.

The potentialities of a gold microwire electrode in acidic conditions [HCl 0.1 $molL^{-1}$ (pH 1) or 1.0 $mmolL^{-1}$ (pH 3) with NaCl 0.5 $molL^{-1}$ medium] using simple and faster subtractive diferential pulse anodic stripping procedures were explored (Chapters 3, 4 and 5, respectively). This microelectrode was used as a WE in two different configurations, i.e., as a vibrating or as a stationary electrode, respectively. The agitation of the WE using a small vibration motor was very efficient to obtain a stable, reproducible and thin diffusion layer during the deposition step, which improved the sensitivity (DLs of the order of μgL^{-1} or sub-μgL^{-1} were attained) and reproducibility of the results (Chapters 3, 4 and 5). In fact, the electrode vibration is very proficient and hence eliminated the need for external stirring of the solution, thus potentially facilitates *on-site* detection using shorter $t_{dep(s)}$. A vibrating gold microwire electrode showed excellent characteristics for the simultaneous determination of As, Cu, Hg and Pb (at pH 1) in unpolluted fresh waters (Chapter 3) and Cu, Hg, Pb and Zn (at pH 3) in a wider spectrum of surface waters, i.e, fresh, drinking and saline waters, respectively (Chapter 4). On the other hand, the gold microwire electrode, when used in the stationary mode, allowed the simultaneous determination of Cu, Hg, Pb and Zn at much higher concentrations (Chapter 4). In fact, performing two sequential measurements using the same gold microelectrode (under the vibrating or the stationary mode), it was possible to perform the monitoring of Cu, Hg, Pb and Zn, in a wide range of concentrations without the formation of Cu-Zn intermetallic compounds (Chapter 4). On the other hand, in chapter 2, mathematical treatments were necessary to be applied to overcome the problems associated with the formation of Cu-Zn intermetallic compounds on a BiFE. Instead, a gold microelectrode showed no evidence of the formation of Cu-Zn intermetallic compounds, for total concentrations of both metal ions commonly found in surface waters.

In conclusion, the procedure used to fabricate and maintain a mercury-free gold microwire electrode is simple and does no require much care and/ or time.

All results obtained with this microelectrode confirmed its applicability and versatility for the multi-element determination of As, Cd, Cu, Pb, Hg and Zn, at trace levels, in surface waters.

Finally, using another branch of the stripping voltammetry, i.e., AdCSV, a solid bismuth electrode, coupled with the vibrating device previously used with the gold microelectrode, was successfully applied for the simultaneous, simple and faster detection of Ni and Co. The analytical performance for detecting Ni with this electrode was comparable or better than the methodologies described in the literature with BiFEs (Chapter 6). The main advantage of this solid electrode, when compared to the bismuth film electrodes prepared by *in-situ* or *ex-situ* deposition, are: (i) its mechanical robustness; (ii) easy handling and (iii) the simpler protocols, which do not require the formation of the bismuth film and cleaning and activating procedures to control the surface of the electrode.

All the voltammetric procedures developed (Figure 7.1) were carried without deoxygenation, which simplifies the stripping protocols and decreases drastically the measurement time. This point is particulary important for *in-line* (flux analysis) and/or *on-site* applications.

The good mechanical (solid and robust electrodes; no medium exchange or film deposition are required) and analytical (sensitive in low μgL^{-1} with 30 s of t_{dep}) features of the gold microwire and the solid bismuth electrodes (Chapters 3 up to 6) make these electrodes easier to convert to automatic flow systems and thus, more suitable for *on-field* measurements.

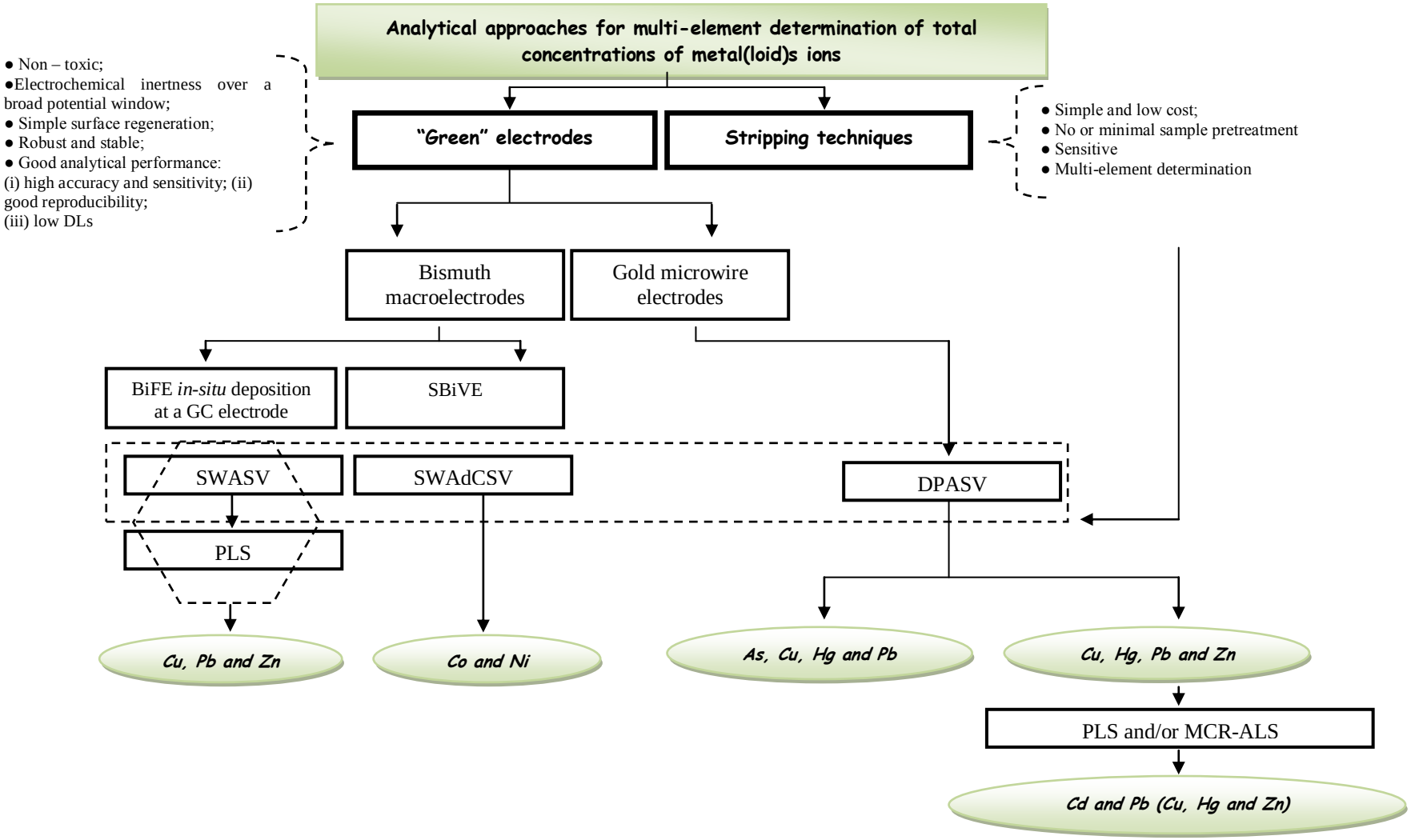

Figure 7.1 – Diagrammatic representation of the overall voltammetric processes developed in this thesis.

7.2. Future work

On-situ remote monitoring of trace metal(loid)s in natural waters is of special importance in order to obtain information about the (i) natural variations of metal(loid) concentrations and the (ii) variations resulting from anthropogenic sources in a rapid and expeditious way. These informations provid to control the pollution and to avoid environmental accidents in a faster way.

Having in mind the arguments presented previously, assembling and optimization of a remote automatic analyser system for continuous *on-site* monitoring of multi-metal(loid) ions is a priority.

Thus, taking into account all the results obtained in this thesis, as a future work, the development of two flow systems configurations, using either a gold microwire or a bismuth solid vibrating electrodes for monitoring total concentrations of (As, Cd, Cu, Hg, Pb and Zn) or [Ni, Co (Cd and Pb) [1]], respectively, is proposed. Briefly, these systems should work automatically, i.e., with *in-line* transport and pre-treatment of the solutions and/ or samples (including a *in-line* UV system) to the cell (quasi-flow cell), subsequently stripping measurement should be carried out (using the WE in the vibrating or stationary mode according to the degree of pollution of the waters) and finishing with cell draining. After the optimization of this *in-line* flow systems on the laboratory, the next step should be the instalation of a *on-field* monitoring station for long time monitoring. In principle, the manual maintenance should be performed every few days.

Furthermore, stripping voltammetric procedures offer speciation capabilities. Meanwhile, having as objective to extend the applicability of gold and bismuth non-toxic electrodes to understanding the ecological impact and fate of trace metals, speciation studies can also be designed.

References

[1] Z.S Bi, C.S. Chapman, P. Salaun, C.M.G. van den Berg, Electroanalysis **2010**, 22, 2897.

“Fight with determination, embrace life with passion, lose with class and win with boldness, because the world belongs to those who dare and life is much to be negligible.”

Charles Chaplin